UNIVERSITY OF SOUTHAMPTON

FACULTY OF HUMANITIES

Archaeology

Volume 1 of 1

The Shape of Childhood:

A Morphometric Growth Study of the Anglo-Saxon to Post-Medieval Period

By

Sarah Y. Stark

Thesis for the degree of Doctor of Philosophy

June 2018

UNIVERSITY OF SOUTHAMPTON

ABSTRACT

FACULTY OF Humanities

Archaeology

Thesis for the degree of Doctor of Philosophy

THE SHAPE OF CHILDHOOD:

A MORPHOMETRIC GROWTH STUDY OF THE ANGLO-SAXON TO POST-MEDIEVAL PERIOD

Sarah Y. Stark

Growth is a heavily studied field in juvenile bioarchaeological studies. The question of shape or developmental trajectories, however, has only recently been investigated as methodological advances such as geometric morphometrics (GM) have become more available. This thesis applied GM to archaeological juveniles and explored how biological processes affect bone shape during ontogeny to answer '*what is bone shape and what do shape trajectories tell us*?' The application of GM allows for a novel analysis of developmental trajectories as whole bone morphology is analysed and visualised in a three-dimensional space. To determine if long bone plasticity is influenced by archaeological site and time period, 178 juveniles of Anglo-Saxon to Post-Medieval foetal to 12 year old long bones were examined; they formed a comprehensive dataset to integrate GM with traditional bioarchaeological methodologies of growth and development.

The objective of this thesis was to develop a reproducible methodology that captures the torsion, curvature, and whole bone growth and development of the juvenile femora, tibiae, and humeri. This was accomplished through two validation studies; the first aimed to determine if GM can be used on cylindrically shaped long bones. Here, the methodological applicability of 3D GM on juvenile long bones examined linear measurements, 3D GM with landmark and semi-landmarks, and automated 3D GM. The second aimed to assess if different scanning methods, inducing laser, photogrammetry, and structured light scanning affect geometric morphometric analyses of bone shape.

This thesis contributes new insights on the applicability and importance of geometric morphometric approaches to the study of human juvenile long bones. The principal findings were that long bone

shape is statistically significant by site and period from foetal to 5 years old and that shape is not a linear progression of increasingly larger shapes but rather fluctuations in the changes of shape. It was also found that the developmental trajectories had different potential in the extent of shape that could be achieved for each age group, and that trajectories could change as a result of developmental pathways such as nutritional or environmental stress that occurred during growth.

Table of Contents

List of Tables

List of Figures

List of Figures

Academic Thesis: Declaration of Authorship

I, Sarah Stark .....

declare that this thesis and the work presented in it are my own and has been generated by me as the result of my own original research.

The Shape of Childhood: A Morphometric Growth Study of the Anglo-Saxon to Post-Medieval Period

I confirm that:

1. This work was done wholly or mainly while in candidature for a research degree at this University;
2. Where any part of this thesis has previously been submitted for a degree or any other qualification at this University or any other institution, this has been clearly stated;
3. Where I have consulted the published work of others, this is always clearly attributed;
4. Where I have quoted from the work of others, the source is always given. With the exception of such quotations, this thesis is entirely my own work;
5. I have acknowledged all main sources of help;
6. Where the thesis is based on work done by myself jointly with others, I have made clear exactly what was done by others and what I have contributed myself;
7. None of this work has been published before submission

Signed: .....

Date: .....

Acknowledgements

First and foremost I am grateful for my supervisory committee, Joanna Sofaer, Sonia Zakrzewski, and Simon Mays for their never-ending encouragement, inspiration, and advice. I am fortunate to have a committee that allowed me to run with ideas for this thesis while keeping it grounded.

I am also in debt to a number of individuals who have provided keen insights and their technical expertise along the way. I would like to thank Pat Tanner and James Miles from the University of Southampton and Jesse Hayes from S2Games for providing me with laser scans, guidance in photogrammetry, and an introduction into structured light scanning. I would also like to thank Jaco Weinstock and Fraser Sturt for their meticulous criticisms and supportive feedback for the earlier version of this draft, and Fraser Sturt for providing a high power computer to run the larger datasets in this thesis. I would also like to thank my examiners, Jay Stock and Alistair Pike for their insightful feedback and engaging discussion. A special thank you also goes to Ellie Williams at Canterbury Christ Church for her critical eye in editing, generous ear in listening, and never-ending support and humour.

I would also like to thank the individuals who provided access to their skeletal collections: Simon Mays at Historic England, Patrick Mahoney and Chris Deter at the University of Kent, Jelena Bekvalac at the Museum of London, and Jo Buckberry at the University of Bradford. I am thankful for their welcoming enthusiasm and scanning accommodation during my visits.

A special thank you goes to Tim Astrop for introducing me to the world of geometric morphometrics over four years ago. Thank you for the guidance and advice during tedious coding sessions, learning new mathematical concepts, and creative ideas for this thesis. I am grateful for your mentorship and friendship.

My family has been an essential source of never-ending support and optimism for every endeavour I pursue. To my parents Terry and Connee Stark, for always being encouraging and enthusiastic about my interests; from ballet, to drums, to archaeological bones. My grandparents Carmen and Lowell Yeager and Ray and Norma Stark, who have always been proud of my pursuits- and for making me critically compose one sentence that describes my research so they can tell their friends. And to my sister Alyssa Stark who has always been an inspiration for following her own aspirations and providing invaluable advice, you leave some big shoes to fill.

Finally, I am eternally grateful to my husband Thomas Dhoop. From building Lego laser scanners, fixing coding errors, providing critical feedback and ideas, to all the laughs along the way. Thank you for the unconditional reassurance and motivation to see this thesis through to the end.

1. Introduction

This thesis seeks to develop and apply a methodological framework using geometric morphometrics (statistical analysis of shape), to archaeological juveniles to explore how biological processes affect bone shape during ontogeny. This research functions as a case study for integrating geometric morphometrics (GM) with traditional bioarchaeological methodologies of growth and development to determine if long bone plasticity is influenced by archaeological sites and/or time period. As growth is the process of enlarging tissues with chronological age, development represents pathways or biological milestones along the life cycle (Agarwal 2016: 132). The rates of growth and developmental timing can differ between individuals based on genetic and environmental influences (Agarwal 2016: 133). This thesis, therefore, explores a specific time frame of growth and development, foetal to 12 years old, from Anglo-Saxon to Post-medieval periods in the UK.

The material properties of bone form a challenge to this work, as it is easy to regard bone as a static rigid structure whereas, in reality, it once was a living organic material. As a result, this thesis incorporates the life course history of an individual through skeletal elements and explores the plasticity of bone as organisms change phenotypes in response to changing environments (Roberts 1995; Agarwal 2016: 132). For instance, stress as a result of poor nutrition can cause an energetic reserve to be reallocated to the development of essential tissues or functions. Early mortality may be prevented but the trade-off ends with a reduced future investment in growth, later seen as growth stunting (Kuzawa 2005; Worthman & Kuzara 2005; Agarwal 2016). The concept of the body as a product of social and biological developments is immensely complicated as multiple variables are intertwined.

This project set out to study the shape of juvenile long bones and investigate how growth and developmental trajectories differ from Anglo-Saxon to Post-Medieval periods in the UK. Juvenile remains provide significant information on the physical and social life of archaeological children as evidenced by their patterns of growth, development, diet, social interactions, and exposure to environmental stresses (Lewis 2011a: 1). To date, an important method of analysing growth trajectories has been plotting long bone length against dental development (Johnston & Show 1961; Tanner 1981; Bogin 1988a; Lewis 2002) and assessing how these trajectories differ from modern populations. A subset of these studies focuses on the biocultural nature of growth and have begun to assess juveniles from different populations, social statuses, and time periods, and have examined how the health and treatment of children vary on social and biological scales. Studies of

health and population stress have been dominant themes as pathological lesions on juvenile remains provide further insight to harsh and often chronic conditions of their environment (Ortner *et al.* 2001; Lewis 2002; 2010; 2011a, Brickley & Ives 2006). This thesis will incorporate these traditional methodologies of plotting growth (age and size), prevalence of stress, and historical contexts to interpret differences in bone shape.

How to capture bone shape is a further challenge of this thesis. Traditional techniques of long bone length only capture the size of the bone while computed tomography (CT) scans provide information on the histological properties and cross-sectional geometries of bone growth. The introduction of CT scans has opened new avenues of morphological research by highlighting regional variations in growth of the long bones through cross-sectional analyses (Gosman *et al.* 2011) which are commonly overlooked with traditional length measurements. Additionally, CT scans and analyses have led to studies of a biomechanical nature and investigated how juveniles interacted with their physical landscape by finding loading patterns in the proximal and distal regions of the femur and tibia during the transition of crawling to walking (Ruff & Hayes 1984; Ruff 1999; Ruff *et al.* 2013). The difficulty with CT scans, however, is that they are time consuming logistically and it is challenging to get permission to borrow material from collections. This is problematic if specimens are in remote locations as it may be difficult to add to analyses or there are additional fees to take them on loan for scanning (Wilson & Humphrey 2017). Another issue to consider is even the highest resolution of Micro CT scans remain largely insufficient for histological characterizations of bone.

The difficulty of obtaining access to methods such as CT scanning and the overall lack of large sample sizes of juvenile remains often leads to researchers combining data that have different methodologies (Pinhasi *et al.* 2005) and results in studies that cannot be repeatable. Limited sample sizes arise due to a range of issues including preservation, excavation methods, and curation of the skeletal remains. Bioarchaeologists, therefore are continuously expanding their analytical tool-kit with methodologies that can work with limited sample size, capture the complexities of bone morphology, as well as be repeatable for other studies. Morphometrics provides one potential solution to these needs.

Geometric morphometrics, the measurement of shape, is a subfield of statistics that goes back to the beginning of mathematics itself (Mitteroecker & Gunz 2009). Until the twentieth century, anthropology and bioarchaeology were confined to the study of bone phenotypes by scoring and measuring changes in shape through linear measurements. It is not until the past three decades when faster personal computers led to a new era of data analysis. This allowed the exploration and visualization of large, high-dimensional datasets in combination with statistical procedures to be

possible, thereby catalysing a new research area in shape exploration (Mitteroecker & Gunz 2009; MacLeod 2008; Slice 2007). This period in morphometric history is now known as the 'morphological revolution' through the invention of coordinate-based methods: geometric morphometrics (GM) became a new subfield, and the development of statistical shape theory has allowed for more theoretical discussion on the relationship of form, function, and allometry in the field of biology as a whole, and in anthropology and bioarchaeology specifically.

1.1 Research Aims

The principal aim of this research is to analyse and visualise ontogenetic trajectories (changes in bone shape with size and age) and investigate developmental plasticity of the left sided juvenile femora, tibiae, and humeri from Anglo-Saxon to Post-Medieval periods in the United Kingdom. In other words, this thesis will address the question, *what makes up bone shape and what do shape trajectories tell us?* To answer this question, a series of validation studies for the data collection and methodological analysis was undertaken. This research, thus, provides both a methodological and bioarchaeological contribution to the field. Marrying qualitative and quantitative data with visualisations of shape patterning is an avenue of juvenile growth and development that has hitherto not been fully explored.

The methodological contribution aims to:

1. Develop a reproducible methodology that captures the torsion, curvature, and whole bone growth and development of long bones.

In order to achieve this aim the following methodological questions were put forward:

a) How effectively can GM be used on small cylindrically shaped bones (Chapter 4)?
b) Do the visible differences in morphological shape change by scanning technique (Chapter 5)?

As indicated above, one of the hindrances to the field (both in bioarchaeology in general and juvenile remains in particular) is the lack of large sample sizes which leads to combining data that have different methodologies and results in non-repeatable studies (Pinhasi *et al.* 2005). This thesis tests a possible solution to expand our analytical tool-kit with a geometric morphometric methodology that has been successful in other fields (O'Higgins 2000; Strand Viðarsdóttir *et al.* 2002; Wilson *et al.* 2008; Mitteroecker 2013) and will limit error rates and provide a replicable method across studies. Another benefit is its ability to work with digital or virtual datasets, thereby not only preserving collections but allows for dissemination of 'virtual specimens' that can undergo rigorous statistical analyses.

The bioarchaeological contribution aims to:

2. Apply the power of geometric morphometric analysis with human juvenile long bones by examining whether plasticity is influenced by archaeological sites and or time period.

To achieve the bioarchaeological aim, the following question was tested:

a) Is plasticity influenced by site and/or time period (Chapter 7)?

This research is based on a multivariate concept of shape by teasing apart growth (age and size), development (age and shape), and allometry (size and shape) of difficult elements such as the long bones. As there has been little previous work on whole bone shape, this thesis analyses juvenile whole bone morphology and uses a repeatable method that can analyse different variables. GM has been used for decades in other fields to explore ontogenetic trajectories but very rarely has been applied to human juvenile remains. GM accommodates for the torsion and assesses the magnitude and pattern of long bone curvature - something that linear measurements have not been able to do. This work, therefore, measures aspects of variation such as curvature that previously have been difficult to capture.

To execute the methodological and bioarchaeological aims of this work, a series of validation studies was needed for data collection and analysis. The following objectives were set that form the framework for this thesis:

a) To synthesize what is currently known about juvenile long bone growth and how the plastic nature of these elements reflect developmental pathways over the life course (**Chapter 2**).
b) To consider how other fields, in particular evolutionary biology and biological anthropology, analyse growth and development trajectories of skeletal elements through the analytical tool-kit of geometric morphometrics (**Chapter 3**).
c) To test the methodological applicability of 3D GM on the juvenile long bones by examining linear measurements, 3D GM (landmark and semi-landmark), and auto3dgm analyses (**Chapter 4**).
d) To asses if scanning methods (photogrammetry, laser, and structured light scanning (SLS)) significantly affect long bone surface morphology (**Chapter 5**).
e) To examine the context of the skeletal case studies (Anglo-Saxon Great Chesterford and Raunds, Medieval Canterbury and Wharram Percy, and Post-Medieval Wolverhampton) and what is already known about the juvenile populations (**Chapter 6**).
f) To analyse and visualise ontogenetic trajectories (changes in bone shape with size and age) and investigate developmental plasticity of the juvenile femora, tibiae, and humeri from Anglo-Saxon to Post-Medieval periods (**Chapter 7**).
g) To summarise the findings of this thesis and evaluate the methodological and bioarchaeological benefits and limitations of GM (**Chapter 8**).

1.2 Structure of the Thesis

The structure of this thesis follows the process of how the research was conducted. First, an evaluation of what is currently known about growth and bioarchaeological studies was undertaken to determine common themes and trends of growth from the past. As geometric morphometrics is

not a common technique in bioarchaeology, it was important to establish the current understandings and accepted hypotheses for studying growth. This identified crucial timings of genetic versus environmental factors (environment being more important before the onset of puberty when genetics begin to take over) which may be problematic to developmental trajectories (Gosman *et al.* 2013). This narrowed the research focus to juveniles from foetal to 12 years old in an attempt to 'control' variables that may impact ontogenetic trajectories and incorporate differences in childrearing practices from Anglo-Saxon to Post-Medieval periods to assess how morphology may differ, not just at a site or in a population level, but also over time.

Before exploring the intricate nature of development and shape, **Chapter 2** synthesises what is known about growth and plasticity of the long bones. An interesting and challenging component of this thesis is the plastic nature of juveniles and the difficulty in capturing developmental changes. Therefore, an understanding of plasticity (the nature of the materials) and life course history (theoretical framework) was needed in order to begin creating a methodological framework. Life course history models offer a unique approach to developmental studies by incorporating stress, environment, temporal period, and biomechanical studies on morphology and plasticity.

Chapter 3 considers how other fields, such as evolutionary biology and biological anthropology, capture the rapid changes in morphology linked to growth. This chapter begins with a general overview of the field of geometric morphometrics, both in terms of history and methodology. The benefits and limitations of linear measurement theory and GM are examined, leading to a series of validation studies for both analysis (Chapter 4) and data collection (Chapter 5).

As the juvenile long bones are small, smooth, and cylindrical in nature, it is important to determine whether GM can work on these elements. **Chapter 4** aims to test the applicability of GM of both landmark and semi-landmark, automated 3DGM, and ratio measurements. GM offers a unique statistical mechanism for quantifying shape, however, it is more labour intensive than traditional linear measurements. Thus, it is crucial to determine if GM uncovers more subtle variations in shape that are not captured with traditional and less labour intensive methods. Juvenile femora from Anglo-Saxon Great Chesterford were digitized using photogrammetry and split into five age groups (Group1: foetal, Group 2: infant to 2 years old, Group 3: 3 to 5 years old, Group 4: 6 to 8 years old, Group 5: 9-12 years old) based on criteria from Gosman *et al*. (2013). Three methods of analyses were applied to each skeletal sample, testing the same questions in order to determine the most appropriate method of analysis for the case studies in Chapter 7.

The findings in the first validation study of Chapter 4 immediately posed the question for **Chapter 5**; *Do the visible differences in morphological shape change by scanning technique?* Photogrammetry is a less expensive but more labour intensive method: This can be useful for pilot studies (such as Chapter 4), but is impractical for larger datasets. Laser scanning is an ideal method for limited scanning error and produces high quality meshes, but was not available in the Department for the case studies used in Chapter 7. Structured-light-scanning (SLS) offered a potential alternative as it is not as expensive as laser scanning but not as time consuming as photogrammetry. The aim of this chapter is to examine scanning techniques by using one femora from each age group (5 groups) and to scan each femora using laser, photogrammetry, and SLS methods. The first objective was to evaluate the technical aspects of each scanning method. This includes costs for equipment, error, resolution, file size, set-up, scanning, and post processing time. Cloud compare was then used to measure the different scans of photogrammetry and SLS against the laser scans to determine if there were significant differences in surface morphology. The second objective was to evaluate whether auto3dgm found significant differences in the surfaces based on scanning type. This validation study was able to confirm that any morphological differences were due to differences in the specimens and not the result of the scanning method used.

The final step, before investigating Anglo-Saxon and Post-Medieval ontogenetic trajectories, was to examine the context of the skeletal material described in **Chapter 6**. As there are very few GM studies of human juvenile long bones, it is important to understand the context of the collections and what is already known through traditional bioarchaeological analysis. Anglo-Saxon Great Chesterford was the first collection used as it was selected for the validation studies. Great Chesterford has medium to poor preservation (Evison 1994: 52) and this was important for refining the scanning methodology. Raunds is a large Anglo-Saxon collection, rare for this period, and offers a good comparison to Great Chesterford. Medieval Wharram Percy is a heavily studied skeletal collection, and is as close to a "known sample" as possible. Canterbury comprises another large medieval collection, with high status individuals, and therefore offers a good comparison to the lower status Wharram Percy juveniles. Lastly, Post-Medieval Wolverhampton was used to include an industrial urban sample.

Following investigation of the variables of growth, validation of techniques, and the context of materials, **Chapter 7** analyses the ontogenetic trajectories of the femora, tibiae, and humeri from Anglo-Saxon to Post-Medieval juveniles. This chapter begins by examining the growth trajectories for each element in terms of length versus age. This is a useful starting point in order to assess the standard growth trajectories of the skeletal collections relative to modern known data from the Denver Growth Study (Maresh 1955). An overview of all femora, tibiae, and humeri sites and ages are then analysed using GM, followed by a closer examination of all three elements by age group.

Each age group begins with an overview of what is known to occur developmentally for that age range, and a hypothesis is made against which to test the GM shape data for each element. A principal component analysis (PCA) is computed, followed by ANOVA of shape (PCA scores) by site, period, and allometry. The results for each element are presented, followed by a small discussion of the findings. The last section of this chapter comprises a summary of the statistically significant patterns in shape for site and age, and contextualises these findings for each site.

Chapter 8 addresses the key findings and limitations of the thesis. By assessing the methodological and bioarchaeological aims, a reflection on the process of addressing, *what makes up bone shape and what do shape trajectories tell us*? and future research will conclude this thesis.

The Appendices supporting this work are found in the back of the document. Appendix A.1 comprises of the intra-observer error tests for the linear measurements of the femora for the Chapter 4 validation study. Appendix A.2 is the GM landmark error test of the femora used in the Chapter 4 validation study. Appendix A. 3 is the auto3dgm error test of the femora for the Chapter 4 validation study. Each femur (Group 1: foetus; Group 2: infant to 2 years old, Group 3: 3 to 5 years old, Group 4: 6-8 years old, Group 5: 9-12 years old) was digitised 3 times to form 3 separate analyses. This series of intra-observer error tests is crucial to the methodology as it demonstrates that any significantly different morphological variation is a result of the bone morphology rather than landmark placement. Appendix B displays the development and allometry for Great Chesterford tibiae and humeri, while the femora are used in the Chapter 4 validation study. Appendix C displays the Raunds site, Appendix C reflects Raunds, Appendix E provides the Canterbury growth data, and Appendix F represents the Wolverhampton development and allometric trajectories. Appendix G comprises of the skeletal specimens used in this thesis.

1.3 Juvenile Growth in Archaeology

The remaining section of this chapter is devoted to exploring the field of juvenile growth and the key subfields that have developed from it. The archaeology of childhood is a growing field of interest as theoretical developments and methodological innovations are becoming more integrated (Baxter 2008: 160). The study of children and childhood in social archaeology is an offshoot of gender theory which, during the 1990s, moved children out of the sphere of women's work. Children became acting agents in their own right with their own social identity, material culture, and interactions to their physical environment (Lewis 2011a: 1). Juvenile osteological remains are an important resource for juvenile studies and provide significant information on their physical and social life as evidenced by their patterns of growth and development, diet, age at

death, social and economic factors, and exposure to environmental stresses (Lewis 2011a: 1). Cultural biases dictate where and how infants and children are buried, when they assume their gender identity, and at what age they are considered adults (Lewis 2011a: 1). Over the past few decades, improvements in excavation techniques, analytical methods, and the integration of other disciplines have slowly brought these 'invisible' members of the past into focus (Baxter 2008: 160).

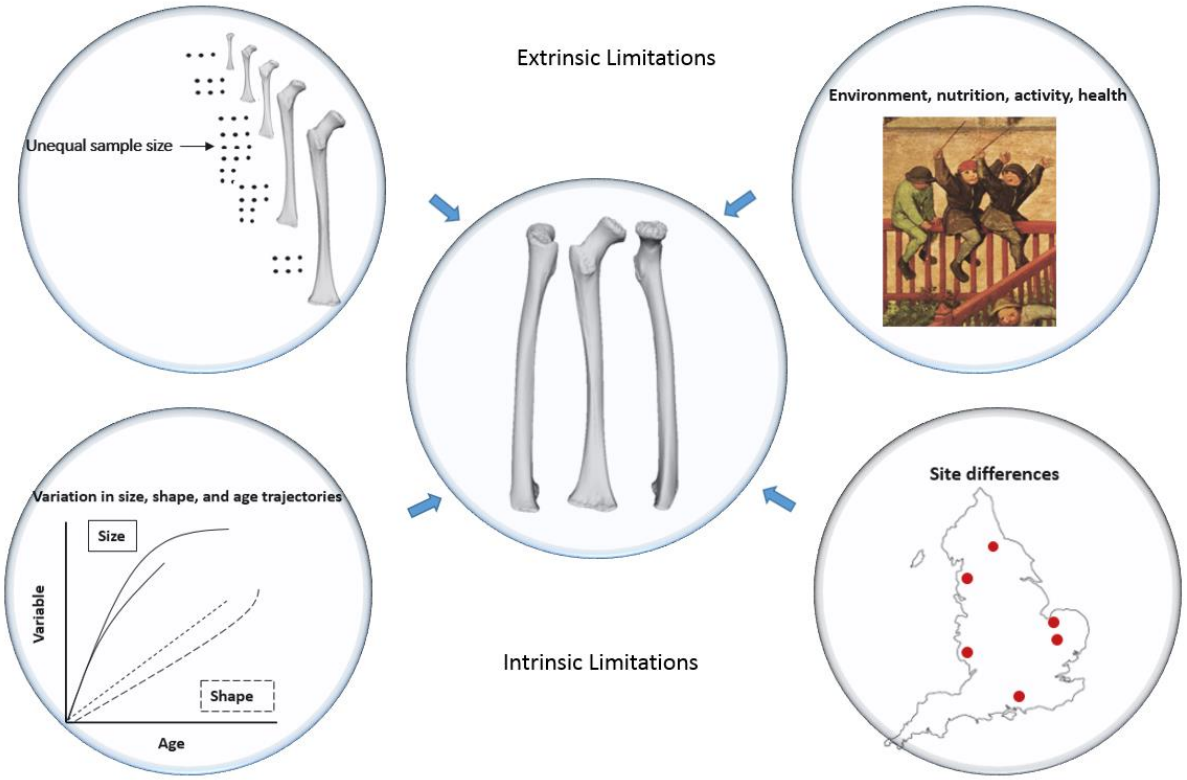

Figure 1.1: Overview of factors impacting growth and development studies of juvenile remains (Image by author: Adapted by Wilson & Humphrey 2017: 35).

1.3.1 Skeletal Growth

Skeletal growth is the most frequently studied field when analysing juvenile remains from archaeological sites (e.g. Tanner 1978: 178-222; Bogin 1988b: 225-263; Eveleth & Tanner 1990; Hoppa & Fitzgerald 1999). The primary interest in juvenile remains came from research on child survival and adult adaption to environmental change (Lewis 2011a:3). Figure 1.1 illustrates the complexity of juvenile growth studies: this is related to unequal sample sizes, environmental differences, site variation, and varying growth and developmental trajectories. During the 1960s, methods of ageing and sexing, adopted from medical studies (Schour & Massler 1941; Boucher 1957:584-592) spurred interest in physical growth of past populations, a theme that has dominated the field for the last forty years. Francis Johnston's work on growth, at Indian Knoll in Kentucky (Johnston & Snow 1961: 240-244; Johnston 1962: 249-253; 1968: 59-63), has been particularly influential as it stimulated many diaphyseal length studies during the 1970s (Armelagos et al. 1972;

Merchant & Ubelaker 1977). Mensforth and colleagues (1978) worked on the prevalence of anaemia and infection in 452 infants and children at the Late Woodland ossuary site of Libben in Ottawa County, Ohio and thereby introduced another avenue of research; for the first time, the health of children in the past emerged as a primary focus, and demonstrated the importance of healed and active lesions for specific ages at which children were most at risk. Interestingly, their findings have yet to be fully integrated into adult studies (Lewis 2011a, 3).

Commenting on the lack of juvenile remains from archaeological sites, Buikstra and Cook (1980:449-452) argued that this issue could be the result of poor preservation, lack of recovery and small sample sizes acting as a severe hindrance to the field. Demands for improved methods of ageing and recording juvenile remains increased as bioarchaeologists finally acknowledged the importance of analysing direct evidence for children in the past (Lewis 2007:8-10; 2011a: 3).

1.3.2 Biocultural Studies

It was not until the 1990s that biocultural studies focusing on growth and health in different populations became a growing theme (e.g. Stuart-Macadam 1992; Grauer 1993; Ribot & Roberts 1996). During this time a surge of studies emerged: this is likely a result of larger collections of juveniles being excavated and available for research. Children of known age and sex from Christ Church Spitalfields and St Bride's Church in London (Molleson & Cox 1993: 145-156) as well as Wharram Percy (Mays 1999:291) and St Thomas Church in Belleville, Ontario (Saunders et al. 1993: 266) became accessible. These collections and research on them inspired methodological discussions of how to estimate the age and sex of juveniles (De Vito and Saunders 1990; Schutkowski 1993; Molleson et al. 1998; Loth & Henneberg 2001). These sites also provided evidence for an abundance of stress indicators in children, and these became a popular focus for study as researchers began to assess the impact of agriculture, colonization, and urbanization on child health (Owsley & Jantz 1983; Blakey and Armelagos 1985 Lewis 2011b). For instance, Goodman and Armelagos (1989: 232, 237) highlighted children under five as the most sensitive members of society to both environmental and cultural stress (Lewis 2011a, 3).

1.3.3 Mortality Bias

The growing focus on juvenile studies led to a critical review by Saunders (1992:15) addressing advantages of working with juvenile remains as well as limitations, specifically mortality bias (Saunders & Hoppa 1993; Sofaer Derevenski 1994: 8; Lewis 2011a: 4). Discussions about the latter are still ongoing as it is argued that we are studying individuals who died prematurely and therefore

may not be an accurate representation of past population growth (Buikstra & Cook 1980). Wood and colleagues (1992) explored this argument but did not find any changes in growth patterns from past populations as they reflected only periods of high and low mortality. Periods of low mortality consist of the sickly children, with delayed and shorter growth, which results in a skewed assumption that the entire population was of shorter stature. The 'non-survivors' will be a result of their disease experience that lead to early deaths and they cannot be compared to modern living children, or considered as an accurate representation of the living population from which they came from (Lewis 2011a: 4).

Sundick (1978) argues that most childhood deaths would result from an acute illness that would have killed children too quickly to affect their growth. The problem is that children susceptible to acute illnesses typically experience previous stress and are likely to be shorter than their healthier peers who survived into adulthood (Humphrey 2000). The early deaths of these individuals presents challenges in the study of paleopathology among juvenile populations. For instance, chronic diseases take time to manifest on the skeleton but children tend to enter the archaeological record from acute stages of diseases before the skeleton has time to respond (Lewis 2011a).

Studies on medieval health and morbidity of juveniles have turned to historical medical documents of child health, such as coroner's rolls (Hanawalt 1977) and reports of saint's miracles reports written by the local churches (Gordon 1991; Finucane 2000). These records share accounts of what children died or survived from (excluding diseases). Hanawalt (1977) studied the coroner's rolls from urban (Oxford and London) and rural (Northamptonshire and Bedfordshire) 'accidental' deaths. The rural children were more frequently reported in these documents, potentially because they had the opportunity to run freely and with less supervision than in a crowed town or city.

Table 1.1 is based on Gordon (1991) who showed the frequencies of accidents that occurred in different ages from miracle records of rural villages or small towns. Drowning was the most common cause of death followed by injury of crushing/piercing, trips/falls, choking, burning, and encounters with animals. Different ages experienced different risks. Infants were commonly killed by accidental strangulation from swaddling: this became an issue in the 14th century by priests who warned parents off this practice. Toddlers often died from drowning (49%) as their mothers would wash clothes in nearby streams or rivers (Gordon 1991). Accident rates dropped after four years of age (Hanawalt 1977) as children could keep up with their parents and more supervision was in place from this age until seven years old. From eight to twelve, children carried out more specific work-related tasks and the accident patterns represent those of adults. Many of these accidental deaths do not manifest in skeletal lesions or stunted growth as they occurred rapidly and damaged the soft tissues. These findings present a more complex picture, indicating that archaeological children are

not all 'sickly'. It should be noted that coroner's rolls did not record deaths through disease so there cannot be any inference about whether deaths from accidents were more common than deaths through disease. Although disease is likely to be more prevalent in any premodern society, it is useful to consider all aspects of health and morbidity in ontogenetic studies, and to examine what types of activities children performed in the past.

Other researchers have expanded on the study of stress and health by focusing on the potential and extent of pathological evidence that can be derived from juvenile bones (Anderson & Carter 1994: 47-48; 1995: 192-195; Lewis & Roberts 1997). By the end of the 1990's, dental microstructure was being explored to refine methods of ageing (Huda & Bowman 1995) and stable isotope analysis dominated the field by addressing the age of weaning in different populations (Katzenberg & Pfeiffer 1995; Herring et al., 1998; Richards *et al.* 2002; Dupras & Tocheri 2007).

Accident and Miracle Records: Rural Medieval Villages									
Accident	Under 1 years old	1 years old	2 years old	3 years old	4-6 years old	7-12 years old	Over 12 years old	No Age	Total
Drowning	3	9	5	1	7	7	3	41	76
Concussion	2	0	3	1	1	1	3	6	17
Lacerations	0	0	3	0	1	2	1	2	9
Choking	2	3	0	1	0	0	2	0	8
Suffocation	5	0	0	0	0	0	1	0	6
Strangulation	1	0	0	0	1	0	0	0	2
Fractures	0	0	0	0	1	0	0	3	4
Abrasions	0	1	0	0	0	2	0	0	3
Burns	0	1	0	0	1	1	0	0	3
Other	2	1	1	0	0	0	1	2	7
Total	15	15	12	3	12	13	11	54	135

Table 1.1: Accident and Miracle records from rural medieval villages (Gordon 1991:150).

1.3.4 Defining the Child

A major stimulus to the field was Scheuer and Black's (2000) volume Developmental Juvenile Osteology which, for the first time, provided detailed images to identify elements of the juvenile skeleton. This handbook led to more studies that focused on a wide range of elements of growth rather in addition to a longstanding emphasis on the femur. Methodological concerns regarding ageing techniques and statistical methods continue to be a research focus (Gowland & Chamberlain 2002) as well as exploring childhood stress (Glencross & Stuart-Macadam 2000; Ortner *et al.* 2001; Lewis 2002; 2010; 2011a; Brickley and Ives 2006). During the 2000s, studies of a biological and mechanical nature emerged, as radiographs and eventually X-ray Computed Tomography (CT) scans were used to capture internal geometries and growth processes (Ruff and Hayes 1984; Ruff 1999; Ruff et al. 2013). For instance, Mays and colleagues (2009b: 411-415) were able to analyse the

cortical thickness of juvenile long bones and found that cortical bone is a more sensitive indicator to nutritional and environmental stress than overall bone length.

Another heavily debated issue with juvenile studies that emerged in the 2000s is determining appropriate 'age ranges' or 'categories'. This issue was raised among Anglo-Saxon archaeologists when comparing grave goods and skeletal age profiles (Hadley & Hemer 2014: 1-2). There have been many attempts to classify the stages of childhood from both biological and cultural perspectives (Sofaer 2000: 11-12; Lewis 2011a: 1-2), however as the field grows, so does the definition of children. Childhood is both a biological and social progression, the child physically grows and matures while learning about their society, gender roles, and labour through aspects of play (Lewis 2011a: 1-2). One of the major difficulties in defining children is the complex relationship of biological, chronological, and cultural ages (Gowland & Chamberlain 2002; Baxter 2008). Skeletal development (biological) is heavily influenced by the chronological (actual age) and cultural (social age) constraints which are temporally and geographically defined (Lewis 2011a: 2). The ages that individuals become independent, play, learn, work, and take on social responsibilities are not clear or universally defined (Lewis 2011a:2).

Biological age marginally precedes how society treats a child, as it affects the child's connection to their physical and social environment. For instance, the transition from crawling to walking allows children to become more mobile or development of speech allows for further communication to those around them (Lewis 2011a: 2). These abilities are physiologically determined as they govern how the child interacts in their environment. Wiley and Pike (1998) recommend developmental stages, rather than chronological ages, to study child mortality rates which incorporate the activity of the child. This approach to archaeological studies encompasses the environment and social life that the child is engaging with physiologically. A detailed review of childhood studies by Kamp (2001) illustrates the age categories that bioarchaeologists select and how they relate to the specific geographical and temporal location of the site. For instance, during the later Medieval period, children from the ages of 8-12 years old represented a period in time when children would begin their apprenticeships (Lewis 2011a: 3). However, in ancient Egypt and Rome, children age 12 to 14 could be married and take on roles as wives or mothers (Hadley & Hemer 2014: 1-2). There have been attempts to define these periods of transition in childhood from the past by analysing the burials of children and the nature of their grave goods at certain ages (Rega 1997; Stoodley 2000; Gowland 2001; Lewis 2011a). Sally Crawford (1991) found that children were sometimes buried with adult gave goods as it was believed that individuals from 12 to 17 years old were still children, however in Anglo-Saxon society adulthood was a legal responsibility that required marriage and could occur as young as 12 years old (Crawford 1991). Incorporating historical contexts is a crucial element that should be considered with the developmental stages of juvenile remains. These

cultural and temporal differences will influence the growth trajectory of the child and can severely skew analytical methods if inappropriate age groups are used for comparisons of childhood life-histories.

1.4 Conclusion

Today, these themes in juvenile archaeological studies are still being explored and refined as digital technologies are becoming more accessible in university and research departments, isotope studies are now being expanded to investigating migration patterns, DNA analysis is incorporated into exploring methods of sexing (Mays 2013: 12-16), and geometric morphometrics is used to create allometric growth trajectories (Strand Viðarsdóttir et al. 2002; Hellier and Jeffery 2006). There have been tremendous improvements in the field which has resulted in a Pandora's Box effect as the archaeology of childhood is immensely complicated and multiple variables of growth, development, allometry, mechanical, nutritional, and environmental effects are all intricately woven together. Nonetheless, an area of study that is severely understudied is the relationship of whole bone morphology during growth and development, as well as the development of a methodology that is repeatable and can be used to analyse relationships in sample variation. Geometric morphometrics has been used for decades in other fields to explore ontogenetic trajectories but has scarcely been used in juvenile archaeology. While a few studies have applied this technique to questions regarding methods of sexing, mechanics, and inter-population variation, little has been done on whole bone morphology of the juvenile long bones. The current study will explores the use of GM as a methodology that captures 3-dimensional shape of the long bones during growth as well as exploring the dynamic relationship between population differences and time periods.

2. Developmental Plasticity and Juvenile Long Bones

In order to assess the different developmental pathways and shape of juvenile long bones, this chapter synthesises the material properties and theoretical framework for the present research. This thesis puts forward the concept that juvenile bone shape is influenced by developmental pathways that occur during the lifecycle. Therefore, it is necessary for this chapter to explore these pathways of bone plasticity, stress, diet, genetics, and biomechanics and how they impact shape during growth. The theoretical framework presented in this chapter is an incentive for alternative ways of thinking about the data generated in this research rather than a rigid structure to fit the empirical data into.

2.1 Developmental Approaches to Plasticity

For the past decade, physical anthropologists and bioarchaeologists have explored questions of phylogeny and functional adaptations. This research has led to the use of more complex explanations of the role of developmental interactions on skeletal morphological variation (Agarwal 2016) including for instance, the experimental models in the understanding of cranio-facial morphology (Martinez-Abadias *et al.* 2012) and the variation in ontogeny of the post-cranial skeleton (Hallgrimsson *et al.* 2002b; Ryan & Krovitz 2006; Gosman *et al.* 2011; Agarwal 2016). These fundamental studies in developmental biology have led researchers in human biology, paleopathology, and bioarchaeology to concentrate on the variation of morphology related to disease, nutrition, and activity in anatomically modern humans (Agarwal 2016). This focus is of great interest in answering questions on the population and individual level. As bioarchaeology is centred in early biocultural approaches with an emphasis on archaeological contexts (Armelagos 2003; Buikstra & Beck 2009; Agarwal 2016), the interaction of bone biology and behaviour in relation to environmental influences on health (Larsen 2002; Agarwal 2016) leads to unique approaches to studying populations and individuals from the past. Studies of bone morphology from archaeological populations are extrapolated by their integration of human life as a result of interrelated events over the individual's lifespan and community level over generations (Agarwal 2016). These studies expand past the concept of early biocultural approaches in the field and make significant contributions to how biologists, anthropologists, and bioarchaeologists think about the role of plasticity (Agarwal 2016).

2.1.1 Plasticity and Developmental Trajectories

Developmental approaches to plasticity have often used life course theory, a melding of several scientific fields such as biology and social sciences (Agarwal 2016). The crux of this conceptual framework is the study of individual lives and their connection to their historical and socioeconomic contexts (Clausen 1985; Elder 1995; Agarwal 2016). This approach includes social and biological experiences and the individual plastic response to exposures that can be viewed as adaptive, intergenerational, or individual changes to the phenotype (Agarwal 2016).

The common elements in approaches to life course models is the trajectory and plasticity of an individual (Roberts 1995; Agarwal 2016). These models view development following an arc trajectory that can change direction along the phase of an individual's life course (Lasker 1969; Roberts 1995; Schell 1995; Bogin 1999; Worthman & Kuzara 2005; Agarwal 2016). Interpreting development as a trajectory allows the incorporation of a range of different influences that alter development to be investigated (Low *et al*. 2012; Halfon *et al.* 2014). Plasticity is the most fundamental piece in life course approaches as it relates to the concepts of growth and development that form the foundation to understanding patterns of phenotypic variability (Agarwal & Beauchesne 2011). Growth is the second variable to be considered as it is the process of enlarging different tissues with chronological age while development incorporates the pathways of biological milestones along the life cycle (Agarwal 2016). The rates of growth and timing of developmental changes can differ among individuals and populations (Lasker 1969; Roberts 1995; Schell 1995; Bogin 1999; Ellison 2005; Worthman and Kuzara 2005).

As previously mentioned, plasticity relates to an organisms ability to change its phenotype in response to environmental changes (Lasker 1969; Roberts 1995). Before the 1950s and 1960s, plasticity was thought to be the malleable mechanism behind human morphology which occurred during growth and development (Bogin 1995). Lasker (1969) redefined the concept of plasticity, and interpreted it as operating within three modes of adaptation. The first was natural selection where the selection of genotypes directly influenced the genetic spectrum of the population (Roberts 1995). The second form of adaptive plasticity is the acclimatization and physiological and behavioural response that adapts an individual to the immediate environment, but is not always permanent (Roberts 1995). The third mode is development or ontogenetic adaptation (Roberts 1995). In this mode, plasticity occurs through growth and development and is seen as changes that are not reversible nor heritable (Schell 1995). Recent studies of variation in human phenotypes through the lens of plasticity are now linked to adaptation and biological trade-offs (Worthman & Kuzara 2005). This model views biological responses to early foetal or childhood life stress as a life history trade-off where early stresses such as poor nutrition cause energetic reserves to be

reallocated to the development of essential functions or tissues. Although early mortality may be prevented, the result is a trade-off with reduced future investment in growth, higher mortality or impaired fertility (Kuzawa 2005; Worthman & Kuzara 2005; Agarwal 2016).

Beyond the adaptationist model of plasticity and development, several researchers have focused on the plastic developmental responses that take place during foetal, early postnatal, and later adolescent growth (Kuzawa 2005; Agarwal 2016). Developmental patterns are believed to be a product of the relationship between genetics and the environment (Roberts 1995). Plasticity is an essential variable of the developmental system that is viewed as the interaction of all variables in development which includes the molecular, cellular, organismal, ecological, social, and biogeographical (Robert *et al.* 2001: 954). Anthropologists and bioarchaeologists have also examined the human body as a developmental system in which human growth is a part of development through engagement with the social world (Ingold 1998; Sofaer 2006).

The study of plasticity in anthropology was historically proposed by Boas (1912), with some earlier migrant studies noting generational changes in growth (Baxter 1875; Bowditch 1879). Boas (1912) examined body size and shape in children of new American immigrants of European decent, a study which became a pivotal point in demonstrating how environmental changes could impact changes in body size and shape for future generations (Agarwal 2016). Boas' work was later supported by Shapiro's (1939) growth study of Japanese children in Japan and Hawaii. It was noted that changes in growth, stature, and development were correlated to environmental triggers. This work inspired numerous migrant studies that have confirmed the correlation between changing environments and changes in growth and development (Baker *et al.* 1986; Bogin 1995; Bogin *et al.* 2002).

From the early 1980s, palaeopathological studies of childhood stress has been a leading field of study (Lewis 2011a: 6), with emphasis on postnatal plasticity on growth as a biological outcome of environmental and behavioural stress resulting in differences in human height or stature (Lewis 2011a). These manifestations are seen as slowing or stunted growth, which allows developing organisms to reroute nutrition to more urgent energetic areas, such as brain growth (Leonard & Robertson 1992; Bogin 1995). These impacts on growth are considered nonspecific as they can have multiple aetiologies including insults from malnutrition and infection (Saunders & Hoppa 1993; Blackwell *et al*. 2001).

Today, recent models have explored how early life factors in particular have been shown to increase the risk of a broad range of diseases (Ben-Schlomo & Kuh 2002) from as early as the foetal period. The Developmental Origins of Health and Disease (DOHaD) paradigm combines early life

environmental events in association with an individual's genetic predispositions to consider how this combination influences an individual's response to the environment and later disease risk (Robert *et al.* 2001; Agarwal 2016). The Barker hypothesis on early foetal, childhood environment, and later disease risk (Agarwal 2016; Barker *et al.* 1989), suggests that poor nutrition during pregnancy could alter foetal programming and change the course of the developing body's function or metabolism (Barker *et al*. 1989; Agarwal 2016). Gluckman and Hanson (2004) expanded this research by associating poor nutrition during pregnancy with a 'predictive adaptive response' (PAR) in the foetus. This means developmental pathways are developed to what is perceived as a better suited postnatal environment (Gluckman and Hanson 2004; Low *et al*. 2012; Agarwal 2016). These findings have also been called the *thrifty phenotype* model of human life history and it is argued that these predictive physiological responses from diseased or stressed individuals reflect a mismatch between foetal development and the actual postnatal environmental landscape (Hales & Barker 2001; Agarwal 2016). These developing pathways can lead to predictive responses such as increased fat storage or reduced insulin production but when nutrition is plentiful, postnatal mismatch can lead to diabetes (Halfon *et al*. 2014).

The role of plasticity is complex as it is a continuous process over the lifecycle. The skeletal manifestations of plasticity and developmental pathways however, has been intently studied by anthropologists and bioarchaeoloigsts for decades. Pathways resulting in differences in stature, stress, diet, and morphology are common themes in anthropological and bioarchaeological studies of growth and development which will be discussed below. These themes in developmental pathway will contribute to the bioarchaeological component of this thesis in Chapter 7.

2.1.2 Stature

Chapter 1 indicated that the most common way to analyse skeletal growth profiles is by plotting bone size (commonly femur length) against age (based on dental development) (Hoppa & Fitzgerald 1999: 3; Mays 1999: 291, 293). Dental development is preferred for determining age at death because eruption is less prone to external factors such as malnutrition and is a more reliable indicator of development (Wall 1991: 276-277). These growth trajectories are then compared to modern children which show secular "improvements" in growth over time as a result of improved living conditions (Bogin 1988: 45). Modern data is a useful guide to maximized growth to which archaeological trajectories can be compared. If the latter have slower growth trajectories than it is likely that the population experienced nutritional and/or environmental stress, resulting in stunted growth (Mays 1999: 293 Lewis 2002; Kemkes-Grottenthaler 2005; Mays *et al.* 2008).

Johnston (1962) carried out one of the first and most impactful archaeological studies of juvenile growth, comparing long bone lengths from 165 prehistoric Native American juveniles from Indian Knoll. The archaeological sample had similar growth curves to the modern Denver children from Maresh (1955). However, there were a few discrepancies in the estimated growth rates between the two samples. On average, the Indian Knoll juveniles had shorter long-bone dimensions than the modern children after two years of age. These differences are thought to be the outcome of different environmental conditions which influence growth trajectories after two years old (Pinhasi et al. 2005). Interestingly, adult populations in the Great Plains are among the tallest and heaviest of Northern Native Americans (Auerbach 2008: 105), which suggests that multiple factors take part in growth outcome, such as improving environmental conditions after early childhood or a genetic predisposition to greater growth in body size (Ruff *et al.* 2013). These studies show that genetics are more important later in childhood, while environment tends to influence younger children (Auerbach 2008: 80).

The influence of the environment in younger children was supported by Frelat and Mitteroecker (2011) who used a multivariate approach to study the ontogeny of the femur and tibia from two populations. A cross-sectional sample of modern South African (N=97) and European (N=81) juveniles was recorded, ranging from infants to 20 year olds. Ontogenetic trajectories found that both the tibia and femur had similar lengths and shapes in both samples until 10 years old. During adolescence, Africans had a higher growth rate which led to longer adult bones and narrower epiphyses relative to the diaphysis. The crural index ratio (a measurement to identify population differences) uses length of the tibiae relative to length of the femora (Davenport 1933) and was found to be higher in Africans than Europeans from birth throughout childhood. This study is important as it attempted to tease apart the role of genetics on limb length proportion (Frelat & Mitteroecker 2011) and showed that genetic potential is indeed mediated by environmental factors.

The main problem with comparing modern growth studies to archaeological datasets is that the first typically records the fused epiphysis while in archaeology usually only the shaft (diaphysis) is preserved and recorded. Powers (1980) attempted to resolve this difficulty by publishing growth data from known age at death juveniles of Post-Medieval assemblages. However, the problem with this study is that the archaeological samples are multi-period with cemeteries spanning over 500 years; this obscures any secular trends in the population means. Another issue when looking at stature is that limb length proportions change dramatically during growth (McCammon 1970; Eveleth & Tanner 1990) and vary between populations (Eveleth & Tanner 1990). These variations

make it difficult to compare between groups as the juveniles may reflect different stages of biological development at different chronological ages.

Although stature estimates have their limitations, they do provide more comparisons to modern studies as stature lengths are the most commonly used method of assessing growth in medical studies (Ruff *et al*. 2013). Mays (1999) used femur-to-stature ratio data on juveniles from Medieval Wharram Percy and found that juveniles with dental ages of 14 years old had the same femoral length as Maresh's (1955) mid-20th century 10 year olds. Bone lengths were converted to estimated stature for Wharram Percy children, which then allowed them to be compared with modern British children and data from an 1833 study of children from work factories (Mays 1999). This study demonstrates that the Wharram Percy juveniles had shorter statures than the modern and 19th century children, suggesting that those from a rural mediaeval community were 'worse off' than children from the Industrial Revolution. These results may imply that secular trends for increasing stature in children started before the first child height surveys in the early 19th century (Tanner 1981; Mays 1999).

2.1.3 Stress Lesions and Developmental Trajectories

Similar to stunting or slowing in growth of the long bones, these indicators of stress reflect a physiological disruption to growth (Larsen 2015). As mentioned above, populations show reduced stature as evidence of greater systemic stress (Bogin 1995; Saunders 2000; Stinson 2000), and as such, bioarchaeologists use stature as an indicator of overall health and stress during growth (Saunders & Hoppa 1993: Hoppa & FitzGerald 2005). Earlier bioarchaeological studies focused on physiological stress responses with a focus on stress as an adaptive response (Temple & Goodman 2014). Several early classic and recent bioarchaeological investigations have noted that early mortality is associated with small stature as well as stress indicators such as linear enamel hypoplasia (Buikstra & Cook 1980; Goodman *et al*. 1980; Duray 1996; Humphrey & King 2000; DeWitte & Wood 2008). Older studies, which will be discussed below, also examined stress in relation to growth arrest such as enamel hypoplasia, cribra orbitalia and porotic hyperostosis, periostitis, rickets, and Harris lines. Recent studies have focused on investigating several of these stress indicators together, or in relation to, dental defects and/or reduced stature (Turner & Armelagos 2012; Watts 2013; Geber 2014; Scott & Hoppa 2015).

Clinical studies have found that there is a strong relationship between childhood infection, malnutrition, and enamel hypoplasia, which makes this lesion a good indicator for studies on socioeconomic conditions and health in archaeological populations (Hillson 2003). Several studies on both American and European groups show that the peak appearance of these defects is two to

four years old; this is around the weaning age for most societies (Lewis & Roberts 1997). This suggests that stress caused by changes in the quality and quantity of food supply can emerge in the formation of hypoplasia (Lewis & Roberts 1997).

Studies on urbanization and decline in human health have also focused on enamel hypoplasia (Lewis 2002). Growth and stress indicators in juvenile skeletons were compared between four English cemetery sites: one early Medieval (Raunds Furnells, Northamptonshire), two late Medieval (Wharram Percy and St Helen-on-the-walls, Yorkshire) and one Post-Medieval (Christchurch Spitalfields, London). Peaks in mortality between the ages of six to ten years were found for Wharram Percy and St Helen-on-the-walls and suggest that the presence of enamel hypoplasia resulted in higher mortality (Lewis 2002). By contrast, Bennike and colleagues (2005) found that juveniles with enamel hypoplasia lived longer than those without. It is possible that both conclusions result from enamel hypoplasia occurring in permanent rather than deciduous teeth, therefore, studies analysing juveniles with enamel hypoplasia will tend to be seven or older as these lesions occur in adult dentition.

Problems with this hypothesis of enamel hypoplasia occurring in juveniles older than seven, include the age estimates of the defects (Lewis & Roberts 1997). Goodman and colleagues (1980) used crown development based on data from Swärdstedt (1966) and Massler and colleagues (1941) to create a table of mean ages for crown development. This method is now used for assessing the age at formation of the hypoplasia line(s), however it assumes that the tooth development rates in ancient juveniles are similar to today's modern and healthy populations. This method also does not account for interpopulation or individual variation in tooth size and its impact on age estimate for the hypoplasia (Lewis & Roberts 1997). It should be noted however, that there are differences in the gross defects of enamel hypoplasia that occur at different regions of the crown and have differing visibilities. Thus, the variation in location and clarity of enamel hypoplasia influences the age at formation based on the gross examination of the remains (Lewis & Roberts 1997).

Another commonly studied stress lesions in bioarchaeological studies are cribra orbitalia and porotic hyperostosis. The latter causes a thinning and porous destruction to the outer compact bone of the cranium and thickening of the diploe-spongy layer separating the inner and outer cranial bones (Stuart-Macadam 1992). Cribra orbitalia causes porosity in the orbits of the skull and both are commonly a result of dietary deficiency (Lewis 2007: 111). One of the main issues with these studies is the mixing of terminology (Lewis & Roberts 1997: 583) as some do not make a clear distinction between the two and refer to both terms as porotic hyperostosis (Grauer 1993).

Recent work has found that there is a range of potential aetiologies linked to cribra orbitalia and porotic hyperostosis (Watts 2013; Scott & Hoppa 2015; Agarwal 2016). In some cases, iron deficiency anaemia can be a possible cause. This was studied by Mensforth and colleagues (1978) with an archaeological sample from Libben Ohio. Clinical observations have shown that low birth weight and iron deficiency anaemia can occur as early as three months (Lundström *et al.* 1977) while in normal birth weight children, iron deficiency anaemia does not occur until after 6 months of age (Saarinen 1978). Study of the Ohio skeletal collection showed that older children were more affected after 6 months, so it is likely that this event was linked to the weaning process. The transition from breast milk to cereal grains can cause gastrointestinal infections and result in a lack of nutrition, thereby leading to anaemia deficiencies (Mensforth *et al.* 1978: 14).

Bacterial infections are another possible cause of anaemia (Lewis 2007: 113). Iron is needed for bacteria to thrive, however, when under attack, the body will withhold iron until the infection subsides (Lewis 2007: 113). A mild deficiency is therefore, not a negative condition as it is one of the body's defensive mechanisms against disease (Stuart-Macadam 1992). Goodman and Armelagos (1989) found that porotic hyperostosis is most common in juveniles from two to six years old and in young adult females. Stuart-Macadam (1985) interpreted the lesions in adults as residual lesions from anaemic periods during childhood. It is possible however, that the higher prevalence in children is from bone marrow physiology in development rather than actual differences in the prevalence of anaemia between adults and children (Stuart-Macadam 1999).

Another frequent stress lesion is periostitis which is the most common form of non-specific infections found on both adult and juvenile remains (Lewis 2007: 135). Periosteal bone formation occurs as a new layer of bone under the periosteum as a result of inflammation of this area from infection or trauma (Grauer 1993). These skeletal lesions are seen as active woven bone which has a disorganised and porous appearance or healing/healed lamellar bone which is smoother with a more organised bone structure. If a mixture of these two types of bone formation are present, it is suggested that the individual suffered a chronic and active infection (Lewis 2007: 135). Non-specific infections are commonly associated with malnutrition, where malnourished individuals are more susceptible to disease and infection negatively impacts the nutritional status of the individual (Lewis 2007: 100).

Rickets provides more information on past population health compared to the previously discussed pathologies as it is more easily identifiable, but is not as commonly studied (Mays 2013). Rickets occurs when there is inadequate absorption of calcium and low levels of vitamin D which result in structurally weak bones that are unable to withstand the mechanical stresses that are placed on them (Mays 2013: 11). Interestingly, rickets was found in infants from the rural settlement of

Wharram Percy and may be a result of already sickly children who were kept inside and lacked the needed sunlight and vitamin D (Ortner & Mays 1998). Rickets was also identified by Lewis (2010) at the Romano-British site of Poundbury. She suggested that swaddling of infants may have been a factor as neither site had high rates of rickets in older children. Historical literature and bioarchaeological evidence suggest that rickets became more common in Britain during the Industrial Revolution as a result of air pollution (Mays 2003). Nineteenth century remains from St Martin's Churchyard from Birmingham showed that the prevalence of rickets was 8% higher than English Medieval remains (Mays *et al.* 2006). The Medieval remains buried in the cemetery also had evidence of healed cases in older children and adults, thereby suggesting that it affected children who already had poor health (Mays 2013).

These studies on health and stress have revealed how growth can deviate in archaeological communities. Recent studies however, have shifted the focus on developmental plasticity to emphasize the potential for different severities of stress on the adult skeletal morphology, mortality, and potential recovery (Agarwal 2016). The incorporation of multiple skeletal indicators enables the study of stress from longitudinally different points along the life cycle. For instance, early developmental stress indicators such as linear enamel hypoplasia on the anterior tooth crowns can reflect development between one and six years of age. Cribra orbitalia however, is found on the frontal bones and is thought to develop before four years of age. Lastly, differences in long bone lengths reflect growth in utero up to late adolescence and early adulthood (Watts 2013; Agarwal 2016). This layered approach was utilized by Watts (2013) in the examination of multiple indicators of stress in an archaeological sample from St. Peters Church, Barton-upon-Humber. This study investigated the impact of environmental and economic change during childhood development from two cemetery phases before and after AD1700, when generally better living conditions occurred (Agarwal 2016). It was found that some stress indicators, for instance vertebral neural canal (VNC) size, showed a positive impact of improved living conditions after AD1700 in childhood health between 5 and 14 years of age (as seen by increased neural canal diameters). Other stress indicators however, such as linear enamel hypoplasia and cribra orbitalia affected dental and skeletal development roughly before 6 years of age and did not show any differences between cemetery phases, indicating that stress was present at these earlier developmental ages (Wats 2013). Watts (2013) investigation of stress indicators by adult age mortality found that individuals who experienced early life stress such as cribra orbitalia no longer experienced reduced adult lifespans after AD1700, which suggests improved living conditions no longer impacted long term health and mortality (Watts 2013; Agarwal 2016).

The inclusion of multiple indicators of stress to investigate changes in development has contributed to more subtle ways of interpreting phenotypic variation in stature by focusing on stunting, trajectories, and tempo of catch-up growth as seen through Harris lines- lesions formed during stressful metabolic periods in developing bones- have been studied since the early 1930s (Harris *et al.* 1933). Once normal nourishment is resumed after a period of stress, a dense layer of bone, a Harris line, is formed. This line may be seen into adulthood through radiographs (Mays 1995). These lines are defined as stress indicators as they only appear after a recovery from stunted growth. Growth is often referred to as 'target-seeking' and once the child's health has been restored it has the ability to 'catch up' with its peers and growth resumes at an increased rate of up to three times its normal velocity (Tanner 1981). The specific mechanisms behind the 'catch-up' period are not fully understood, however if the stress state lasts too long (especially near puberty), growth cannot return to optimal levels (Geber 2014, Scott & Hoppa 2015). There are some difficulties with interpreting Harris lines as they vary based on the rate of stress (Mays 1995). Children with Harris lines from Wharram Percy had deficient bone length and cortical bone (Mays *et al*. 2007: 101) which implies insufficient resources were available for the individual to catch-up in either longitudinal or appositional growth after the events that led to the Harris lines. On the other hand, Poundbury, a Romano-British town in Dorchester demonstrated the opposite (Mays 1985). Juveniles who did not show deficient appositional or longitudinal growth did have Harris lines which suggests that they received enough nutritional resources to resume growth (Mays 1985). These studies show how the severity of stress impacts bone growth differently. The individuals from Wharram Percy most likely experienced poorer and more chronic health conditions as they were a lower social status community with harsher environmental impacts than Roman Dorchester (Mays *et al.* 2007: 101-102).

Interestingly, catch-up growth can also occur if the growth rate stays the same but individuals grow for a longer period of time in order to achieve normal adult potential (Bogin 1995; Cameron & Demerath 2002; Stinson 2012; Agarwal 2016). Temple (2008) discussed catch-up growth in his comparative study of stress indicators and phenotypic variation in prehistoric Japan. The comparison of dental defects and stature between Jomon foragers from eastern and western Japan found the latter region experienced environmental stressors. Although foragers from eastern Japan showed a higher frequency of enamel hypoplasia, there was no difference in stature between the two regions. Temple (2008) argues early childhood stress results in indicators such as enamel defects that could represent an episodic event that may not affect long-term phenotypic variation in stature. Stature was found to decrease temporally between the middle, late, and final Jomon phases which reflects chronic bouts of systemic stress such as infection and dietary stress (Temple 2008).

Incorporating skeletal evidence of stress and overall health of juvenile remains into studies of juvenile growth has vastly improved our understanding of the delicate synchronicity of growth and environment. However, one of the main difficulties with paleopathology is the unknown aetiology of the many stress related diseases. There is nonetheless a vast amount of literature in both clinical and bioarchaeological studies that have found important trends in different stresses. For instance, the 'catch up' period in Harris lines can infer periods of stress and whether proper nutrition are restored to that population (Mays 2013). Different ages of cribra orbitalia potentially shed light on weaning diarrhoea versus parasitic infections found in older juveniles (Mays 2013).

2.1.4 Diet and Developmental Trajectories

As seen in the previous section, stress and lack of proper nutrients can lead to stunting of skeletal growth and a variety of skeletal lesions. During the early 2000s, researchers began investigating aspects of diet, nutrition, and weaning practices through the use of stable isotope analysis (Katzenberg *et al*. 1996, Lewis 2011a: 6). Stable isotope analysis has been ideal for assessing diet and weaning through carbon and nitrogen isotopes (Mays 2013; Jay 2013) and studies on diet and paleomobility have taken a life course approach (Agarwal 2016: 135). Although trace elements and stable isotopic analyses have become common methods for reconstructing diet in past humans, recent studies have used isotope signatures from different skeletal elements and teeth to reconstruct diet changes over the life course (Agarwal 2016: 135).

The ratios of the carbon and nitrogen stable isotopes vary between food types as unique signatures are left in the tissues of the individual (Mays 2013: 5). Carbon stable isotope δ13C ratios vary in plants as they undergo different photosynthetic pathways to produce carbohydrates. The C3 pathway is more commonly found in temperate vegetation zones while plants from warmer regions (e.g. maize) use a C4 pathway, although this is not a common food type in pre-modern north-west Europe. Additionally, carbon and nitrogen stable isotope ratios differ between marine versus terrestrial foods (Mays 2013: 5).

Nitrogen isotope ratios are fundamental when investigating trophic levels as they show more significant franctionation between trophic levels compared to carbon (Waters-Rist & Katzenberg 2010). Once there is an equilibrium with a new diet after food conditions change (e.g. weaning), fractionation represents the difference in stable isotope ratios between the diet and the tissue of the consumer. Typically, δ15N fraction reflects differences of +3-4% from dietary protein to the consumer's whole body tissues (Waters-Rist & Katzenberg 2010). By using species or tissue-specific

fractionation differences can improve the accuracy of predicting trophic levels or stable isotopic signatures of organisms from known isotopic data (Waters-Rist & Katzenberg 2010).

Nitrogen isotope ratios, δ15N, from bone collagen in infants, can be used to identify the weaning processes in past populations as infants have higher trophic levels than adults. Breastfeeding infants are exclusively consuming a product of their mother's body and are one trophic level higher. These values decrease to adult signatures once other foods are introduced to the infant during weaning (Mays 2013), which makes this a useful technique to study the duration of breastfeeding in past societies (Jay 2013; Waters-Rist & Katzenberg 2010).

In most modern cases, δ15N in children who have been weaned show similar values to adults; however, several studies in archaeological populations from around the world found that children have slightly lower δ15N signatures than adults (Richards *et a*l. 2002; Katzenberg *et al*. 1996; Nitsch *et al.* 2011; Turner *et al*. 2007). This was seen at Wharram Percy and it has been suggested that the depression of nitrogen values in childhood and adolescence may reflect physiological factors connected with growth (Schurr 1997). Some researchers state that the effects of growth on bone collagen δ15N is small (Waters-Rist & Katzenberg 2010), but likely to be the result of dietary changes as lower δ15N suggests the consumption of lower proportions of meat or marine resources compared with adults (Mays 2013).

There are some difficulties with the interpretation of isotopic data as the rate of collagen turnover in young individuals has not been studied in detail (Mays 2013). Additionally, time lags appear between changes in dietary intake and its reflection in the stable isotope ratios which can leave a grey area of breastfeeding duration (Mays 2013). One possible solution proposed by Nitsch and colleges (2011), showed that infants of known age at death had elevated δ15N at five to six weeks old as found in the infant rib bone collagen. The rapidity of the change in δ15N in collagen reflects the decline in breastfeeding as older infants are weaned onto solid foods and therefore, creates a time lag in infants which reflects the decline in bone turnover rates (Frost 1969) and growth (Tanner 1978) with age (Mays 2013). The relationship between weaning and growth was studied at Wharram Percy and found that growth in long bone lengths was similar to modern infants until 18 months old (Mays 2007). However, once breastfeeding ended (as indicated by the nitrogen isotope data) the effects of breast milk were gone and growth trajectories stunted (Mays 2007).

A more recent approach to avoiding these 'lag' periods is to use dental hard tissues instead of rib collagen because they do not turn over and instead preserve the isotopic signals from tissues formed during childhood (Mays 2013). This process can be used to study breastfeeding in older individuals who did survive to adulthood and analyse regions of their teeth that formed at different times during childhood (Mays 2013). This approach was applied to Wharram Percy where teeth of

adults and juveniles who survived the weaning period were subjected to analysis. The δ15N were consistent with isotopic analysis from ribs at Wharram Percy (Mays 2013), which suggests that breastfeeding continued for 1 to 2 years post-partum. Interestingly, by combining the isotopic data with the skeletal lesions from juveniles at Wharram Percy, it was found that the formation of enamel hypoplasia peaked at 1.5 years but child mortality, cribra orbitalia and non-specific infections peaked much later on. This study found that weaning was successful in maintaining a healthy child (Lewis 2002: 2011a) but the children became sickly during the post-weaning period.

Isotopic work on the diet of children has also become more abundant in the last few years (Mays 2013: 9). Redfern *et al*. (2012) studied diet in Late Iron Age and Romano-British juveniles from southern England and it appears that there were more marine resources used by the Iron Age population. Reitsema and Vercellotti (2012) also used stable isotopes in bone and dentine to look at diet variation with age, sex, and social status in Medieval Italy. Females and high status males showed a childhood diet that was similar to adults for both δ15N and δ13C. The δ13C suggested however, that lower status males consumed more millet as adults than as children. Historical evidence supports these findings, as millet was less desirable so children and females had preferential access to more valued foods (Mays 2013:9). It is also possible that the adult male labourers may have had access to a much less varied diet as their work was often further from the kitchens. Isotopic analysis has also found interesting results with changes in subsistence practices. Beaumont *et al*. (2013) found that C4 food consumption, from isotopic analysis of bone collagen in some of the juveniles from Kilkenny Workhouse cemetery, was associated with the Great Famine in Ireland in the mid-nineteenth century. Documentary evidence showed that imported maize-based foods were used for famine relief and are likely responsible for the C4 signal in the juveniles δ13C (Mays 2013: 9).

Other studies have shown gradual introduction to weaning foods (Schurr 1997: 1998). The ability to measure an increase or decrease of nitrogen values in infants shows the potential for indicating children who may have died at certain points in the weaning process (Waters-Rist 2010). Isotopic studies have helped provide further explanations of pathological stress lesions by determining the time of weaning as well as diet intake. There are many complex interactions with the environment, diet, and overall stress and by combining these approaches bioarchaeologists are able to determine the extent of stress in past populations. Improvements in ageing methods, microscopic imaging of enamel defects, and refinement of diagnostic criteria for skeletal lesions (Ortner & Mays 1998; Ortner *et al*.1999) have shown that the interaction of childhood nutrition, infection, mortality, and

environmental changes in past societies is more complicated than previously thought (Lewis 2011a: 6).

The introduction of isotope analysis to determine weaning and diet in skeletal populations has greatly added to juvenile studies. Studies of isotopic signals in the past that use both dental and skeletal tissues are interesting avenues for life course research, especially in combination with other stress indicators or measure of bone morphology (Agarwal 2016: 237). Strontium and stable oxygen isotopes can be used for studies regarding paleomobility and, in addition to other isotopic analyses, build a life history of diet and childhood residence (Chenery *et al.* 2010; Agarwal 2016: 137). The incorporation of the carbon and nitrogen signatures with historical sources provides a more detailed picture of not just the dietary intake of juveniles but the cultural and environmental constructs around them. These historical and dietary studies will be used to interpret the developmental trajectories for the study sites in Chapter 7.

2.1.5 Canilization Continuum and the Effects on Growth and Plasticity

As discussed above, the relationship between the environment and phenotypic plasticity has been a key concept within biological anthropology and bioarchaeology (Roberts 2012). Through the movement of the human genome project, it has been found that "Genes aren't what they used to be…" (Fortun 2009: 255). This has led to more focus on the 'epigenome,' which is known as gene expression rather than changes to the genetic code (Gowland 2015). This term was coined by Waddington (1942) in his article 'The Epigenotype' which describes the relationship between the environment and genotype and the production of phenotypic plasticity (Gowland 2015).

Today, studies on the epigenome examine morphological variation by comparing canalized verses plastic traits (Stock 2012:5). Canalized traits are developmentally stable and show minimal variation in different environmental conditions. These traits include brain size and dental morphology as they are closer to genetic regulated traits during development rather than influenced by environmental changes (Stock 2012:5). Plastic traits are more susceptible to environmental conditions and are notably flexible in variation during early life. This flexibility allows for modification of the phenotype during the lifespan and allows for more rapid adaptation than is possible through intergenerational genetic change (Stock 2012:5).

Stature is the most commonly used trait when investigating variables that influence phenotypic variation. More specifically, twin studies are often used and have found that there is between 60-90% heritability in height (Stock 2012:5). These findings suggest that there is an underling genetic mechanism for stature and any proportion of variation that is not attributed to shared genes (by heritability estimates) is assumed to be environmental variation. It has been found that stature is

associated with 180 specific genes, each contributing a very small effect (Allen et al. 2010; Lanktree et al. 2011). Until recently, these genes were believed to account for as little as 5% of the variation in adult stature (Lettre et al. 2008; Weedon et al. 2008). Yang and colleagues (2010) however, found that approximately 40% of variation may be controlled deeper within the genome (Stock 2012). It is also possible that heritability estimates from the twin studies have an artificially inflated result as twins experience a common foetal environment. During development twins will experience similarities in genetic regulation in response to similar environmental conditions, or epigenetic effects and other intergenerational mechanisms (Wells & Stock 2011). These varying issues suggest that the human phenotype is a continuum between plasticity and genetic canalization and some environmental effects may artificially inflate heritability estimates (Stock 2012).

A number of mechanisms have been proposed for the maintenance of genetic variation in traits under selection, many of which apply to growth rate. In general, interactions between the genotype and its environment may act to maintain genetic variation within populations (Dmitriew 2011). Wells and Stock (2007) suggest that a biological emphasis on mechanisms of plasticity is crucial for adapting to differing environments. It was found that there are levels of plasticity which can be seen as intermediate biological mechanisms to buffer the genome from the necessity to commit to adaptation or a selective response to environmental stress. Additionally, there are several mechanisms of physiology and biology which can be manipulated through changes in life history (Stock 2012). For instance changes in body size, physique, energy stores, variation in developmental trajectories, and metabolic plasticity.

Genetically based differences in growth rates have been observed in populations along latitudinal clines (Dmitriew 2011) and it is suggested that growth rates increase with latitude. At low latitudes where season length is longer, slower growth appears to be selected. The prevalence of submaximal growth within populations and the tendency for slower growth to predominate in certain populations suggests that costs of growth may be considerable (Dmitriew 2011). These mechanisms are necessary for modifying the phenotype to fit local environmental conditions without taking a greater risk to genetic adaptation (Stock 2012). In this context, genetic adaptation would commit an individual or population to phenotypic characteristics that are slow to respond to the future environmental variation. Plastic mechanisms can also allow adaptation of the phenotype within the lifespan and specifically during development (Stock 2012).

As seen in previous sections, secular trends are the most common comparisons across generations. The phenotypic effects are not restricted to a single generation and rather, are found in subsequent generations (Wells & Stock 2011). This transgenerational phenotypic covariance is not through

direct transmission of DNA but is known to biomedical researchers as 'intergenerational effects' (Emanuel 1986). The inheritance of the effects of adverse environmental or social conditions from grandparents to grandchildren has been established within the framework of DOHaD and epigenetic inheritance (Gluckman et al. 2011; Barker 2012; Gowland 2015). For instance, longitudinal studies of the Dutch famine victims showed that three generations were directly affected by the famine, the expectant mother, offspring, and her grandchildren (Barker 2012). As a result, an individual's phenotype will be the outcome of a lifelong remodelling of the epigenome due to complex interactions between the genotype and the ancestral and current environments (Hochberg et al. 2011: 194; Gowland 2015). The importance of intergenerational inheritance is unique within the life course history framework and suggests that an individual's physical and social world in early life can shape not only their own biological processes during their lifetime, but also those of their children and grandchildren (Thayer & Kuzawa 2011; Rando 2012).

The significance of intergenerational inheritance to bioarchaeological studies relates to the interpretations of growth trajectories which extends to biocultural circumstances occurring prior to conception. In addition to offspring being influenced by their parents environment (in which the offspring never experienced) (Rando 2012: 703), food availability for parents are linked to offspring for generations through epigenetic mechanisms (Kaati et al. 2002). Therefore, poor health may arise as a consequence of the accumulation of chronic conditions across generations rather than a single life course event (Davey Smith 2011). The interpretations of health from past skeletal remains can be seen as 'linked lives' as well as a continuous biography of past generations (Gowland 2015). This idea is important when interpreting pathological lesions of stunted growth from the bioarchaeological record, where the tendency is to consider the immediate life history event (Gowland 2015). The difficulty however, of investigating plasticity in life-history traits is that they are not confined to genetic or environmental factors. Instead, these the two sources of variability are intertwined and result in a continuum of genetic canazliation and levels of plasticity that can be seen throughout the life course (Wells & Stock 2011).

2.2 Long Bone Morphology

As mentioned above, studies on bone development and plasticity have focused mainly on growth, stress and diet. However, studies investigating long bone strength through cross-sectional geometries is a widely used method to understand behaviour, specifically changes in mobility from past populations (Agarwal 2016). Studies on bone strength examine the formation and maintenance of long bone shape and size over time, with interest in understanding bone growth and remodelling over the life course (Agarwal 2016). For instance, it has been shown that bone shape is a better indicator for changes in mobility than bone size (Ruff & Larsen 2014). Additionally,

shape and rigidity in the lower limb relate to ontogenetic changes in loading during the different phases of learning to walk and maturing gait patterns (Wescott 2006; Cowgill *et al.* 2010). There have only been a few studies on the variation and trajectory of robusticity and strength in juveniles (Ruff *et al.* 1994; Wescott 2006; Cowgill *et al.* 2010), and a continued understanding of the relationship between bone size and shape over the life course is therefore needed (Agarwal 2016). The remaining chapter will explore how function in terms of biomechanics, bone remodelling, the musculoskeletal system, Wolff's law, and activity levels impact an individual's life course history and developmental pathways.

2.2.1 Biomechanics and Bone Remodelling

Traditional studies on human bipedalism focus on the proximal and distal epiphyseal morphologies of the femur (Richmond & Jungers 2008; De Groote *et al.* 2010; De Groote 2008; 2011). Morphology of the diaphysis has seen less detailed attention, primarily because of the difficulty of obtaining three dimensional morphometric measurements as most studies use length, diameter, and cross-sectional properties (Ruff 2007; Young *et al.* 2010).The process of long bone growth occurs as new bone is deposited at the diaphyseal growth plates and subperiosteal surfaces (Scheuer 2000; Serrat et al. 2007). The variability in growth results in variation from external or the subperiosteal surface and cortical bone thickness. This relationship is correlated with musculoskeletal topography (Lovejoy *et al*. 2003; Morimoto *et al.* 2011) and cross-sectional biomechanical properties (Ruff 2003).

As bone is constantly changing in response to external variables of stress and diet, it is important to explore the functional and biomechanical nature of bone. The current research covers the period of crawling to walking, thus it is useful to understand how this transition affects developmental plasticity and shape of the long bones. Ontogenetic development of bone shapes relies on normal muscle activity and weight bearing behaviour (Lanyon 1980) which is not always influenced by individual variation in body weight. Locomotor modes change during ontogeny from limited mobility of crawling (quadrupedal) which occurs around 9 months old, to supported walking (bipedal) by 12 months, and independent walking by 18 months (Morimoto *et al.* 2011). It has been found that the onset of bipedal locomotion is associated with increased mechanical loadings while there is an increase in rigidity of the lower limbs (Ruff *et al*. 1994; Sumner & Andriacchi 1996; Ruff 2003; Morimoto *et al*. 2011). Immature long bones are wider with more anterior-posterior and medial-lateral expansion relative to length compared to mature individuals (Young *et al*. 2010; Morimoto *et al*. 2011). These shapes are thought to prevent potential risks of injury during

locomotion when the musculo-skeletal structures are not fully developed (Carrier 1996; Young *et al*. 2010; Morimoto *et al*. 2011). The results presented in this thesis incorporate visual components of shape change, therefore, it is important to consider the musculoskeletal system and remodelling process of bone and its possible effects on shape.

2.2.1.1 Musculoskeletal System: Lower Limb

Movement of the lower limbs occurs with the majority of leg muscles contracted and then relaxed (Morimoto *et al.* 2011). The functional demands placed on the lower limbs vary during the development of crawling to walking. For instance, in order to propel the body forwards, muscle forces extend from the hip to knee. Table 2.1 and Figure 2.1 summarizes the main muscle groups of the lower limb used for walking.

The hamstrings are found at the back of the thigh and allow movement in the hip and knee (De Groote *et al*. 2010; De Groote 2008; 2011). The hamstrings extend the hip but do not create significant bending in the bone as it is loaded in axial compression (Frost 1969). The short head of the biceps femoris creates a posterior bending force to the femur. The gluteus maximus and two gastrocenemii apply a bending stress to femur so that it bends convexly in the posterior direction (Frost 1969; Duda *et al*. 1997; Trinkaus *et al.* 1999; Hall 2004).

The quadriceps are the strongest and leanest muscles in the leg and are the major extensors used to extend and straiten the knee (De Groote *et al*. 2010; De Groote 2011). These muscles exert stress to the femoral shaft in the opposite direction of the other muscle groups (Carter & Beaupre 2001: 193). The shaft must create a balance of muscle forces to minimise bending stress, resulting in an anteriorly convex shape (Frost 1969). The calf muscles are essential for movement in the ankle, foot, and toes. Lastly, the Achilles tendon is one of the most important tendons for mobility (found at the back of the calf and ankle) as it stores an elastic energy that is needed for running, jumping and other physical activity (Carter & Beaupre 2001: 193).

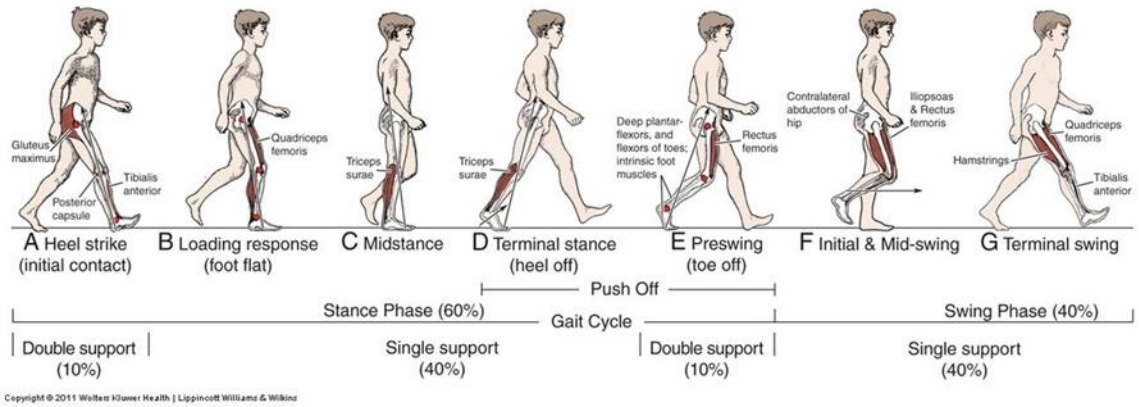

Figure 2.1 Gait cycle (Physiopedia: Wolters Kluwer Health, Lippincott Williams and Wilkins, 2011).

Quadriceps	
Vastus lateralis	Outside of the thigh and is the largest of the quadriceps. It extends from the top of the femur to the kneecap or patella.
Vastus medialis	A teardrop-shaped muscle of the inner thigh and attaches along the femur and down to the inner border of the kneecap.
Vastus intermedius	Between the vastus medialis and the vastus lateralis at the front of the femur, it is the deepest of the quadriceps.
Rectus femoris	This muscles attaches to the kneecap and has the least effect on knee flexion.
Hamstrings	
Biceps femoris	Long muscle that flexes the knee. It begins in the thigh area and extends to the head of the fibula near the knee.
Semimembranousus	This long muscle extends from the pelvis to the tibia along the thigh which flexes the knee and rotates the tibia.
Semitendinosus	This muscle also extends the thigh flexes the knee.
Calf	
Gastrocnemius	One of the largest muscles of the leg, it connects to the hell. It also flexes and extends the foot, ankle, and knee.
Soleus	This muscle is found form the back of the knee to the hell and is important in walking and standing.

Table 2.1: Muscle groups for bipedal locomotion (Carter & Beaupre 201: 194).

2.2.1.2 Musculoskeletal System: Upper Limb

The shoulder joint is surrounded by three ligaments, which is where most of the stability and muscle power occur in the rotator cuff (De Groote *et al.* 2010; De Groote 2011). The rotator cuff is made of four muscles, supraspintus, infraspinatus, subcapularis, and teres minor (Figure 2.2). Each muscle has its origin on the scapula and inserts in the humeral head. The tendons of these muscles surround the support of the humerus while the contraction of muscles rotates, adducts, or abducts the humerus.

The elbow joint is a leaver made up of the huemero-ulnar (flexion and extension), humero-radial (flexion, extension, supination, and pronation), and proximal radio-ulnar (pronation and supination) joints (Frost 1969; Hall 2004). The large number of muscles that create a range of motion in the elbow is complicated. The elbow is not a weight-bearing bone but it does receive large loads during activity. The elbow experiences most of the compressive loadings which are generated when the hands are rotated in pronation.

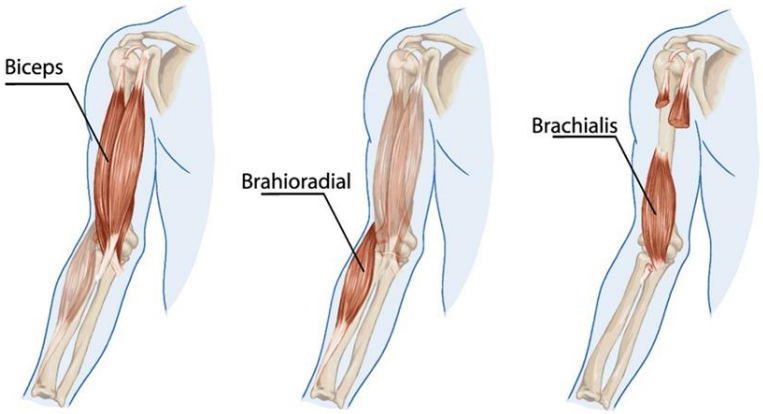

Figure 2.2: Upper limb anatomy (Human Anatomy Library: 2017).

2.2.1.3 Wolff's Law

In addition to changes in the musculoskeletal systems of the limbs, changes in bone remodelling occur during the life course. According to Wolff's Law, bones grow and remodel throughout an individual's life in order to adapt to their mechanical environment (Pearson & Lieberman 2004; Ruff *et al.* 2006). There have been several studies investigating the absence of loading from muscle activity and weight-bearing during ontogeny as long bones fail to develop their appropriate bone mass or longitudinal curvature, despite reaching a normal length (Lanon 1980). Lieberman and Pearson (2001) tested cortical bone growth (known as modelling) and repair in response to exercise-induced mechanical loading and found remodelling varied with loading and position in the skeleton. Ruff and colleagues (2006) suggest that the rates of remodelling and rates of bone turnover vary at different sites of the skeleton (Lieberman & Pearson 2001; Ruff *et al*. 2006).

The relationship between forces, modelling, and remodelling of long bones is complex (De Groote *et al*. 2010; De Groote 2011). By considering the long bone as a slender beam, it is assumed that the optimal function is to resist the applied stresses and minimise strain through axial compression (Frost 1969; Bertram & Biewener 1988; Hall 2004). Through this loading regime, most material is distributed to the plane of deformation and cortical bone becomes stronger under compression than tension (Frost 1969; Bertram & Biewener 1988; Hall 2004).

The femur articulates with muscle attachments such as the medial displacement of the femoral head (Trinkaus 1993; Anderson & Trinkaus 1998) and the contraction of the adductor and gluteal abductor muscles cause the femur to undergo mediolateral bending (Ruff 1999). Ruff (2000) has suggested that the anteroposterior bending may be the cause of an anteroposterior expansion of the femoral midshaft as a response to high activity and mobility levels (Ruff 2000). Taylor and colleagues (1996) tested one-legged stance and found the femur to be loaded through compression

rather than torsion or bending (Taylor *et al*. 1996). It was also found that the anterior and posterior stresses of the femur may be a reduction of overall bending stress as a result of muscle forces. If a bone is loaded in bending, this would increase the biological cost of bone production as it would need to resist these stresses and become more robust (Tayler *et al.* 1996).

Duda *et al.* (1996) found differences in muscle attachments as a result of different biomechanical properties from different individuals. Thus, not only do bones remodel as a result of different stresses but so do the muscles and tendons. The intricate nature of muscles or parts of muscle contractions and joint reaction forces during gait make it difficult to fully understand the strains on the lower limbs, especially as there is evidence for the variation in the femoral muscles which would affect the muscle forces applied to the femur (Duda *et al.* 1997). Experimental studies have found that the curvature of long bones increases during bending strains and the direction of that curve does not necessarily correspond with tension surface of a bone when loaded (Lanyon & Bourn 1979; Swartz 1990). Weight-bearing bones displaying longitudinal curvature may be crucial as it reduces the ability to withstand high levels of loading and compromises between bone strength and predicting strains and material failure (Lanyon 1980; 1987). A curved bone is more likely to bend in the direction of its longitudinal curvature regardless of the orientation of the bending movement applied to the bone. Alexander (1981) noted that structures are likely to be subjected to unpredictable loads as a means to build a safety factor and maintain their biological structure, even if that safety factor is more metabolically costly (Alexander 1981).

Lanyon and Bourn (1979) found femoral bending may result in larger muscle packing and allow the position of more slender attachments to be closer to joints. Muscles that are adjacent to the bone exert pressure on the periosteum which leads to an increase in bone resorption leading to curvature. Reduction of loading then leads to a decrease in bone mass (Lanyon & Bourn 1979; Ruff *et al*. 1991; Carter *et al.* 2000; Lieberman *et al.* 2001; Pearson & Lieberman 2004; Ruff *et al*. 2006).

Recent studies have found that the periosteal surface is more sensitive to mechanical influences during growth and before adolescences, whereas the endosteal surface is more sensitive to mechanical influences after this period (Ruff *et al.* 1994; Gosman *et al.* 2011; Ruff & Larsen 2014). The bone modelling and remodelling process and material properties of bone change dramatically during growth and ageing (Currey 2003; Agarwal & Beauchense 2011; Gosman *et al.* 2011). Two recent studies have considered the relationship between mechanical influences on bone structure and biology from archaeological samples. Temple and colleagues (2014) compared growth and stress between early Neolithic and late Neolithic foragers from Cis-Bakal, an eastern Siberian site by examining stature, cortical thickness, and medullary width. It was found that early Neolithic

samples had previously shown evidence for stress which resulted in stunting in the femoral length. It was suggested that biomechanical strain may have been present in the early Neolithic group despite systemic stress affecting growth as there was no difference in cortical bone measures between the two (Temple *et al*. 2014). Schug and Golman (2014) examined midshaft femoral morphology to investigate bone turnover during periods of stress in the second millennium BC from prehistoric subadults from India. It was found that immature femora differed in cross-sectional shape which is consistent with locomotion behaviour. Children during the first 10 years of life show reduced compact bone mass that is consistent with increased cortical bone porosity (Schug & Goldman 2014). These studies suggest that surface morphology is a more useful indicator of growth and development in earlier age groups, a feature of bone that has yet to be fully understood in juvenile growth studies, to which this thesis will contribute to.

2.3 Morphometric Approaches to Long Bone Diaphyses

It has been demonstrated throughout this chapter that the use of long bones has many practical applications for assessing growth patterns in past populations. Their robust nature has a higher preservation rate which lends to more comparative studies (McCammon 1970; Ruff 2007; Ruff *et al.* 2013). During the last decade, an interest in morphological shape has taken a hold of the field of growth and development. The use of CT scans has moved these studies beyond the use of linear measurements, towards appositional growth through cross sectional geometries. Growth in terms of body mass (weight) is also important for health in modern populations but has not been fully explored in bioarchaeological studies. These approaches have broadened the field significantly and introduced further methods of geometric morphometrics to analyse and visualize changes in development. The consideration of other aspects of skeletal morphology and geometric methods can provide insights into the functional and physiological bases of growth (Ruff *et al.* 2013) from the past.

2.3.1 Activity Levels through Cortical Bone

Measurement of cross-sectional geometric properties of long bone diaphyses are a common approach to bioarchaeological studies investigating biomechanical properties (Ruff & Hayes 1984; Sumner & Andriacchi 1996; Ruff *et al.* 1999; Ruff 2009; Morimoto et al. 2011), and more specifically, patterns of skeletal robusticity (Larsen 1995; Stock & Pfeiffer 2004; Stock 2002; 2006). This research is based on the repetitive anteroposterior loading on the lower limb during mobility which results in a thickening of the cross-sectional geometry in the anteroposterior plane (Ruff 1987, 1999; Stock & Pfeiffer 2004; Shaw 2009; Macintosh *et al.* 2017) and its significant relationship with diaphyseal curvature (Macintosh *et al.* 2015). Recent studies have shown that postcranial robusticity, mobility,

and activity patterns are not as straightforward as originally thought, rather, there are levels of robusticity that vary at different sites of the bone (Stock 2006).

In addition to nutritional and environmental stress, mechanical considerations can be inferred from variations in cortical growth (Ruff *et al*. 2013). Long bone cortices continue to grow for a longer period of time than long bone lengths and articular dimensions (Ruff *et al.* 1994; Humphrey 2000) as a reflection of their primary mechanical role in supporting body mass and resisting muscular forces (Sumner & Andriacchi 1996; Ruff 2003). Differences in the growth patterns of long bone cortices reflect the complex interactions between environmental variables. For example, periosteal apposition may be more dependent on mechanical stimuli while endosteal apposition may be more sensitive to nutritional influences (Van Gerven *et al*. 1985; Ruff 1999; Mays *et al.* 2009). These considerations also suggest that both periosteal and endosteal dimensions are needed for assessing bone growth and possible growth disturbances (Ruff *et al.* 2013).

Gosman *et al*. (2013) looked at the relationship between ontogenetic growth periods and changes in femoral and tibial diaphyseal shape from neonate to skeletally mature individuals (n=46) from Noris Farms (Gosman *et al*. 2013). The diaphysis of each bone was divided into five cross sections to look at the relationship between cross-sectional shape, total subperiosteal area, cortical area, and medullary cavity area for each slice location. The study found that the femoral and tibial midshaft shape are conserved during growth, but the proximal and distal femoral diaphysis and proximal tibial diaphysis are more sensitive to developmental changes as a result of mechanical loading. Interestingly, two time periods were found for accelerated cross-sectional change in early childhood (0-1.9 years and 2-4.9 years). The second period was during pre-puberty (9-13.9 years and 14-17.9 years), which reflects the shift in increasing hormones and body mass which instigate periosteal expansion and endosteal reshaping (Gosman *et al.* 2013: 783). The first two patterns in the study showed that the medio-lateral proximal femur and anterior-posterior tibial expansions are consistent with previous studies which suggest changes in locomotor loadings. The other patterns of the distal femur anterior-posterior expansion and minimal change in the midshaft femur are consistent with regional heterogeneity and the sensitivity to mechanical loads (Gosman *et al.* 2013: 783). The importance of this study is the demonstration that the midshaft of cortical bone shape of the femur is fairly constant throughout development and is the most conserved region as the proximal and distal portions of the femoral diaphysis undergo change. The tibia, in contrast, shows a different pattern where there is a higher cross-sectional shape variability proximally and less change distally during development (Gosman *et al*. 2013: 786), possibly because more load bearing occurs in the femur and proximal tibiae.

Although there are limitations to the study by Gosman *et al.* (2013: 786), such as a small sample size for some of the age categories (3 to 5 year olds) and pooling of the sexes, this is one of the few quantitative studies of the whole bone diaphysis (Gosman *et al*. 2013). Most studies focus on only the midshaft (Ruff 1987; Wallace *et al*. 2012), thereby missing the regional cross-sectional geometry and the developmental heterogeneity in bone morphology resulting from dynamic patterns of growth (Gosman *et al*. 2013). Studies that look at age-related morphological variation from both a surface and region-specific perspective need to develop and define the spatial characteristics and regional significance of diaphyseal cortical bone during growth as well as the shift towards mature cortical bone geometries (Gosman *et al*. 2013).

2.4 Concluding Remarks

Skeletal morphological variation is a combination of multiple biocultural trajectories of individuals that are embedded in the larger communities from which they are drawn (Agarwal 2016). Indeed, capturing these subtle changes in shape is not as straightforward as it might seem. The plasticity and morphology of skeletal elements, especially long bone diaphyses, is difficult to quantify reliably. Different elements grow and develop at different rates and exploring the internal structure of the bones not only provides information on stress but mechanical loadings and movement of juvenile remains. Bioarchaeologists have the opportunity to continue to make more deliberate contributions to understanding and interpreting plasticity (Agarwal 2016: 143). As noted by Agarwal (2016: 143) 'we need a holistic approach that uses our empirical testing of skeletal data as well as our imaginations.' An imaginative approach and fascination of bone shape is discussed in Chapter 4, as the biologist, bioanthropologist, and statistician inspired a field of quantifying shapes known as geometric morphometrics.

3. Geometric Morphometric Method and Theory

Chapter 2 discussed the nature of plasticity in relation to the life course history of juvenile remains, and suggested that a more sensitive and forgiving technique, such as geometric morphometrics, is needed to capture growth and development. This chapter will begin with the history of morphometrics, outline the differences between traditional measurement theory, traditional geometric morphometric methodologies (GM), and automated 3D geometric morphometrics (auto3dgm). This chapter will consider with how GM can be used to describe and analyse developmental pathways.

3.1 Introduction to the Measurement of Form

The measurement of form has a long and continuous history within the fields of statistics, biology, and anthropology. Historically, the study of taxonomic classification of organisms and the diversity of biological life were based on descriptions of morphological forms (Adams *et al.* 2004: 5). These studies were less concerned with testing hypotheses of the morphological shapes and more with testing hypotheses concerning how biological processes affect shape (Zelditch *et al.* 2012: 16). During the early twentieth century biology began to transition from a descriptive field to a quantitative science, and morphological analyses experienced a 'quantification revolution' (Bookstien 1998; Adams *et al.* 2004: 5) known as biometrics.

This connection between shape and function has led biologists and anthropologists to play an important role in the development and application of new methods to quantitative biology in general, and morphometrics in particular. The founders of modern statistics were motivated by questions concerning patterns of variation, association, causation, and inheritance in human populations. The development of statistical methods such as correlation coefficient (Perason 1895), analysis of variance (Fisher 1935), and principal components analysis (Pearson 1901; Hotelling 1933) included quantitative data for one or more measurable traits. During the 1900s-1930s, professional anthropologists were eager consumers of the new methodologies and applied them to their research questions within their own fields. G.M Morant (1939) and Franz Boas (1912; 1922) made a huge impact on both the anthropological and statistical literature (Sparks & Jantz 2002) by using statistics to address questions on growth and development.

A second historically important driving force in morphometrics came from D'Arcy Thompson's pioneering book *On Growth and Form* (1917). This work highlighted the importance of the

relationship between the form or shape of a biological structure and its function (Small 1996: 2). Thompson's (1915; 1917) famous illustrative approach (Figure 3.1) of "Cartesian Transformations" (incorporating qualitative anatomical comparisons with quantitative methods) is still used in contemporary geometric morphometric analysis. The deformation grids produced by Thompson depict how part of one specimen may be described as a distortion of the same part in another specimen through a visualized mapping of boney homologous point locations along the same form.

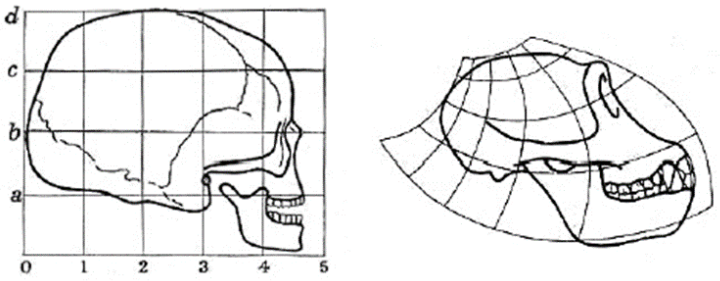

Figure 3.1 Thompson's (1917) drawings of a Cartesian transformation of a human (Fig. 548: 1082) to chimpanzee skull (Fig. 550. 1083).

The role of anthropologists as both the adopters and promoters of sophisticated methods of shape analysis has continued throughout the twentieth century (Slice 2007). The quantitative description of morphological shape was combined with statistical analyses describing patterns of shape variation within and among groups, leading to the development of the modern field of morphometrics (Adams *et al.* 2004: 5). Worldwide recognition of this approach followed by W.W. Howells (1973; 1989) work on craniometrics variation, and Charles Oxnard's research (1973; 2000), who developed and applied sophisticated and innovative methods in engineering to questions of functional anatomy.

3.2 The Biometrician and Traditional Morphometrics

The close relationship between statisticians, anthropologists, and biologists has persisted through recent shifts in the methodology and types of data for morphometric analysis. During the 1960s and 1970s, biometricians began using a range of multivariate statistical tools to describe patterns of shape variation within and between groups. This approach is now called traditional morphometrics (Reyment 1991) or multivariate morphometrics (Blackith & Reyment 1971). These datasets are typically acquired through measurements of length, depth, width, counts, ratios and angles (Zelditch *et al.* 2012: 3). Many of these studies investigated questions of allometry, changes in shape with changes in size (Jolicoeur 1963).

The relationship between size and shape is one of the most debated subjects in traditional morphometrics (Zelditch *et al.* 2012: 11). One of the main reasons for this are the many definitions

of size and shape (Bookstein 1989: 574) which results in different methods of teasing these two variables apart. Some researchers argue that size separated from shape is not really size (Zelditch *et al.* 2012: 11) as they are linked through biological processes. Functional morphologists, anthropologists, and biologists however, are interested in the relationship between these two variables.

The field of traditional morphometrics had difficulty with combining multivariate statistics and quantitative morphology (Adams *et al.* 2004: 6). For example, methods of size correction were proposed in an attempt to tease apart the size and shape of a specimen, however there was little agreement on which method should be used. This is an important issue because different size correction methods produce slightly different results (Adams *et al*. 2004: 6). Issues with removing size coincides with difficulty of holding information about shape (Zelditch *et al.* 2012: 3) because linear measurements often overlap or run in similar directions (Figure 3.2, B). The most obvious overlap is when several measurements radiate from a single point. This will cause datasets to contain less information than could have been collected because of redundant measurements (Zelditch *et al*. 2012: 3-9). Similarly, the same set of distance measures could be obtained from two different shapes because the location of where the distances were made relative to one another was not included in the data. For instance, if the maximum length and width were both measured on an oval and a teardrop, both objects could have the same height and width values, however they are clearly different shapes.

Another source of crucial information that is missing from these analyses are the spatial relationships between measurements (Slice 2007). For instance, this information can be line segments between points which do not fully capture an objects entire morphology. Rather, they consist only of a list of observed values of such lengths (Zelditch *et al.* 2012: 3-9). Once the line segments from traditional measures are taken away, and only the landmarks that connected the measurements are left (Figure 3.2 B), it can be seen that some are closer together than others (Zelditch *et al.* 2012: 9). Information about positions, which is crucial for morphological studies, is not found in distances between landmark points. However, landmarks made of coordinates (found in geometric morphometric methodologies) will hold all positional information as well as distances between all of the points (Zelditch *et al.* 2012:8-10). Algebraic manipulations can then be used to separate information into size and shape and remove irrelevant information like position or orientation of the specimen in the model or photograph (Zelditch *et al.* 2012: 14-15). Lastly, the linear measurements may not sample homologous anatomical points or landmarks of the organism,

thereby making it difficult to interpret the results and may overestimate the amount of shape information collected (Zelditch *et al*. 2012: 3).

3.3 Geometric Morphometrics

The difficulties with traditional morphometrics inspired researchers to explore alternative methods of quantifying and analysing morphological shape (Adams *et al.,* 2004: 6). Data that captured the geometry of a morphological structure was a key interest, which led to the development of outline and landmark methodologies. Archaeologists Kendall and Kendall (1980) and other statisticians developed a rigorous statistical theory for shape analysis that made it possible to combine the use of multivariate statistical methods with direct visualization of form. The distinct approaches that were earlier attempted by Thompson's (1917) work of combining shape description (biometric traditions) with the evaluation of shape change (geometric traditions) were later fused into *geometric morphometrics (GM)* in the 1980s by Fred Bookstein (1989, 1991), Colin Goodall (1991), D.G Kendall (1984), and F.J. Rohlf (1986; 1998; 1999;2000). The key ideas and methodologies behind GM are described in the following section.

3.3.1 2D Geometric Morphometrics: Outline Shapes

One of the first GM methods used were outline methods (Slice 2007). This approach digitizes points along an outline (with a mathematical function such as Fourier analysis) and compares the curves by using coefficients of the functions as shape variables in a multivariate analyses (Adams *et al.* 2004: 6). The points in this multivariate space can be transformed back to the physical space of the organism and visualized as outlines. The earliest methods fit lengths of equally-spaced radii from a central point, either a landmark or centroid of the specimen. This approach is, however, limited to simple outlines, so other methods were suggested such as changes in the angle of tangents at each point along an outline (Rohlf 1990). These methods worked technically, however the statistical analyses based on the different methods of changes in angles gave different statistical results and there was no agreed theory that would allow a researcher to select the best approach for their research (Rohlf 1986; Addams *et al.* 2004: 6).

3.3.2 Landmark Methods

Landmark-based GM started with the collection of two or three-dimensional coordinates of biologically definable landmarks. Landmarks are any corresponding, relocatable points on a biological structure of interest, similar to measuring with sliding callipers. Each landmark point is described with a Cartesian coordinate (X,Y,Z) and is used to represent the shape of a structure (MacLeod 2002: 769). Specific points are selected for measurements by placing a stylus or remote-controlled cursor on the desired point, instructing the measurement system to record the coordinates of that location. Each system has a spatial resolution that determines the degree to which two adjacent points can be recognized as having different coordinate values (MacLeod 2002: 769- 770, Zelditch *et al.* 2012; 3, 7), presently, the resolutions of tenths to hundredths of a millimetre are common in morphometric measuring systems. Each landmark contains its own coordinate, and it is the sets of landmarks located in either two or three dimensions which represents the structure during the analysis. There are three types of landmark classes (Bookstein 1991):

Type I: Located at junctions between different tissues or structures, such as a nutrient foramen.

Type II: Maximum curvature along the boundary or outline of a specimen, found at the extreme points or width of a specimen.

Type III: A miscellaneous category that currently includes external points and the entire set of boundary coordinates that comprise the trace of a specimens or structure's outline, commonly referred to semi-landmarks (Figure 3.2A).

Direct analysis of these coordinates as variables would be inappropriate as the effects of variation in position, orientation, and scale of the specimens are still present (Zelditch *et al.* 2012: 11, 34).Therefore, the non-shape variation must be mathematically removed before the analysis of such variables. Once non-shape variation has been eliminated, the variables become shape variables and can be used statistically to compare samples with graphical representations of shape for comparison (Adams *et al.* 2004: 6).

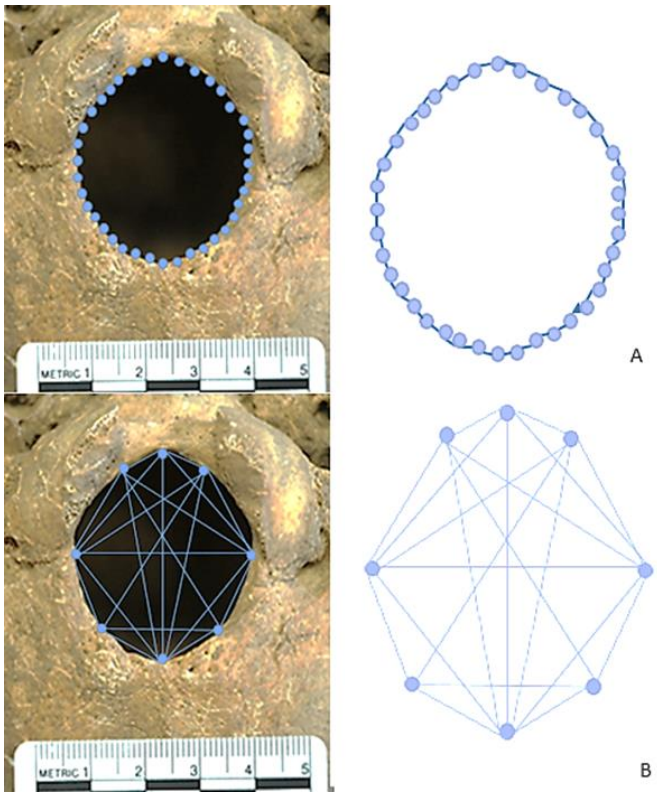

Figure 3.2: Metric and Geometric measurements of the foramen magnum of a 25 year old male from Great Chesterford. A. represents the GM analysis of the foramen magnum with a series of semi-landmarks (n=38) that were digitized clockwise around the structure. B. represents the traditional metric analysis of the same foramen with a series of linear measurements with 8 landmark locations and 20 linear distances (Stark 2013: 25).

3.3.3 Analysis of Landmark Data

The definition of shape in geometric morphometrics is, "all the geometric information that remains when location, scale and rotational effects are filtered out from an object" (Kendall 1977: 428). This process is computed through Generalized Procrustes Analysis (GPA). The coordinates that are left behind in the final configurations can be used to analyse shape differences. These include curves between landmarks and removal of any non-shape variation resulting from arbitrary choices of where to sample points on a curve (Zelditch *et al.* 2012: 11, 34).

According to Kendall's (1977: 428) definition of shape, scale is removed; this implies that the definition of size is 'scale' and is complementary to shape (Zelditch *et al.* 2012: 13). Ideally, the two variables are geometrically independent and the concept that highlights geometric scale is clear (Zelditch *et al*. 2012: 11-16). To calculate geometric scale, all of the distances of landmarks to the centre of the form (centroid) are assed to account for configurations of an organism that are larger and have landmarks further apart (Zelditch *et al.* 2012: 13). The location of the centroid and segments connect the landmarks to it, thereby allowing computation of geometric scale by taking the square of each distance from the landmark to the centroid and summing the squares to take

the square root of their sum (known as 'centroid size' (Zelditch *et al.* 2012: 13)). This creates a size measure that is mathematically independent of shape. This process of GPA enlarges or reduces shapes to achieve a standard and equal size (Zelditch *et al.* 2012: 62). The landmark configurations of all specimens are computed into a common coordinate system where the differences in landmark coordinate values reflect the differences in configuration shapes. The coordinates of landmarks on each (superimposed) specimen are then used as shape variables, or rather as geometric variables invariant to position, orientation, and isometric size. Although size and shape are now teased apart, it does not mean that they are assumed to be biologically separate or that their separation causes information to be lost regarding the relationship between size and shape (Zelditch *et al.* 2012: 13). For example, in biological data, the centroid size may be correlated with shape because larger organisms are shaped differently than smaller ones (Zelditch *et al.* 2012:13). These variable can then be used in traditional multivariate testing procedures to quantify and identify covariance structure, group differences, and functional relationships.

3.3.4 Graphical Outputs

It was not until computers, and improved digital recording techniques became more widely available, that the field of GM took off. Once all specimens have undergone GPA, visualization techniques can provide insight into the covariation among the shape variables through an ordination procedure called Principal Component Analysis (PCA). The similarity and differences of the sample shapes are visualized through scatter plots, where the first Principal Component Analysis (PC1) represents the largest axis of variation followed by the second Principal Component Analysis (PC2) representing the next largest axis of variation and so on. The closer objects or specimens are plotted, the more similar they are in shape (Slice 2007: 268-269), and variation of shapes are visualized through a thin-plate spline (Figure 3.3). While, as described above, deformations were Thompson's (Figure 3.1) idea as a means of analysis and mapping function from one form to another (Bookstien 1989, 1991). Fred Bookstein introduced thin-plate splines for visualizing shape differences (Bookstein 1989, 1991) (Figure 3.3). The idea comes from physics where it models an infinitely thin and large metal plate which covers the form and causes deformations or warps in the areas that have the most morphological variation (Rohlf & Marcus 1993). Thin-plate spline grids show how much shape varies along PC1 and PC2, and allows the investigator to explore how landmarks differ on each grid, and indicate how to interpret the morphospace that is presented through principal component analysis (Bookstein 1989). The variation in shape can then be analysed through traditional multivariate statistics.

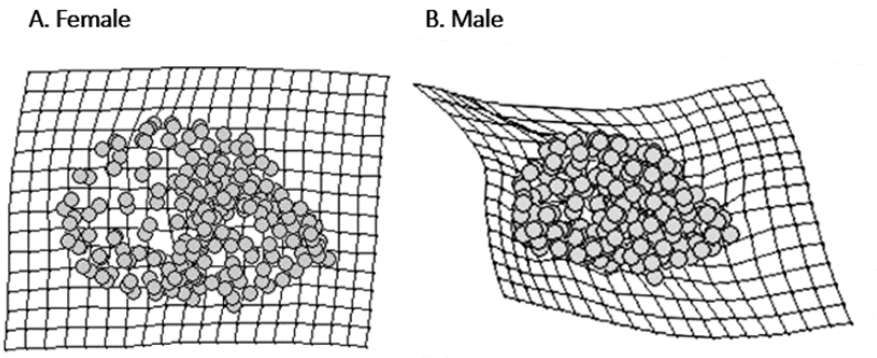

Figure 3.3: Thin-plate spline (TPS) deformation grid for Oceanic Female and Male human skulls (Image by author). The male skull reflects more shape or rubusticity in the supraorbital brow and skull vault as indicated by the warping of the grid.

Many of the latest innovations, extensions, and new applications in the field of GM are more commonly seen in the anthropological and anatomical literature such as Hartman's (1989) early three dimensional GM study of hominoid molars, O'Higgins and Jones's (1998) GM modelling of three-dimensional facial growth, Bookstein and colleagues (1999) use of sliding landmarks to study frontal bone morphology, and various works by Slice (2005) in *Modern Morphometrics In Physical Anthropology*. One of the main reasons for this trend is that anthropologists and archaeologists are often faced with limited sample sizes. For this reason, these disciplines are always in need of new methods that aid analysis from a limited amount of material. With advancing digital techniques, the range of recording and digitising materials for GM analysis and the dissemination of resource materials are becoming more abundant. These will be discussed in more detail in Chapter 5.

3.3.5 Analysis of Outline Data

A clear limitation to landmark-based geometric morphometric methods is that a sufficient number of landmarks may not be available to capture the shape of a structure (Adams *et al.* 2004: 10). In some instances, shapes or curves can provided important biological information but may lack obvious sampling points, as seen with the foramen magnum in Figure 3.2. One solution is to sample a curve at points along its length on each specimen. These landmarks are called 'semi' landmarks where the coordinates are allowed to slide along their curve (Bookstien 1991; Slice 2007: 271), as seen in Figure 3.2A. These points are placed arbitrarily using an algorithm that often defines endpoints at biologically homologous points and places a specific number of semi-landmarks between them. To calculate surface morphologies of a 3D object, semi-landmarks create a mesh or grid over the specimen and landmarks help anchor this grid to fully capture the entire morphological shape.

3.3.6 3D Data Analysis: Landmarks and Surfaces

The next logical progression of GM was the extension of sliding landmark methods for curves to extend to surfaces (Adams *et al.* 2004: 12). As surfaces lack biologically homologous landmarks (for instance Figure 3.4 of the diaphysis of a femur), attempts to capture their geometry were difficult (Wilson & Humphrey 2017: 40). Sliding semi-landmarks are able to remove the arbitrary placement of semi-landmarks (found in curve analysis) and surface sampled are considered to be the point of geometric homology between specimens rather than individual landmark points (Gunz *et al.* 2005; Wilson & Humphrey 2017: 40).

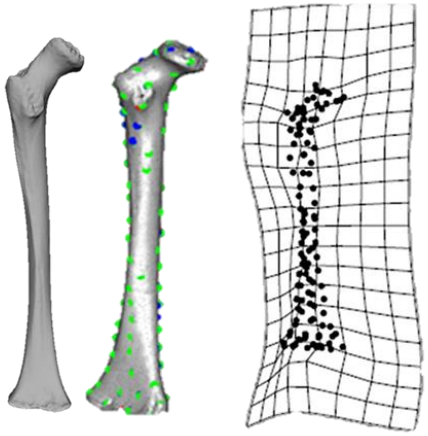

Figure 3.4: Digitized 12 year old femur with landmarks, semi-landmarks, and a thin plate spline. The warping's or grid deformations show were the most amount of variation is seen in the femur. The proximal region of the femoral head and neck as well as the distal metaphysis and midshaft (Image by author).

3.3.7 Interpretation of 3D Data Analysis: Thin-plate splines and Navigating the Shape Space

Interpreting GM results through principal component analysis (PCA) can be difficult. Figures 3.5-3.7 represent a hypothetical data-set of juvenile femora. The PC1 image reflects the shape changes that occur along the first principal component axis (x- axis of the PCA), while the PC2 image relfects shape changes along the second principal component axis (y- axis of the PCA). The minimum PC1 and PC2 thin plate splines (TPS) reflect the shapes found in the negative quadrents of the PCA. Therefore, the maximum PC1 and PC2 TPS reflect the shapes found in the postivie quadrents of the PCA. For this thesis, shapes that reflect a further degree of development with more distintictive long bone landmarks (e.g. trochanters), curvature, and torsion are referred to as *robust*. Specimen

which reflect a lesser degree of devlopment with fewer defined landmarks, smoother contours, and less torsion are referred to as *gracile*.

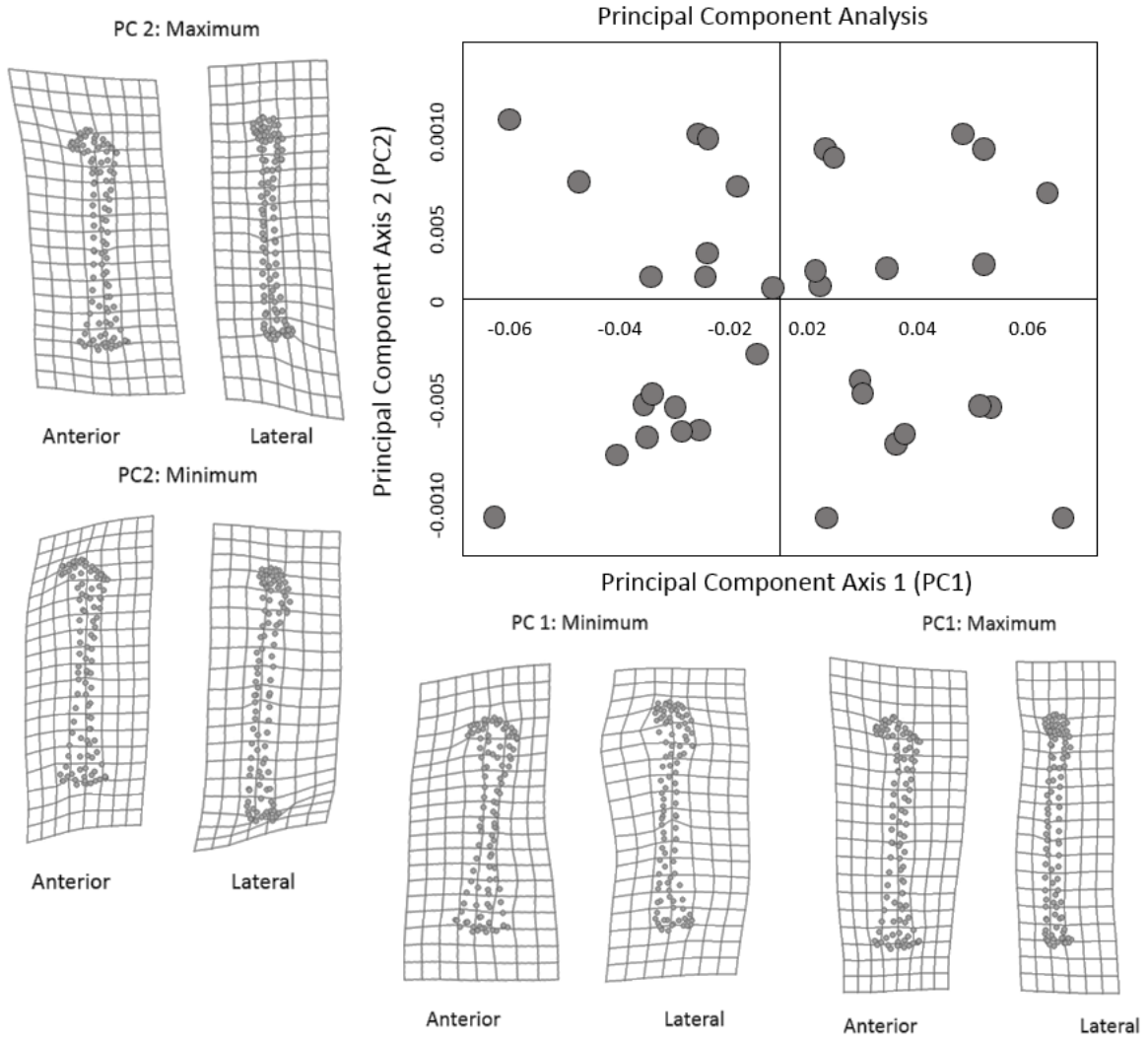

Figure 3.5: Principal Component Analysis of a hypothetical dataset of juvenile femora. PC1 Maximum TPS reflects the shape at the furthest positive shape space along the x- axis while PC1 Minimum TPS reflects shape at the furthest negative shape space. PC2 Maximum and Minimum TPS reflect the furthest positive and negative shape space along the y-axis.

The first principal component (Figure 3.5-3.6), reflects shape deformations in the proximal metaphyses and diaphyses of the femora. Specimen plotting negatively in PC1 have rounder and more convex curvature of the proximal metaphysis (PC1 minimum: Anterior veiw) and an overall more gracile architecture. In addition, there is more expansion in the anterior posterior plane of the lateal proximal meatphysis and some curvature at the disal diaphysis (PC1 minimum: Lateral view). Specimen plotting positively in PC1 have a more elongated proximal metaphysis and splitting of the trochanters (PC1 Maximum: Anterior veiw). Additionally, femora in postive PC1 have more curvature in the anterior posterior expansion of the proximal metaphyses and more mid-diaphyseal curvature (PC1 maximum: Lateral view), therefore reflecting a more robust architecture.

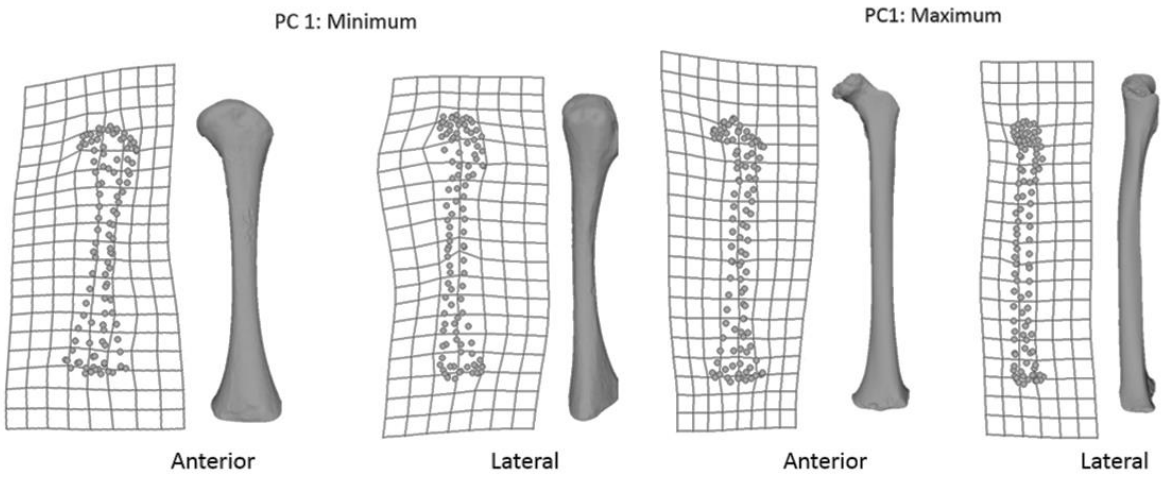

Figure 3.6: Principal Component Axis 1 TPS for the Maximum and Minimum shape space (x-axis).

The second principal component axis (Figure 3.5 and 3.7) reflects changes in the distal metaphysis into the diaphysis. Specimen plotting negatively in PC2 reflect rounder distal metaphysis (PC2 minimum: Anterior view) with a concave inter-metaphyseal angle and curved distal diaphysis (PC2 minimum: Lateral view). Specimen plotting positively in PC2 reflect a straighter distal metaphysis (PC2 maximum: Anterior view) with a convex inter-metaphyseal angle and a slight curvature in the mid-shaft (PC2 maximum: lateral view). Although PC2 is not as distinctive in shape variation as PC1 (which is to be expected as PC1 reflects an overall higher percentage of shape variation), specimen in positive PC shape space will be more robust while those in negative PC shape space will be more gracile in shape development.

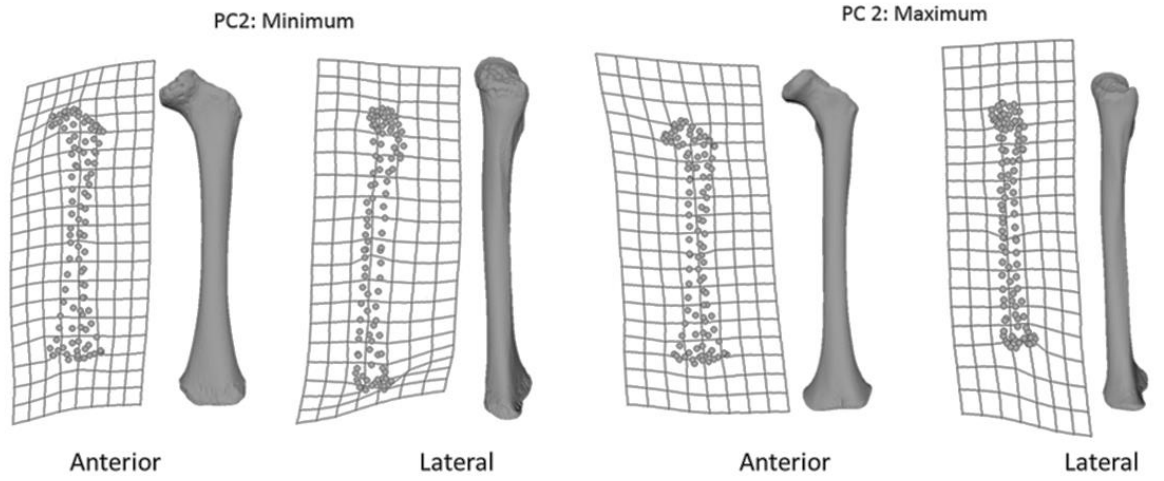

Figure 3.7: Principal Component Axis 2 TPS for the Maximum and Minimum shape space (y-axis).

Navigating and interpreting the shape space can prove difficult as some data-sets and Principal Component Axis are more descriptive than others. For instance, PC1 will typically hold more shape variation than PC2, while PC2 will reflect more variation than PC3 and so on. Additionally, studies which analyse skeletal morphology among different species will typically have more variation in shape than perhaps a dataset of only one species at different ages.

3.3.8 Auto3dgm: Automated 3D Methods

Combined with improved computational power and flexible open-source coding languages (Orme *et al.,* 2011; R Coding Team 2012), there have been growing methodologies for automation of shape quantification, which began with semi-landmarks over 3D surfaces (Bookstein 1997; Bookstein *et al.* 1999; Perez *et al.* 2006; Mitteroecker & Gunz 2009). The desire to improve shape analysis to 3D specimens has brought its own set of problems. Three-dimensional shape analyses are tied to two-user determined landmarks (Polly & MacLeod 2008), and 3DGM analyses are not meaningful without four or more (Gunz *et al.* 2005; Wiley *et al.* 2005). As a result, these methods have brought us back full circle to the same limitations in morphological studies that occurred 30-40 years ago. These limitations include subjectivity and observer-error in the interpretation of measurements, time invested for generating large datasets, and incomplete or biased representation of specimen morphology and sample variation (Boyer *et al.* 2015: 5).

MacLeod *et al.* (2010) raised the importance of bringing morphological studies to a new level of objectivity, standardization, efficiency, and accessibility by investigating automated methods to determine patterns of morphological similarity and differences (Boyer *et al.* 2015: 5). Many of the automated techniques available, even for 2D specimens, require direct interaction with the study materials to determine at least one 'corresponding point' that is common to all shapes of the study sample (MacLeod 2008).

Boyer and colleagues (2011, 2015) have worked to remedy these issues with automated 3D analysis through the development of auto3dgm (Wilson & Humphrey 2017:40). This freely accessible R package can match corresponding points on different locations of the same bone, estimate species classification at a higher success rate than user selected landmarks, and allow for different correspondence hypotheses based on the assumed path to shapes in the dataset. The placement of large numbers of points on 3D models with auto3dgm and the effectiveness of this method on difficult shapes includes tibial curvature (Frelat *et al.* 2012), talar surface shape (Parr *et al.,* 2014), rib curvature (Bastir *et al.* 2013: García MartÍnez *et al.,* 2016), endocranial shape (Neubauer *et al.* 2009) and juvenile ilia (Wilson & Humphrey 2017). This program determines features which correspond objectively or algorithmically and it can assess morphological differences with less

measurement sensitivity. This allows for greater insight into patterns associated with morphological disparity (Boyer *et al.* 2015).

3.3.8.1 Auto3dgm Workflow

As this method represents the alignment of pairs of surfaces with landmark like feature points, each bone is represented with the same number of points. The algorithm then configures each point consistently (with biological features) across all bones of the sample. Each of these points is analogous to an observer-placed landmark. However, they are not identified based on any of the criteria for determining type I, II, or III landmarks (Zelditch *et al.* 2004), or semi-landmarks (Bookstien 1997; Mitteroecker & Gunz 2009), as they are known as 'pseudolandmarks' by Boyer *et al.* (2015).

There are four computational steps for this methodology. The first is re-sampling the surface coordinates to a specified standard number of points. The user must determine the number of points used for the low resolution version of the alignment, the number of points to represent the high resolution or final alignment, and the number of principal alignments, usually this number is set to eight possible combinations of the alignments along the first three principal axes, but additional principal alignments can be used for more complex specimens. This allows the pseudolandmarks to be evenly spread over the surface (Boyer *et al.* 2015). The algorithm uses these surface pseudolandmarks to align each pair of bones using an iterative closest points (ICP) procedure (Besl & McKay 1992), and the best alignment is found by computing a Procrustes distance. A Procrustes distance matrix is produced and a computation by a minimum spanning tree (MST) which connects all specimens in the dataset using the shortest edge length possible (Figure 3.8). The addition of a MST offers a unique solution to visualizing the automated alignment, apart from datasets where several cases are exactly equidistant from each other (Boyer *et al.* 2015). Datasets with high degrees of shape variability may have specimens with biologically meaningless Procrustes alignments as artefacts of the high dimensionality of the dataset give false results. Therefore, instead of attempting to directly align pairs of shapes that have large Procrustes distance separating them, alignments between such pairs are generated by diffusing alignments between intermediate shapes and ultimately allow very different shapes to be aligned indirectly (Boyer *et al.* 2015).

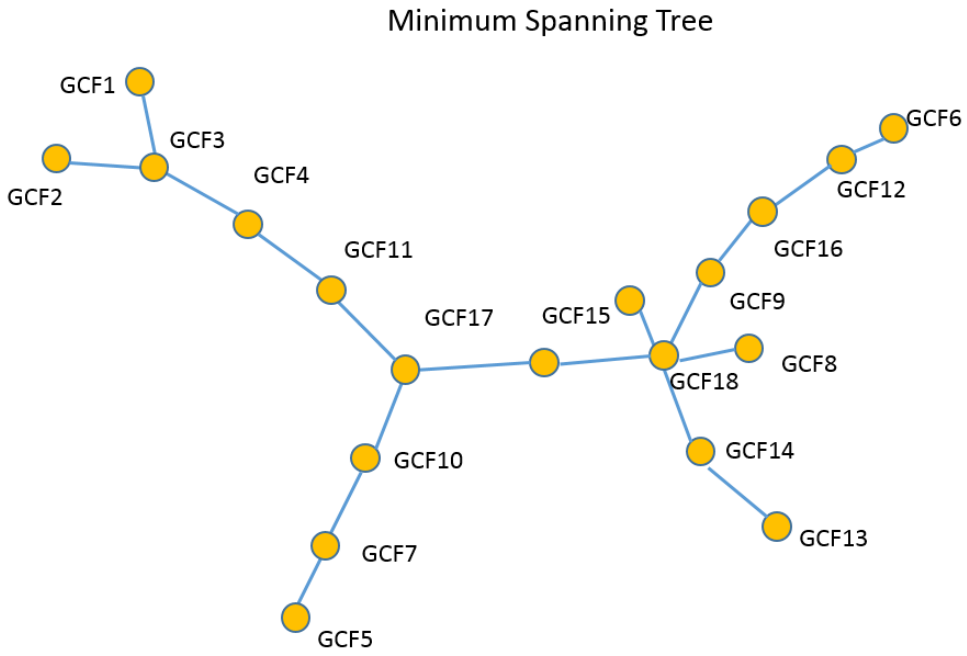

Figure 3.8: Minimum Spanning Tree of 18 femora from Great Chesterford (foetal to 12 years old) (Image by author).

The output files include an 'alignment file' which is a 'multi-surface.off' file that includes displays of user-supplied low resolution renderings of all specimens shown in the algorithm determined alignment (Boyer *et al.* 2015). An 'MDS file' is another multi-surface file which embeds the same aligned renderings of specimens in a coordinate space determined by a multi-dimensional scaling (MDS) analysis of the distance matrix of aligned specimens. A 'scaled'.txt file contains all of the coordinate data for all specimens scaled to the same centroid size and an 'unscaled'.txt file contains all of the coordinate data for all specimens at the scale of the original input files (Boyer *et al.* 2015). Finally, a folder with copies of the original input files, the coordinates which have been multiplied by the rotation matrix used in the final alignments is produced (Figure 3.9).

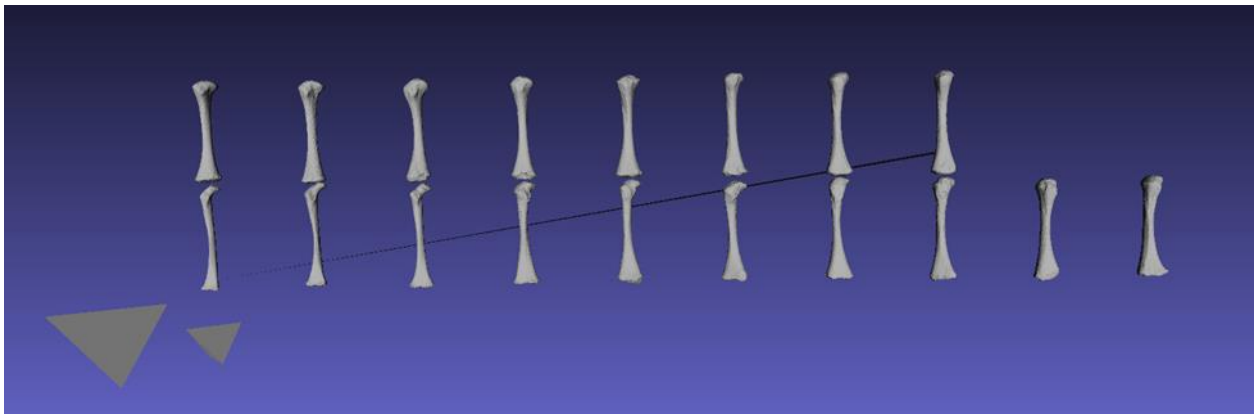

Figure 3.9: Auto3dgm alignment of 18 femora from Great Chesterford (infant to 12 year olds) (Image by author).

The purpose of the alignment file is to check for the errors that may be generated by the alignment algorithm. In cases when errors are found, Boyer and colleagues (2015) provide a detail outline of functions that can remedy common alignment errors such as gaps between specimens or groups of specimens (Wilson & Humphrey 2017). Figure 3.10 illustrates how the pseudolandmarks capture the minimum and maximum shapes of the first PC axis of Great Chesterford femora. These images can be rotated 3-dimensionaly in R to examine if the entire surface has been captured. The same multivariate statistics can be then be used for analyses to determine PCA, Pairwise matrix, Group ANOVA, and allometric plots (Boyer *et al.* 2015).

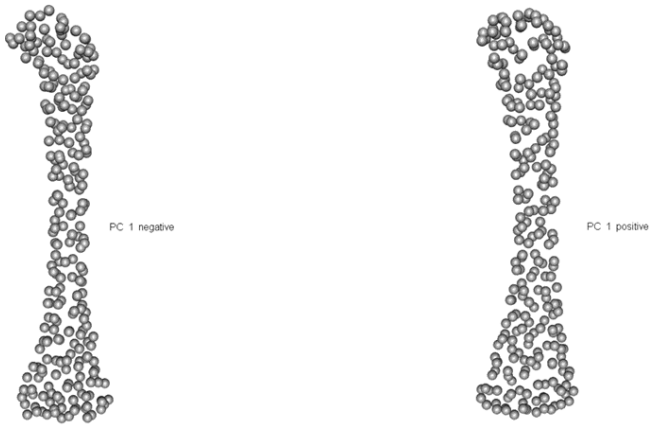

Figure 3.10: Great Chesterford femora of the minimum (right) and maximum (left) femora shape of the first principal component (Image by author).

3.3.8.2 Limitations to Auto3dgm: Determining Correspondence between Surfaces

Although there have been substantial improvements to GM, including new automated approaches, this brings a new set of challenges. The need to compare 3D surfaces with a high level of precision is a common goal to many fields that deal with geometric processing and the development of algorithms to automate correspondence mapping between surfaces (Wilson & Humphrey 2017). Computationally rapid automated methods that process high levels of surface geometric data (>600 semi-landmarks) for large datasets are highly sought after for the development of ontogenetic trajectories, sex and age estimation methods, and taxonomic classification (Wilson & Humphrey 2017). The difficulties with these methods are associated with establishing corresponding surfaces for alignment.

Attempts at resolving the problem of identifying correspondence between surfaces have been made by computing a map that minimizes the distortion between a given pair of shapes, as measured by a distance matrix (Bronstein *et al.* 2006; Wilson & Humphrey 2017). Reasons for specimens that are incorrectly aligned may be singular, such as a mesh that is incorrectly aligned to

the rest of the sample dataset. Multiple misalignments may occur if any one group of shapes is aligned to one another but misaligned to the rest of the dataset (Wilson & Humphrey 2017). The singular misalignments happen when multiple maps between two surfaces exist and the algorithm is unable to determine which one is correct (Wilson & Humphrey 2017). Multiple misalignments occur when shapes are highly dissimilar, for instance 3D models of a bone for individuals belonging to two species. Boyer *et al.* (2015), addressed this issue by incorporating minimum spanning trees of pairwise distance which guides their algorithm through intermediate shapes and improves the alignment. An ontogenetic sample of bone surfaces may be less affected by this issue, as those surfaces will more closely represent continuous gradual shape variation associated with growth, which are less likely to result in misalignment (Wilson & Humphrey 2017). The sample-dependence of the alignment outcome is a concern that remains difficult to address (Boyer *et al.* 2015; Wilson & Humphrey 2017).

Preliminary tests on meshes of teeth and post-cranial bones for a diverse sample of primates indicate that automated landmark free approaches may offer a fast and more robust solution to surface comparisons (Koehl & Hass 2015; Wilson & Humphrey 2017). However, more needs to be done to test how different methods of landmark and semi-landmark, auto3dgm and traditional ratio measurements can be applied to small 'shapeless' juvenile long bones.

3.3.9 Morphometric Analysis of Developmental Pathways

It has been expressed throughout this chapter that the common themes in morphological studies are to understand the difference in both form and function (Zelditch *et al.* 2012: 270). There are several methods that can be used for modern morphometric analysis in order to examine processes that underlie observed morphological variation, allometry, and ontogeny (Cobb & O'Higgins 2004, Rozzi *et al.* 2005, Leigh 2006) which will be discussed below.

3.3.9.1 Ontogenetic Trajectories

Many statistical and graphical methods have been developed to compare ontogenetic shape change (Mitteroecker 2007). Early attempts to formalize evolutionary effects on ontogeny focused on the concept of heterochrony. Gould (1977), developed his 'clock model' to visualize evolutionary changes of developmental timing. Alberch and colleagues (1979) developed a broader conceptual framework to describe and compare ontogenetic sequences. For instance, a given organism can be represented as a point in a 3-dimentional plot with axes for size, shape and age (Mitteroecker 2007). The size and shape changes of a particular developing individual creates a trajectory, or as Alberch *et al.* (1979) coined, the ontogenetic trajectory.

Gould, Alberch and several authors compare phenotypic changes during ontogeny by focusing on a single shape or form variable (Shea 1983; Rice 1997). The term ontogenetic trajectory has been adopted to describe the ontogenetic sequence of shapes in a multivariate shape space. It is also used to signify the ontogenetic path in an age-shape space (Mitteroecker 2007). Instead of describing individual development, as found in most empirical studies, the term is applied to describe population-specific or species-specific average form change during ontogeny (O'Higgins 2000; O'Higgins *et al.* 2001; Vidarsdottir *et al.* 2002; Cobb & O'Higgins 2004; Mitteroecker *et al.* 2004; 2005). For this thesis, the term 'ontogenetic trajectory' is used to describe the average of a population sample(s) specific ontogenetic pathways in multivariate shape space.

Some authors characterize ontogenetic form change by *a priori* selected mathematical growth function (Rice 1997; Zollikofer & Ponce de Leon 2004). These individual trajectories are displayed graphically as curves which connect the developing shapes in a low-dimensional data representation such as plots of principal component scores. Mitteroecker *et al.* (2004) demonstrated how to construct a size-shape space (or rather form space) using geometric morphometrics. The data matrix of Procrustes coordinates are augmented by a column that holds the natural logarithm of Centroid Size of all forms (Mitteroecker 2007).

One of the earlier juvenile studies in biological anthropology that employed this methodology was by Strand Viðardóttir *et al.* (2002) who looked at regional differences in ontogeny of the cranium. This study on interpopulation variation of 10 modern human populations looked at distinctive features of the adults from each population and found the extent that population differences occur with ontogenetic scaling and allometric trajectories. It is one of the few studies that clearly defines growth (size and age), development (shape and age), and allometry (shape and size) in an attempt to tease these variables apart. This study demonstrates the plasticity of facial shapes through growth and highlights a method (GM) that can be used on juveniles to capture whole bone morphology and statistically analyse trajectories of growth, development, and allometry.

Hellier and Jeffery (2006) looked at the plasticity of the juvenile talus (a structure crucial to the distribution of body weight). Interestingly, it was found that three of the talar articular facets correlated significantly with increases in body weight. Adult morphological structures focus on muscle attachment sites as they change in shape according to muscle mass. This study demonstrated that, for juvenile remains, the joint facets are much more malleable and change in shape and direction according to body mass. This presents an interesting field of research, as juvenile joints have been severely understudied in the past, but would be useful in looking at activity patterns in archaeological children.

Regression analysis can also be used to relate shape to other variables such as size for allometric studies (Penin *et al.* 2002, Frost *et al.* 2003), extrinsic variables such as time (Jonke *et al.* 2003, Kimerle & Jantz 2005, Wescott & Jantz 2005), or developmental environments (Fink *et al.* 2005). This type of analysis can be combined with hypotheses of group differences through multivariate analysis of covariance (MANCOVA) as was done by Rosas and Bastir (2002), who identified independent effects of sex and size on cranial shape in modern humans. Analysis of ontogeny and sexual dimorphism from data at Bolton-Brush was done by Dean *et al.* (2000), the study of facial growth and sexual dimorphism in the Papionin face by O'Higgins & Collard (2002), the interspecific allometric comparisons of African apes by Berge and Penin (2004), as well as the study of sexual dimorphism and allometry in extant hominds by Schafer *et al.* (2004).

More recently, geometric morphometrics have been used to assess the morphological features of the pelvis to provide a more detailed picture for juvenile assignment of sex than traditional measurements. Wilson *et al.* (2008) found that the sciatic notch morphology was able to correctly identify sex in 96% of juveniles from Spitalfields. This is a significant improvement on Schutowski's (1993) linear attempt. Wilson *et al.* (2011) also combined geometric morphometric studies of Spitalfields and a Lisbon collection and found that, although sexual dimorphism was greater in the sciatic notch in both materials, the notch morphology varied with individual age, confirming previous work (Valk *et al.* 2008). A discriminant function from one of the populations was applied to the other and it was found that the success rate for sex determination was little more than chance (Wilson *et al.* 2011: 42). This also supports earlier work (Boucher 1957, Weaver 1980) in indicating that inter-population differences in the greater sciatic notch morphology are greater in magnitude than sexual dimorphic features of the pelvis and prevent reliable sex determination (Mays 2013, 13). GM was successful in showing that sex determination was not reliable because of sensitively to shape and highlights the potential of this method of quantifiable shapes that can be applied to various regions of the juvenile skeleton, as GM is more sensitive to slight changes in surface morphology than other approaches.

3.3.9.2 Allometry

Allometry has been an influential concept in biology and morphometrics since Huxley's *Problems of Relative Growth* in 1932. Huxley's work was based on multiplicative growth models for size measurements such as bone lengths, linear distances, areas, organ weights or volumes (Mitteroecker 2007). Allometry was expressed as a power function between traits or equivalent, as a linear relationship between the log-transformed traits (Mitteroecker 2007). Logarithmic transformation of variables is also common as a method of overall size correction and to account for different units (Gould 1966; Bookstien *et al*. 1985; Mitteroecker 2013: 61).

From a biomechanical viewpoint, it is expected that organisms change shape when they change size, whether from ontogeny or evolution (Zelditch *et al.* 2012: 304). When organisms grow or evolve to larger sizes without changing shape, they are likely to decrease their ability to perform crucial functions from locomotion and feeding to respiration (Zelditch *et al.* 2012: 304). If one takes a cross-sectional area of a femur or weight-bearing limb, then the geometric scaling of length (x), area (x^2), and mass (x^3) would have the proportions of 2:4:8, larger organisms would be 4:16:64 and even larger organisms would be 10:100:100 (Zelditch *et al.* 2012: 304). Geometric scaling would cause the limb to buckle much quicker under increasing mass and would cause load-bearing bones to bend under the force generating muscles (Zelditch *et al.* 2012). Allometric scaling maintains the functional equivalence over a range of sizes for basic physical properties such as surface area to volume relationships (Zelditch *et al.* 2012: 304). These might be expected to scale predictably over an entire ontogenetic series even though children or young animals are not just small but are ecologically different from the older and larger members of their own species (Zelditch *et al.* 2012). For this reason, they do not undergo the same functional demands but could have the *length: surface area* or *surface area: volume* relationships (Zelditch *et al.* 2012:304). Otherwise it could be expected that the scaling relationships that alter proportions would suggest that, over an individual's life-time, the increases in size and changing shape will experience transitions in functional demands at every age and the individual must be competent to perform the function that is needed while continually changing both form and function (Zelditch *et al.* 2012: 304). The direction of specific functional demands has been documented in many mammalian species (Zelditch *et al.* 2003; Bastir & Rosas, 2004; Tanner *et al.* 2010). Meaningful conclusions can be made about evolving morphologies, whether trajectories are linear, curving, or abruptly reorienting (Zelditch *et al.* 2012: 305)

Geometric morphometric studies of allometry require a methodological approach that differs to classic allometry studies (Mitteroecker 2013: 61). Procrustes shape coordinates are shape variables, not size variables, and they have no natural zero point (they are on interval scales not ratio scales) and cannot be log transformed. Allometry is usually a linear function of the Procrustes shape coordinates, estimated by multivariate regression of the shape coordinates on centroid size or logarithm of centroid size (Bookstein 1991; Klingenberg & McIntyre 1998; Mitteroecker *et al.* 2004).

Ontogenetic allometry, the association between size and shape across different age stages, is used to estimate a population's ontogenetic trajectory (average growth pattern) (Mitteroecker 2007). Static allometry, the association between size and shape within a single age stage is used to explain

the coevolution of size and shape and act as a model for functional and behavioural adaptations (Gould 1966, 1977; Klingenberg 1998; Schaefer *et al.,* 2004; Gunz 2012).

In the classic concept of allometry, a trait is considered negatively allometric if it increases less in size than other traits or overall size of the specimen. A trait with a positive allometry increases more in size than other traits do. For instance, head size compared to body size is negatively allometric during human growth, whereas limb length is positively allometric (Mitteroecker 2013:62). The variables used in geometric morphometrics are the shape coordinates of the landmarks. Positive or negative allometry cannot be inferred from single shape coordinates as they are shape variables rather than size variables and depend on the superimposition. All shape coordinates must be visualized together to draw inferences about the relative size increase or decrease of specific parts described by the landmarks (Mitteroecker 2013: 62).

Comparisons of two or more groups of individuals raise the question on how allometry might differ across groups (Mitteroecker 2013). In recent years, a large body of literature on the morphometric comparison of growth and ontogenetic allometries has advocated different morphometric and statistical approaches (O'Higgins *et al.* 2001; Zelditch *et al.* 2003; Mitteroecker *et al.* 2004, 2005; Gunz 2012; Mitteroecker 2013). An effective way to compare ontogenetic or static allometry across groups is the visual comparison of deformation grids or series of reconstructed shapes representing group-specific allometry. These deformations can easily be described in qualitative morphological terms, but the comparison of deformations leads to useful biological inferences (Mitteroecker 2007).

Ordinations such as principal component analysis or between group principal component analysis (Mitteroecker & Bookstein 2011) can be useful to explore ontogenetic and allometric trends in different groups. Growth trajectories and allometric vectors can be plotted within a principal component plot, either as linear vector or as nonlinear estimates such as local linear regressions (Bulygina *et al.* 2006; Coquerelle *et al.* 2011). Alternatively, multiple allometric vectors can directly be compared by principal component analysis (Mitteroecker *et al.* 2004, 2005; Gerber *et al.* 2007).

Parallel ontogenetic trajectories in two or more groups indicate that the groups have the same linear patter of relative growth during the observed age periods, even if they differ in the initial or adult morphology (Mitteroecker 2007). If the average morphology of a species differs from its ancestral average morphology, specifically by the extension, truncation, or the developmental timing of an otherwise conserved ontogenetic trajectory, the underlying evolutionary process is known as allometric scaling or heterochrony (Gould 1977; Alberech *et al.* 1979; Klingenberg & McIntyre1998).

3.4 Concluding Remarks: Shape, Size, and Form

Size and shape are classic geometric concepts, and it is a long standing tradition in morphometrics to analyse and interpret variation in shape separately from variation in size (Mitteroecker 2007). However, every organism and every part of an organism has a certain form, meaning a certain size and shape. Modern geometric morphometrics offers two modes of analysis: an analysis of shape separately from size, and the combined analysis of size and shape in single form space (Mitteroecker 2007). Form is a more comprehensive description of an object than shape alone and should be used for classification studies whenever groups of organisms differ both in size and shape. Predictions of variables, such as age from morphological form is better than shape alone whenever size is related to the variable. In most studies of growth and development, changes in both size and shape may be of statistical relevance and can be analysed together (Mitteroecker 2007).

Geometric morphometrics offers a powerful technique for the visualisation of both shape and form differences. Deformation grids and series of reconstructed shapes can be successfully interpreted within a biological context (Bookstein 1991). Ordinations and other multivariate statistical analyses of high dimensional shape spaces or form spaces can be useful when comparing relationships between multiple groups, but meaningful biological interpretations of such analyses are more difficult (Mitteroecker *et al.* 2004, 2005; Mitteroecker 2011).

This chapter has outlined the history of geometric morphometrics and its application to the fields of biology and anthropology. The geometric morphometric tool-kit has only recently made its way to juvenile bioarchaeological studies and its benefits and limitations have yet to be fully understood. Chapter 4 therefore, acts as a validation study of the traditional linear measurements, landmark and semi-landmark GM, and automated 3D GM, by testing if there is an effect of shape on the juvenile femora, and if so, what is it? This study will assess if there are any similarities or differences between the three methods in order to determine which was the most appropriate to be used for the main study analyses in Chapter 7.

4. Capturing Shape: Linear Measurements, 3DGM, and Auto3dGM of the Juvenile Femora

Chapter 3 has demonstrated the potential of teasing apart size and shape with a visual component and its appeal for anthropologists and bioarchaeologists. However, very little use of 3D geometric morphometrics (3DGM) has been applied to juvenile remains. As discussed in Chapters 1 and 2, juvenile femora are the most commonly used element in growth studies as femora have the highest survival rate in the archaeological record. However, apart from CT scans of internal geometries of the midshaft, little is known about the entire bone morphology of juvenile long bones. This is a result of the complex 3-dimensional structure of juvenile long bones which have smooth, even boundaries, and complex curvatures that are challenging to quantify by traditional metric analysis (Gould 2014: 1-2). This is problematic as comparative anatomists have noted that these aspects of shape information vary qualitatively based on modes of locomotion and ontogeny (Polly 2008). Gosman *et al.* (2013: 783-786) found that the proximal and distal regions of the femur were most sensitive to changes during growth and development, however, as discussed in Chapter 3.2, these regions are potentially overlooked using traditional linear measurements.

Applications of quantitative 3D surface analysis (those discussed in Chapter 3) of the femur may significantly increase the amount of qualitative or morphological information examined in ontological studies of the lone bones. Some researchers (Polly *et al.* 2011; Gould 2014) explored the differences between traditional and geometric morphometric methods and auto3dgm (Boyer *et al.* 2015) and have concluded that there was not much difference between metric and GM shape data, and thus the latter requires much more effort than necessary. Others have argued that there is a constant need to improve the quantitative methods for analysing models of biological shapes to further expand the morphological field (Evans *et al.* 2007; MacLeod 2008). The important distinction between analyses of geometric shape data and conventional morphometric data is that the analyses of landmark configurations are multivariate. According to the earlier definition, shape is a feature of the whole configuration of landmarks. Thus, shape data is multidimensional and is best described by multiple coordinates (Zelditch *et al.* 2012: 75).

It would be useful therefore, to test the power of linear measurements (through ratios), 3D geometric morphometrics (3DGM), and automated geometric morphometric (auto3dgm) methods on complex bone morphologies (Gould 2014: 2). This chapter presents a validation study of shape analyses by using three analytical methods to test the same hypothesis on the same skeletal

material. The aim of this study is to determine if, and how, linear ratios, 3D GM, and auto3dgm analyses can even be used on juvenile long bones and if these methods reveal developmental pathways differently in juvenile remains. This validation study assesses the utility of GM applications to juvenile long bones and the sensitivity of these analyses on difficult to capture shapes. The analytical methods will be examined through the following questions and hypotheses:

1. Is there an effect on morphological shape and size?

Null Hypothesis: there is no effect on femur shape in relation to size

Bookstein (1991) presents the most common question asked in morphological analysis, which '*is there an effect on shape?'* This can be answered by determining the probability that the association between variables is no greater than chance (Zelditch *et al.* 2012: 14). These questions are typically analysed by regressing shape on centroid size using a multivariate regression. This question is tested by examining ontogenetic trajectories from linear, 3DGM, and auto3dgm methods of the juvenile femur. The ratios will be regressed onto femur size through a linear regression and through the geometric mean to create a proxy for the 3DGM and auto3dgm allometric plots. The null hypothesis can be accepted (there is no effect) or rejected (there is an effect) for all three methods.

2. What is the effect on femur morphology in response to mechanical loading?

Null Hypothesis: there is no significant change in the proximal and distal regions of the femur during this growth period

If the first hypothesis is rejected and there is an effect on shape, the second question is *'what is the effect?'* and relies on a description of morphological similarities and differences. For the ratio analysis, this is assessed with a MANOVA and principal component analysis of the ratios and their differences with ages. 3D GM and auto3dgm analysis is addressed by depicting the changes in landmark positions and grid deformations (Zelditch *et al.* 2012: 15) represented by the principal component analysis (PCA) and thin-plate splines. This hypothesis tests a previously confirmed observation by Gosman *et al.* (2013: 783) through CT scans of the internal geometries of the femur during infancy to 18 years old. He found that there were two periods of accelerated cross-sectional change in early childhood (0-1.9 years and 2-4.9 years) and during pre-puberty (9-13.9 and 14-17.9). There was a shift in medio-lateral expansions both in the proximal and distal regions of the femur during these ages, thereby suggesting changes in locomotor loadings (Gosman *et al.* 2013: 783). This test determines whether linear ratio measurements, 3DGM, and/or auto3dgm, are able to pick up the subtle changes of morphological surface shape in these regions.

4.1 Skeletal Materials

The skeletal material used for this methodological study comes from Great Chesterford, an Anglo-Saxon settlement in Essex, UK, curated at the University of Southampton. This collection was used because of unlimited access, which was necessary for testing both the analysis and data collection methodology. Secondly, the preservation is poorer than the other skeletal collections used in the main analysis (Wharram Percy, Canterbury, Raunds, and Wolverhampton). Thereby testing the validity of these shape analyses on moderately preserved bone which is the common preservation of archaeological juvenile remains. As a result, any difficulty in either the data collection or analysis would be addressed before scanning the other study collections, which had limited periods of access granted.

The ages selected for this study are found in Figure 4.1 and range from foetal to 12 years old (N=18). As discussed in Chapter 1 and 2, this age range reflects more environmental than genetic influences. Additionally, only the diaphyses and metaphyses are present for the individuals in this age range as the inclusion of epiphyses (both fused and/or fusing) would further complicate these analyses. This study heavily relies on the surface and completeness of each element, therefore specimens were excluded if they were fragmented or had poor preservation that altered the surface morphology.

The classification of the age groups were selected using Gosman and colleague's (2013: 783) criteria, reflecting the general changes in musculoskeletal features of the lower limb as different forms of movement, such as crawling to walking, are seen in this age range. These groups are intended to give a base-line of the general types of movements that occur at certain ages and therefore are reflected in bone shape (Lewis 2011: 2; Gosman *et al.* 2013: 783). Additionally, movement, nutrition, and environment influence this age range, while puberty to adulthood is shaped by secondary influences such as hormones (Gosman *et al.* 2013:783). Dental development (Schour & Massler 1941) was used to age the individuals because it is less likely to be influenced by environmental stress (Lewis & Garn 1960; Lewis 201), and has been shown to be a highly reliable method for estimating age at death (Smith 1991; Richards *et al.* 2002: 206). Ageing the individuals by diaphyseal length would be inappropriate for this research as the differences in developmental, growth, and allometric trajectory of the long bones is under study. Dental development was recorded using Schour and Massler (1941) which is more appropriate for British archaeological material. This method was tested by Liversidge (1994) who assessed a variety of dental aging standards on immature individuals of documented age at death from the 18th-19th century AD crypt at Christ Church, Spitalfields, London. It was determined at Spitalfields that the mean difference

between actual age and age estimated using Schour and Massler (1941) was only 0.1 years in those under 5 years old.

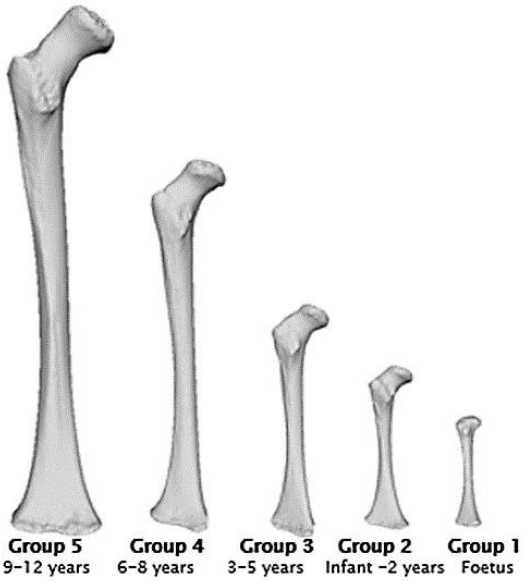

Figure 4.1: Femur development from foetus to 12 years old. Group 1 (n=3) : No movement; Group 2 (n=11): Supportive sitting, crawling, pulling to stand, cruising, and beginning stages of walking; Group 3 (n=1): Intermediate walking and running; Group 4 (n=1): Adult walking, climbing, and jumping; Group 5 (n=2): Adult walking with more refined musculoskeletal features (Lewis 2011: 2; Image by author).

4.2 Linear Measurement Data Collection: Ratios

Six ratios were recorded and calculated from linear measurements on each specimen with Mitutoyo digital sliding callipers. Each measurement was taken two times to calculate the measurement error (Appendix A.1). Figure 4.2 describes the measurements used for the traditional linear portion of this study. Ratios are expressions of proportional rather than absolute differences and are less prone to the autocorrelation found in body size differences (Gould 2014: 2-3). Ratios are also biomechanically significant and a good approximation for functional demands, such as joints, and provide a better expression of shape differences, as described in the comparative literature (Carrano 1999). The ratios were selected based on Gould's (2014: 3) study on metric versus geometric morphometric morphology of the distal femur and Toogood *et al.* (2009) on proximal femoral anatomy in order to capture as much shape as possible from the juvenile long bones.

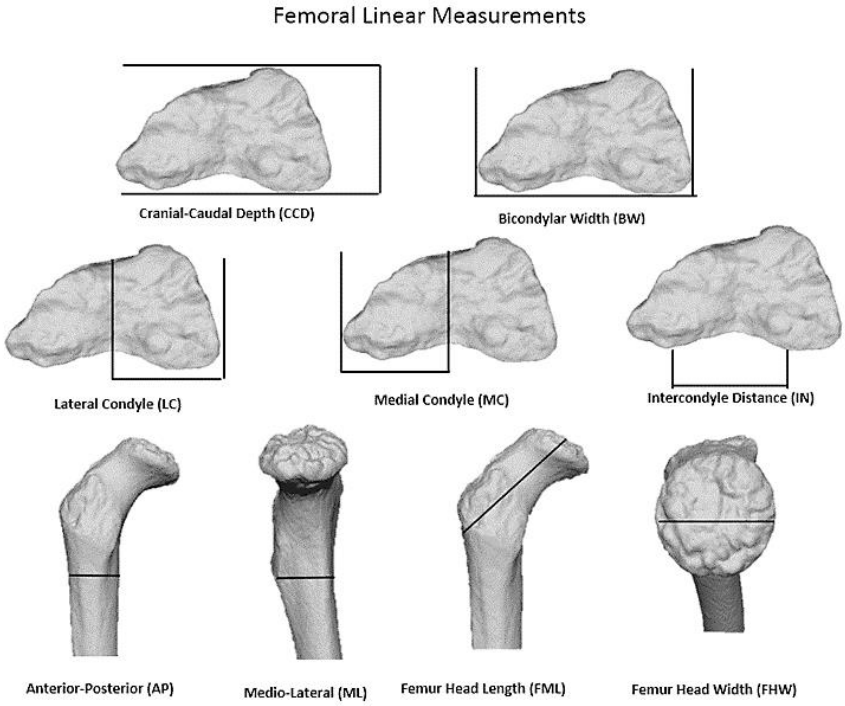

Figure 4.2 Femoral linear measurements (mm) of maximum lengths and widths used to compute ratios. CCD/BW: Cranial caudial depth/bicondylar width; IN/BW: Intercondylar distance/Bicondylar width; MC/LC: Medial condyle/Lateral condyle; AP/ML: Anterior-Posterior/Medial-Lateral; FHL/FHW: Femur head length/Femur head width (Image by author).

4.3 GM Data Collection: Photogrammetry

Photogrammetry was used to create the 3D models for the geometric morphometric analyses. Due to current technological advances in digital cameras, software, and computational techniques, photogrammetry has become a portable and powerful tool in producing dense and highly detailed 3D surface data. The key principle behind photogrammetry is to take multiple overlapping images of good quality (Falkingham 2012: 3). By applying orientation and transformations of digital photogrammetry, it is feasible to create 2D or 3D coordinates from one or more photos. This is an objective method that can be reliable with CAD software (Falkingham 2012: 5).

4.3.1 Acquisition of Photographs for Each Specimen: Photogrammetry Set Up

Photographs were captured with a DSLR Cannon 1200D with settings of an F-number of 10, ISO at 200, and shutter speed of 1/50. The larger F-number allowed for more of the bone to be in focus. The slower shutter speed of 1/50 ensured that the image was lit enough and the ISO number improved the camera's light sensitivity. The ideal lighting is when the object does not have harsh

shadows and is evenly lit. A table lamp was used as well as placing the object under a florescent light from the ceiling. This combination was able to provide a lit object with few shadows.

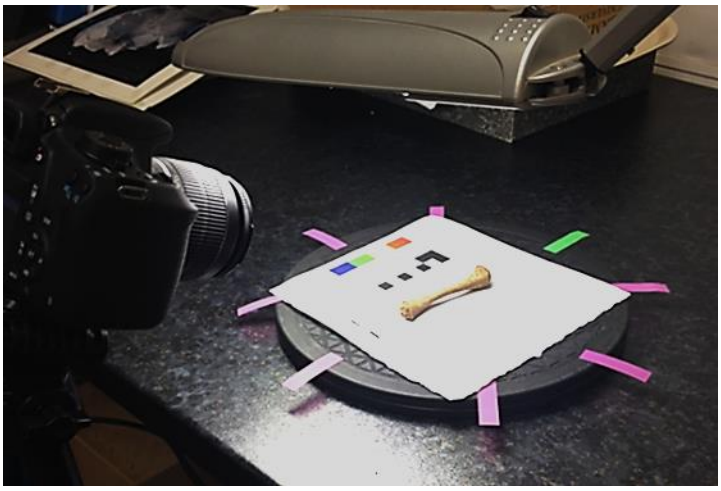

Figure 4.3: Photogrammetry set up with a foetus (Group 1) femur. The green tab marks the start of each series of photos and the purple tabs mark the 45^{o} intervals (Image by author).

As the bones were very small and cylindrical in shape there was not a lot of surface area to capture in each image, therefore it was best to divide the bone into two segments (anterior and posterior) and lay the bone on a turntable marked at 45^{0} intervals (Figure 4.3). It was more efficient to mount the camera on a tripod and use a turn table rather than move the camera as the images from the foetal bones were sensitive to slight shaking from holding the camera versus mounting it on a tripod. This allowed for more surface to be covered with each image as the bone was rotated, as well as a more reproducible set up that could be used for all angles and sides for each bone. Two scale bars were placed on the turntable to get a scale of the length and width of the object; this is needed for the final scaling of the model.

Each segment consisted of roughly 16 images (to make a full rotation every 45^{o}) and the camera was raised at 30^{o} intervals to capture the bone from three different angles. In short there were three sets of photos taken at different angles (at 30^{o} intervals), each set consisting of 16 images in a clockwise rotation for the anterior and posterior sides separately. This results in approximately 96-105 photos for each bone.

4.3.2 Building a Point Cloud

Once the images were taken they were edited with Photoshop and then imported into Agisoft Photoscan Pro (Agisoft L.L.C., 2013) to build the sparse and dense point cloud. Each image had the background masked and a sparse point cloud was created for each segment individually as each photo was lined up by their masks (Figure 4.4).

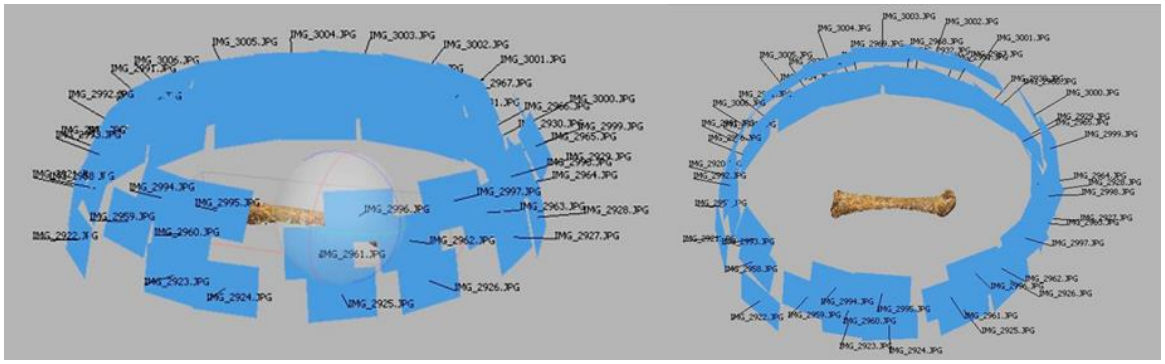

Figure 4.4: The sparse point cloud in Agisoft Photoscan of a foetus femur. Each blue square represents the photo taken from that viewpoint (Image by author).

There was significant overlap between the anterior and posterior segments, and the lower edges around both were edited to delete the bad data, such as shadows and the underside of the bone, that was captured in both point clouds. As this method relies on photographs, rather than a direct measure of XYZ positions found in laser scanning, the point cloud is scale-less. Therefore, once both segments were edited, a scale was added. This process involved using 2 distance points from both scale bars and inputting the distance in at least 3 photographs for each segment. The next step was aligning segments; this was carried out by visual inspection to see if they lined up and determine whether any more editing was needed. Once both segments were sufficiently aligned, they were merged and the mesh for the entire bone was created.

4.4 3D Geometric Morphometric Digitization

All GM digitization and analyses was done in R geomorph package (Adams *et al.* 2014) and auto3dgm. Procrustes (GPA), was used to align shapes and minimize differences between them so only real shape differences were measured (Bookstein 1996). For the 3DGM analyses, ten type I, II, III landmarks were used (Table 4.1 and Figure 4.5) as well as 100 semi-landmarks to describe the curves and surfaces between the fixed landmarks to provide the quantified long bone shapes (Bookstein 1996). The fixed landmarks are digitized onto each specimen and the template of sliding semi-landmarks are projected onto the remaining specimens. The template was created with Specimen 119 (Group 5: 9-12 years old) because it was found that creating a template of the semi-landmarks was easier to scale down with age rather than ‘grow up’. When using the foetal femur, the semi-landmark meshwork tended to slip off of the proximal end once the trochanters and femoral head began developing. Landmark placement was tested through an inter-observer error test which is found in Appendix A.2.

Landmark Points and Description		
Landmark	**Description**	**Landmark Type**
1	Lesser Trochanter	Type I
2	Capital surfaces (further down on femoral head)	Type II (maximum posterior curve)
3	Second trochanter	Type III (extremal point)
4	Greater trochanter surface (top peak)	Type II (maximum peak)
5	Anterior hollow	Type II (maximum curvature)
6	Flat Posterior border	Type III (extremal point)
7	Medial metaphyseal condyle	Type III (extremal point)
8	Lateral metaphyseal condyle	Type III (extremal point)
9	Lateral curve of midshaft*	Type II (maximum curvature)
10	Medial boarder of midshaft curve*	Type II (extremal point)

Table 4.1: Landmark descriptions for Geometric Morphometric Analysis

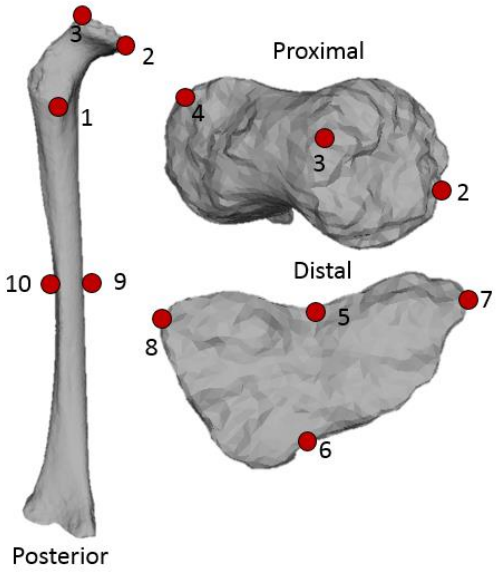

Figure 4.5: Landmarks used for the GM analysis taken from a 12 year old femur. *The maximum curvature of the femur was captured with landmarks 9 and 10. The femurs were oriented so landmarks 1-3 could be visible and facing straight forward (Image by author).

4.5 Auto3dgm Digitization

As discussed in Chapter 3.2.3, the package auto3dgm produces landmark datasets that can be analysed similarly to traditional GM landmark datasets. Unlike the tedious manual landmark placement of traditional GM studies, there is very little pre-processing for auto3dgm. Surface files are exported into Open file format (.off) which can be converted from .ply files in the free software MeshLab (Boyer *et al.* 2015).

The methodology of auto3dgm was developed by Puente (2013), and the input files are a set of surface mesh files in .off format. The user supplies a set of 'low and high resolution' versions of the mesh files that are used by the algorithm to generate summary images (Boyer *et al.* 2015). The parameters needed to run the analysis include: the number of points used to represent shapes in

the low resolution version of the alignment, the number of points to represent shapes in the high-resolution (or final version) of the alignment, and the number of principal alignments (typically this number is set to eight possible combinations of the alignments (Boyer *et al.* 2015). This thesis used 250 initial points and 300 final points (as surface sliders) with 8 principal alignments. The alignment of all 18 femora can be seen in Figure 3.9 and an inter-observer error test is found in Appendix A.3.

4.6 Question 1: Effects on Morphological Shape and Size

The first question '*is there an effect on morphological shape and size?*' is used to examine if each method can capture both size and shape of the juvenile femora. Chapter 2 and 3 demonstrated the close relationship between age and size for growth. However, allometry, the relationship between size and shape is rarely discussed in bioarchaeological studies, although it can demonstrate different tempos in growth and development both between and within population samples. The ratio data was analysed through a linear regression of shape (ratio) onto femur length. The GM studies were analysed through a similar technique but regressing shape through PCA scores onto centroid size.

4.6.1 Multivariate Linear Regression: Ratios vs Length

A Bonferroni adjustment was made to determine significance among ratios and femur length. The alpha level was set to 0.008 (0.05/6). Table 4.2 shows the only ratio with a significant correlation (p=0.001) to increasing femur size is the Femur Head Length by Femur Head Width (FHL/FHW) ratio. It is possible that the other variables do not contribute, as there is more overlap with one another in the model. These regressions show that there are changes in the proximal and distal regions of the femur; this is to be expected, as the femur becomes more load bearing. Figure 4.6 is a regression of the geometric mean of the ratios against the femur length. By using the geometric mean, a proxy of ratio data can be compared to the allometric plots for the 3DGM and auto3dgm data. It can be seen that Group 4 (6-8 year olds) are within ratio range of Group 5 (9-12 year olds) femora. Groups 1 (foetal), 2 (infant to 2 years old), and 3 (3-5 year olds) are within ratio range, despite differences in femur length. Although minor, there is an effect on shape as the femur increases in size, therefore the hypothesis that there is no effect on femur shape in relation to its size is rejected.

Multivariate Linear Regression: Ratios vs. Length				
Ratio	Slope	Intercept	R^2	p-value (0.008)
CCD/BW	-0.003	0.5527	0.1253	0.432
IN/BW	0.0002	0.1876	0.2179	0.375
MC/LC	-0.0002	1.0758	0.0122	0.540
IN/CCD	-0.0002	0.2652	0.5033	0.05
AP/ML	-0.0001	0.8877	0.0155	0.079
FHL/FHW	0.0022	1.266	0.535	**0.001**

Table 4.2: Multivariate Linear Regression of Ratios against femur length (mm). Femoral linear measurements (mm) of maximum lengths and widths used to compute ratios. CCD/BW: Cranial caudial depth/bicondylar width; IN/BW: Intercondylar distance/Bicondylar width; MC/LC: Medial condyle/Lateral condyle; AP/ML: Anterior-Posterior/Medial-Lateral; FHL/FHW: Femur head length/Femur head width.

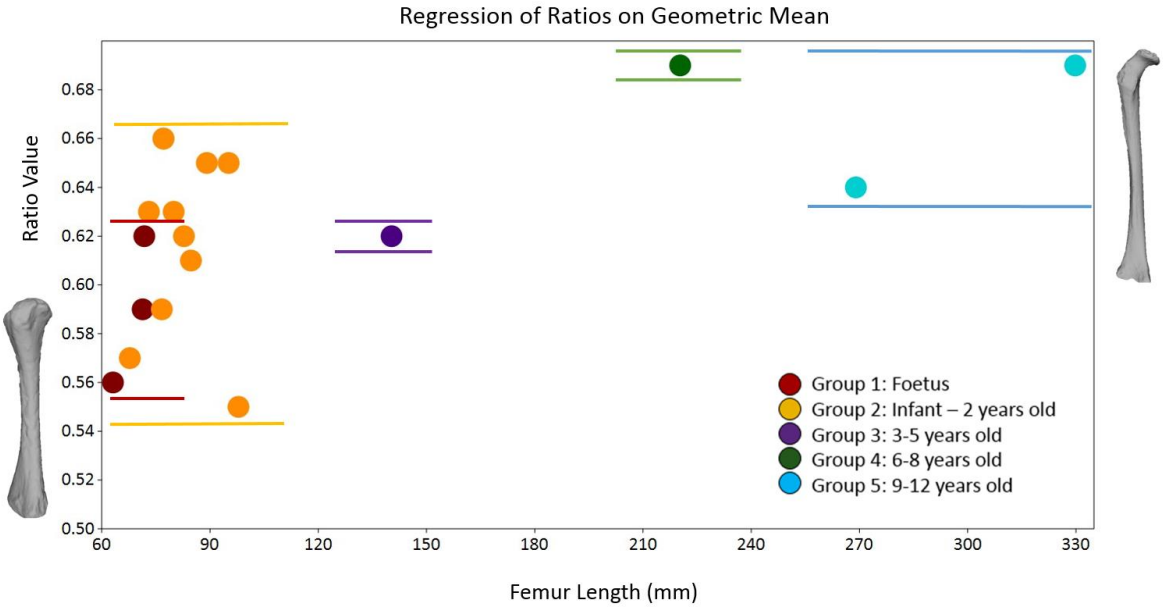

Figure 4.6: Regression ratios geometric mean against femur length (mm). Femoral linear measurements (mm) of maximum lengths and widths used to compute ratios. CCD/BW: Cranial caudial depth/bicondylar width; IN/BW: Intercondylar distance/Bicondylar width; MC/LC: Medial condyle/Lateral condyle; AP/ML: Anterior-Posterior/Medial-Lateral; FHL/FHW: Femur head length/Femur head width. The lines delineating the age groups of the femora reflect the variation of size and shape that are found within each age group.

4.6.2 3DGM: Allometry PCA (shape) by Centroid Size

The allometric function in geomorph R creates a plot that describes the multivariate relationship between size and shape from landmark data by performing a regression of shape on size (Figure 4.7). The allometric plot reveals that size and shape show a statistically significant relationship (p=0.01; Rsq= 0.42) with a steady increase in size and little change in shape development from infancy to one years old (Group 1-2). Once the development of walking (Group 3) is established, there is a significant increase in size with very little increase in shape morphology and robusticity. However, as walking becomes the primary form of movement (Group 4-5), there is a significant jump in shape development. This plot suggests that there is more variation in shape and size during

infancy. Once the bone becomes large enough (around 2 – 5 years old) and is used for more refined upright movement, there is a sudden increase in the development of shape. In conjunction with the ratio data, the geometric morphometric analysis also supports the rejection of the hypothesis, as there is a clear effect on shape with increasing femur size.

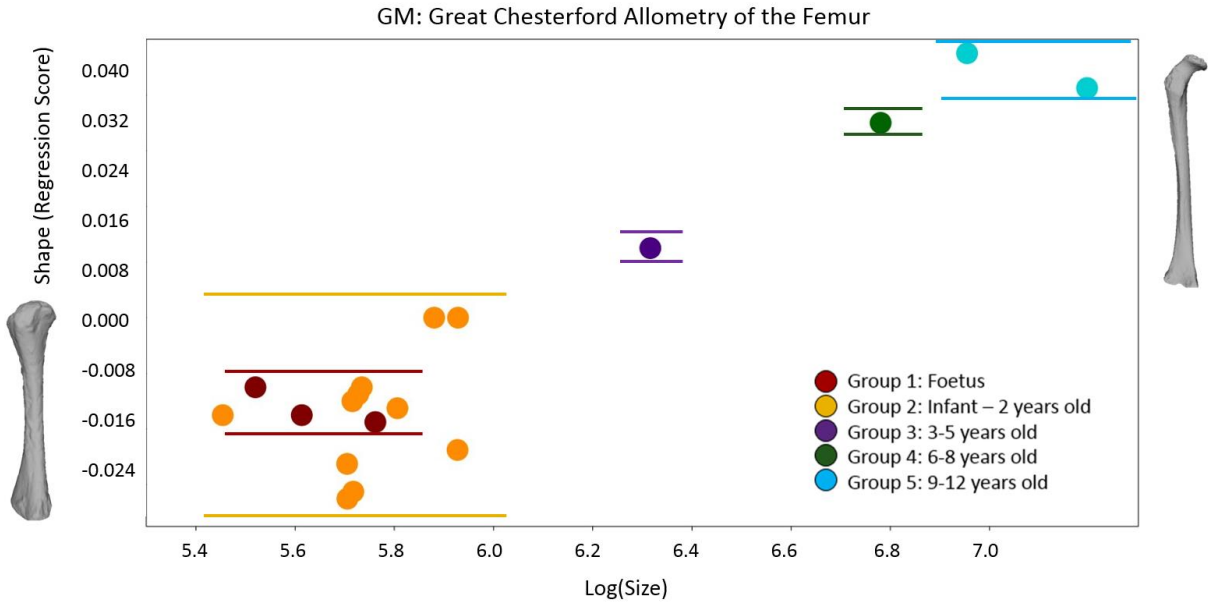

Figure 4.7: Allometric plot of principal component scores (regression score) against centroid size (log size) from traditional GM analysis of the Great Chesterford Femora. The lines delineating the age groups of the femora reflect the variation of size and shape that are found within each age group.

4.6.3 Auto3dgm: Allometry PCA (shape) by Centroid Size

The same allometric function that was used in 4.6.2 was applied to the auto3dgm shape analysis (Figure 4.8). The allometric plot shows a similar trajectory of statistically significant size and shape ($p=0.01$; $Rsq=0.31$). The largest range of variation comes with Group 2 (infant to 2 years old), which is to be expected as it has the most specimen in this age category and represents the most varied range of movement (crawling to walking). There is a clear increase in femur size followed by shape with an increasing tempo until Group 3 (3-5 years old) and a slowing in shape variation for Groups 4 and 5 (6-12 years old). Similarly to the ratio data and traditional geometric morphometric analysis, auto3dgm rejects the hypothesis, as there is an effect on femoral shape with increasing size.

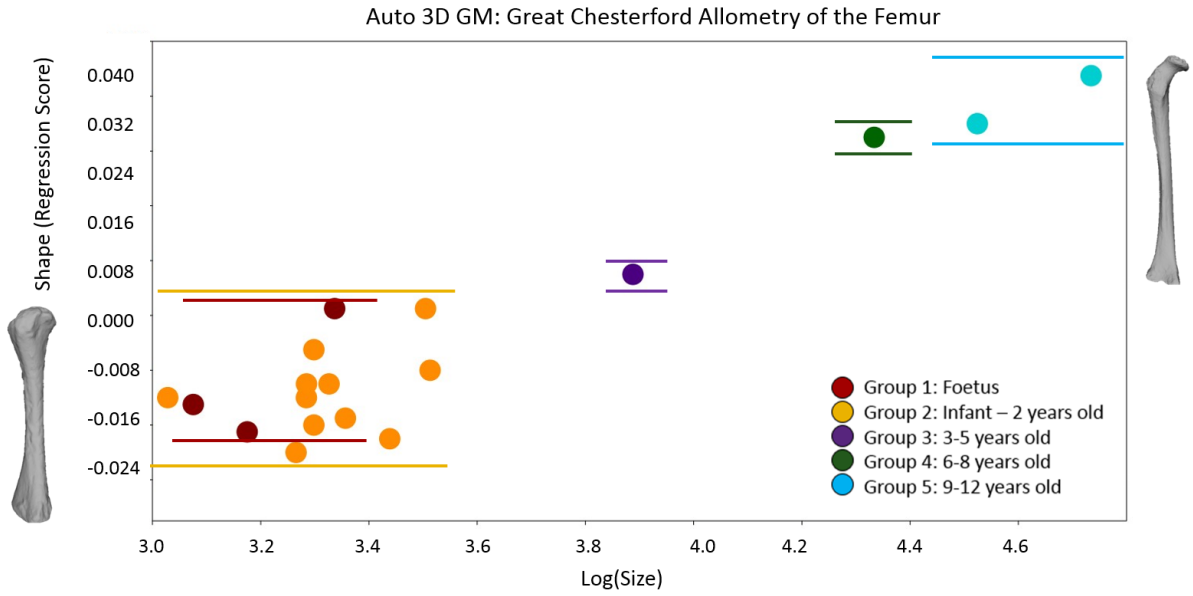

Figure 4.8: Allometric plot of principal component scores (regression score) against centroid size (log size) from auto3dgm of the Great Chesterford Femora. The lines delineating the age groups of the femora reflect the variation of size and shape that are found within each age group.

4.6.4 Discussion: Is there an Effect on Morphological Shape and Size?

The ratio, 3DGM, and auto3dgm analyses revealed significant differences in femoral shape and its relationship with size. The multivariate linear regression of ratios and femur length showed that the proximal region of the femur, Femur Head Length by Femur Head Width (FHL/FHW), exhibited the only statistically significant variation against Femur Length ($p<0.001$). The regression equation only found a small correlation with the ratio of Femur Head Length by Femur Head Width (FHL/FHW: 53%), while the other ratios were weak. This pattern is supported by the allometric plot in both traditional GM and auto3dgm, which includes both size and shape of the juvenile femora. Interestingly, the main differences between the GM analyses is auto3dgm grouped the last two age groups of 6 to 12 year olds (Groups 4 and 5) (Figure 4.8). This could be a result of the different scaling seen in Figure 4.7 and 4.8. Auto3dgm used 300 pseudolandmarks while 3DGM used 10 landmarks and 100 semi-landmarks. It is possible that auto3dgm captured more of the surface mesh that was missed with the 3DGM landmark and semi-landmarks. The additional 'points' or pseudolandmarks were able to find that Group 4 was in size and shape range of Group 5. The rest of the allometric trajectories show similar patterns between the two GM analyses as Groups 1 and 2 have a wide range of shape variation. Group 3 (3-5 years old) is separated from the first stages (foetus to 2 years old), while the later stages (6-12 years old) represents a period of 'catch-up' in development (shape). This trend suggests that the femur grows more in size and then shape changes in response.

The results from the current study are in agreement with studies suggesting that the elongation of the femur precedes its diameter or robustness (Bass *et al.* 1999; Bradney et *al.* 2000; Pujol *et al.* 2014; Rauch *et al.* 2001) as mass and muscle strength are important for overall bone robusticity (Moro *et al.* 1996; Pujaol *et al.* 2014; Schoenau 1998; Schoenau *et al.* 2000; Van der Meule *et al.* 1993). Results from the ratio and GM analyses with respect to Question 1 showed that both size and shape vary significantly during this period. In addition, the GM studies showed a large shift from group 3 (3-5 years old) to groups 4 and 5 (6-12 years old) which could be a result of a post-weaning period. It is possible that the children from Great Chesterford had a conservative period after weaning and, once the dangers had passed, there was a 'catch-up' in developmental shape. Another possibility is that children reflect adult-like walking patterns by age 5 (Gosman *et al.* 2013: 783) (Group 3) and it is possible that the refinement of this new mobility results in increased morphological development and robusticity of the femur. These interpretations are difficult to prove with a small sample size, however, they warrant further investigation.

The ratio and both GM tests show that as the femur increases in size, changes in shape follow. The regression analysis of the ratio data revealed that femoral head (Femur Head Length by Femur Head Width (FHL/FHW)) is the only region that changed significantly with size. The GM data did show clear changes in tempo as this encompasses whole bone shape against whole bone size, whereas the ratio data had overlapping measurements which contains less geometric information of the long bone shape.

4.7 Question 2: The Effect on Femur Morphology in Response to Mechanical Loading

The analyses conducted in response to Question 1 demonstrated that there was an effect on femur size and shape for all three methods The second question is now '*what is the effect on femur morphology in response to mechanical loading?*' seen by age groups. The second question will determine the sensitivity of capturing and analysing shape by age from all three methods.

4.7.1 MANOVA of Ratios: Ratios and Age

To test if the ratio shape data was statistically significant by age group, a multivariate tests analysed the significance of the ratios between ages and a principal component analysis (Figure 4.9) determines which ratio contributes the most to femoral shape variation. As this sample is small with unequal n values, Pillai's trace is used instead of Wilk's Lambda (Gould 2014). Although non-

significant (p<0.066), Pillai's value of 2.396 shows a tendency towards a relationship between ratios and age.

A Bonferroni adjustment was made to determine statistical significance among ratios and femur length. The alpha level was set to 0.008 (0.05/6). Table 4.3 demonstrates that the variables that exhibit significant change by age are the Medial Condyle by Lateral Condyle (MC/LC: p= 0.004) and Femur Head Length by Femur Head Width (FHL/FHW: p=0.004). The principal component analyses confirmed these findings as PC1 (64%) represented variation in the femoral head length by width (loading: 0.90648). The second principal component axis (29%) represents variation in the Medial Condyle by Lateral Condyle which was also found to be statistically significant. The partial ETA squared represents the proportion of variance for the ratios that is explained by age. MC/LC (0.675) represents 67.5% of the variance of age group while FHL/FHW (0.677) represents 67.7%. This test also rejects the hypothesis that there is no effect on femur morphology in response to mechanical loadings, as seen in the distal region of the knee joint (MC/LC) and the proximal region of the hip joint (FHL/FHW).

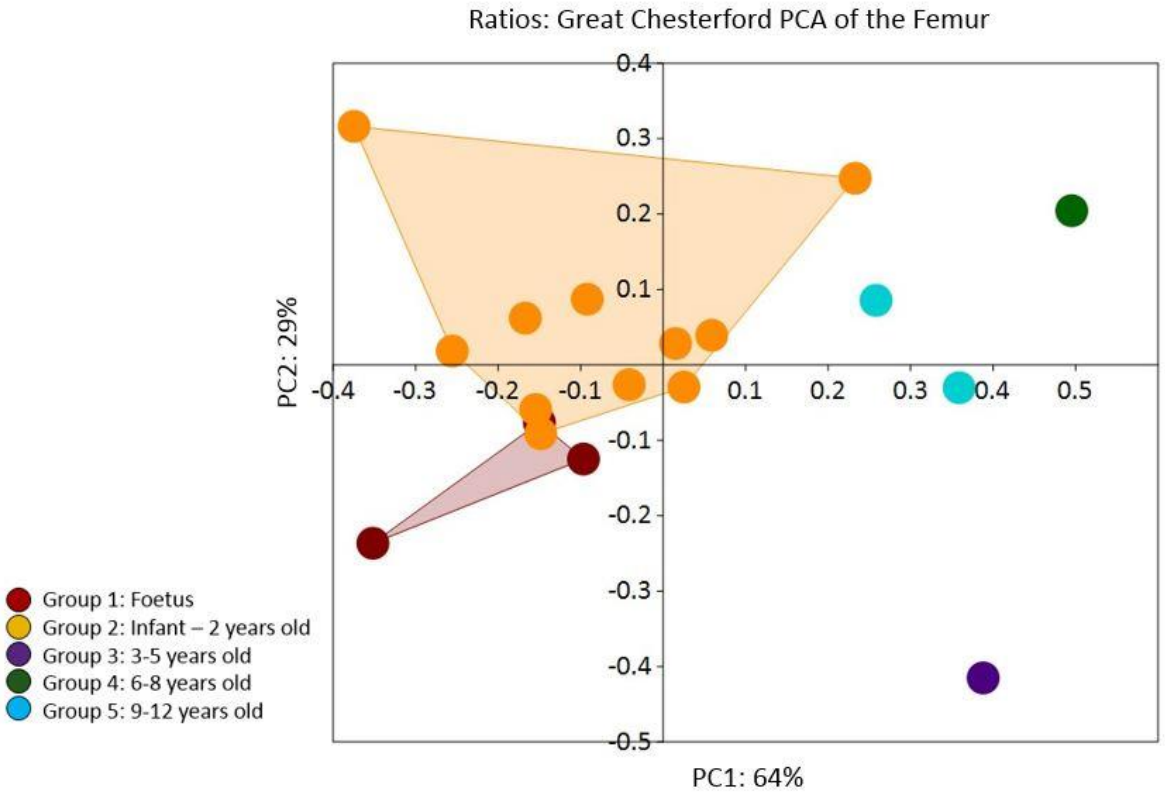

Figure 4.9: Principal Component Analyses of Femur ratios by age group. PC1 represents 64% of all ratio variation and PC2 represents 29% of all ratio variation.

MANOVA: Ratios and Age						
Ratio	F	R^2	p-value (0.008)	Partial Eta Squared	PC1 Loadings	PC2 Loadings
CCD/BW	3.862	0.402	0.028	0.543	-0.18316	-0.017192
IN/BW	1.273	0.060	0.330	0.281	0.065445	-0.034674
MC/LC	6.743	0.575	**0.004**	0.675	-0.22352	**0.95724**
IN/CCD	4.021	0.415	0.025	0.553	0.29764	-0.058232
AP/ML	0.634	0.094	0.647	0.163	-0.043749	0.1074
FHL/FHW	6.800	0.577	**0.004**	0.677	**0.90648**	0.25937

Table 4.3: MANOVA of Ratios and Age to determine if shape is represented by changes in locomotion. Femoral linear measurements (mm) of maximum lengths and widths used to compute ratios. CCD/BW: Cranial caudial depth/bicondylar width; IN/BW: Intercondylar distance/Bicondylar width; MC/LC: Medial condyle/Lateral condyle; AP/ML: Anterior-Posterior/Medial-Lateral; FHL/FHW: Femur head length/Femur head width.

4.7.2 3DGM: Generalized Procrustes by Age (PCA and ANOVA by Age)

The GM test underwent a PCA and an ANOVA by age group. In Figure 4.10, Principal Component 1 represents 42% of all shape variation of the femur, while Principal Component 2 represents 15%. The same trend with the ratio data is seen in the GM results as most shape development occurs in the proximal and distal metaphyses (as illustrated in the thin plate splines for each PCA quadrant). However, the PCA also shows that there is a slight curvature in the midshaft with older juveniles as a result of increasing loading and movement.

Plotting positively on PC1 are foetuses to 5 year olds (Groups 1, 2, and 3). The thin plate spline (TPS) for this quadrant shows slight deformation in the curvature of the proximal femur along the neck, with little change along the proximal metaphyses and the splitting of the trochanters. Substantially more warping or robusticity is seen from the neck to the proximal end of the midshaft, with little change along the distal metaphysis which remains relatively flat. A slight depression in the proximal head is seen, yet not as distinct as the splitting of the trochanters in those plotting negatively along PC1.

Femora plotting negatively on PC1 are the 6- 12 year olds (Groups 4 and 5). There are substantial changes in shape occurring along the proximal metaphysis and neck, as the curvature in the neck angle becomes more pronounced, and the development of the second trochanter on the metaphysis starts. There is also some slight warping in the lateral metaphysis which represents the development of the metaphyseal angle increasing with bipedal movement. The TPS shows more angling of the shaft as it curves medially and begins to warp along the distal end.

Plotting in this area, negative PC2 is made up of Groups 1, most of 2, and 4 (which has very little deformation in this quadrant and reflects more gracile shapes). There is slight lateral curvature in the distal metaphysis (TPS), representing slight changes in the metaphyseal angle. Those plotting positively on PC 2 is made up of Groups 3, 5, and some 2. The majority of deformations are seen in the neck, and proximal shaft curvature and distal metaphyseal angle. This could be a result of remodelling as a 'catch up' in length, rather than shape, as was seen in the allometric plot (Figure 4.7) in Question 1.

Similar to the ratio data analysis, the Procrustes ANOVA reveals a significant relationship ($p<0.003$) between femur shape and age group. The 3DGM ANOVA, however, also provides a pairwise comparison function, which identifies shape among groups and displays how similar the mean shape of each femur is between groups. The matrix in Table 4.4 shows the significant values between individual group shapes. Anything that is not significant ($p>0.05$) can be confused with another group shape in the morphospace (Collyer *et al.* 2015). Groups 1-3 appear similar, which may reflect the transitional stage of crawling to walking in Group 2.

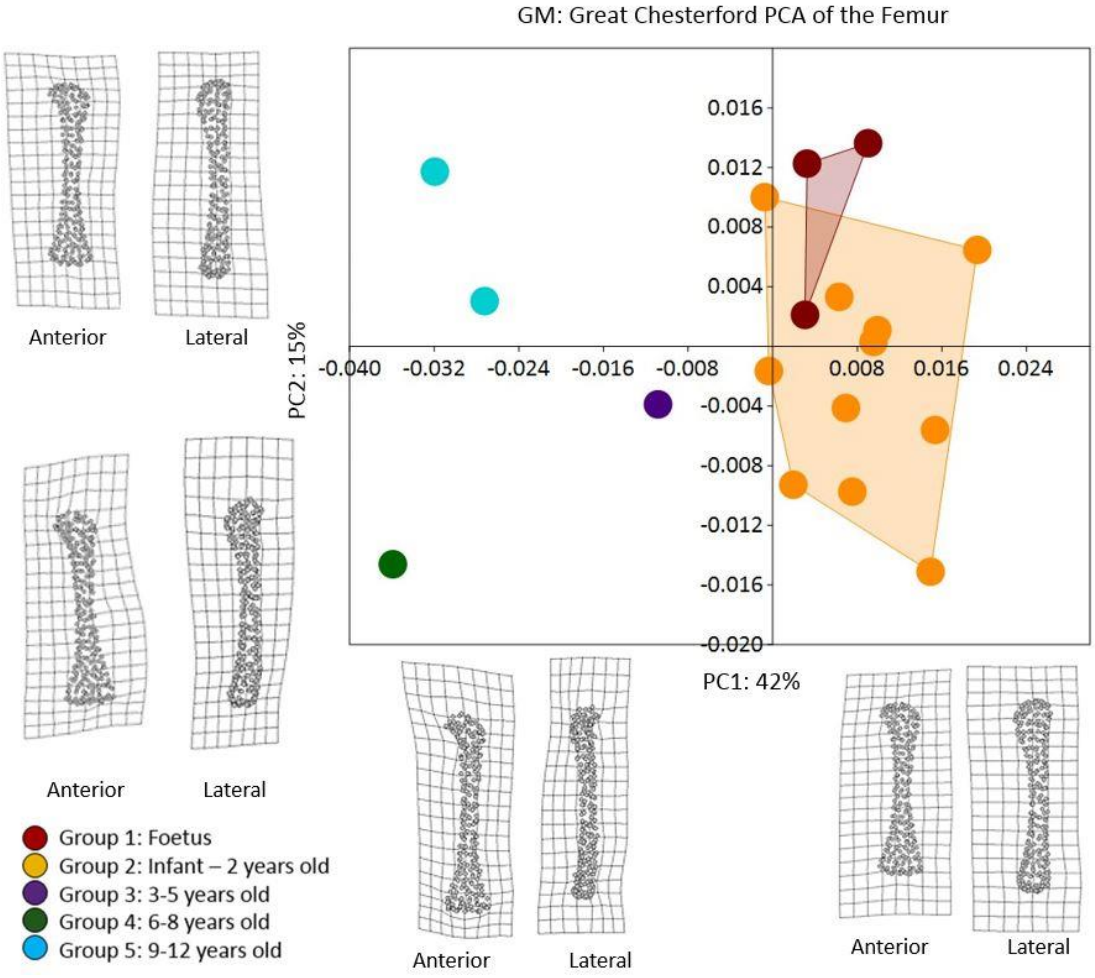

Figure 4.10: Principal Component Analysis of femur shape by age group. PC 1: 42% of all shape variation and PC 2: 15% of all shape variation.

Procrustes ANOVA: Femora by Group (p < 0.03)					
Prob.dist	1	2	3	4	5
1	1.000	0.121	**0.003**	0.058	**0.017**
2	0.121	1.000	0.746	**0.048**	**0.030**
3	**0.003**	0.746	1.000	**0.044**	**0.044**
4	0.058	**0.048**	**0.044**	1.000	**0.047**
5	**0.017**	**0.030**	**0.044**	**0.047**	1.000

Table 4.4: Procrustes ANOVA of femur shape by age group shows a statistical significance (p<0.03). Pairwise ANOVA displaying significance (p-values) of mean shape by groups.

4.7.3 Auto3dgm: Generalized Procrustes by Age (PCA and ANOVA by Age)

The auto3dgm analysis produced similar results to the 3DGM analysis (section 4.7.2). The Principal Component Analysis in Figure 4.11 shows similar patterning to Figure 4.10. Principal Component Axis 1 represents 40% of all shape variation and 20% on Principal Component Axis 2. As Group 2 has the most specimens, it is not surprising that this group has the most shape variation along the PC1 and PC2 Axes. Plotting positively for PC1 are foetuses (Group1) and infant to 2 year olds (Group 2). The TPS for this quadrant is more warped than the traditional 3DGM analysis in Figure 4.10, with changes occurring on the lateral metaphysis and slight curvature in the femoral neck.

Femora plotting on negative PC1 include some Group 2 specimen (infant to 2 years old) and Groups 3 to 5 (3 to 12 year olds). There is extensive warping in the shapes found in this quadrant (negative PC1) compared to negative PC1 in Figure 4.11. The majority of shape deformation is in the metaphyseal angle of the distal metaphysis and the developing trochanters in the proximal metaphysis. These hip and knee developmental shapes are reflective of walking patterns as more loading is placed on these joints.

The negative PC2 shows similar shape deformations to positive PC1 as more shape is occurring in the lateral condyle of the distal metaphysis and more deformation in the femoral head. Only half of the Group 2 (and all of Group 3) specimens are in this quadrant which may represent the transitional phase of early walking and upright movement as there is more loading in the knee and angling in the hip. Positive PC2 is where Group 4-5 femora (6 to 12 year olds) and half of Group 2 are plotted and reflect more deformation and robusticity in the proximal and distal metaphyses and the midshaft, which coincides with refined upright movement.

Similar to the ratio and traditional 3DGM analysis, the Procrustes ANOVA for auto3dgm found a statistically significant relationship (p>0.03) with femur shape and age group (Table 4.4). The pairwise matrix (Table 4.5) found a different pattern than the traditional GM analysis (Table 4.5). In

this instance only Group 2 was statistically significant from all groups. This could be a result of unequal sample sizes as this group was the largest and captured an age range of a variety of moments (stationary, crawling, and walking) which are not seen in the other age groups.

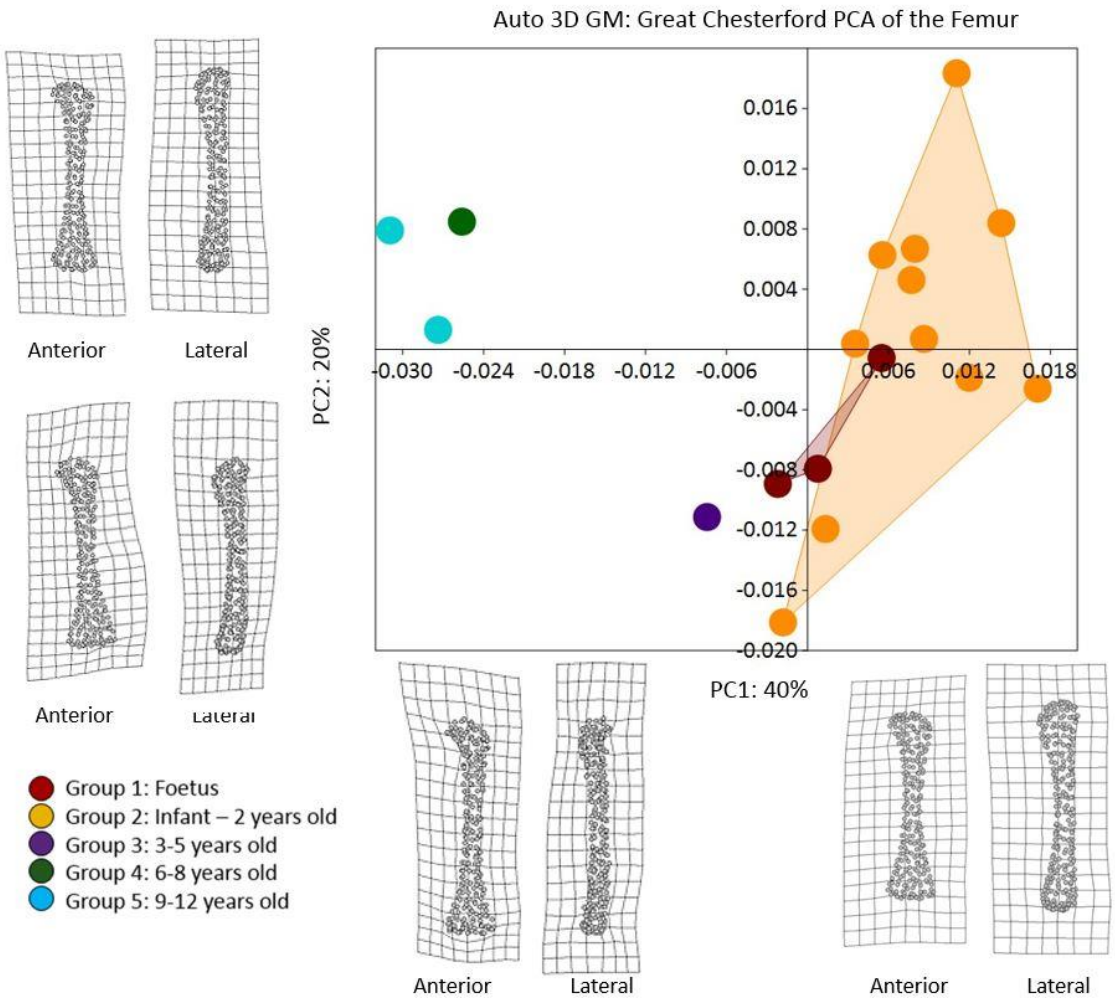

Figure 4.11: Principal Component Analysis of Femur shape by age group for auto3dgm. PC1: 42% of all shape variation and PC2: 18% of all shape variation.

Procrustes ANOVA: Group p< 0.03					
Prob.dist	1	2	3	4	5
1	1.000	0.008	0.842	0.842	0.966
2	0.966	1.000	0.001	0.001	0.026
3	0.857	0.001	1.000	1.00	0.612
4	0.857	0.001	1.00	1.000	0.612
5	0.008	0.026	0.612	0.612	1.000

Table 4.5: Procrustes ANOVA of femur shape by age group. Pairwise ANOVA displaying significance of mean shape by groups.

4.7.4 Discussion: What is the Effect on Femur Morphology in Response to Mechanical Loading?

The ratio (FHL/FHW and MC/LC: p=0.004) for the linear measurement study and the Procrustes ANOVA (p=0.03) for both GM studies showed that there was a significant change in morphological shape in the proximal and distal regions of the femur associated with age and locomotion. The Great Chesterford children, from foetal to 2 years old (Groups 1 and 2), show more emphasis on the curvature of the proximal femoral neck (Figure 4.10 and 4.11: PC 1) but very little morphological change in the proximal head as there was no clear distinction of the splitting of the trochanters. It is only with the auto3dgm (Figure 4.11) that shows a slightly more varied range of morphological shape with the Group 2 (infant to 2 years old) femora. This split may represent the changes in locomotion where some Group 2 (infant to 2 years old) individuals are within shape range of Group 1 (foetus). The other Group 2 (infant to 2 years old) and Group 3 (3-5 years old) individuals reflect similar, yet less defined diaphyseal curvature, to the older age groups of 5 to 12 years old.

The age groups from 6-12 years old (Groups 4 and 5), show a much more substantial change in shape occurring along the femoral head, neck, and metaphyseal angle, as the curvature in the neck is more pronounced and the second trochanter begins to form along the metaphysis. These morphological changes are in agreement with studies by Pujol *et al.* (2014) who studied the ontogeny of known male and female femora of modern Spanish children with 2-dimensional GM. The metaphyseal angle is the skeletal feature that permits the adduction of the lower limb in humans. The metaphyseal angle allows the knee and ankle joints to be placed under the centre of gravity of the body, making the human displacement more economical, as the load transmitted by the lower limbs is close to the vertical axis of gravity to the body during the phases of walking and running. This angle undergoes major transformation from the beginning of locomotion to 8 years old, and continues until 12 years old (Pujol *et al.* 2014; Tardieu & Damsin 1997). This patterning in metaphyseal angle is seen in the auto3dgm (Figure 4.11) TPS for Groups 4 and 5 which suggest more loading occurs in these two groups.

The pairwise analyses for both GM studies (Table 4.3 and Table 4.4) show that not all groups are statistically different from one another. This displacement of a non-linear morphological development could be a result of remodelling as there is a 'catch up' period in overall size of the femur rather than shape. This is consistent with relevant studies (Gosman *et al.* 2013; Pujol *et al.* 2014) as the size and shape of the trochanters are related to the increase in mass of the gluteus maximus, gluteus minimus (greater trochanter) and pectineus (lesser trochanter) muscles, as these

are actively used in locomotion and stabilization of the femoral-pelvic and femoral-tibial joints (Pujol *et al.* 2014: 8).

The distal epiphyses and metaphyses react to mechanical loads as a result of changes in angulation of the femur. Pressures generated in the bicondylar region cause this shape modification. Stress exerted by the different muscle groups, as well as the patella, create an asymmetrical load in the condyles, while focusing the force mainly on the medial condyle. This causes more robusticity and angulation of the distal femur (Shefelbine *et al.* 2002). This is seen with the Great Chesterford children from foetal to 2 years old (Groups 1 and 2) as there is very little change to the distal metaphysis, and this has very little depth in the condyle region. There is some angling along the metaphysis, with slight curvature along the distal shaft. The older children, of 6 to 12 years old (Groups 4, 5), show more warping and depth in the lateral metaphysis; this is expected as the metaphyseal angle increases to an adult gait pattern by this age (Gosman *et al.* 2013: 783).

It is possible that with an improved sample size there would be more data to determine mean femur shape for each group and this might help tease these groups apart. Unlike size and growth, development in shape is not necessarily linear. There is more plasticity in the morphology of the juvenile limbs and this is better captured with GM. The auto3dgm analysis showed similar patterning to traditional GM methods. The main difference, however, was a larger range of variation with the Group 2 juveniles which may reflect the transition from possible crawlers to possible walkers (as seen in differences of the TPS quadrants in Figure 4.11). The TPS were also more detailed and revealed a clearer picture on the variation of shapes found in this sample. Additionally, the larger variation may be an artefact of more individuals found in Group 2 than the rest of the Groups.

4.8 Concluding Remarks

The aim of this chapter was to determine if long bone shape could be captured with GM. The first objective of this chapter was to determine the relative effectiveness of traditional multivariate analysis, based on linear measurements versus 3D geometric morphometric, and automated geometric morphometric analysis of the entire femur morphology. This study, like Gould's (2014) of adult distal femur morphology in mammals, shows that all three methods uncover significant patterns of morphological variation of the femur. The graphical outputs of the GM studies however, can be related to qualitative descriptions of morphological differences. These differences form the basis of much comparative anatomical work that is found in morphological studies (Mitteroecker *et al.* 2005; O'Higgins & Jones 1998; Strand Viðardóttir *et al.* 2004). GM methods also permits the

inclusion in analysis of biologically interesting but difficult to measure aspects of variation, such as changes in curvature and outline (Gould 2014: 9-10).

Gould (2014: 10) noted that ratios do not attempt to quantify many aspects of shape contained in the GM analysis. This is a result of the limitations of calliper measurements as there are only so many measurements that can be reliably taken from the femur. Linear measures and traditional GM landmark techniques also represent predetermined choices by the investigator as to which aspects of shape they consider relevant to the question (Zelditch *et al.* 2012: 61). The addition of semi-landmarks however, does not make the same assumptions as linear measurements about what aspects of shape are to be considered most relevant to the question, but instead reveal aspects of shape. Auto3dgm takes this essential difference between user subjectivity of linear and landmark placement even further by removing all user predetermined choices (Terhune 2013).

4.8.1 Biological Significance of Automated Pseudolandmarks

The main difference between pseudolandmarks and traditional landmarks is that points associated with a particular feature (i.e. the second trochanter or the linea aspera), or an articular surface on one bone, may not be located on those features in another bone. This may cause friction with some morphologists if they feel that they know the foramen is homologous between two taxa or samples, but the algorithm does not find the correlation of these landmarks (Boyer *et al.* 2015: 272). For the current study of slender cylindrical femora, auto3dgm eliminated the ambiguity of finding appropriate landmarks that captured the complete specimen and that could be repeated across a sample dataset. Although there is no current error test for auto3dgm (Boyer *et al.* 2015), the 3D GM landmark test (Appendix A.2) showed varying landmark placement replicability by the user over three intra-observer tests. Auto3dgm was run on three separate intra-observer tests (Appendix A. 3) and it is seen that there is no difference in the plotting of specimen for each PCA plot.

Comparisons between 3DGM and auto3dgm found similar results with the allometric and principal component analyses of the juvenile femur. Auto3dgm displayed a slightly larger variation of shape for the largest group (Group 2). Nearly half of the individuals plotted with Group 4 and 5 juveniles in PC2, which reflected more deformation in the proximal and distal metaphysis and midshaft, which coincides with refined upright movement. Another possibility for the difference in clustering between traditional and automated approaches is the sensitivity to errors caused by noise in the surface mesh (Boyer *et al.* 2015: 37). Boyer and colleagues (2015:37) found this to be the case as some of their clustering errors of traditional and automated approaches occurred as a result of

small and unequal sample sizes and less surface detail found in some specimens which were misclassified with the auto3dgm method.

4.8.2 The Curse of Dimensionality

In both statistics and machine learning, the difficulty of modelling high-dimensional data is commonly referred to as 'the curse of dimensionality' (Boyer *et al.* 2015:273, Wilson & Humphrey 2017: 42-43), an issue that is also prevalent in many areas of biology where there are large numbers of variables (v), and v is often much larger than the number of samples (n) (Wilson & Humphrey 2017: 43). Capturing surface geometry with hundreds of landmarks leads to n<v, as seen with the current studies dataset. Another issue with large matrices of landmarks is the propensity to oversample morphology. In this context, oversampling refers to separate landmarks that are recording the same traits on a 3D model. Wilson and Humphrey (2017:43) described this as a hypothetical dataset of 500 landmarks, in which 'feature A' varies independently of other landmarks in the data set, and five landmarks are used to capture its morphology, accounting for a small part of the variance. Instead of using 5 landmarks, say 20 landmarks are used to describe feature A (Wilson & Humphrey 2017: 43).These 20 landmarks would now vary independently, adding more covariance with feature A without changing the variance in any of the other landmarks in the data set. In this example by Wilson and Humphrey (2017: 43), the sampling of a feature is likely to have an effect on the total variance in the data set and also the weighting of one feature relative to another. While this issue might be relatively straightforward to identify in small data sets such as the current study, pinpointing the source of oversampling in large landmark data sets (1000s landmarks) is more challenging and controlling it in automated landmarking algorithms has yet to be attempted (Wilson & Humphrey 2017:43).

A further limitation to this study is the small and unequal sample sizes from the Great Chesterford collection. There are only one or two individuals representing the last three age Groups (3 to 12 year olds) which will skew the results and interpretations. The aim of this chapter however, was to determine the logistics and the practicality of quantifying shape of juvenile femora from archaeological collections, thus, Great Chesterford represents a realistic dataset with extensive taphonomy. This makes an ideal collection to test if GM can work on such datasets and how these results confirm or deny previously accepted hypotheses of shape by systematically testing three methods of shape quantification.

4.8.3 Moving Forward

Clearly, there is no silver bullet: there is no perfect methodology. Three-dimensional analysis using GM has certainly become more user friendly, yet it is still much more labour-intensive than caliper measurements. The linear measurements for this study took on average 15 minutes (including repeating two times), while the three-dimensional models took up to 5 hours from start to finish. Each surface specimen in this analysis is represented by a vector of roughly 90,141 vertices, which makes these datasets extreme from a statistical point of view. The advances in geometric morphometrics have undergone many changes to cater to large multivariate datasets, and the field is currently growing towards the application of more varied techniques for geometric morphometric analysis (Slice 2007: 273), such as the addition of auto3dgm.

The criticisms presented at the start of this chapter regarding all approaches are valid. For instance, the time invested in not only creating the digitized bones, but carrying out the GM analyses, is significantly more demanding than the use of traditional measurements. The automated approach requires less user digitization of landmarks, however it did take 2 hours to align this sample dataset. This can simply run in the background of the user's computer, however this time commitment should be noted in terms of larger and more computationally complex datasets. Thus, linear measurements may be more suitable for specific questions or if time is a limiting factor as the results are similar, although GM methods are more sensitive in capturing whole bone shape. An advantage of three-dimensional data however, is that it allows the researcher to take the virtual collection with them so they can spend more time on analyses.

This study has determined that auto3dgm is more beneficial than the ratio and traditional 3DGM methods as it was able to shed light on how the femur develops and grows as a whole structure and was able to give more detailed analyses in the allometric (Figure 4.8) and PCA (Figure 4.11) plots. This fundamental advantage of 3D models and GM-based approaches over a selection of discrete aspects of morphology which are treated as independent features is the drive to continue exploring GM in juvenile long bones (Wilson & Humphrey, 2017: 40). The ability to automate data collection improves the efficiency of processing time, reduces observer error, and increases the accessibility of a method for non-specialist users (Wilson & Humphrey 2017: 41). Research questions can now be redesigned to explore aspects of bone morphology that differ between ages or sample populations, rather than by how much does 'trait 1' differ between ages or regions (Wilson & Humphrey 2017:41).

Although both GM analyses took 2 hours to digitize, the essential difference was the automated alignment in auto3dgm which could run in the background. This eliminated any subjectivity in the landmark placement and required less 'hands on' time for the user. It was also able to identify interesting patterns of overlapping shapes and highlight possible conservative periods of development. Chapter 2 reflected on the intricate nature of juvenile development and growth and GM has provided a more sensitive and forgiving method to capture these ontogenetic trajectories. Although the questions of this validation study (*Is there a morphological effect on shape and size?'* and *'what is that effect?)* are fairly complex, it answered a crucial question which is '*can this method even be used for juvenile long bones?*' This methodological study of linear and GM analyses confirmed previously understood concepts of allometry and biomechanical features of the femur. This permitted validation of the technique, and it can thus be used to answer more complicated questions regarding different sample populations ranging from Anglo-Saxon to Post-Medieval periods in the UK. To do this, a larger set of data was collected and the question of *'what is the most cost-efficient data collection method?'* posed itself. To cope with this, Chapter 5 tests several scanning methods to determine a more efficient means of digitization and to test how much surface meshes from different scanning methods influence the automated alignment of the auto3dgm method.

5. Comparison of Scanning Methods

As 3D documentation and preservation of archaeological datasets moves to more open sourced data, there is a need to explore the sensitivity of these digitization methods and their analytical robustness. This chapter explores three different non-contact scanning techniques; FARO laser scanning, structured-light-scanning (SLS), and Photogrammetry to determine if and how financial and labour costs, resolution, and scan quality affect 3D GM analysis.

The Chapter 4 validation study on the application of GM to juvenile long bones demonstrated that auto3dgm is the most effective method for capturing and quantifying patterning of shape changes. Auto3dgm relies heavily on scan quality to align specimens for the GM analyses. This raises the question *'do the visible differences in morphological shape change by scanning technique?'* An overview of the benefits and drawbacks of each scanning method (FARO laser scanning, SLS, and photogrammetry), in terms of image and data quality, costs (both financial and time), and applicability to capturing changes in shape with GM analysis, are assessed. This rigorous testing was designed to determine which method is most suitable for the main research data collection and analysis, in order to eliminate any uncertainty as to whether the results are from the actual morphology of the bones or the scanning method.

5.1 Excavating the Data Mine: An Overview of Digitization Processes in Archaeology

Digital technologies have been adding value to archaeological research by diminishing barriers to access and providing researchers with the ability to re-examine, compare, and integrate primary sources from a variety of collections (Limp *et al.* 2011; Selden *et al.* 2014). Three-dimensional scanners have been available for decades, but they have only recently made their way out of engineering laboratories and into the hands of biologists, anthropologists, and archaeologists in museums and universities (MacLeod 2008). As digital recording methodologies are becoming more integrated into archaeological excavation and curation, it was not until the early 2000s, that the application of GM for shape analysis been considered as another possible toolkit for assessing patterns in biological and cultural contexts.

It was only after the 2000s that more inexpensive laser, mechanical and optical 3D digitizers were available, which led to a burst of new algorithms and procedures that could take advantage of these complex geometric datasets. Bioarchaeological and zooarchaeological studies have experimented

with 2D and 3D methodologies to explain morphological variation in ontogenetic, sexually dimorphic, and taxonomic phenomena seen in the archaeological record (Polly & MacLeod 2008; Wilson *et al.* 2008, 2011; Frelat *et al.* 2012; Terhune 2013). Dissemination and access to the GM toolkit in these fields is owed to the close proximity of their anthropological cousins who have been utilizing GM for the past three decades to look at form and function, development, and taxonomy (Bookstein *et al.* 1999; O'Higgins & Jones 1998; Strand- Viðarsdóttir *et al.* 2002). Although, the application of three-dimensional scanning is not new to archaeology or bioarchaeology, it was not until Selden and colleagues (2014), broached the subject that there is more to just scanning and recording 3D artefacts or specimens for documentation. Selden *et al.* (2014) raises many important questions regarding how digital images can be expanded past recording techniques and incorporated into analytical research projects through the use of GM. The ability to use different scanning methods without compromising quality of data, as this Chapter tests, will allow for more researchers to examine morphological variability in biological and cultural contexts.

5.2 Materials for Comparison of Scanning Methods

The skeletal material used for this scanning test comes from the Anglo-Saxon site of Great Chesterford. Five left sided femora were chosen, one from each age category described in Chapter 4 (Group 1: Foetal, Group 2: Infant to 2 years old, Group 3: 3 to 5 years old, Group 4: 6-8 years old, and Group 5: 9-12 years old). Each specimen was digitized through photogrammetry, SLS, and laser scanning. The technical aspects of time and cost were documented for each method. Scan quality was assessed though cloud compare and GM analysis to determine if there was statistical difference between scanning method. As discussed in Chapter 4, photogrammetry is the most accessible method of digitization. Structured-Light-Scanning is becoming a more common method for digitizing data, it can be a faster method than photogrammetry and more inexpensive than laser scanning. Laser scanning is the most accurate method for producing highly detailed models, however, this equipment was not available for the main data collection process. The laser scanned models therefore act as a proxy for the most accurate meshes to test photogrammetry and structured-light-scanning against.

5.3 Photogrammetry

Photogrammetry is a means of producing measured 3D models from photographs (Falkingham 2012: 1). Due to current technological advances in digital cameras, software, and computational techniques, photogrammetry has become a portable and powerful tool for producing dense and relatively accurate 3D surface data. There is a range of software available, from free online versions (123D Catch), to more expensive packages (e.g. Agisoft Photoscan). It can be used for complex objects involving high surface detail, however, the quality of the models relies heavily on the level of detailed photographs (Falkingham 2012).

Photogrammetry is used on different spatial scales, ranging from the object level to entire site excavations (something other methods cannot do). This method provides an accurate record of not just the location of finds that have been removed from the site during an excavation but also offers the ability for geospatial referencing to geomorphological features or other dig sites in the surrounding area (Falkingham 2012). It can be useful when direct access to the object under study is limited (Pavlidis *et al.* 2007). The methodology for photogrammetry used in the validation study is the same as that used in Chapter 4 for the validation study of the applicability of GM to juvenile long bones and is illustrated in Figure 5.1.

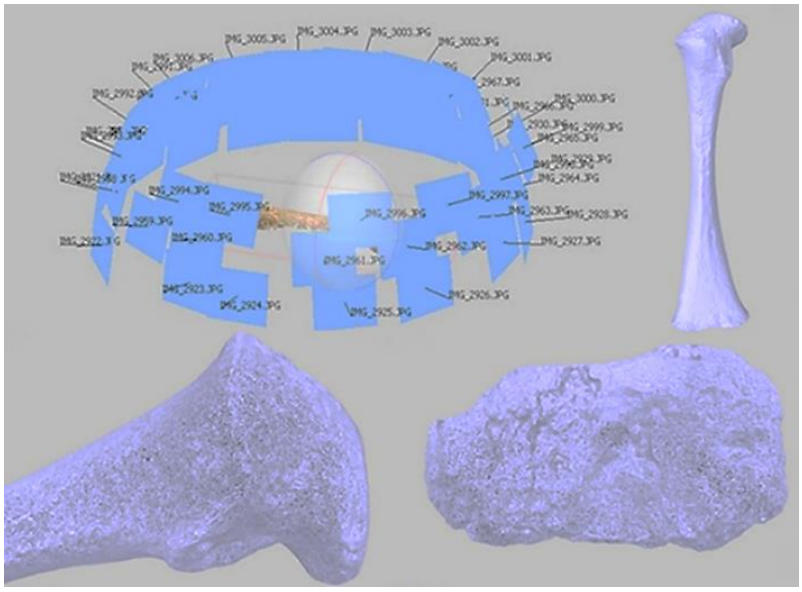

Figure 5.1: Aligning the anterior segment and building a dense point cloud from a 2 year old femur from Great Chesterford (Image by author).

5.4 Structured-Light-Scanning (SLS)

Structured-Light-Scanning (SLS) is a 3D scanning method that uses a data projector to cast patterns of light onto an object (Figure 5.2) and calculates the deformation of the projected patterns (Weber & Bookstein 2011: 99). A camera is positioned at an angle to the projector to find curves that move away from the light source. The angle between the camera axis and the projector axis is calibrated through optical triangulation, which determines the distance from the camera to every projected point. Each line in the pattern moves across the entire field of view, and thereby encompasses the surface of the object which is digitized line by line (Weber & Bookstein 2011: 99).

SLS is a low cost method, requiring a LCD projector, standard digital camera, and program. The speed can be adjusted to rapid and almost instantaneous acquisition as the entire field is registered in one procedure rather than point-by point (Weber & Bookstein 2011: 101). The accuracy is controlled by the projected pattern and camera resolution and the process is completely non-intrusive as it captures images through near-infrared emitters (Weber & Bookstien 2011: 101).

5.4.1 SLS Methodology

Similar to photogrammetry, SLS requires overlapping scans to create 3-dimensional models. The camera is mounted on a tripod and is positioned higher than the projector and closer to the object so that its central axis lies in the X-Z plane and is parallel to the projector axis (Figure 5.2). For the smaller bones (foetal and 1 year old), the camera was zoomed in significantly to capture as much detail in these more featureless shapes. Unlike photogrammetry, it was found that placing the long bones vertically upright provided more detailed features of the surface that could be captured from the light patterning and subsequent scans. The DAVID 4 SLS program measured the position, orientation, focal length, and distortion coefficients of the camera (Friess 2012: 11).

After set-up and calibration, the default setting was selected: the fast scan setting produced noise and the quality setting produced almost identical scans as the default setting but took twice as long. Each bone was then rotated 10-15 intervals clockwise to capture the superior and inferior surfaces. Separate scans were then taken for the proximal and distal ends of each bone (totalling 12-17 scans). Post-processing included deleting background noise and cleaning the edges of each scan so they could be fused in .ply file format (Figure 5.3). The smaller bones required more manual adjustments to align the scans as the lack of surface detail made meshing difficult.

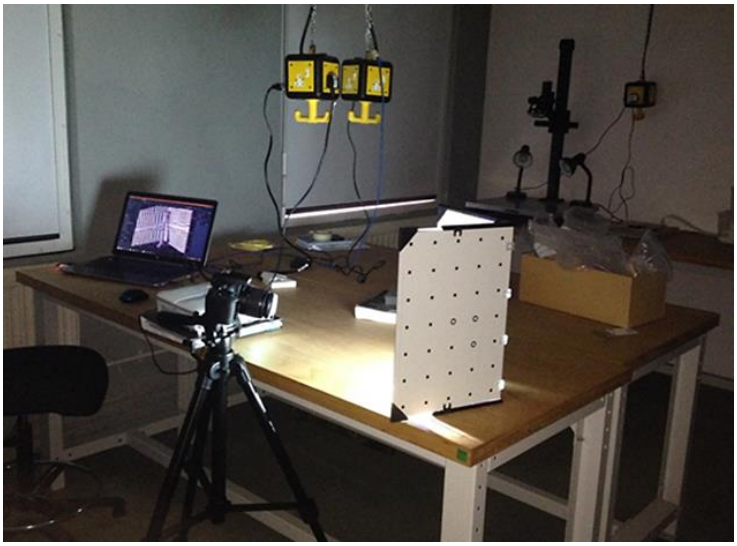

Figure 5.2 Structured Light Scan set up (Image by author).

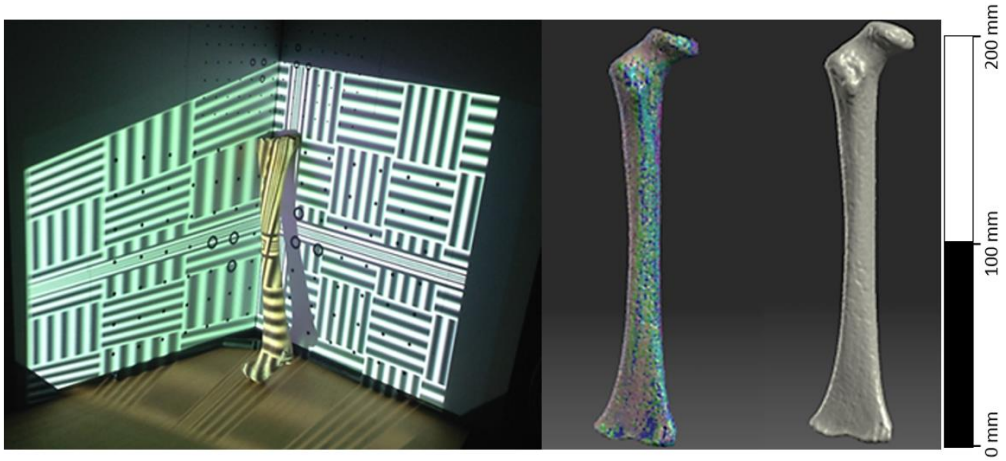

Figure 5.3 Projected light pattern (left) and final mesh (right) of an 8 year old juvenile (Image by author).

5.5 FARO Laser Scanning

Laser scanning operates by using transmitted light to record the object's surface by measuring the time the reflected laser light needs to return to the transmitter (Weber & Bookstein 2011: 99). This triangulation method of emitting laser light by the transmitter and simultaneously the receiver (or camera), measures where the laser dot is located on the object and the sensor element of the camera forms a triangle (Weber & Bookstein 2011: 99). The distance between the laser source and the light sensor element of the camera is known, as well as the angles at the corner of the laser source and camera because they follow from the position of the laser dot in the camera's field of view. The shape and the size of the triangle are fully determined once the position of the laser dot on the object has been determined and the coordinates can be stored. At small distances, up to a

few meters, the accuracy of this method can be as high as a few tens of microns (Weber & Bookstein 2011: 99). In addition to the spatial registration of the geometry, colour information can also be obtained with complex measuring systems. This is an expensive but useful technology which creates realistic representations for archiving and analysing heritage objects (Weber & Bookstein 2011: 99).

5.5.1 FARO Methodology

The difference between the FARO scanning compared to other methods is the ability to use manual movement of the arm to capture the surface geometries rather than rotating the bone. Each bone was placed horizontally on a small stand in order to digitize the full circumference (Figure 5.4). This technique allowed for more attention to detail in the difficult regions of the bone (features that are not as pronounced in the foetal to 2 year old long bones) to produce more accurate models. The arm was calibrated and the meshes were processed with Geomagic.

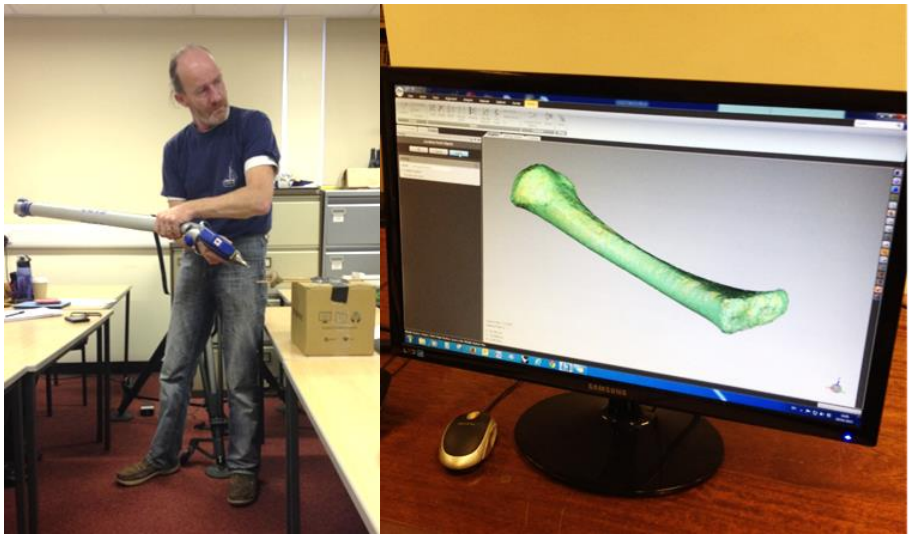

Figure 5.4: Scanning set up with Pat Tanner (left) and real time scan of a 2 year old femur from Great Chesterford (right) (Image by author).

5.6 Technical Aspects: Photogrammetry, SLS, FARO Laser Scanning

The first task of this study is to evaluate the technical aspects of each digitization method in terms of financial and labour cost, time, and mesh quality. This was achieved by documenting the financial cost and time for each method, while mesh quality was tested and quantified through cloud compare.

5.6.1 Method Practicality

The technical aspects to consider for each scanning method are summarised in Table 5.1. The main differences were time and cost. Photogrammetry was the most inexpensive method, although the better the camera and program, the better the final mesh. The Agisoft licenses were available through the University of Southampton and the DSLR camera was already owned, which made this method least expensive for this study. The error rate was very low at 0.169 mm and both the set-up and imaging process averaged from 45 minutes to 1 hour per bone. The mesh quality is highly detailed (depending on the camera used) as seen in Figure 5.5. The post-processing time, however, which includes editing the images, masking the background, and deleting noisy data in the point cloud, averaged to 4 hours per bone, thus making photogrammetry impractical for large data collection. An attempt to decrease the post processing time was made by automatically masking the background during the data capturing process. It was found however, that the smaller bones from foetal to 2 years had larger sections of the surface masked during this stage as Agisoft had difficulty finding the difference between the black background and slight shadowing on the surface of the bone.

Structured-Light -Scanning (SLS) is more expensive than photogrammetry as it requires a camera, projector, tripod, calibration boards, and program (the DAVID kit is the most inexpensive on the market and the entire set-up is £2,000). The error is lower than photogrammetry (0.1mm) and the entire process from set-up to final mesh takes 1 to 2 hours (depending on the complexity of the scan and/or lack of morphological features that require more scans). In terms of image quality, it was found that SLS produced the least detailed scan of the three, as the bone appeared to have smoother features compared with the other scan types (Figure 5.5). It is possible that this could be remedied by the use of a macro lens.

The final method, the FARO laser arm, is significantly more expensive than the other methods and produces the lowest error rate. It takes the longest to set up and falls in the middle in terms of processing time as it takes 2.15-2.45 hours per bone. The image quality is very detailed as the taphonomic changes to the bone as well as the second trochanter were crisply presented. This is to be expected as the FARO arm is manually moved by the user and allowed for more flexibility in capturing the difficult features of the bone while the data collection of photogrammetry and SLS is stationary. The file size, however from the FARO scans are significantly larger (12,387-29,833 KB) and require high power computers to operate, not only for the scanning, but also for the post-processing of each model.

Technical Aspects of Scanning Techniques			
Variable	**Photogrammetry**	**Structured Light Scanning (SLS)**	**FARO Laser Scanning**
Cost of Equipment (£)	£350- £3,000	£250-£2,000	£16,000
Error (mm)	~0.169mm	~0.1mm	~0.024mm-0.064mm
Resolution (vertices)	86,342 -90,141 vertices	82,856-102,163 vertices	612,031-2,121,818 vertices
File Size (KB)	6,895-7,121 KB	5,889-7,319 KB	12,387-29,833 KB
Set-Up (Time)	15 minutes	15 minutes	1 hour
Scanning (Time)	30-40 minutes	15-20 minutes	15 minutes
Post-Processing (Time)	3.5-4 hours	30-40 minutes	1-1.5 hours
Time per bone (Time)	4.45-5 hours	1-2 hours	2.15-2.45 hours

Table 5.1 Technical aspects of different scanning techniques as of 2017.

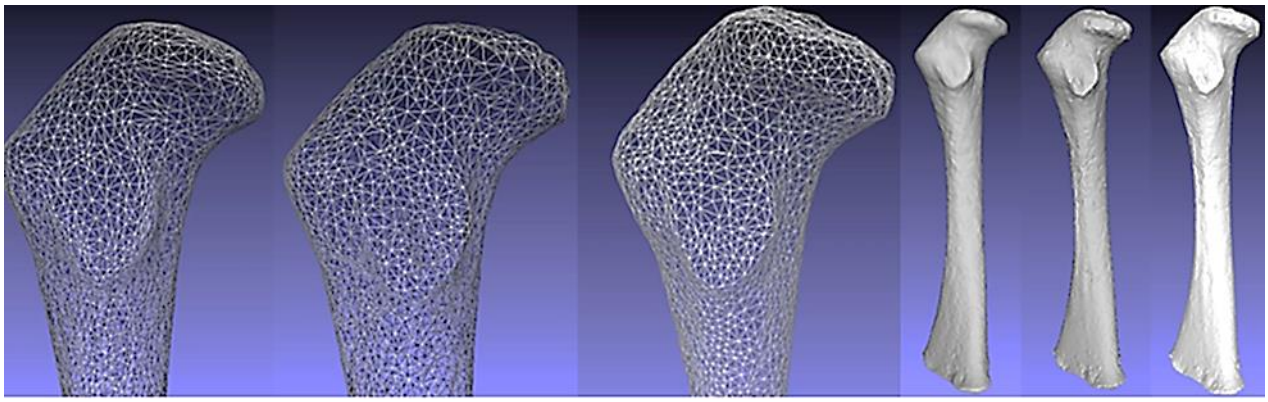

Figure 5.5: Comparison of femur meshes from a 2 year old femur from Great Chesterford. SLS (Left), Photogrammetry (Middle), FARO (Right) (Image by author).

5.6.2 Scanning Deviations

In addition to practical differences between scanning methods in terms of time, cost, and file size, resolution is a variable that can describe morphology differently. The laser scanned models were compared with photogrammetry and SLS to determine whether there is any significant measurement differences between methods and where such deviations occur in the femur. Cloud compare (Version 2.7, 2016) was used to measure these differences and determine whether the models produced were rounder or flatter than the high quality laser scans. Figure 5.6A shows the measurement differences between the SLS scan of an 8 year old (Group 4) femur and the histogram indicates that the SLS scans tended to produce rounder and larger areas of the proximal and distal metaphyses compared to the laser scans. Figure 5.6B of a 4 year old femora (Group 3) shows a common difference between the laser and photogrammetry models, once the texture is removed (which is needed to run the GM analysis in R), they are more flat relative to the laser scans. The

histograms for both SLS and Photogrammetry show that although there are some deviations from the laser scans but they do not reveal any significant differences between the laser scans.

The image quality for SLS is the poorest relative to both photogrammetry and the FARO laser arm. The Cloud Compare measurements also showed that the proximal and distal metaphyses vary in size compared with the FARO scans, thus the SLS method produced rounder metaphyses. Chapter 4 demonstrated that this was an important region of morphological variation. According to Cloud Compare, this does not statistically impact scan morphology, however, if GM identifies differences between scanning techniques, it is likely to be a result of the metaphyseal regions. The second phase of the comparison of scanning methods therefore tests the applicability of GM to the different models in order to identify how much the differences in proportions of the metaphyses (rounder in SLS and flatter in photogrammetry) affects the overall morphological shape of the specimen.

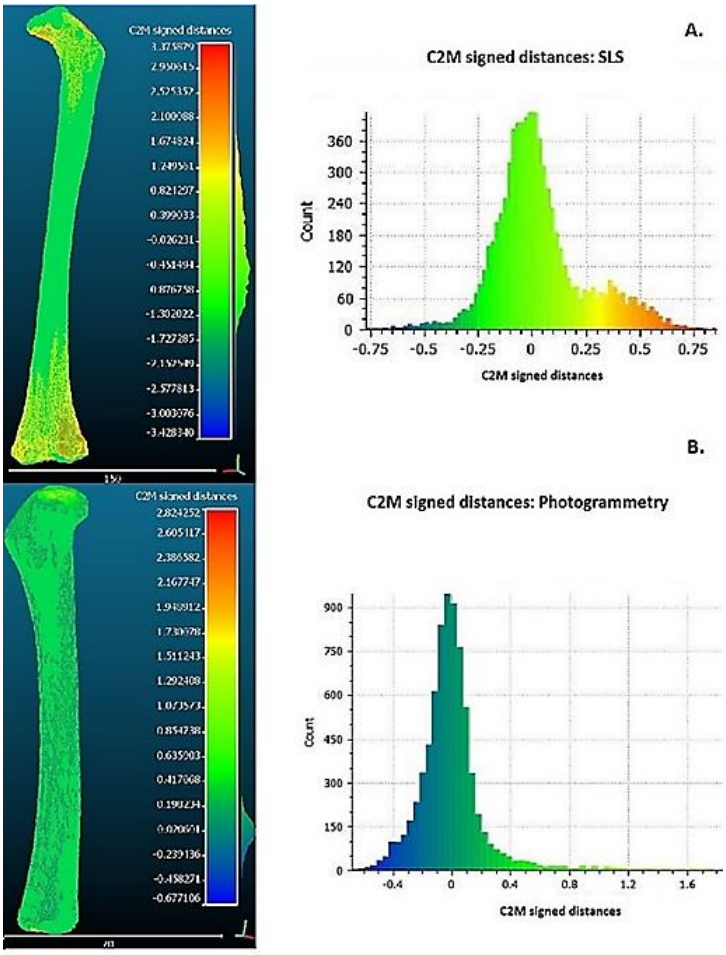

Figure 5.6: Cloud Compare of FARO scans against SLS (A.) and Photogrammetry (B). The femora used for both histograms (A: 12 year old and B: 4 year old) were selected based on the most extreme differences from their chosen methods (SLS and Photogrammetry) to the laser scans. The more negative values (blue) represented a flatter surface while the higher positive values (red) represent a more rounded surface compared to the FARO scan.

5.7 GM Analysis of Different Scanning Methods

The technical aspects of time, cost, and Cloud Compare results revealed differences between digitization methods and final meshes. The second part for this study examines if there are differences in morphological shape as a result of different scanning methods.

5.7.1 The Effects of Scanning Methods on Morphological Shape

The auto3dgm methodology discussed in Chapter 3 and 4 was used for this study. Each bone (3 scans of 5 bones, resulting in 15 'specimens') were subjected to a geometric morphometric analysis to assess variation in shape between capture methods. After running a GPA ANOVA, it was found that there was no statistical significance between the methods ($p<0.9991$) when projecting the same bone in tangent space. The SLS scans grouped closely with the FARO scans while the photogrammetry shapes are slightly further away. Cloud Compare revealed different, although normally distributed, measurements in the metaphyses for both methods. The GM analysis supports these findings as size differences are not statistically significant in terms of morphological shape (Figure 5.7).

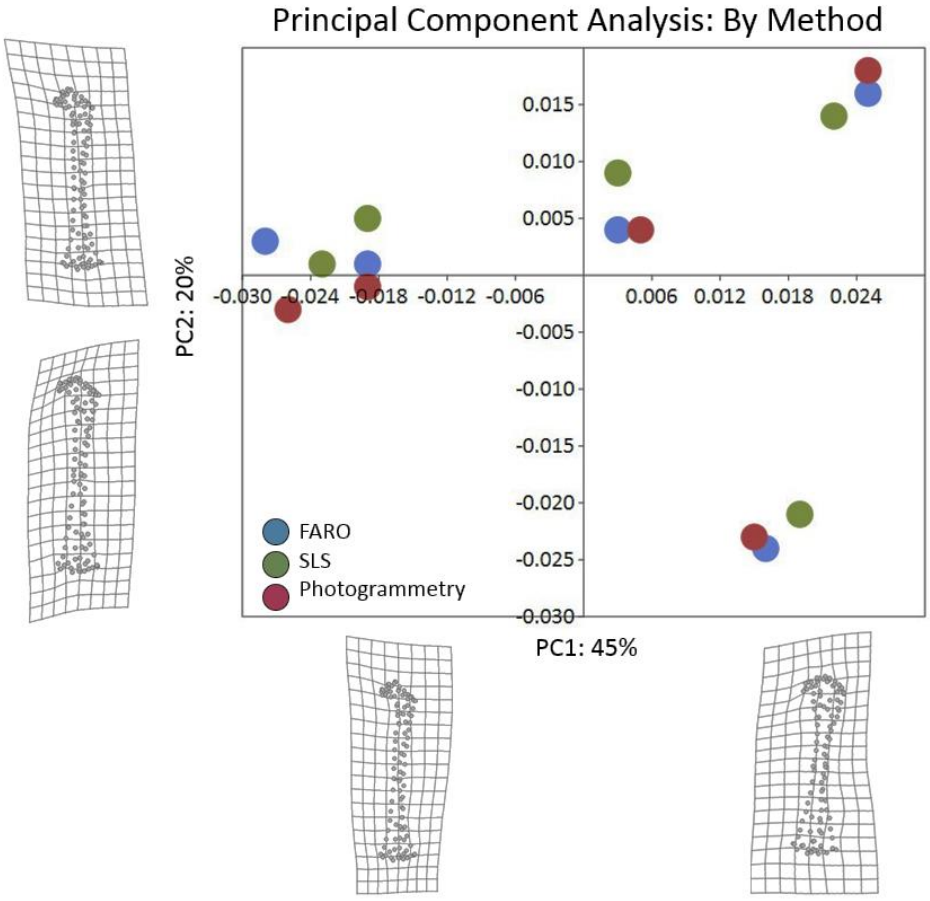

Figure 5.7 PCA of juvenile femora by scanning method.

5.7.2 The Effects of Scanning Method and Specimen Groups

Although there is no statistically significant difference between scanning methods, the question now arises as to whether the age groups vary by method. The same femora meshes were examined to see if scanning method (i.e. FARO, SLS, and photogrammetry) could be grouped by specimen (i.e. GC 49, GC 111, GC 118). It was found, using an ANOVA, that bone specimens are significantly different ($p>0.001$) and can be separated, regardless of method. According to the morphological disparity, most specimens can be distinguished from each other, however, it is possible for Group 5 and 4 to be categorized together. This was found in the Chapter 4 auto3dgm PCA analysis, as Group 4 represents the transition stage between child and adult gait patterns and it is possible that, with a larger sample size and more variation in shape, these groups can be more easily distinguished from one another. In Figure 5.7, it can be seen that this age group varied the most by method type, and this could be a result of the bone being more slender in this age range as the bone is growing more in size than morphological shape. Similarly to the PCA between method types (Figure 5.7), and the findings in Chapter 4, the proximal and distal metaphyses of the femora represent the most variation in shape by age (PC1: 45%; PC2: 20%).

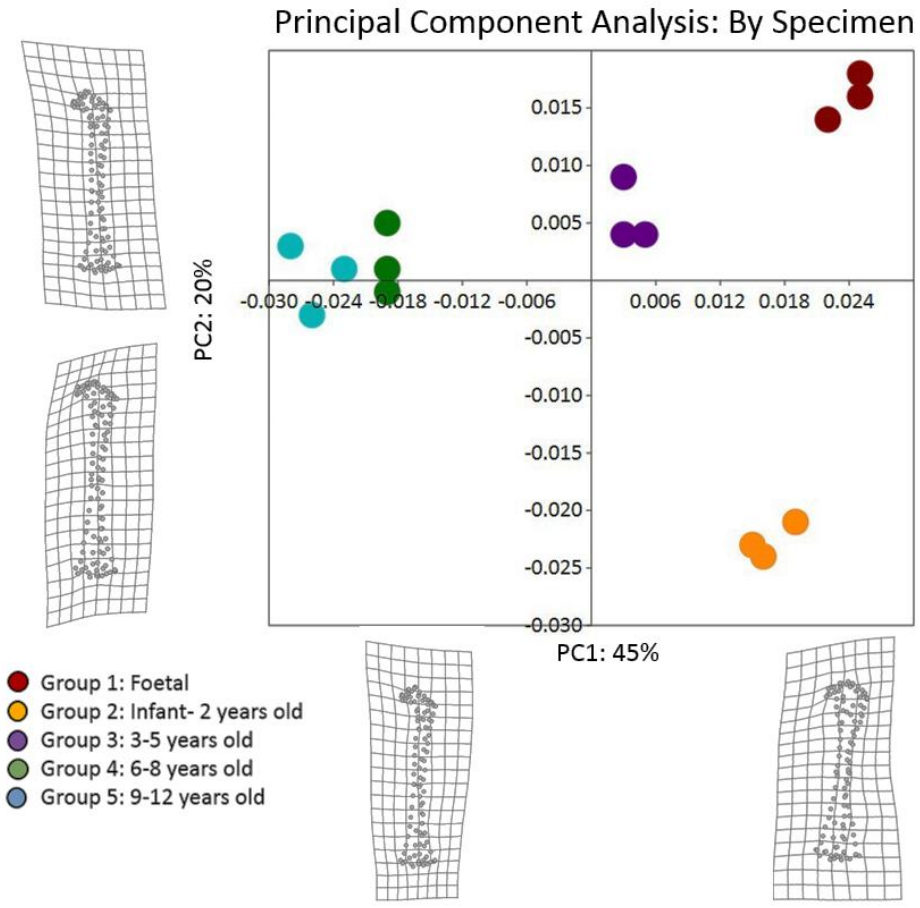

Figure 5.8: PCA of juvenile femur by specimen

5.8 Discussion: Scanning Methods and Morphological Shape

Although image quality was noticeably different between scanning methods, it did not over-or-under produce femur morphology as there were no differences between scan method and morphological shape. The assessment of each technique, morphological differences of each method, and practicalities of 3D dataset dissemination are discussed below.

5.8.1 Limitations of Each Method

Although photogrammetry was the most inexpensive technique for this study (as the author had a DSLR camera and tripod and used the department Agisoft license) it was also the most labour intensive. It required over 100 images for each mesh which was edited, masked, and aligned manually. The infant bones were the most difficult to capture because of the small cylindrical shape with little surface area and few distinguishable features. It was difficult to get the most accurate focal length for these bones specifically when they were at their most narrow position (medially-laterally to the camera) and often the images would not be entirely in focus. This method also took the most processing time, 4 hours would be needed from set-up to final meshed model. The amount of time spent during post-processing the images is impractical for large data-sets. In order to perform the GM analysis in R, all texture must be discarded from the scan which caused additional problems. In Figure 5.7, it is seen that the photogrammetry models are slightly more distinct from the FARO and SLS (apart from Group 4). This could be a result of the removal of texture as this leaves the photogrammetry models slightly flatter in shape than the other methods. Another possibility for these differences is a result of the 'noise' from the multiple elements being stacked which leads to small misalignments that occur all over the bone models.

SLS is also difficult to find an adequate set-up for the foetal and 1 year old bones. This method proved difficult to create good quality scans with minimal noise while capturing the overlapping features needed for alignment. Like photogrammetry, for SLS, once bones were turned to the narrowest position, it proved difficult to capture the shape as the method relies on surface area. The striped patterns produced in SLS created more noisy scans, and as a result, more manual alignment was required for these regions.

Although laser scanners are reducing in price, this was by far the most expensive in terms of hardware (FARO-Arm) and software (Geomagic). Furthermore laser scanning requires a computer that is fast enough and big enough to hold the large data files produced. Most universities have laser scanners available and, in most cases, they can be portable for data collection. The large file size needed for these models also requires more computer storage both to save the files and run the GM analysis through R. Furthermore, the size of files often results in crashed or corrupted files.

This method is challenging both financially and practically as there are often waiting lists within university settings. Desktop laser scanners (NextEngine 3D Laser Scanner) are becoming more affordable as they range from £2,000 and are fast and reliable. For the main study collection in Chapter 7, the department does not have a suitable laser scanner for digitizing skeletal material, so alternative methods are needed. However, for the validation studies in this Chapter, laser scanning was an essential proxy to compare alternative methods too.

5.8.2 The Drawbacks of Digital versus Physical Specimens

Another notable difference between methods was how each technique combats 'missing' or difficult to capture surface data. For any surface that may be broken or damaged by taphonomic processes, or where there was a very narrow range of surface area where images could not overlap as much as needed, photogrammetry filled in these areas of missing data with what Agisoft believed to be the shape of the bone. Although these filled-in spaces are minor in terms of the entire morphology of the bone, they can give a false sense of mesh quality. Both SLS and the FARO arm show these imperfections in the data collection process. As a result, these errors can be remedied by filling in the spaces (like photogrammetry), or scans can be re-taken during data collection. The user must be aware of these flaws and make an appropriate decision during the data collection (rather than finding out during post-processing). This study also demonstrates the importance of a good mesh, rather than texture. As seen in Figure 5.6B, the photogrammetry models fell relatively 'flat' once the texture was removed for GM analysis. Although this was not detrimental, it may alter the morphological integrity of the bone as some features are lost.

The overall SLS scans showed fewer morphological features as they were smoothed out during post-processing (Figure 5.5) and tended to produce models that were slightly larger than the laser scans (Figure 5.6A.). Although this did not prove to be significant in terms of morphological shape, (Figure 5.7) it is a limitation to this method as features were less distinct. For specimens that lack much surface detail, in this instance juvenile long bones, this can be a problem.

In addition to issues of missing data, it was found that some specimen could not be properly meshed during the scanning and/or post-processing stage, even with acceptable scans. Table 5.2 indicates the physically available skeletal material for Great Chesterford femora and a subset of these that could be scanned as the digital skeletal elements used in this thesis. The first criterion of this study was to analyse juveniles from foetal to 12 years old. These age ranges are known to be difficult to acquire large sample sizes from the archaeological record. The second criterion was to only use left sided complete long bones. Unfortunately, some individuals had undergone destructive analysis or

the preservation (mainly deep root etchings) could not be used in the current study as the analysis relied on complete surfaces. To further reduce the already limited skeletal sample, some specimen could simply not be used as the 3D models could not be meshed properly (even after repeated scanning attempts). This resulted from differences in colour or texture of the bone, specifically darker regions where the light patterning from the structured light scanner or photogrammetry images could not effectively capture the surface of the long bone. The most problematic regions for SLS and photogrammetry was when the skeletal elements were at the narrowest focal point, resulting in a lack of surface area that could not be matched up with the subsequent scans. This was a severe limitation to the study as it is seen that the digital skeletal elements are less than half of the available physical collection.

Physical Skeletal Elements versus Digital Skeletal Elements for Great Chesterford			
Ages	**Number of Individuals**	**Complete Left Femora**	**Digital Femora**
Foetal	5	5	3
Infant- 2 years old	50	35	11
3 – 5 years old	11	6	1
6-8 years old	12	6	1
9-12 years old	5	3	2
Total	83	55	18

Table 5.2: Physical femora from Great Chesterford versus the useable digital versions for photogrammetry and SLS.

The differences in physical versus digital specimens and mesh quality are crucial elements that must be considered during data collection. However, once these datasets have undergone post-processing and analysis another obstacle faced by researchers is what to do with these large files. In most cases, 3D datasets incur a financial cost of publishing these collections which are proportional to the amount of data being stored (Berquist *et al.,* 2012; Davies *et al.* 2017). Some repositories such as MorphoSource do not have a charge for data storage and dissemination. Other popular digital repositories however, such as Dryad currently charges £92 per data package of 20 GB plus £39 for each additional 10 GB (Davies *et al.* 2017). Publishing such datasets can quickly become expensive. While many journals offer to fully or partially cover the costs of depositing digital datasets, they do not have a clear policy for datasets that are hundreds of GB to TB in size (Davies *et al.* 2017). Applications for research funding are increasingly budgeting for data storage costs, but this does not assist projects making use of pre-existing data or those where funds for data publication are not available. Davies and colleagues (2017) proposed a possible solution to this by reducing the total size of data published without compromising the quality. For instance,

cropping of redundant space around a volume that represents the specimen or lossless compression of individual image files is another route to reduce data storage for image stacks in certain formats (Davies *et al.,* 2017). ZIP archives are another solution for reducing disc space through compression and is convenient for downloading. ZIP and VOL archives however, are less secure for long-term data storage as one file within a larger dataset can become corrupt and affect the entire dataset. Some repositories do have procedures in place to detect and remedy bitrot (Boyer *et al.* in press; Davies *et al.* 2017), but data storage is another aspect of 3D datasets that must be considered.

In addition to finding a suitable recording methodology and storage, ownership of 3D datasets is another issue that has emerged. Although the principles of open data have been recognised by the majority of funders (Davies *et al.* 2017), publishers, collection facilities, and researchers, there is still a struggle to meet the new challenges of 3D datasets (Davies *et al.* 2017). The main issue is over ownership of digital data which must be resolved between the funders of the research, researchers who collect specimens and create the digital datasets, research facilities where data is collected, museums who have the duty of care for the physical specimens, and research publishers. Funders, researchers and publishers may have constructed a system of open data, however, the institutions responsible for the physical specimens have not been involved in the development of open-data policy. This is a crucial problem as museums will have to change the most in terms of their polices on the nature of what they consider fundamental aspects of the physical specimens they curate. One solution proposed by Davies *et al.* (2017) is for museums to comply with research funder's requirement and waive copyright over digital representations of their collections as well as the associated income stream. Another possibility is for these institutions which are best placed to inform policy on the curation, storage and distribution of data, to develop digital collections with the stability to match that of their physical inventory (Davies *et al.* 2017). For instance, the Archaeology Data Service is an open access digital archive at the University of York.

5.8.3 Benefits of Scanning Methods and 3D Dissemination

Despite the difficulties and deficiencies outlined above the advantages of 3D models are the potential to generate and disseminate virtual databases which can remedy the limitations associated with access to collections in remote locations or expanding sample sizes with collections from various institutions (Wilson & Humphrey 2017: 39). Scanning is also non-invasive which results in virtual records of specimens, these virtual repositories can be accessed repeatedly and even shared through collaborative networks without the risk of damaging, commingling, or losing the

original specimen(s). Even when most carefully curated, collections undergo wear and tear when they are continuously used for research projects. Although no 3D model can ever replace the original specimen, as they are only virtual representations, the potential of scanning specimens, before becoming damaged or undergoing destructive analysis, allows for a wider range of research questions to be explored. Fruciano *et al.,* (2017) assessed measurement error with combining 3D datasets with automated geometric morphometric methods. It was found that datasets must be subsampled to the same resolution if they are digitized with different techniques. However, as bioarchaeologists and archaeologists struggle to find sample sizes large enough to produce meaningful studies, the ability to expand datasets through virtual methods and produce statistical analyses on morphological variation would be a vital addition to the field.

The question of determining a suitable scanning method depends on the aim of the research. For instance, it has been shown that photogrammetry has many limitations for large scale data collection. Chapter 4 however, demonstrated that photogrammetry was a useful method for running a validation study on GM when no other equipment was available. The use of a decent camera and Agisoft Photoscan Pro allowed for an initial trial of the study, thereby permitting small adjustments to be made to the overall project aims and analysis. Muńoz- Muńoz *et al.* (2016) found that photogrammetry was a useful technique to capture small mammal crania as it was able to capture the fine detail of these small skeletal features. Studies involving smaller specimens would benefit more from photogrammetry (rather than SLS or FARO scanner) as photogrammetry has the ability to capture fine detail with a MACRO lens.

SLS remained in the middle of the other scanning methods. Although it did not have the highest scanning quality, it did have a small measurement of error of 0.1mm and was one of the fastest techniques for all areas of data collection. The lack of surface area for the smaller bones was the main challenge and it required several days to refine the methodology. In terms of recording larger data sets however, the overall time and financial cost proved this method was a suitable alternative to photogrammetry.

As with any form of laser scanning, the FARO method produced the most detailed meshes. This was the only process where the bone remained stationary while the laser was manually rotated around the bone. This allowed for a more complete scan of the entire surface area of the bones, and captured the areas in which other techniques struggled. As the scanning process happens in real-time, the problematic areas could be identified immediately and more attention spent capturing such details.

5.9 Concluding Remarks

This study demonstrates that reliable GM analysis can be done using models captured by a variety of scanning methods as the technique of the scan does not statistically change the morphological shape. Structured-Light-Scanning was found to be the most reasonable method for the main data collection for this thesis as it was not as labour intensive as photogrammetry, was affordable, and portable. Although features were not captured as well as with laser scanning, the analyses demonstrated no significant variation between techniques in the captured shapes of juvenile long bones. This chapter has shown that through rigorous testing of different methodologies any morphological variation found in the main study results derives not from scanning method, but is real.

Each research project has different criteria and parameters that need to be considered before choosing an appropriate method. These are mainly time, cost, and availability of equipment. The validation study in this chapter demonstrates that researchers with limited access to expensive and high powered equipment can still produce meaningful studies on morphology as there is no statistical difference by scanning method. There is potential here: as more datasets become publicly available, more quantifiable studies can be undertaken. As Selden *et al.,* (2014) have stated, there is more to 3D scanning than documentation and curation, but an analytical approach can be incorporated into many publicly accessible 3D datasets. The validation study in this chapter has shown that an alternative method to laser scanning and photogrammetry, SLS can be used for the main study collection and it is the most affordable and portable and does not compromise the outcome of bone shape.

6. Skeletal Materials

This chapter examines the context of the skeletal materials employed in this thesis. It has been discussed in Chapter 2 that developmental pathways such as varying levels of exposure to environmental stress, diet, period, and urban versus rural communities affect growth rates. Therefore, the sites chosen for this thesis provide a range of differing geographical locations, time periods, juvenile collections, and urban versus rural settlement structures that can be analysed (Table 6.1 and Figure 6.1).

Great Chesterford in Essex dates to the seventh century and has a large collection of juvenile remains which is rare for Anglo-Saxon sites. Raunds Furnells in Northamptonshire is an Anglo-Saxon settlement with a cemetery dating between the tenth and twelfth centuries. These Anglo-Saxon communities would have practised subsistence agriculture and lived in rural environments. Medieval Wharram Percy dates from the mid-11th to 13th century and is one of the largest and most extensively studied medieval juvenile collection through long bone lengths, isotopic analysis, cortical bone geometries, environmental stress, and population variation. Wharram Percy remains are the closest to a 'known' collection because of the breadth of research that has been studied over the past 30 years (Mays 1995; 1999; 2003, Mays *et al*. 2006; 2009), thereby making it an ideal collection to test the success of geometric morphometrics in addressing these growth patterns. Canterbury is another large and well preserved urban and rural medieval assemblage from the 11th to early 16th century which makes an ideal comparison to Wharram Percy. Post-Medieval (AD 1800-1850) Wolverhampton is a smaller urban assemblage but offers an extreme contrast of industrial developmental trajectories. These five sites offer rural and urban juvenile trajectories that span from Anglo-Saxon to Post-Medieval periods in the United Kingdom.

This chapter will begin with the history and archaeology of each site, followed by the demography, infant mortality, weaning, diet, and health of the juvenile samples. The background in this chapter is intended to aid the interpretations of the geometric morphometric results in Chapter 7 by providing the context of the juveniles studied and how their life history may affect their developmental trajectories.

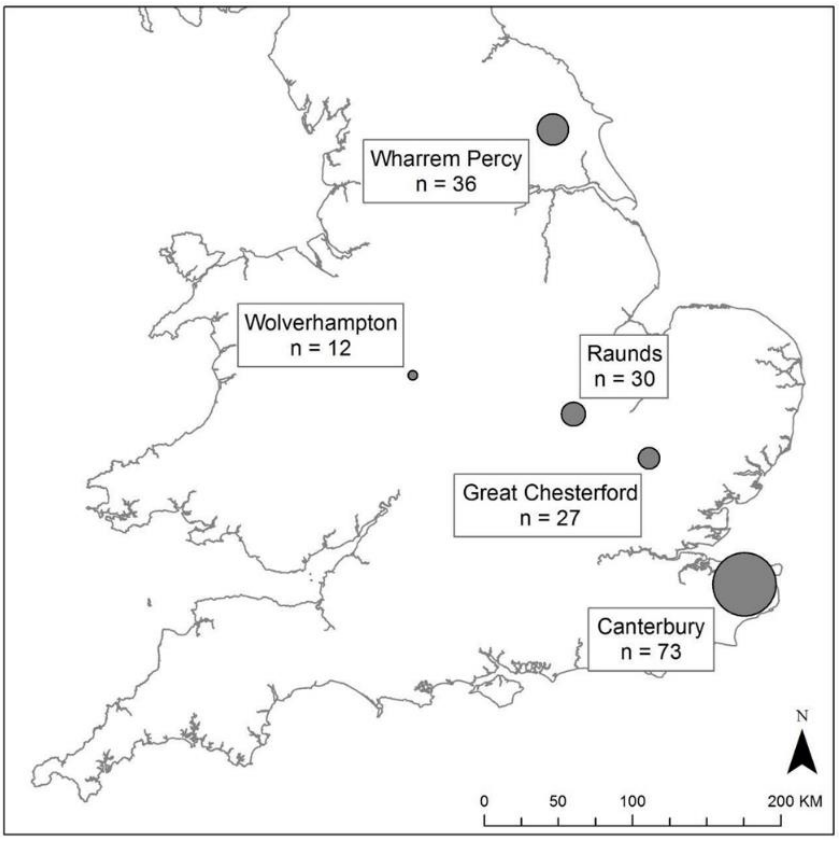

Figure 6.1. Map of the UK showing the location of skeletal collections and the number (n; and circle proportion) of individuals used for this thesis from each site (Image by author).

Skeletal Material					
Site	**Date**	**Environment**	**Demography**	**Juvenile Sample (n)**	**Reference**
Great Chesterford	AD 601 - 700	Rural	Agricultural Community	83	Evison 1994
Raunds	AD 850-1100	Rural	Agricultural Community	162	Boodington 1996
Canterbury	AD 1100-1501	Urban and Rural	Urban Ecclesiastical and Rural Community	294	Hicks & Hicks 2001
Wharram Percy	AD 1066-1348	Rural	Agricultural Community	327	Mays *et al.* 2007
Wolverhampton	AD 1800-1850	Urban	Industrial Community	58	Adams & Colls 2007

Table 6.1 Skeletal Material by site, date, environment, demography, and total number of juveniles excavated from each site (n).

6.1 Archaeology of the Sites

The archaeological contexts, excavations, and a brief history of Anglo-Saxon Great Chesterford and Raunds, Medieval Canterbury and Wharram Percy, and Post-Medieval Wolverhampton are described below.

6.1.1 Great Chesterford

Anglo-Saxon Great Chesterford is located east of the River Cam, south of Cambridge (National Grid Reference: TL 501435; Evison 1994: 1). There is extensive evidence of prehistoric activity which dates back to the Mesolithic period onward (Evison 1994:1). A large circular feature was found in the region of a Roman fort and is thought to be a Bronze Age barrow. There was substantial Late Iron age settlement on the river next to the later Roman town, with a Roman fort constructed north of the existing settlement in the first century AD. The settlement developed during the second century into a more urban site and went through a period of decline during the third century before expanding again in the fourth century. There is evidence suggesting a large Anglo-Saxon settlement existed at Great Chesterford from the end of the Roman period until the seventh century (Evison 1994: 2). The evidence, however, largely comes from the burials as the location of the settlement is unknown and it is likely that the medieval town was built over the Anglo-Saxon settlement (Evison 1994: 1). After the Norman Conquest, Great Chesterford became a royal manor and was a prosperous settlement during the Medieval period due to the cloth trade (Evison 1994). The area declined in the Post-Medieval period because of the collapse of the cloth trade and little passing through due to development of the road link with Newmarket, Cambridge and the London-Cambridge railway (Evison 1994: 1).

Excavations began commercially in the 1950s as a gravel extraction project was commissioned for the area (Evison 1994: 1). According to the site report by Evison (1994), this resulted in a loss of 100 Anglo-Saxon graves. The looming threat of more gravel extraction spurred a single excavation commissioned to the north-western border of the Roman town and a subsequent excavation report was published (Evison 1994:1). Excavation of the Anglo-Saxon graves found in the area resulted in 160 burials and 33 cremations excavated by 1955 (Evison 1994:1). The excavated area is believed to be within the centre of the cemetery. Evison (1994) defined four phases in the cemetery's usage from the period 450-600.

The depth of the burials are not known, however, the ones which were recorded vary from just beneath the sand and gravel topsoil to at least six feet deep (Evison 1994:1). There are 65 infant

and foetal burials exhumed from shallow earth cuts (Evison 1994: 28). The graves at Great Chesterford were mixed in orientation as some were South-North and others West-East. The latter are assumed to be typical for Anglo-Saxon cemeteries (Evison 1994: 36).

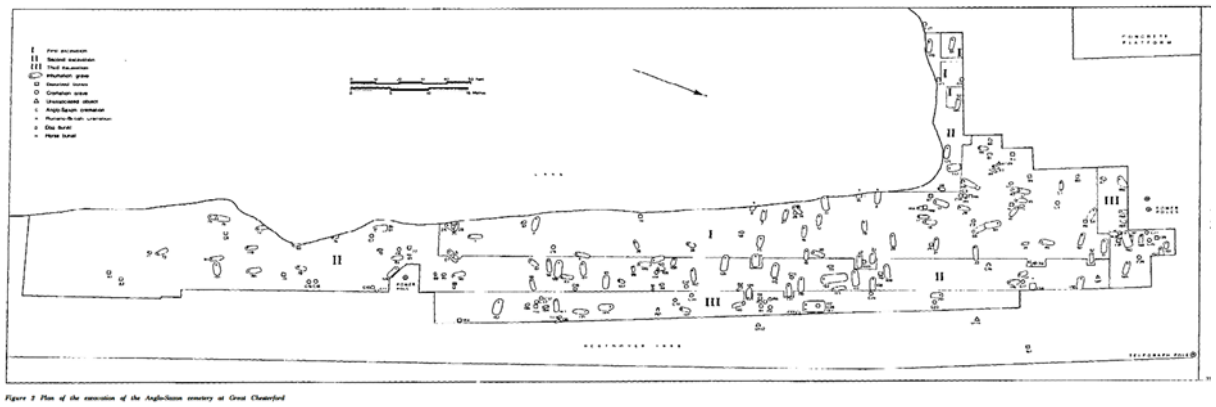

Figure 6.2 Figure 6.3 Excavation plan of Great Chesterford Cemetery (Evison 1994: 3).

Of the 167 inhumations, 83 (48.5%) were juveniles (Evison 1994: 31). In comparison to other Anglo-Saxon populations, this is an extremely high percentage of juvenile remains. The preservation of Anglo-Saxon sites for juvenile remains is generally regarded as fair to poor as infant and juvenile remains fail to survive extreme soil environments (Buckberry 2000). Other factors that play a role in the low level of infant and juveniles remains could be shallower burials, being found further away from the rest of the population, or differential disposal (Inskip 2008). Crawford (1999:66) suggests that the foetuses found at Great Chesterford demonstrate that even infants who had not reached full term were seen as sufficiently worthy to be buried in the main cemetery.

6.1.2 Raunds

The Anglo-Saxon site of Raunds is found in the valley on the eastern side of the River Nene in Northamptonshire (National Grid Reference NGR 999733). Archaeological evidence suggests that the village existed since AD 850 (Boddington 1996). During the Late Saxon period (AD 850-1100), Raunds was the most dominant and largest settlement in the region which was continually occupied from the sixth to late fifteenth centuries. In AD 1066, Raunds was held by two manors of Burgred and Gytha, and had six dependent villages (Damna & Foard 1984). The manor of Burgred was originally at the site of Raunds, to the north of the present village, and was the primary manor of the area until the Medieval period, when Gytha became prominent (Lewis 2002).

Raunds was excavated by the Northamptonshire County Council Archaeological Unit between 1977 and 1979 when a manor, church and churchyard were found (Boddington 1996). Excavations revealed that the site initially contained timber buildings in a rectangular enclosure. By the eleventh century, they had merged to form a single manor house. A church was found at the site from the

early tenth century and during the next 100 years was enlarged to include a graveyard (Figure 6.3). By the twelfth century, the church and churchyard at Raunds fell into secular use and the churchyard was abandoned with the church building incorporated with the manor house (Cadman & Foard 1984).

The individuals from the churchyard were interred during the tenth to twelfth centuries (Bodington 1996). Most of the burials were in the south and east of the cemetery, with a concentration of infants on the south side of the church wall, suggesting 'eaves-drip' burials were children could be indirectly baptised (Boddington 1996). The skeletal material excavated from Raunds contains 361 individuals, with 103 males, 82 females, and 162 juveniles (Craig & Buckberry 2010: 13).

Figure 6.3. Raunds Furnells cemetery displaying burials of juveniles and the location of the earliest church (Boddington 1996).

6.1.3 Canterbury

Medieval Canterbury is a local district of Kent and lies on the River Stour (National Grid Reference TR 1525 5826). Archaeological evidence suggests that Canterbury started as an Iron Age settlement and was an important town centre in the first century AD (Hicks & Hicks 2001: 2). In AD43 the Romans invaded Britain and took over the settlement and called the new town Durovernum Cantiacorum (Hicks & Hicks 2001: 2). After the Romans left Britain in AD407 town life dwindled and the remaining farms survived by growing crops and raising animals. In 597AD, Pope Augustine was sent to convert the Saxons in Canterbury (Hicks & Hicks 2001:3). By AD598 Augustine and his monks built an abbey outside the walls of the old Roman town and in AD602 he rededicated a deserted Roman church which later became the seat of the first Archbishop in AD603 (Hicks & Hicks 2001: 3). This event spurred a new revival in the town as craftsmen, such as leather and wool workers

came to Canterbury (Hicks & Hicks 2001:3). Another important industry in Canterbury was providing the needs of pilgrims. The town of Canterbury was known for its several religious houses and cathedral which held the shrine of Thomas Beckett (Hicks & Hicks 2001: 4). The shrine brought many pilgrims to the town who bought souvenirs such as badges or a pewter containing holy water.

By the 9th century, Canterbury had grown into a busy town. However, this made it an easy target for Danes raiding in England because of its close proximity to the eastern shore of England (Hick & Hicks 2001: 3). Canterbury was raided twice in AD842 and 851, and in 1011 the Danes returned to lay siege to Canterbury. They burned the Archbishop as well as the cathedral and most of the houses in Canterbury (Hick & Hicks 2001: 3). Unfortunately, Canterbury Cathedral suffered many fires, the first in 1067. The cathedral was rebuilt in 1070 by the Normans, burned in 1174, and was rebuilt again in 1175.

The priory of St Gregory, Canterbury was founded between AD1084 and AD1086 by Archbishop Lanfranc (Knowles & Hadcock 1971; Hicks & Hicks 2001:3) and was in use from the mid-11th to early 16th century. It is found 300 m north of the present day Canterbury Cathedral, outside of the Medieval city wall (Mahoney *et al*. 2016: 131). It was originally for six priests who ministered to the nearby hospital of St John the Baptist (Knowles & Hadcok 1971; 152), and provided free burial for the poor in the cemetery (Sparks 1988: 371; Mahoney *et al.* 2016: 132).

The cemetery was established just before the Priory (Sparks 1988: 31), with a total of 1,342 skeletons recovered during the excavation (Figure 6.4). Historical textual records reveal that the cemetery served poorer families from local parishes, people who could not afford burial fees and patients from nearby St. John's hospital (Somner 1703; Mahoney *et al.* 2016: 132). The cemetery was in constant use until a few years after the priory dissolved in the 16th century (Sparks 1988: 32; 2001: 376).

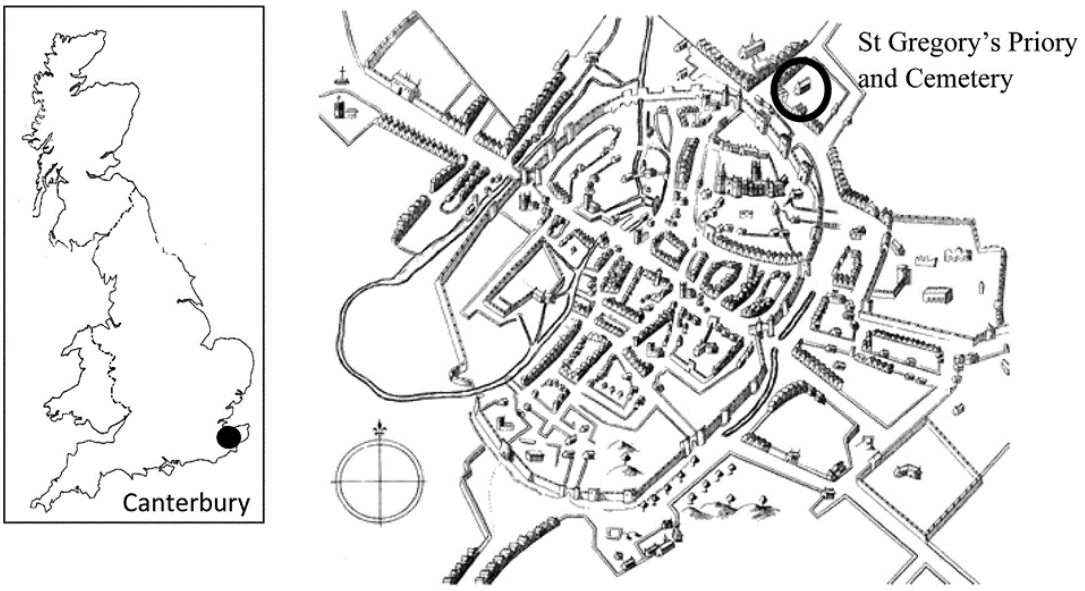

Figure 6.4 St. Gregory's Priory and Cemetery Map (Mahoney *et al.* 2016: 131).

Excavations of the Priory and cemetery of St Gregory's were undertaken between 1988 and 1991 by the Canterbury Archaeological Trust (Hicks & Hicks 2001: 1). Details of the cemetery excavations to the south of the church have not been published, partly because of a lack of funds for the project. A total of 1,342 skeletons were excavated from the cemetery, church and priory of St. Gregory's (Anderson & Andrews 2001: 338). The skeletons were previously excavated (Anderson & Andrews 2001: 338-370) with a total of 91 burials recovered from inside and around the priory. These were members of wealthier families (Hicks & K Hicks 2001:1), who paid for the prestigious burial location, which was a popular way of displaying socio-economic status for wealthy lay people during this period (Daniell 1997: 96-97). Anderson (Hicks & Hicks 2001:1) notes 1,223 skeletons from the cemetery; of these, 294 are listed as sub-adults and 929 adult burials. The unpublished notes by Anderson are located at the University of Kent, along with the collection of skeletal remains from the site (Hicks & Hicks 2001: 1).

As a result of the excavation, the majority of the individuals are located in the cemetery which was situated to the south of the church, although a large proportion of children were found to the west of the church, in close proximity to the building (Hicks & Hicks 2001). Only children over two years of age were recovered from within the priory (Hicks & Hicks 2001). The presence of children and females within the church shows that there were lay benefactors and their families rather than an enclosed monastic community (Mahoney *et al.* 2016: 132). The male and sub-adult mortality at St Gregory's is similar to those found in other medieval urban and ecclesiastical sites (Hicks & Hicks 2001).

6.1.4 Wharram Percy

Wharram Percy is a medieval village found in the North-West Yorkshire Wolds (National Grid Reference SE 8583-6421). The site has been abandoned since the early 16th century and archaeological investigations began in 1950 and continued for four decades. The church and cemetery were excavated in 1962-74 and research on the site has produced a large reference series of thirteen reports in XI 'The Churchyard' (Mays *et al.* 2007). The village of Wharram Percy was continuously occupied for nearly 600 years (Figure 6.5). St Martin's church was one of the earliest structures built between AD950 and 1050 and was replaced by a newer and larger building in the early 12th century when the members of the noble Percy family lived in the village.

The area was first settled in the Bronze Age; by the Iron Age at least two farms were established which grew to five during the Roman period. It was not until the Anglo-Saxon period that the site began to grow, and, by the 9th century, there was a corn mill followed by a small chapel (Beresford 1987: 10). During the 12th century, St Martin's church served Wharram Percy as well as four other townships in the ecclesiastical parish: Towthorpe, Burdale, Raisthorpe and Thixendale (all 2km to 4km away on the south side of the Wolds watershed) (Mays *et al.* 2007: iii).

During the Medieval period, there were two manors at Wharram. One was held by the Chamberlain family and the other by the Percy family (lords of Northumberland). By the 13th century, the Percy family had bought the Chamberlain manor and house (now known as the South Manor) and the church was constructed in the early 14th century. The lord of the manor died during the Black Death in 1347, but Wharram Percy and its neighbours survived and the village continued to grow, reaching to 30 houses by 1368 when a mill, corn barn, and kiln were erected (Beresford & Hurst 1990: 57-59).

The prosperity of the growing community quickly ended when the Hilton family took over the manor in 1403 (Mays *et al.* 2007: iii). Changing prices and wages, during the 15th century, had shifted production from crop farming to sheep wool. The population began to dwindle in 1458, and by the middle of the 16th century Burdale and Wharram Percy were deserted, with Towthorpe and Raisthorpe also deserted by the end of the 17th century (Mays *et al.* 2007: iii). Today, the church is the only standing Medieval building on the site and the overgrown foundations of the two manor houses and 40 peasant houses surround it (Mays *et al*. 2007: iii).

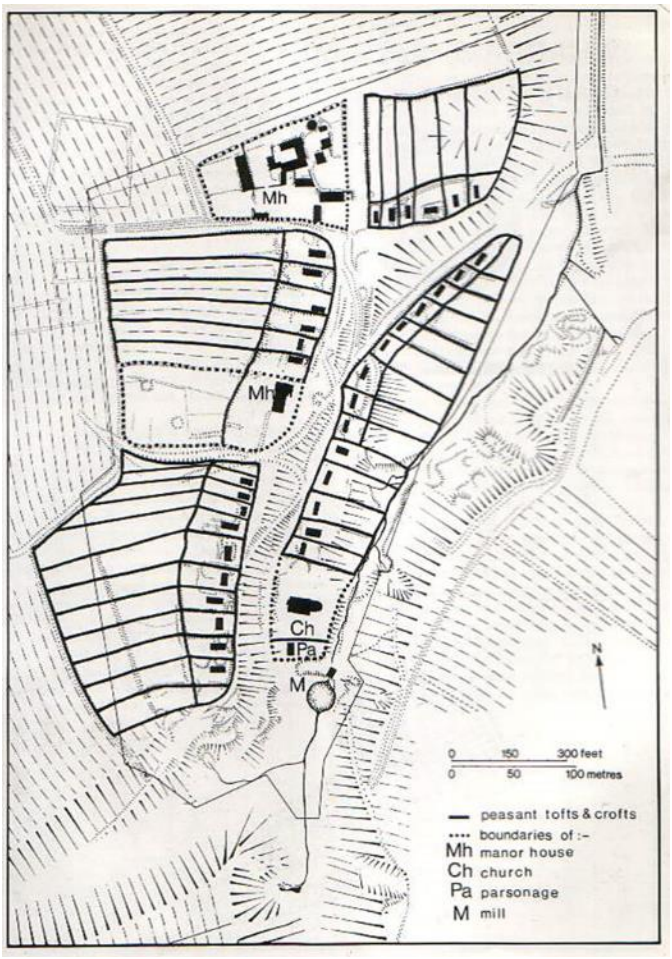

Figure 6.5 Wharram Percy site (Mays *et al*. 2007: 84).

The site of Wharram Percy was rediscovered in 1948 and underwent extensive excavations over the following decades (Mays *et al.* 2007: iii). The skeletal remains of 687 articulated burials found in the church and churchyard span 900 years, from the commencement of burial in the churchyard in the mid-10th century to the mid-19th-century (Mays *et al*. 2007: 77). The people who lived in the parish were the only ones interred in the cemetery and thus it represents a geographically and socially confined population, primarily comprising peasants (Richards *et al*. 2002: 206). Of the 687 skeletons, 327 juveniles (Mays *et al*. 2007: 88) were recovered.

There was a clear division in mortality rates during the Medieval period for pre- and post-Black Death groups (Mays *et al*. 2007: 77). Historical Documents show population depletion during the mid-14th century as the Black Death resulted in better living conditions for those who survived. Labourers were scarce, so wages increased and lower numbers of burials were found in the later Medieval period (Mays *et al.* 2007: 77).

The juvenile burials were localized in the East End of the church (EE) (Figure 6.5 and Figure 6.6) of the churchyard and nearly half of the excavated juvenile burials were under 10 years old (Heighway

2007: 229). Statistical testing of burial location and age found significant bias towards burying juveniles north of the church from foetal to 1 year old, while older infant burials were found within 30 ft. of the north church wall (Mays 2007: 87; Table 17). There was a change in appropriate burial location from 1-2 years old, which may be loosely related to baptism. Juveniles aged 1-17 were buried in higher frequencies in the North Churchyard (NA) than adults who were found in higher proportions at the south (SA) and west (WCO) regions of the church. Mays (2007: 86-87) noted this strong relationship between age and burial location and its reflection of the transition from childhood to adulthood.

The majority of the burials at St Martins were intercut thereby affecting the overall completeness of skeletal remains. Preservation was recorded as 'poor', 'moderate' or 'good' (Mays 2007: 79). The soil was beneficial to bone survival however the lack of on-site sieving was a likely factor in the lesser skeletal completeness of infants (Mays 2007: 79-80: 88).

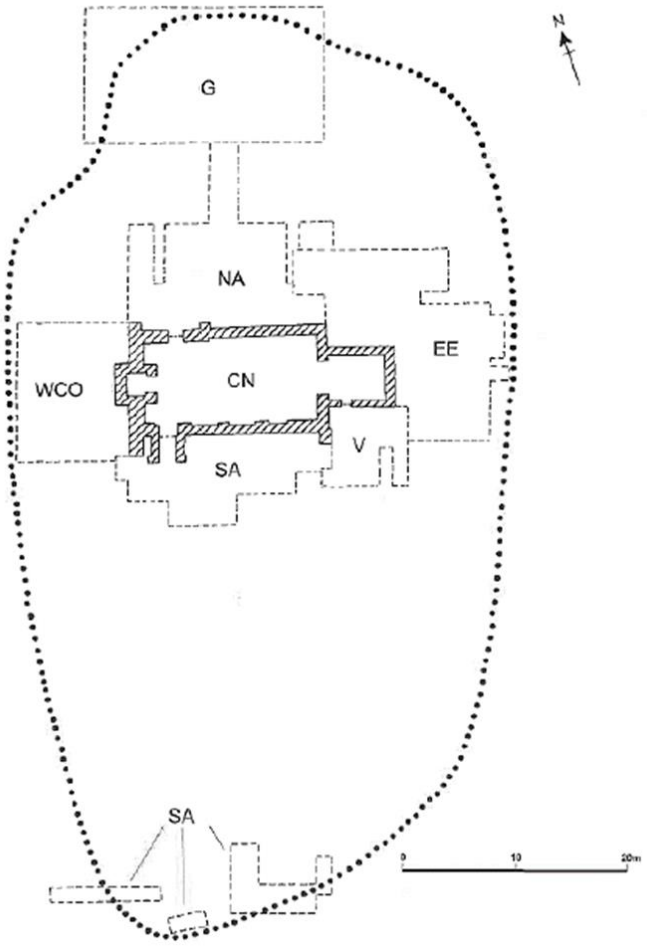

Figure 6.6 Excavation zones, limit of burial and standing remains at St Martin's, Wharram Percy (E.Marlow-Mann; Mays 2007, 78 fig. 115).

6.1.5 Wolverhampton

The Post-Medieval community of Wolverhampton is located in the West Midlands (National Grid Reference NGR SO 3914 2989). The earliest reference to Wolverhampton comes from AD985 when an area of land at 'Hampton' was granted by King Aethelred to Wulfrun, a Mercian noblewoman (Adams & Colls 2007: 6). Despite the outbreak of plague in the 14th century, the town flourished over the next 100 years and saw developments in the woollen trade (Adams & Colls 2007: 6).

The 16th century saw the discovery of coal and ironstone which transformed the area (Mander & Tildesly 1960: 143; Figure 6.7). Several small ironworking businesses developed and the town became well known for the numerous small items it produced. During the Civil war many ironmasters profited by making arms and ordnances for both sides (Adams & Colls 2007: 6). It was the growth of the lock industry however, that dominated the local economy in the 17th century, with locks and keys produced as early as 1603 (Adams & Colls 2007: 6). Jewellery become fashionable and more elaborate, often with the inclusion of semi-precious stones and steel. Until the early 1790s, this jewellery was in great demand and gradually became less fashionable with cheaper production methods developed in nearby Birmingham (Adams & Colls 2007: 6).

During the 19th century, industrialisation continued and the lure of employment attracted immigrants to the town, not only from outlying rural areas but also from Wales and Ireland (Adams & Colls 2007). As production methods improved, the emphasis changed from small scale manufacturing to heavier forms of engineering with bicycles, cars, lorries and buses being made in the town (Adams & Colls 2007: 6).

As the effects of industrialisation spread across the country, Wolverhampton was already a manufacturing centre with a population of 7,454 people living in 1,400 houses (Adams & Colls 2007: 6). The 19th century saw an increasing pattern of growth; the existence of a rich coalfield with supplies of iron ore and fire clay immediately to the east of the town fuelled this growth as Wolverhampton benefited from its location as one of the major towns of the area which became known as the 'The Black County' (Adams & Colls 2007: 7). The population increased significantly from 12,565 at the start of the century to 94,187 at its end as people migrated from the country attracted by the promise of work and industry (Adams & Colls 2007: 7).

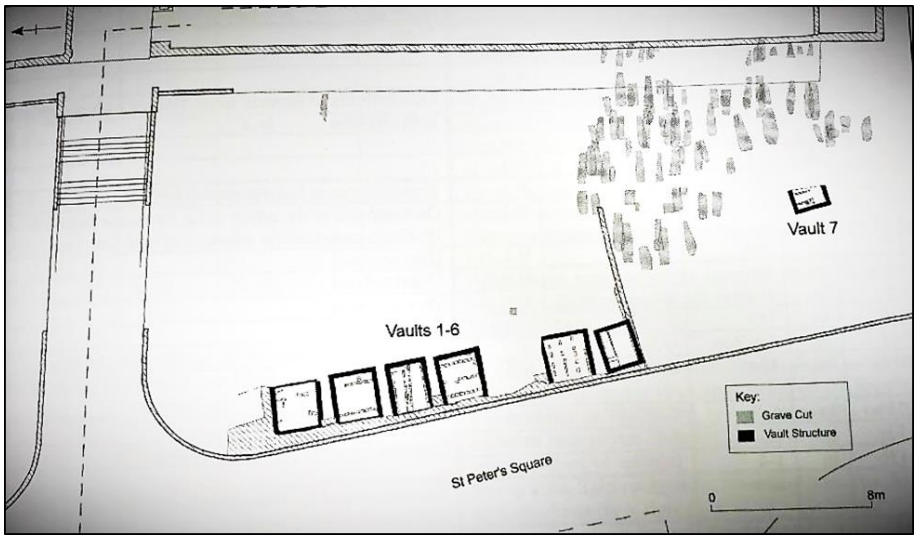

Figure 6.7: Wolverhampton St Peters Church Phase 2 plan showing burials and vaults (Adams & Colls 2007: Figure 8: 19).

The Birmingham University Field Archaeology Unit (Now Birmingham Archaeology) carried out archaeological excavations for Thomas Vale Construction between October 2001 and January 2002. They carried out excavation of an overflow burial ground of St Peters Collegiate Church Wolverhampton in advance of the construction of an extension of the Harrison learning centre (Adams & Colls 2007).

The earliest parts of St Peters Church date from the 13th century (Adams & Colls 2007). St Peters churchyard was the only Anglican burial ground in the immediate area until 1727 when the churchyards of St Leonards, Bilston and St Giles Willenhall were constructed. Between 1539 and 1900, 62,031 people were listed in the St Peters burial register. The majority of burials took place in the open churchyard but there is documentary evidence in the parish burial records that list 21 vaults along the wall on the east side of the churchyard. This latter group is recorded with associated names and dates from 1774-97.

The excavations recorded 152 burials, with 52 juveniles dating to the mid-19th century. The majority of burials were found with few remains of wooden coffins, and evidence of intercutting graves and truncation by later building activity (Adams & Colls 2007). Seven brick vaults were found; six had been emptied during an earlier graveyard clearance. The intact vault and earth cut burials were found in the south-eastern part of the site which appeared to not have been clad (Adams and Colls 2007). The preservation of the human bone was good, despite high levels of truncation. Out of the individuals investigated, 42% died before the age of 20 and 76% of the sub-adults died before the age of five (Adams & Colls 2007).

6.2 Demography of the Sites

It has been demonstrated that the study sites represent a range of past population groups. Both Anglo-Saxon and Medieval Wharram Percy are rural settlements. Medieval Canterbury is a mix of both urban and rural inhabitants and Post-Medieval Wolverhampton is an urban community. Sorokin and Zimmerman (1970) compiled a table that outlines the key characteristics of urban and rural environments (Table 6.2). The classifications of urban versus rural settlement structure provides more context for the inhabitants from the sites used in this thesis and will aid in the interpretations of the developmental trajectories in Chapter 7. For instance, rural settlements such as Great Chesterford, Raunds, and Wharram Percy, are described as more homogenous and closer to the natural environment. Rural communities are believed to have smaller populations undertaking agricultural activities (Williams & Galley 1995). These communities are likely to have a close kinship network compared to urban areas such as Canterbury and Wolverhampton, where there is more population density, heterogeneity and isolation from nature. Urban communities are typically larger with dense populations and a diverse range of economic functions, as well as evidence for an established administration, politics, and religion (Ottaway 1992).

Characteristics of Rural and Urban Environments		
Variables	**Rural**	**Urban**
Occupation	Totality of cultivators and their families. There may be some representatives of non-agricultural works.	Totality of people engaged in manufacturing, mechanical pursuits, trade, commerce, professions, governing, and other non-agricultural occupations.
Environment	Predominance of nature over social environment.	Greater isolation from nature and predominance of human environment.
Size of Community	Open farms or small communities. Agriculturalism and size of the community are negatively correlated.	Typically within the same country and period, the size of the urban community is larger than the rural community.
Population Density	During the same country and period, the density is lower than the urban community. Agriculturalism and density are negatively correlated.	Greater than in the rural community. Urbanity and density are positively correlated.
Heterogeneity and Homogeneity of Population	Rural groups are more homogenous.	Urban groups are more heterogeneous.
Social Differentiation and Stratification	Rural differentiation and stratification are less than urban.	Urban differentiation and stratification are positively correlated.
Mobility	Territorial, occupational, and other forms of social mobility are much less than urban. Typically migration carries individuals from the country into the city.	Urbanity and mobility are positively correlated. Only during social catastrophe is migration from city to country greater.
System of Interaction	Less contacts per person as there is a narrower area for the interaction system and its members. More prominent primary contacts of personal relationships.	More numerous contacts as there is a wider area of interaction system and its members. Greater complexity with a predominance of secondary contacts and impersonal, casual, and short-lived relationships.

Table 6.2: Characteristics of rural and urban environments (After Sorokin & Zimmerman 1970: 75).

6.2.1 Rural Environments and Everyday Activities

Rural communities were often dependent on their own agriculture which led to limited and less varied diets. In the event of crop failure, individuals would become susceptible to pestilence and famine (Lewis 2002), which may have occurred at Medieval Wharram Percy (Mays 2007). Settled communities led to greater local environmental contamination as permanent housing and land attachment meant that people were no longer free to leave an area before pathogens could become established. Increases in population size resulted in closer contact with other humans and livestock and made the agricultural settlement an ideal place for disease and infections to spread person-to-person or animal-to-person (Manchester 1992; Roberts and Manchester 1995; Cohen 2009). The domestication of cow, pig, sheep, cat, and dog also brought rats, mice, ticks, fleas, and mosquitos which acted as vectors for disease (Cockburn 1971).

New tracts of land for agricultural exploitation also exposed people to new vectors and pathogens (Cohen 2009). Contact with soil exposed people to fungal diseases such as *Aspergillus fumigatus*, and the inhalation of silica-containing dust could cause lung diseases. The spreading of faeces on the land increased contact with pathogens directly or indirectly through the plants they fertilised and typhoid, roundworm, hookworm, and amoebic dysentery could all be transmitted (Cockburn 1971).

Little is known about Anglo-Saxon crafts and their industry due to the perishable nature of Anglo-Saxon artefacts. Individuals at Raunds and Great Chesterford however, were likely to have engaged in subsistence agriculture and had use of the meadows and woodland within the surrounding area. Environmental evidence from neighbouring villages at Raunds shows that wheat, barley, rye, and flax were grown (Campbell 1994), and it is likely that similar crops were cultivated at Raunds. These crops would have been used to produce bread, porridge, beer, clothing, and fodder for animals (Campbell 1994).

The houses were probably consistent with the period as timber-framed rectangular buildings with stone or clay floors. Close contact with cattle would have left the occupants susceptible to infections such as zoonoses, allergies and parasitic infections (Campbell 1994). Both Great Chesterford and Raunds settlements however, pre-dates any of the major industrial activity that developed in England during the thirteenth century.

More is known about Medieval Wharram Percy, which was a rural agricultural settlement that also produced wool (Mays 2007). Mays (2007: 191) conducted a demographic study of the adult skeletal population from Wharram Percy compared to the urban centre in York. The osteological data showed that the adult population from Wharram Percy had more males than females while the

reverse is seen at York. A possible interpretation of this pattern was that female-led migration into York occurred from surrounding rural settlements such as Wharram Percy, a pattern for which there is Medieval documentary evidence (May 2007: 191). Goldberg (2013) suggests that this was associated with labour imbalances resulting in social disruption caused by mid-14th century Black Death and an increased demand for female labour in urban centres. At Wharram Percy, the sex imbalance is in all phases. If a female-led migration pattern is the correct explanation, then it is the result of events before the Black Death, and the occurrence of this outbreak only accentuated trends already present before the mid-14th century (Mays *et al*. 2007: iii).The osteological data also shows evidence for trading links between Wharram Percy and other settlements (Mays 2007). Carbon and nitrogen stable isotope analyses show that both Medieval and Post-Medieval diets had small but significant quantities of seafood which have been acquired from coastal settlements or indirectly through trade with inland towns (Mays 2007). Regular links between Wharram Percy and larger settlements may have impacted the disease experience of the community and affect juvenile growth. DNA analyses show that tuberculosis at Wharram Percy was acquired from other infected humans (rather than animals) (Mays 2007: 189). Two specific infectious diseases were identified: tuberculosis (nine adults) and advanced leprosy of a 10 year old child (Mays 2007: 189). The human form of tuberculosis is a population density dependent disease and regular contact with large urban centres may have helped to maintain the disease even in the less populated countryside (Mays 2007).

6.2.2 Urban Environment and Everyday Activities

The common characteristics of urban communities are specialised craft, trade, and religious centres (Lewis 2002). The centres are the result of a shift in subsistence with population movement and occupational hazards adding to the problems of overcrowding and poor hygiene (Lewis 2002). Pre-industrial urban centres, such as Canterbury in the Medieval period, relied on their rural hinterlands to provide the food for increasing populations of specialists inhabiting the urban areas (Storey 1992). These changes lead to metabolic diseases such as rickets and scurvy which prevalence increased due to dietary deficiencies and overcrowded centres (Fildes 1986).

Studies on Medieval Canterbury have found that males were living longer than females, with only 2% of males classed as young adult, whereas over a fifth of females died before their 30's (Hicks & Hicks 2001: 230). Over a fifth of all adults displayed evidence of extra spinal osteoarthritis occurring in males - almost three times more frequently than in females. The most frequently affected joint was the shoulder, followed by the foot and ankle (Hicks & Hicks 2001). The relatively low level of

degenerative disease in the spine suggest that activities resulting in excessive wear and tear of joints was not a major problem for those buried within, or surrounding the church (Hicks & Hicks 2001). In both sexes, the vertebral column is the most frequent site of osteoarthritis.

The skeletal sample from within the church and the surrounding cemetery appears relatively healthy when compared to other medieval material (Hicks & Hicks 2001). The mean stature of both adult sexes does not display evidence of stunting which is common when individuals do not receive adequate nutrition during childhood. The adults from this population also show low levels of joint disease and trauma which suggests a sedentary lifestyle (Hicks & Hicks 2001). There was a high prevalence of cavities and poor oral health which may be related to eating between set meals and a diet low in fat coupled with a high carbohydrate intake (Hicks & Hicks 2001: 370).

Similarly to Wharram Percy, increases in trade and migration of people from other areas introduced new diseases into the communities. The range of different groups of people traveling into urban settlements provided the perfect breeding ground for infections (Lewis 2002). Population dependent diseases such as tuberculosis thrive in these conditions, however, as people became immune to diseases the infections became endemic (McGrath 1992).

The differences between larger towns and rural communities became more distinct in the seventeenth century. As towns grew, however, they became dependent on exports to maintain the population and the rural areas providing for towns also grew (Schofield & Vince 1994). Rural areas provided urban centres with food and in the event of crop failure, both groups were affected. Despite having different microclimates, both areas experienced the same climatic changes and were equally vulnerable to natural disasters and the interaction between urban and rural populations provided the opportunity for similar diseases to become endemic (Lewis 2002).

The Industrial Revolution in the eighteenth century was a period of rapid technological change with the establishment of new urban centres, population growth, rural-urban migration and subsequent rural depopulation (Storey 1992; Lewis 2002). Fully industrial centres grew larger and more dependent on external food supplies. The gap between the social classes became more distinct and industrial advance resulted in an increase in environmental pollution (Lewis 2002).

By the 1820s, industrialisation reached its peak and people complained about the effect of urban and industrial environments on their health, specifically contamination of food and water supplies (Adams & Colls 2007: 9). Wolverhampton suffered from endemic disease at the time including tuberculosis, typhoid, scarlet fever, measles, and various forms of pneumonia (Adams & Colls 2007: 9). In the early 19th century, pulmonary tuberculosis was the most common cause of death in the newly emerging urban centres (Adams & Colls 2007: 9). With poor housing and inadequate

ventilation in the narrow streets it is likely that many people suffered from the condition (Adams & Colls 2007: 7). Syphilis had also become a significant problem by this time in the many urban centres (Adams & Colls 2007: 9), which is supported by strong evidence of the disease in town burials (Adams & Colls 2007: 9).

A disease that affected the inhabitants of Wolverhampton several times in the early 19th century was cholera, an acute infectious disease that spread to Europe from the Indian subcontinent in the early 1800s (Adams & Colls 2007: 7). In 1849, nearly 500 people died which highlighted the inadequacies of medical facilities in the town. During the 1832 outbreak, those who were able to pay went to the dispensary in Queens Street, while some free treatment was available at the Medical Hall and Vapour Bath in Dudley Street. By 1849, the south Staffordshire general hospital had been built but it refused to accept any cholera patients, preferring to isolate them in the workhouse or in specially erected tents on Gold Thorn Hill, two miles out of town (Adams & Colls 2007).

It is impossible to know how many of the people buried in St Peters were victims of cholera as there are no skeletal manifestations of the disease. Instead, one of the characteristics of the disease was the speed with which it affected the victim, death occurring within hours of the first symptoms (Adams & Colls 2007). It was not until the 1850s, that the cause of the disease was linked to contaminated water supplies (Adams & Colls 2007).

As well as disease, accidents were a major cause of death. The Children's Employment Commission reported deaths (not only children) associated with fire, drowning, murder, suicide, and accidents associated with horses, wagons and pigs, and falls from ladders (Adams & Colls 2007). Additionally, deaths are recorded associated with mining induced falls within coal shafts, deaths from falling coal, clods and rubbish, drowning, suffocation, and explosion. There were accidents at ironstone pits, ironworks and lime works (Adams & Colls 2007: 11).Three cases of amputation were found at Wolverhampton. One individual's ulna and radius was represented as stumps which suggests a traumatic event such as catching the arm in a machine. The second case was an amputation of the left tibia and fibula, and the third was of the right femur. Whether the amputations were carried out as a result of disease or an accident is unknown (Adams & Colls 2007). The archaeological evidence and documentary research suggests that Wolverhampton was a population largely suffering from bad health and poor living conditions in an urban centre and employed in hazardous and stressful working environments (Adams & Colls 2007).

6.3 Infancy and Mortality of Anglo-Saxon to Post-Medieval Juveniles

It has been demonstrated that the environments from both urban and rural communities, spanning from Anglo-Saxon to Post-Medieval periods had many challenges. Table 6.3 refelcts the mortality rates of each site by age group. Childbirth was a particularly dangerous time for women and infants in all periods. Beginning with the Anglo-Saxons, the adult females from Raunds had high mortality peaks in early adulthood, while the juvenile samples peaked during infancy (Craig & Buckberry 2010). Forty-four per cent of all adult females died between 17-25 years old, with a gradual decline in mortality peaks for adult females. Nearly 71% of all females recorded from Raunds died during the childbearing age range of 17-35 years (Boddington 1996: 114). The majority of first pregnancies might be expected to occur during the 17-25 year age range, usually associated with higher risk of death than subsequent pregnancies (Craig & Buckberry 2010). It cannot be established whether the females at Raunds were dying during childbirth or subsequent to the birth. The low number of neonates found does suggest that the majority of pregnancies continued through to full term (Craig & Buckberry 2010). The smaller, though not insignificant number of females dying in the next age range of 25-35 suggest a continuing risk from the hazards of childbirth. These difficulties are a result of poor medical attention and hygiene standards during childbirth. This high mortality spike of females in early adulthood can be associated with the high infant mortality during the first year of life. If a mother died at childbirth or within the first year of an infant's life, the nutritional standard of the infant would fall dramatically and increase the risk of infant mortality (Boddington 1996: 114-115).

Birth to two years old had the highest risk of death for all sites, specifically the first year of life (Boddington 1996: 114). While birth is indicated as a time of high risk of death, other factors play a more important role in infant mortality. The first year of life is a dangerous period because of the many new elements an infant is introduced to. Two different nutritional sources, one from the mother and subsequent weaning, and the development of immunity to infection are common examples of normal pressures on an infant that may have been responsible for high infant mortality. Similar to the high death rate in younger females, it appears that poor medical and hygiene standards during or after the pregnancy is likely to have contributed to the death rate. Seventeen per cent of the entire population of Raunds died in infancy (0-12 months), and in early childhood (-3 years); 1.2% in middle childhood (4-7 years); and 4.7% in older childhood (8-12 years; Craig & Buckberry 2010). Great Chesterford supports these findings as 63% of females died between 25-35 years old and 45% of all juvenile died in infancy (0-12 months).

Similar trends were found at Medieval Wharram Percy, which had high mortality rates in infancy, decline during later childhood and adolescence, and a final gradual rise during old adult age (Mays

2007: 95-99). Individuals under 16 years old comprise of 312 burials; these are 45% of the total burial population (Mays 1993). There is a flat age distribution of natural deaths in the perinatal period and it loosely represents trends of stillbirths and natural deaths soon after birth (Mays 1993). The pattern of infant deaths at Wharram Percy is consistent with what is expected for a historic population (Mays *et al.* 2007: iii). Wharram Percy however, has more infant burials than other medieval skeletal assemblages, although it is still unclear as to the reasons behind this.

The trend of difficult early years is also seen at Canterbury. Just under a quarter of the burials at Medieval Canterbury failed to reach adulthood, with the greatest sub-adult mortality occurring between 1-6 years old (Hicks & Hicks 2001). In addition to the high mean stature for the whole sample of juveniles, this suggests an overall high standard of health and growth during childhood, at least for those who survived to adulthood (Hicks & Hicks 2001:370).

Concern about the health of children in towns was highlighted in 1848 as a result of the Public Health Act, a government inspector visited towns and reported that one in six children died in their first year and that life expectancy at birth was only just over 19 years. This was confirmed by the skeletal analyses which shows that Wolverhampton infant mortality, especially in the weaning age of 2 years old, contributed to 40% of all juvenile burials. The Children's Employment Commission Report of 1843 also attributed the high death rate in infants to the custom of administering 'Godfrey's Cordial' to infants and young children to keep them quiet or 'sleeping them' while their parents were out at work (Adams & Colls 2007: 8). This was a mixture of boiled treacle water and a dose of opium made by the local chemist or his wife, the ingredients of which were not always precisely calculated. This could result in varying amounts of opium being administered to the child, often while the mother was out at work.

Mortality Profiles of Juveniles by Site						
Site	**Group 1 (Foetus)**	**Group 2 (Infant-2 years)**	**Group 3 (3-5 years)**	**Group 4 (6-8 years)**	**Group 5 (9-12 years)**	**Juvenile Sample (n)**
Great Chesterford	57.83% (n=16)	59.03% (n=49)	2.40% (n=2)	13.25% (n=11)	3.61% (n=3)	83
Raunds	1.23% (n=2)	6.17% (n=10)	5.55% (n=9)	4.93% (n=8)	5.55% (n=9)	162
Canterbury	18.70% (n=55)	24.49% (n=72)	12.59% (n=37)	9.52% (n=28)	4.08% (n=12)	294
Wharram Percy	23.24% (n=76)	23.24% (n=76)	16.82% (n=55)	15.29% (n=50)	10.70% (n=35)	327
Wolverhampton	6.90% (n=4)	51.72% (n=30)	12.07% (n=7)	3.45% (n=2)	5.17% (n=3)	58

Table 6.3: Mortality Profiles of the juveniles from Great Chesterford (Evison 1994), Raunds (Boodington 1996), Canterbury (Hicks and Hicks 2001), Wharram Percy (Mays *et al.* 2007), and Wolverhampton (Adams & Colls 2007).

6.4 Weaning Problems and Practices

As mentioned in Chapter 2, after the first six months of breastfeeding, breastmilk loses some of its nutritional content and, if not sufficiently supplemented, infant growth trajectories are altered and they become more susceptible to disease (Mays 2007). The supplementation of external foodstuffs may have led to infection and fatal diarrhoeal disease known as 'weanlings dilemma' (King & Ulijaszek 1999). The transition to solid foods during weaning exposed children to a wide array of bacterial, viral, and parasitic infections (Fildes 1988).

At Anglo-Saxon Raunds, Haydock and colleagues (2013) investigated stable-isotope ratios for evidence of weaning for the late Anglo-Saxon population. Nitrogen and carbon values of rib collagen were obtained for individuals of different ages to assess the weaning age of infants within the population. Anglo-Saxon infants are thought to have been weaned relatively swiftly (Crawford 1999: 73). Data from Haydock *et al*. (2013) supports this interpretation since the Raunds infants appear to have changed from exclusively breastfed to an adult diet within 1 year. The final shift to adult diet occurs between 2 and 3 years old which corresponds with archaeological and documentary evidence of a change in the status and attire of children aged 2-3 years old in the Anglo- Saxon period (Crawford 1999: 70-73; Haydock *et al.* 2013: 609). This suggest that the completion of weaning was a significant rite of passage in later Anglo-Saxon England, as it is in many societies, as it marks the end of the vulnerable infant period (Van der Vlliet 1974). Although there is no isotopic analysis for Great Chesterford, the weaning period of 12 months to 2 years is the second highest morality peak for this sample, as 28% of all juveniles died during this period. This suggests that after the dangers of childbirth, weaning was the second most problematic period for Great Chesterford juveniles.

Studies of Medieval Wharram Percy have revealed that long bone growth shows no evidence of stunting until after 2 years of age, by which time it is likely that women were supplementing infant diets with other foods during weaning. There was no change in nitrogen stable isotope ratios until after eighteen months. It is likely that supplementation was based on cereal foods as there was a lower level of ð15N in indivduals after this age (Mays *et al.* 2002). Appositional bone growth was deficient even in individuals under one year compared with modern reference data. Despite the evidence for effectiveness of the infant feeding strategy, it suggests that breast-feeding could not completely insulate infants from environmental insults (Mays *et al.* 2007).

In the seventeenth and eighteenth centuries, the mean weaning age dropped from 18 months to 7, a reduction that is a reflection of female migration to cities to find work (Fildes 1986). It was suggested by Thompson (1984) that artificial feeding may have resulted from poor mothers in urban centres not being able to feed their infants as a result of severe malnutrition. The development of

a rural industry in the eighteenth century provided employment opportunities for women in textile factories which may have lowered the quality of their health care, changed breastfeeding practices, and resulted in higher infant mortality (Lewis 2002).

The demography of the Wolverhampton population shows nearly 40% of the entire population were children. St Brides Lower Churchyard in London, a known Post-Medieval urban site found a similar demographic profile (Bowman *et al*. 1993). Analysing the juveniles according to their age-at –death category indicates that the peak in mortality occurred between six months and five years (Adams & Colls 2007). This could be related to the hazards associated with weaning. In the Victorian period it was known to feed the growing infant with 'papa' or 'panda' which led to a defective nutrition resulting in a poor immune system. As a result, children of weaning age were at a higher risk of contracting diseases and gastro-intestinal infections (Lewis 2002: 10-11; Roberts & Cox 2003: 307). Other archaeological sites form this period with high infant mortality associated with weaning include Christchurch Spitalfieds, London (Molleson & Cox 1993: 183).

6.5 Children's Diet and Changing Lifestyle

Once the child survived the difficulties of weaning, diet continued to be a source of poor health for children of the past (Lewis 2002). Different climates, soil types and terrain determine local diet from the Anglo-Saxon to Post-Medieval periods. Some societies would have access to wild foods, while others traded thus providing a wide variety of produce year round (Dyer 1989). The Anglo-Saxon diet primarily consisted of wheat, rye, barely oats, and legumes which provided folic acid, iron, B complex vitamins and fibre, but was low in vitamin C. Dyer (1989) proposed that the consumption of leeks, cabbages and apples may have prevented deficiencies that would cause scurvy. Excessive amounts of fibre in the diet could have resulted in poor absorption of calcium which would be problematic for young children and older adults (Pearson 1997).

Meat consumption was restricted to three days a week by monastic rules (Schofield & Vince 1994). Fish, such as Herring and eel were common in the medieval and later urban centres (Dyer 1989). By the fourteenth and fifteenth centuries, an increase in wheat consumption occurred as people ate more bread instead of pottages and ale became more popular (Dyer 1989). By the sixteenth century in Britain, cane sugar imports increased and the first sugar factory was opened in Britain in 1641. These changes meant that an expensive commodity was now affordable for most of the population. New milling methods were also introduced which led to an increase in refined flour (Dyer 1989).

Increased population density and agricultural intensification would have had some impact on the rural communities of Great Chesterford and Raunds, but more specifically on Medieval Wharram Percy. Manual labour meant that nutritional requirements of the rural inhabitants were greater than those in urban settings. Estates would provide rations for their tenants, however, the need to produce a surplus to feed the growing urban population may have affected the rural communities (Schofield & Vince 1994). Medieval Wharram Percy revealed no difference in diet between adult males and females but differences in diet by ages were found. Juveniles from 4-8 years old consumed a higher plant-based diet and lower protein than older children and adults, whose diet consisted of terrestrial sources of food with small but significant amounts of marine protein (Mays 2007: 93-95).The introduction of the mouldboard plough and a three field crop rotation system in the seventh century meant that more land could be cultivated and a wider variety of foods grown; in addition, animals could be reared on fallow land (Tannahill 1973: 23).

Inhabitants from developing urban towns in the Medieval period could grow vegetables and herbs in their gardens and kept animals such as pigs, chickens, and ducks in their yards (Keene 1983). During the sixteenth century, households became subdivided which lead to a reduction of urban gardens. This shift in household structures resulted in an increasing reliance on rural food production (Tannahill 1973). Although Medieval towns were able to store food and inhabitants had more variety in their diet due to trade, including importing meat and fish, the poor could no longer rely on their own plots to grow food (Schofield & Vince 1994). Mahoney and colleagues (2016) conducted a novel microware study on the juveniles (1-8 years old) from Canterbury. They found that diet became tougher from four to six years old. The variation in microware texture surfaces was related to historical textual evidence which refers to changes in lifestyle for these age groups (Mahoney *et al.* 2016). These changes in diet from four years old was also found in the isotopic study at Medieval Wharram Percy and suggests that the age of 4 marks a change in social status of Medieval children. During the 19th century, refined flours, fermentable carbohydrates and high consumption of sugar resulted in a sharp rise of caries (Mays 1998) which was seen in the Wolverhampton skeletal remains (Adams & Colls 2007: 48).

6.6 The Effects of Poor Health during Childhood

As discussed in Chapters 1 and 2, juvenile growth studies are most commonly used to understand a past population's health. The Anglo-Saxon sites of Great Chesterford and Raunds display varying levels of juvenile stress and health. Waldron (1994) indicated only three of the Great Chesterford juveniles had signs of cribra orbitalia. The condition was found in a neonate, in a 6-8 year old and 8-10 year old. These three juveniles have substantial new bone growth throughout the skeleton, specifically along the long bone diaphyses. The lesions are symmetrical and all three have visceral

rib lesions (Inskip 2008). For a large juvenile site, there is a relatively low frequency of stress markers in the juvenile remains. The Great Chesterford juveniles follow trends noted by Hoppa (1992) in that Anglo-Saxon juveniles tend to have the smallest rates of growth and that by early adolescence, the difference in stature between the modern and Anglo-Saxon individuals could be as much as four years of growth (Hoppa 1992). Mays (1999) noted that nutritional stress can delay epiphyseal fusion and prolong growth periods. Dental development is less affected by environmental factors than skeletal growth (Ubelaker 1989) and children living around the modern poverty line show slight delays in dental eruption (Garn *et al*. 1973), as is seen in the Great Chesterford juveniles. This could be another explanation as to why the number of individuals from Great Chesterford have unfused proximal and distal long bones but adult dentition with some M3 (third molar) occlusal wear. Cribra orbitalia and hypoplasia may be additional evidence for nutritional stress within the Great Chesterford population, but the level of severity is minor as there are no clear cases of rickets or scurvy. The pattern of lesions for Great Chesterford juveniles is less likely to be a result of malnutrition (Inskip 2008) and rather a fast-acting infection as there is a low frequency of cribra orbitalia or any other pathological lesions in the collection.

In contrast, the prevalence of stress markers in the Raunds population is relatively high. Out of 361 individuals recorded, 85 out of 286 with orbits had skeletal evidence of cribra orbitalia (29.72%), 46 out of 187 with at least one canine had linear enamel hypoplasia (LEH) (24.6%) and 109 out of 316 with at least one tibia present had tibial periostitis (34.5%). Several correlations between stress markers and grave elaborations produced statistically significant results (Craig & Buckberry 2010). Stress related lesions is most frequent in children from 2 years to adolescence, with nearly half of the adolescents showing signs of stress. Females also showed higher prevalence compared to males. This distribution would suggest that nutritional deficiency, in particular anaemia, would cause the pitting in the orbits. Children and in particular adolescents have high nutritional requirements with growth and development, while females have high nutritional standards to produce healthy offspring (Craig & Buckberry 2010).

As discussed in Chapters 1 and 2, children who grow up in adverse conditions tend to be short for their ages, yet, the growth period may be extended so that final adult stature may only be marginally affected (Eveleth & Tanner 1990). The burial population at Wharram Percy showed many signs of stress (Mays 2007: 184). Mays (2007) used femur length from four archaeological assemblages (Raunds Furnells, St. Helen-on-the-Walls, and Christ Church Spitalfields) to examine differences in stature. Additionally, the classic study of Maresh (1955) on recent American White children was used in Mays (2007) study as a modern comparison. The Wharram Percy femoral

length data is shorter and substantially stunted relative to the modern children. A fourteen year old from Wharram Percy is roughly the same height as a modern ten year old (Mays *et al.* 2008; Mays 2007). This shows that disease and poor nutrition were greater in the Wharram Percy individuals than modern American children. Additionally, a study of 19th century urban children show that children from Wharram Percy were no taller than factory children during the Industrial Revolution (Mays 2007). This suggests that the health and nutrition of the Medieval children may have been no better than the 19th-century urban poor. Further evidence of adverse conditions during this growth period are seen through Harris lines. These revealed that children suffering episodes of growth interruption, resulting in Harris lines, and failed to catch up either in appositional growth or in bone length, so that they remained short for their ages and deficient in cortical bone (Mays 1995; 2007). These findings show that chronic poor nutrition and disease were a problem for the Wharram Percy juveniles (May 2007).

It can be argued that mortality bias is partly responsible for the growth deficit seen at Wharram Percy and the rest of the sites, as the growth profile might not be fully representative of healthier children who survived to adulthood. Based on archaeological comparisons it can be seen that, even over 1500 years, there is very little deviation in stature and femur length, suggesting that diaphysial growth patterns changed very little. Despite no statistical significance in femur length, physical health and environmental stress was evident at Wharram Percy (Mays 2007: 133-192) as out of the 194 juveniles studied, 31 had dental caries and 6 had dental abscesses. Enamel dental hypoplasia, indicative of nutritionally deficient diets and poor health, affected 93 individuals (47.94%) and mostly formed around 2-3 years old. Porotic hyperostosis, including cribra orbitalia, associated with anaemia, was found in 30.8% of juveniles and 19.2 % of adults. The lesions were more commonly active in juveniles at time of death than the adults. Similarly, active rickets was found in eight juveniles, thus suggesting that they were already sick or unwell children who were kept indoors and as a result had deficient vitamin D leading to rickets. Twenty-nine juveniles (14.94%) had non-specific periostitis which is indicative of periosteal inflammatory responses. Three juveniles (1.54%) and 69 adults (19.16%) had evidence of fractures; one of these was a 5-6 year old with unhealed blunt trauma to the skull (Mays 2007). Wharram Percy was compared to urban York and it was found that Wharram Percy had more active lesions compared to the healed stress found at York (Mays 2007). This is also consistent with the idea that a greater pathogen load in the urban environment and long term exposure from birth to a pathogen rich environment might be expected to lead to greater resistance to infectious disease (Mays 2007).

In contrast, the juveniles from Canterbury showed very little sign of pathological stress compared to other southern Medieval England sites, such as Taunton and Gloucester (Hicks & Hicks 2001). They all followed similar long bone length trajectories that are seen with archaeological versus

modern growth studies, where the archaeological children become stunted after 2 years old and become smaller for their age compared to modern children (Hicks & Hicks 2001). One possibility for the lower prevalence of porotic hyperostosis and generally low prevalence of nutritional stress may relate to the possibility that lower status individuals at Canterbury are associated with the hospital and free burial for the poor (Hicks & Hicks 2001). These individuals may have died before the bone formation associated with periostitis has had time to manifest. Wood *et al.* (1992) have suggested that it may be the advantaged groups in society that are more likely to survive a stress episode and survive long enough for a skeletal lesion to become visible. it is possible that the most stressed individuals died relatively quickly when a stressful assault occurred, thereby not surviving long enough for the skeletal manifestations to be seen. This may explain why a higher prevalence of stress was seen in the assumed higher status burial areas (Hicks & Hicks 2001).

Poor diet combined with overcrowded living conditions at Post-Medieval Wolverhampton resulted in vitamin deficiency related conditions. The 1843 Children's Employment Commission highlighted the problem of poor diet, stating that the quality of food was not adequate. Rickets, was also prevalent during this time, partially because a lack of sunlight. It affected the pelvis (Roberts & Cox 2003: 309) and may have contributed to high maternal and infant death rates in the town. In addition, a diet that lacks fresh fruit and vegetables may be deficient in vitamin C, resulting in scurvy, a problem that also affected bone and dental development. Skeletal analysis found evidence of both conditions together with osteomalacia, which results from deficiency of vitamin D in adulthood (Adams & Colls 2007). The evidence for cribra orbitalia is also high, the explanation for which could be the poor diet that infants received (Roberts & Cox 2003; 307).

6.7 Concluding Remarks

This chapter has demonstrated the breadth of research already undertaken on the juveniles from Great Chesterford, Raunds, Wharram Percy, Canterbury and Wolverhampton and how these sites vary across different periods, settlement types, and exposures to environmental stress. For instance, the urban communities of Wolverhampton and Canterbury are exposed to more pathogens as they have higher population density and mobility, than rural environments. Wolverhampton however, represents an industrial population with higher rates of accidents, activity related pathologies, and poorer health conditions compared to the more sedentary and ecclesiastical site of Medieval Canterbury. Rural agricultural settlements of Medieval Wharram Percy and Anglo-Saxon Raunds also have high prevalence of pathological stress which may be

related to the trade routes found along these sites, while Anglo-Saxon Great Chesterford was a more rural isolated settlement.

Weaning occurred from 2 to 3 years old for all sites and children of this age were mostly kept indoors. It was not until 3 to 7 years old, that children from all sites were likely to engage in 'play' with light work related activities around the home, fields, and/or workshops. After seven, children began more gender related tasks (Heywood 2014: 123), as girls worked around the home and watched younger siblings while boys would work with their fathers in the fields or workshops. Serious work began around 12-14 for all sites as puberty signalled a transition into adulthood. The context of each site provided in this chapter will aid in the interpretations of the developmental trajectories in Chapter 7, and how bone shape may be influenced by site and time period.

7. Ontogenetic Trajectories from Anglo-Saxon to Post-Medieval Juveniles

As discussed throughout this thesis, current understandings of juvenile development is limited by the prevailing methods used to examine growth trajectories. This chapter analyses and visualises ontogenetic trajectories from Anglo-Saxon (Great Chesterford and Raunds), Medieval (Canterbury and Wharram Percy), and Post-Medieval (Wolverhampton) juveniles (foetal to 12 years old) of European origins. Following the validation study described in Chapter 5, structured-light-scanning was used to create the meshes for all femora, tibiae, and humeri and auto3dgm was used to analyse the trajectories following the validation study in Chapter 4. The first section of this chapter addresses growth (age and size), developmental variation (shape and age) and allometric trajectories (size and shape) for all individuals, sites and ages for femora, tibiae, and humeri (PCA and allometric trajectories by individual site and element are found in Appendix B-F and skeletal material in Appendices G). The rest of the chapter takes a closer look at each element by age group and explores how plasticity may or may not be influenced by site and time period. Each age group will begin with a hypothesis that was developed based on the overall developmental and allometric trends of all sites and ages presented in the first section of this chapter. Each hypothesis is then tested against each element (femora, tibiae, and humeri) for all five age groups. The PCA for developmental variation and allometric trajectories will be used to accept or reject these age group hypotheses for each element, followed by a short discussion on the findings and interpretations for each age group. This chapter will conclude with a summary discussion on the GM results and their applications to the archaeological materials presented in this chapter. By drawing on the historical context of the sites, Coroner Rolls (in order to deduce possible movement), and stress that occurs at each age group, this study sheds light on the varying tempos and rhythms of growth and development from children of the past.

7.1 Growth, Development, and Allometry

This chapter begins with a standard growth trajectory of long bone diaphyseal length (mm) by age (dental development) for the study samples (Great Chesterford, Raunds, Canterbury, Wharram Percy, and Wolverhampton) and a modern sample from the Denver growth study (Maresh 1955). The modern sample is of known age and was used to determine if there was any statistical significance in growth for the archaeological versus modern sample. Although it was demonstrated

in Chapter 4 that linear measurements are not as useful as GM for capturing shape, they are still the most commonly used method for juvenile growth studies and allow for comparisons with modern known juveniles. Unfortunately, it was not feasible to use a known age sample for the GM analyses for this thesis. Therefore, this growth comparison is used to create a baseline for the developmental and allometric interpretations discussed in this chapter. After the growth analyses, development was tested through a PCA for each element to investigate if there is statistical significance in shape for age and site. The last analyses in this section is an allometric trajectory of regressing bone shape against size. This regression determined if there was significant a correlation between bone size and shape and revealed developmental rhythms for each element. The analyses presented in this section provides an overview of the entire growth, developmental, and allometric trajectories for all ages, sites, and elements and highlights age ranges of interest for the remaining chapter that analyses shape and allometry by age group.

7.1.1 Growth Trajectories of the Femora, Tibiae, and Humeri from Anglo-Saxon to Modern Juveniles

The long bones were recorded to the nearest millimetre using an osteometric board and age was recorded using dental development (Schour & Massler 1941). The collections (Table 7.1) used were all from European decent and include: Anglo-Saxon Raunds (Boddington 1996) and Great Chesterford (Evison 1994), Medieval Wharram Percy (Mays 2007) and Canterbury (Hicks & Hicks 2001), Post-Medieval Wolverhampton (Adams & Colls 2007), and modern American White children (Maresh 1955). It should be noted that the modern collection was recorded in mean lengths for boys and girls as there are hundreds of individuals in the modern study that fall within this age criteria for this thesis. As it is difficult to sex juvenile archaeological remains, this thesis consequently pools the archaeological males and females together. Therefore, it is necessary to pool the modern data for a homogenous comparison. For the current study, an average of the diaphyseal mean lengths for boys and girls was taken and plotted to create a proxy of expected normal growth. A polynomial curve of the 2nd order was fitted for the regression of size against age and the residuals for each site were analysed through an MANCOVA to determine if there was any statistical significance between age and length between sites.

Growth Trajectory Samples					
Site	Period	Femur	Tibia	Humerus	Reference for Data
Great Chesterford, England	10^{th}-14^{th} century AD	18	9	12	Evison (1994)
Raunds, England	10^{th} century AD	17	12	11	Boddington (1996)
Canterbury, England	11^{th}-16^{th} century AD	40	40	27	Hicks and Hicks (2001)
Wharram Percy, England	10^{th}-14^{th} century AD	18	17	23	Mays (2007)
Wolverhampton, England	19^{th} century AD	6	5	7	Adams and Colls (2007)
Denver, United States of America	20^{th} century AD	1,866	1,866	1,866	Maresh (1955)

Table 7.1: Comparative archaeological data for femoral diaphyseal length.

MANCOVA: Polynomial Residuals of Femur length, Site, and Age						
Site	Great Chesterford	Raunds	Canterbury	Wharram Percy	Wolverhampton	Modern
Great Chesterford		**0.027929**	**0.004621**	**0.017663**	0.82693	**0.0019956**
Raunds	**0.027929**		0.99985	0.9892	0.5637	0.80232
Canterbury	**0.004621**	0.99985		0.98724	0.50218	0.71827
Wharram Percy	**0.017663**	0.9892	0.98724		0.50817	**0.0019956**
Wolverhampton	0.82693	0.5637	0.50218	0.82693		0.33007
Modern	**0.0019956**	0.80232	0.71827	**0.0019956**	0.33007	

Table 7.2: MANCOVA of Polynomial Residuals from the Femur Growth Trajectories.

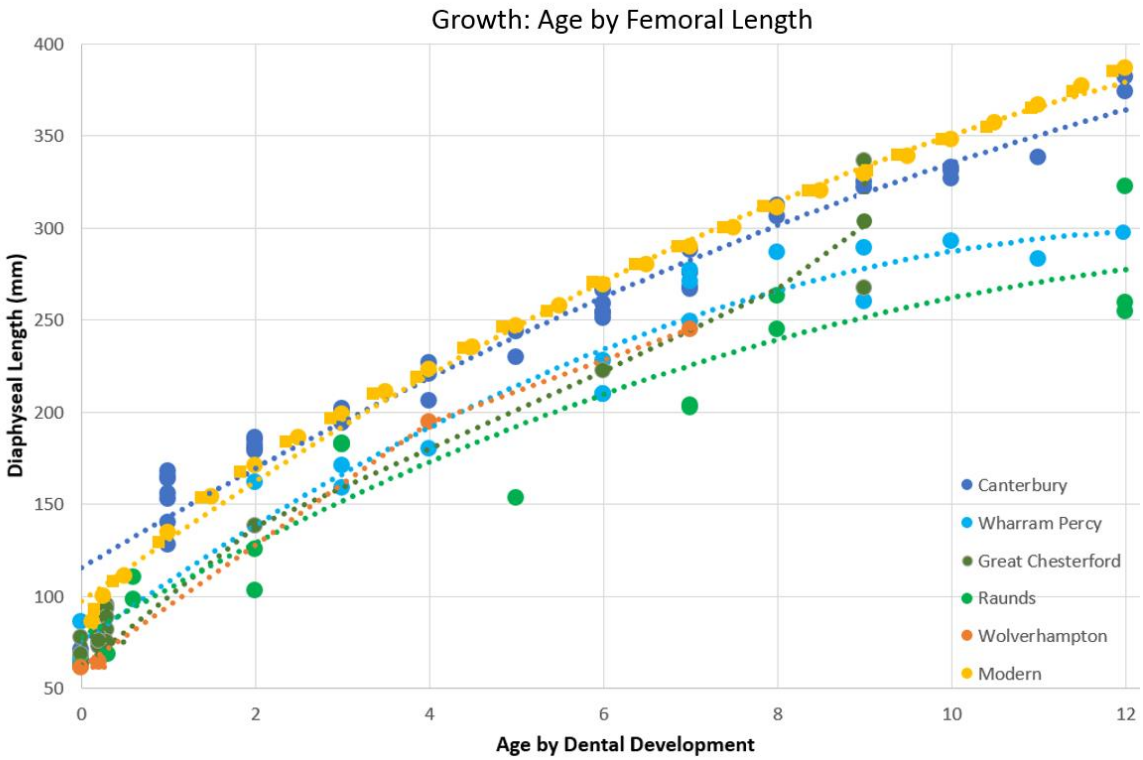

Figure 7.1: Juvenile growth from Anglo-Saxon to Modern populations. Femoral diaphysial length (mm) versus dental age for Great Chesterford, Raunds, Canterbury, Wharram Percy, Wolverhampton, and Source data for Modern (Meresh 1955) populations. The modern data was plotted by males (yellow dots) and females (yellow squares). As males and females plotted ontop of one another it can be suggested that there is little to no significant difference bewtween long bone length and age for males and females during this age range.

The linear growth trajectory for the femora (Figure 7.1 and Table 7.2) reveal that Canterbury and the modern samples have a slightly faster trajectory at birth but the trajectories begin to separate from one another at 2 years old. Once the juveniles reach 2 years of age, the Raunds growth trajectory slows, followed by Wolverhampton and Great Chesterford. This pattern continues until an interesting shift in growth trajectories occurs at 7 years old. Canterbury and the modern sample continue to have the largest amount of growth. Wharram Percy, Great Chesterford, and Wolverhampton continue to fall in the middle range of growth trajectories and Raunds falls into the smallest size range. A MANCOVA of the polynomial residuals (Table 7.2) found that the Great Chesterford femora growth trajectory was statistically different for all sites apart from Wolverhampton, which follows a similar growth trajectory. This may be a result of the lack of older indivdiuals (10-12 year olds) from Great Chesterford. Wharram Percy was also statistically significantly different from the modern growth trajectory, which may reflect growth stunting that occurred at Wharram Percy. As discussed by Mays (2007: 97-99), this growth stunting continues as 11 year olds from Wharram Percy are similar to a modern 8 year olds.

MANCOVA: Polynomial Residuals of Tibia length, Site, and Age						
Site	Great Chesterford	Wharram Percy	Raunds	Canterbury	Wolverhampton	Modern
Great Chesterford		0.64112	0.35091	0.18154	0.29761	0.19323
Wharram Percy	0.64112		0.777	0.59138	0.57365	0.58369
Raunds	0.35091	0.777		0.99678	0.87656	0.98773
Canterbury	0.18154	0.59138	0.99678		0.8664	0.99353
Wolverhampton	0.29761	0.57365	0.87656	0.8664		0.90002
Modern	0.19323	0.58369	0.98773	0.99353	0.90002	

Table 7.3: MANCOVA of Polynomial Residuals from the Femur Growth Trajectories.

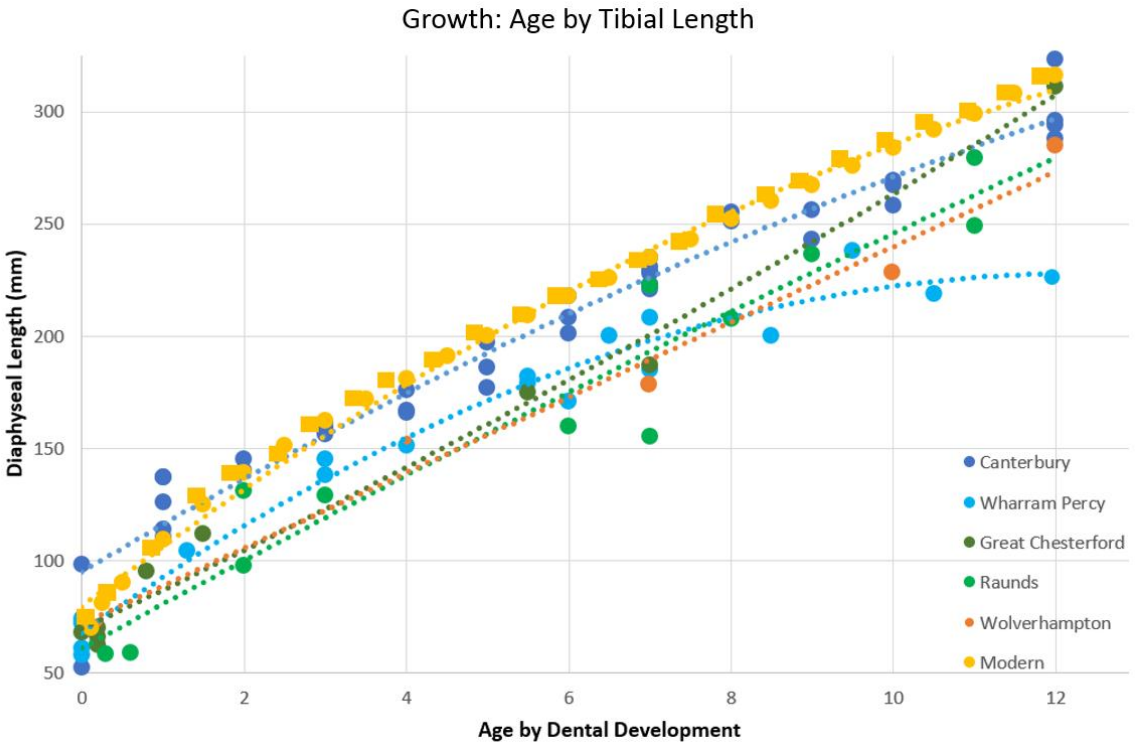

Figure 7.2: Juvenile growth from Anglo-Saxon to Modern populations. Tibial diaphysial length (mm) versus dental age for Great Chesterford, Raunds, Canterbury, Wharram Percy, Wolverhampton, and Source data for Modern (Meresh 1955) populations. The modern data was plotted by males (yellow dots) and females (yellow squares). As males and females plotted ontop of one another it can be suggested that there is little to no significant difference bewtween long bone length and age for males and females during this age range.

The tibiae growth trajectories (Figure 7.2) show a similar pattern to the femora. The Canterbury and modern samples have longer tibiae than Wharram Percy, Raunds, Great Chesterford and Wolverhampton. Similarly to the femora, by 2 years old the growth trajectories separate and by 7 years old there is another shift in growth trajectories. The Wharram Percy tibiae, become stunted in size and become the smallest followed by Great Chesterford, Raunds and Wolverhampton.

Despite these changes in growth trajectories, the MANCOVA (Table 7.3) does not show any statistically significant difference between growth and site.

MANCOVA: Polynomial Residuals of Humeral length, Site, and Age						
Site	Great Chesterford	Wharram Percy	Raunds	Canterbury	Wolverhampton	Modern
Great Chesterford		0.85686	0.097923	**0.008797**	11.059	**0.0073187**
Wharram Percy	0.85686		3.6395	1.7941	7.6026	1.4475
Raunds	0.097923	3.6395		14.923	1.4945	15
Canterbury	**0.008797**	1.7941	14.923		0.6941	14.864
Wolverhampton	11.059	7.6026	1.4945	0.6941		0.5969
Modern	**0.0073181**	1.4475	15	14.864	0.5969	

Table 7.4: MANCOVA of Polynomial Residuals from the Humerus Growth Trajectories.

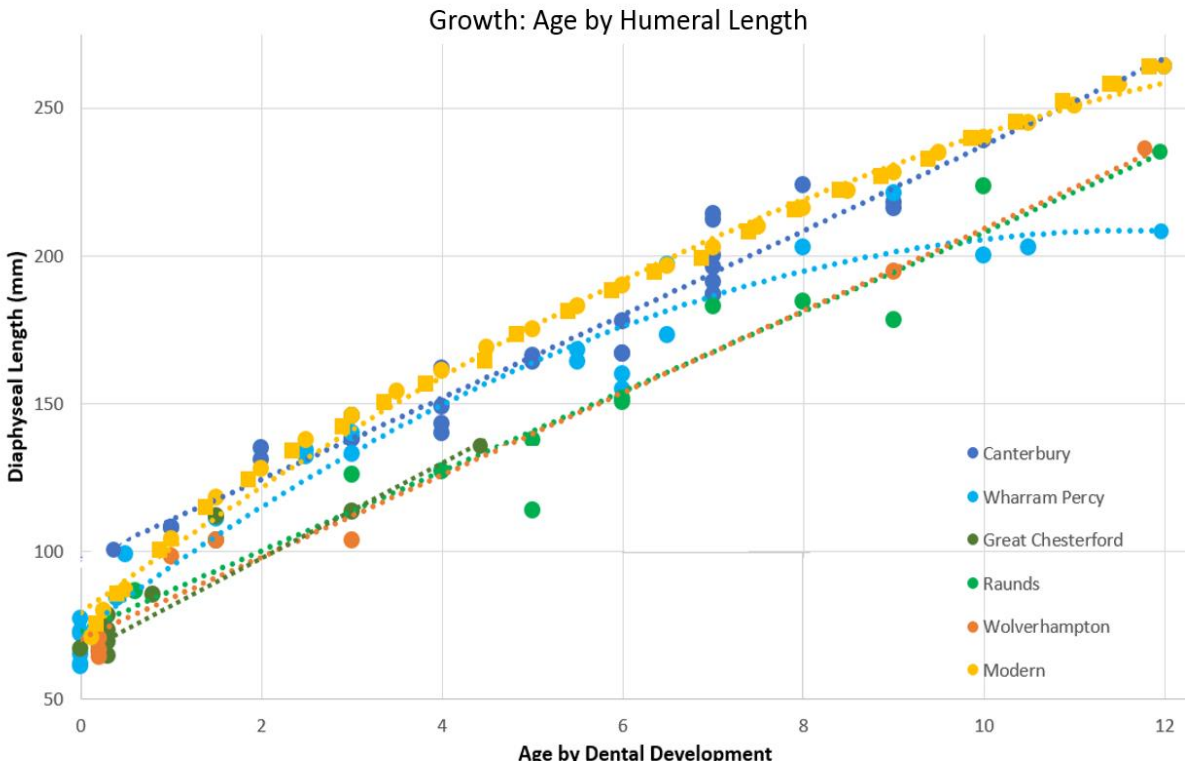

Figure 7.3: Juvenile growth from Anglo-Saxon to Modern populations. Humeral diaphysial length (mm) versus dental age for Great Chesterford, Raunds, Canterbury, Wharram Percy, Wolverhampton, and Source data for Modern (Meresh 1955) populations. The modern data was plotted by males (yellow dots) and females (yellow squares). As males and females plotted ontop of one another it can be suggested that there is little to no significant difference bewtween long bone length and age for males and females during this age range.

The humeri growth trajectory (Figure 7.3) is similar to both femora and tibiae trends. The modern and Canterbury sites have larger humeri followed by Wharram Percy, Raunds, Great Chesterford, and then Wolverhampton. These trajectories begin to separate at 3 years old rather than the 2 year mark of the lower limbs. This is to be expected as the humeri experiences a slight pause in growth

during the acquisition of bipedalism (by 2 years old) and then resumes at a later age of 3 years old and onwards (Mays 2007). The Wharram Percy growth trajectory begins to plateau at 7 years old, while Raunds and Wolverhampton become larger in size. The MANCOVA (Table 7.4) revealed statistical difference in growth between Great Chesterford and Canterbury and Great Chesterford and the modern samples. However, this may be a result of sample size (as seen in Figure 7.1) as the Great Chesterford Trajectory ends before 9 years old, while the rest of the sites continue until 12 years old.

7.1.2 Developmental Variation for the Femora, Tibiae, and Humeri for Anglo-Saxon to Post-Medieval Juveniles

The growth trajectories described above indicate interesting differences between the Anglo-Saxon and Post-Medieval juveniles. Canterbury had the highest growth trajectory, which closely paralleled the modern sample. Raunds, Great Chesterford, and Wolverhampton revealed a stunted growth after 2 years old which continued for the rest of the growth trajectory. Wharram Percy juveniles plateaued at the 7 year old age mark and then underwent a slowed period of growth. Development, the relationship of age and shape would be expected to show differences in where shape occurs for each element. The principal component analyses (PCA) for each element describes the variation of shape by site and age group. The same procedure of auto3dgm as described in Chapter 4 was used for the following analyses in order to analyse statistical differences between shape, age, period, and site. The number of skeletal elements used in the PCA and allometric trajectories may be found in Table 7.5 and the statistical results in Table 7.6.

Skeletal Materials					
Site	Period	Femur (n)	Tibia (n)	Humerus (n)	Total
Great Chesterford	Anglo-Saxon	18	9	12	39
Raunds	Anglo-Saxon	17	12	11	40
Canterbury	Medieval	42	40	27	109
Wharram Percy	Medieval	18	17	23	58
Wolverhampton	Post-Medieval	4	4	7	15
Total		99	82	80	261

Table 7.5: Sample size for developmental and allometric trajectories.

Shape (PCA Scores): ANOVA Results (p-values)			
Variable	Femur	Tibia	Humerus
Site	0.01	0.07	0.01
Age Group	0.01	0.01	0.01
Period	0.01	0.34	0.07
Allometry	0.01	0.01	0.01

Table 7.6: ANOVA results of site, age Group, period, and allometry for femora, tibiae, and humeri.

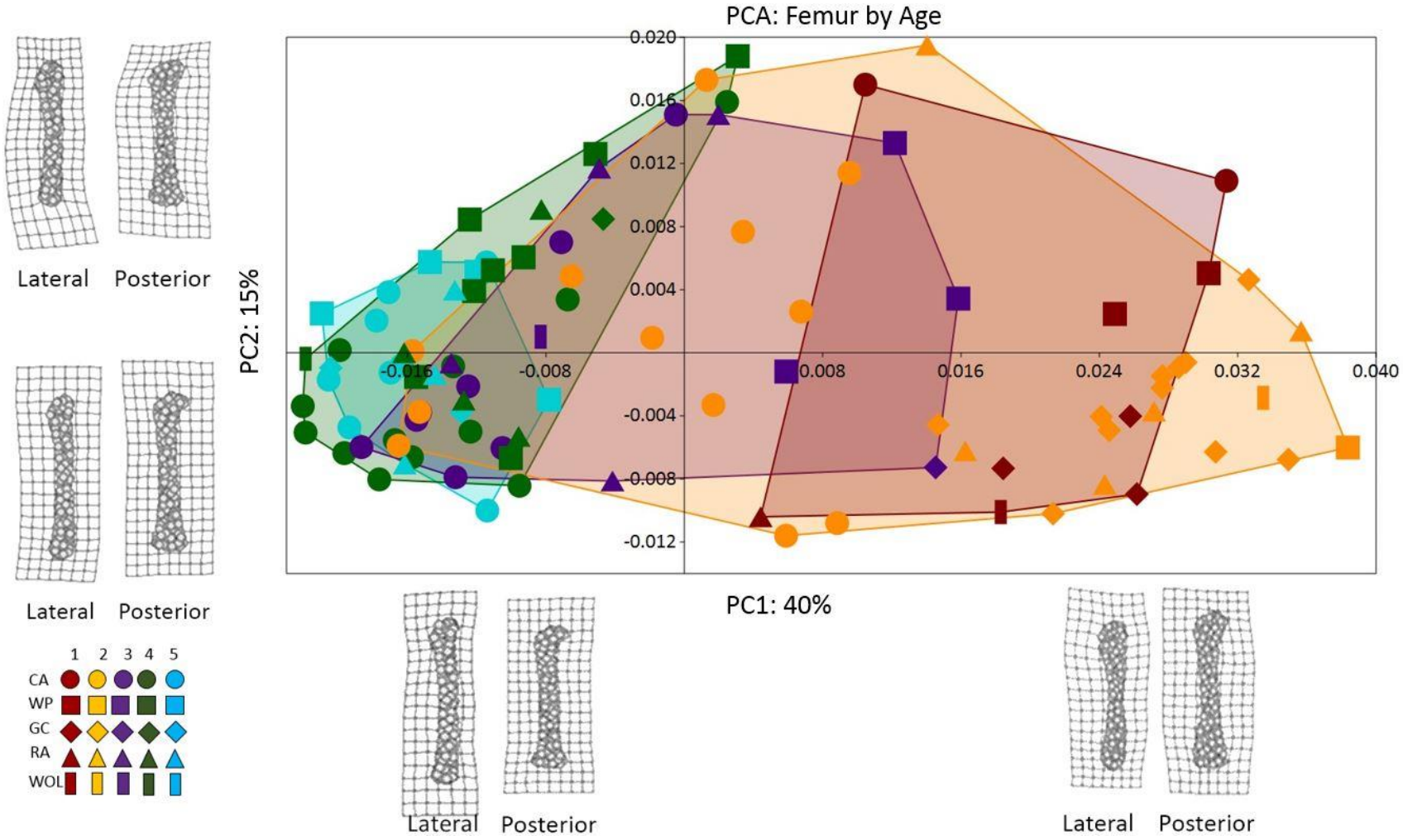

Figure 7.4: Principal Component Analysis for Group 1 (foetal: red), Group 2 (infant to 2 years old: orange), Group 3 (3 to 5 years old: purble), Group 4 (6 to 8 years old: green), and Group 5 (9 to 12 years old: blue) Femora for Canterbury (circle), Wharram Percy (square), Great Chesterford (dimond), Raunds (triangle), and Wolverhampton (bar).

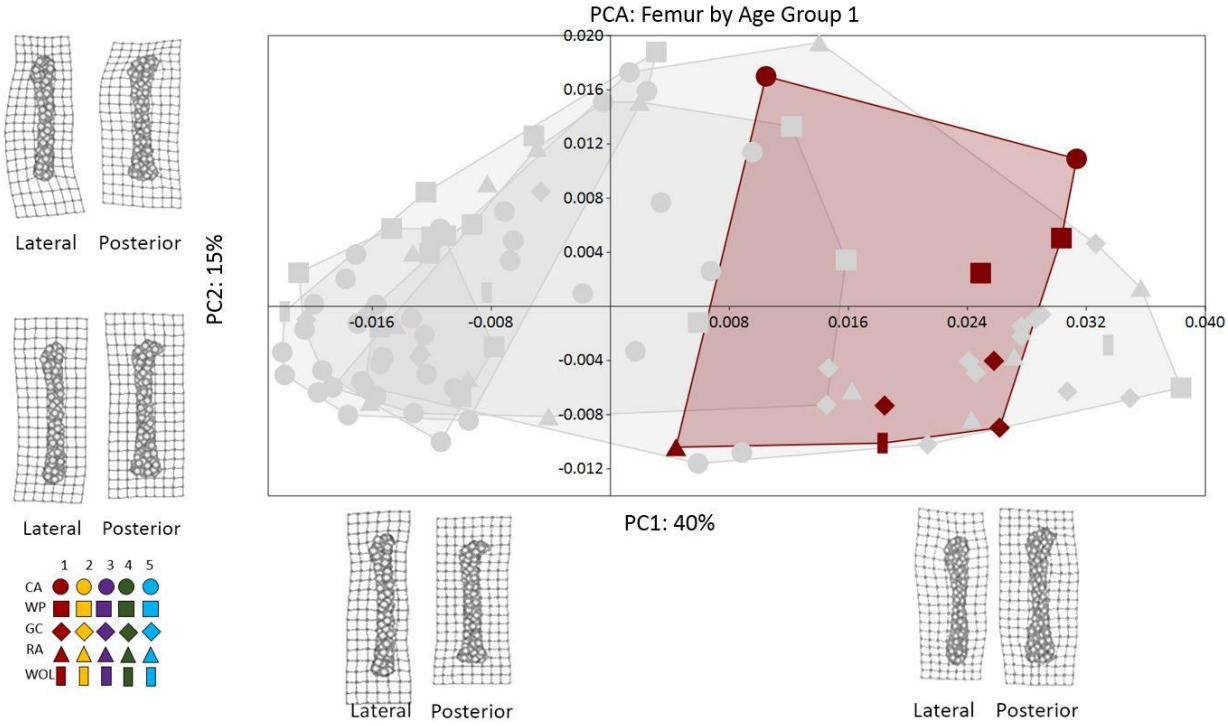

Figure 7.5: Group 1 (foetal) highlighted Principal Componenty Analysis of the Femur.

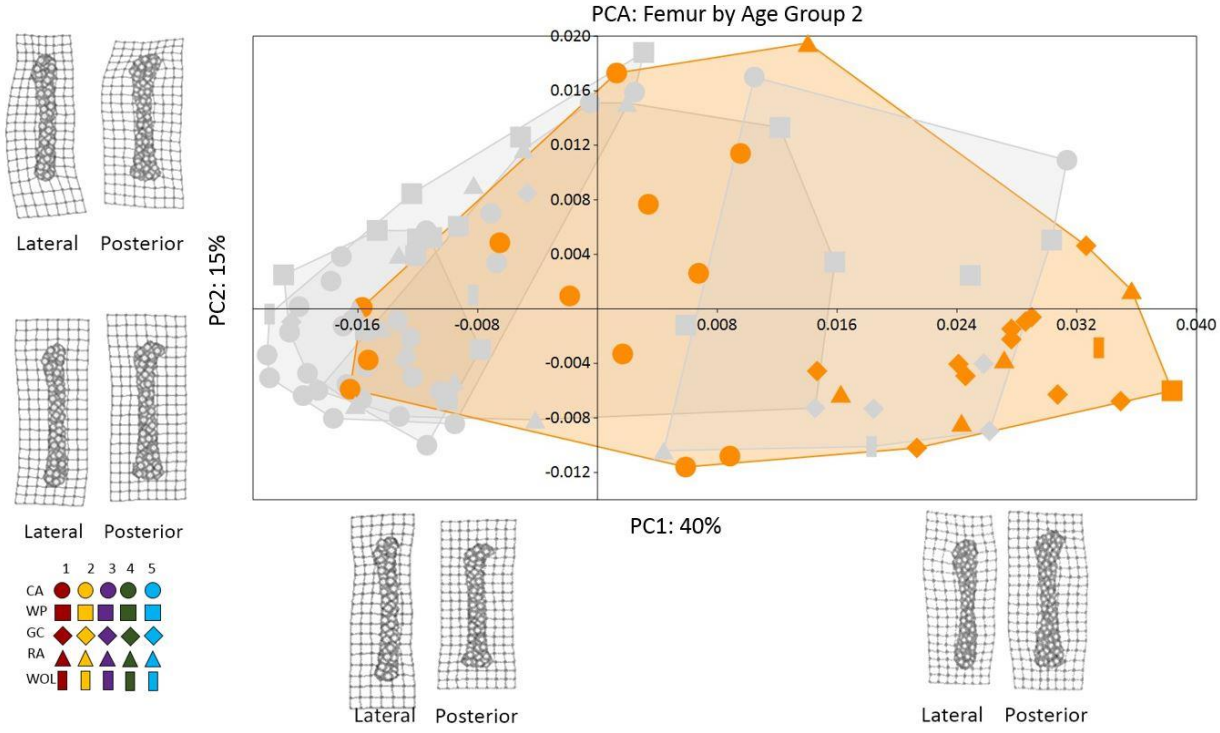

Figure 7.6: Group 2 (Infant to 2 years old) highlighted Principal Componenty Analysis of the Femur.

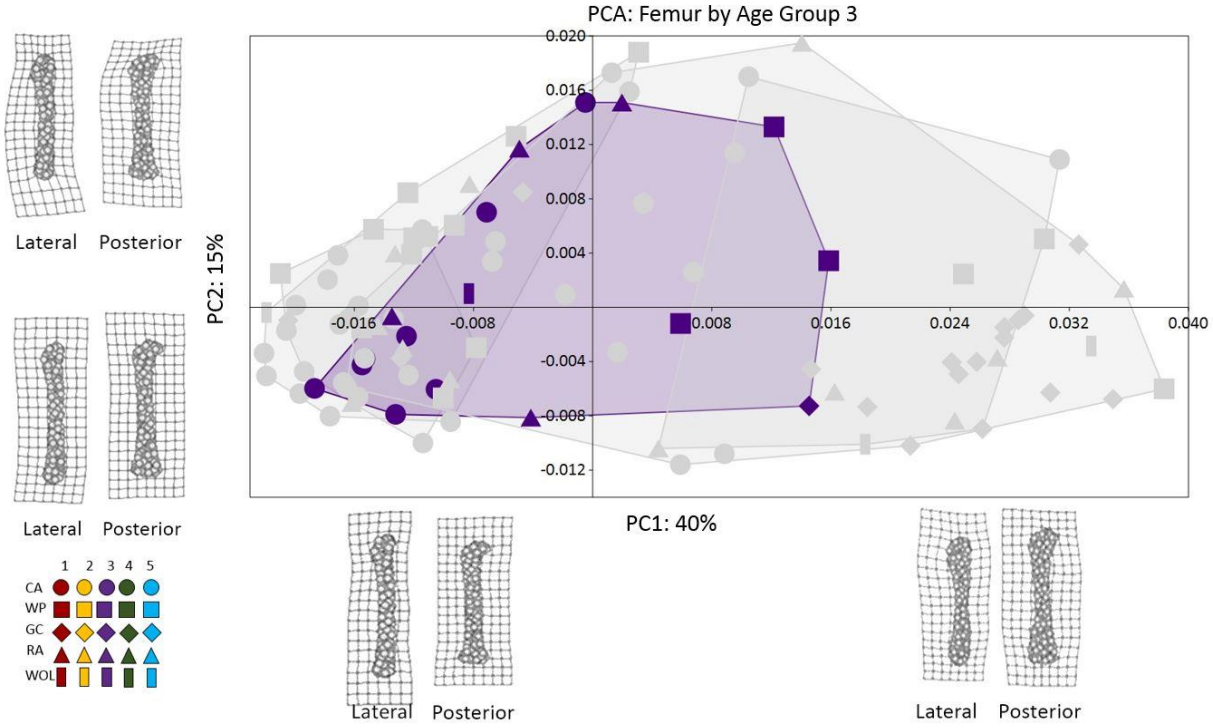

Figure 7.7: Group 3 (3 to 5 years old) highlighted Principal Componenty Analysis of the Femur.

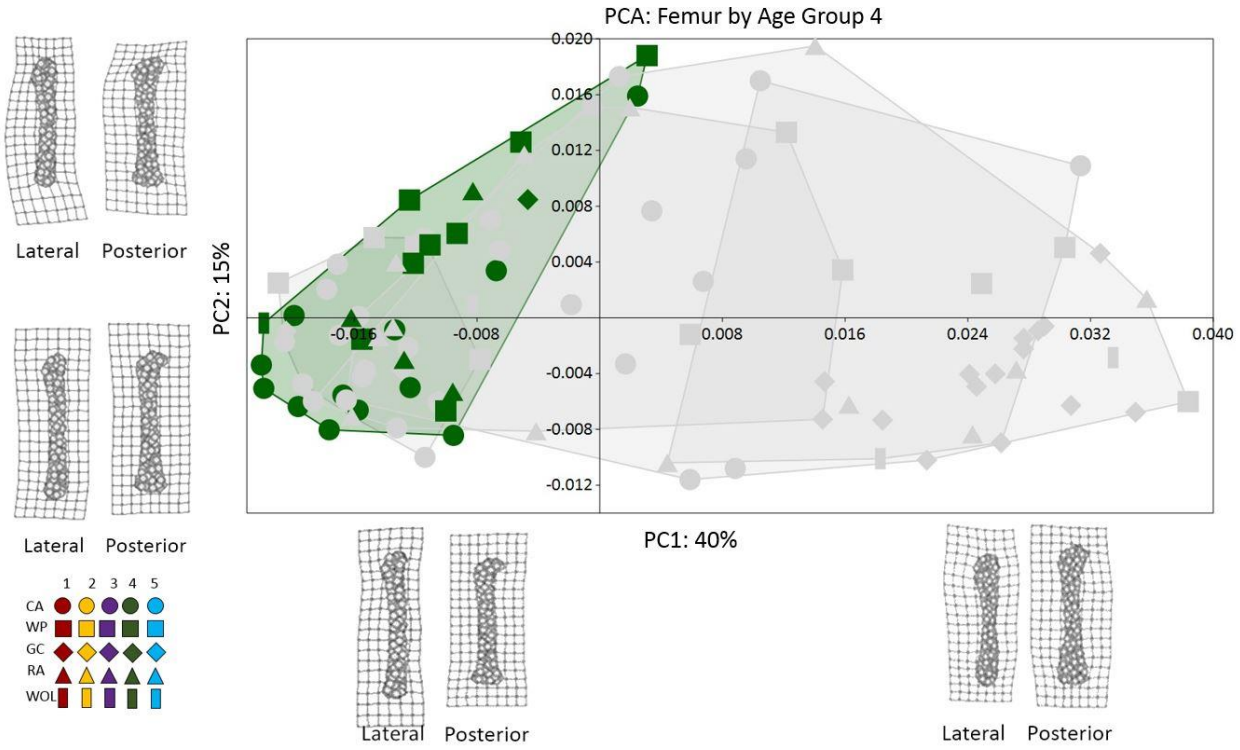

Figure 7.8: Group 4 (6 to 8 years old) highlighted Principal Componenty Analysis of the Femur.

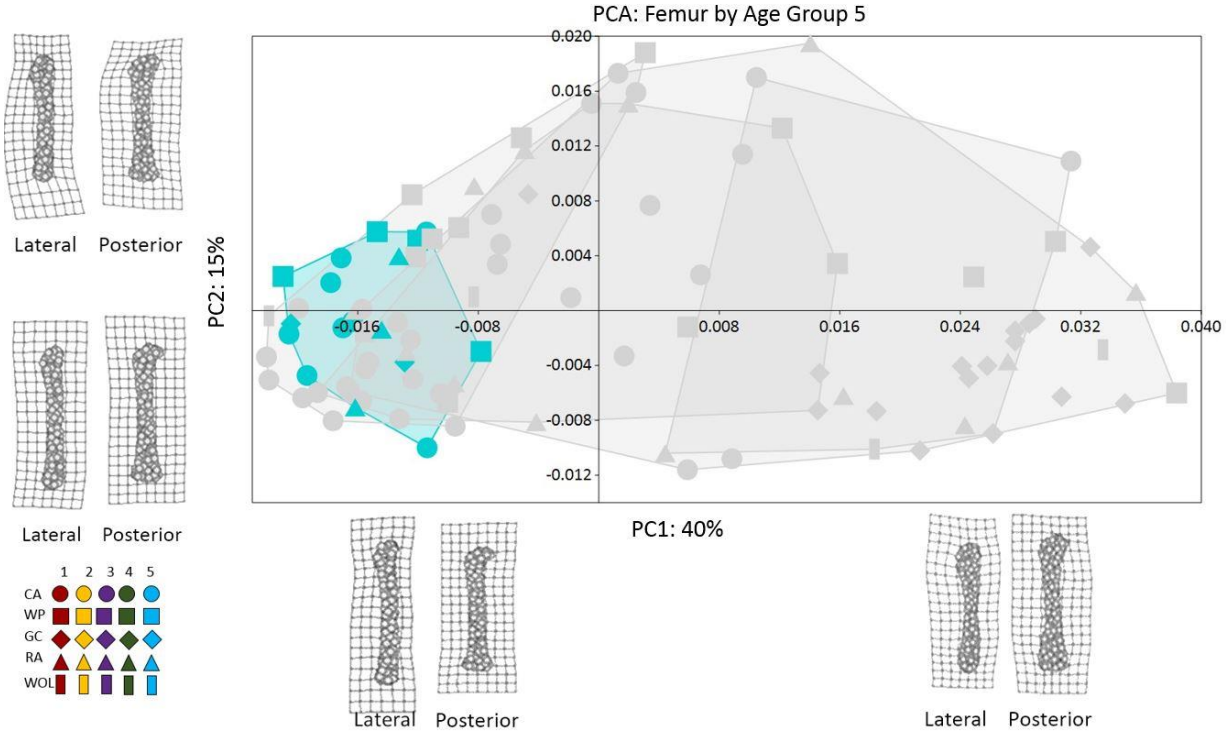

Figure 7.9: Group 5 (9 to 12 years old) highlighted Principal Componenty Analysis of the Femur.

The PCA's for the femora (Figure 7.4-7.9) found statistically significant results for shape by site ($p>0.01$), age group ($p>0.01$), period ($p>0.01$), and allometry ($p>0.01$). The PCA shows that femora plotting positively on PC1 (40%), represents the younger age groups of foetal (Group 1) to 3 years old (Groups 2 and 3). While negative PC1 represents the older juveniles of 4 (Group 3) to 12 years old (Groups 4 and 5). The first principal component axis shows the relationship between the proximal metaphyseal length, metaphyseal width, and curvature of the midshaft. Positive values represent a wider and shorter proximal metaphyses with a straighter diaphyses (representing the Groups 1 -3). Negative values represent a longer and narrower proximal metaphases with more curvature in the midshaft (Groups 4-5). The second principal component (15%) represents differences in the angle of the proximal metaphyses. Positive values (Groups 2 to 4) have a concave proximal metaphyses with more curvature and torsion from the lateral plane of the metaphyses into the diaphyses. Negative values (Groups 1, 3, 5) have a convex and sharper degree of curvature in the proximal metaphyses. The second PC axis is not as clear for younger versus older age groups. Instead, this axis is likely showing the modelling and remodelling process of the developing femora as shape is not a linear progression of large shapes but rather fluctuating shapes.

Figures 7.5-7.9 reflects the variation of shape found in each age group and highlights delayed growth trends (stunting) within groups. For instance, Group 1 Canterbury reflects similar shapes to Raunds and Great Chesterford Group 2 femora. This pattern of Canterbury femora accelerating into

older age group shape spaces continues for the rest of the trajectory. By Group 2, Great Chesterford, Raunds, Wharram Percy, and Wolverhampton reflect delayed shape development for the remaining age groups. It can also be seen the Anglo-Saxon sites are clustered more in gracile (see Chapter 3.3.7 for robust and gracile definitions) shape spaces (Postive PC 1 and PC2) while the Medieval juveniles are in the robust shape spaces (Negative PC1 and PC2). Post-Medieval data is found equally between the two shape quadrants. Therefore, general patterns reveal that Anglo-Saxon femora have a wider and longer proximal metaphyses and straighter diaphyses. According to De Groote and colleagues (2010; De Groote 2011), this patterning is representative of moderate activities. In addition to De Groote and colleagues (2010), this thesis found that Medieval femora have a shorter and higher proximal metaphyseal angle and shorter femoral neck with more torsion in the midshaft, which represent highly active individuals. Post-Medieval femora from both this thesis and De Groote *et al.* (2010) are a combination of these trends as the femora have a slight curvature in the midshaft of the diaphyses and elongation of the proximal metaphyses which also represents moderate activities (De Groote *et al.* 2010).

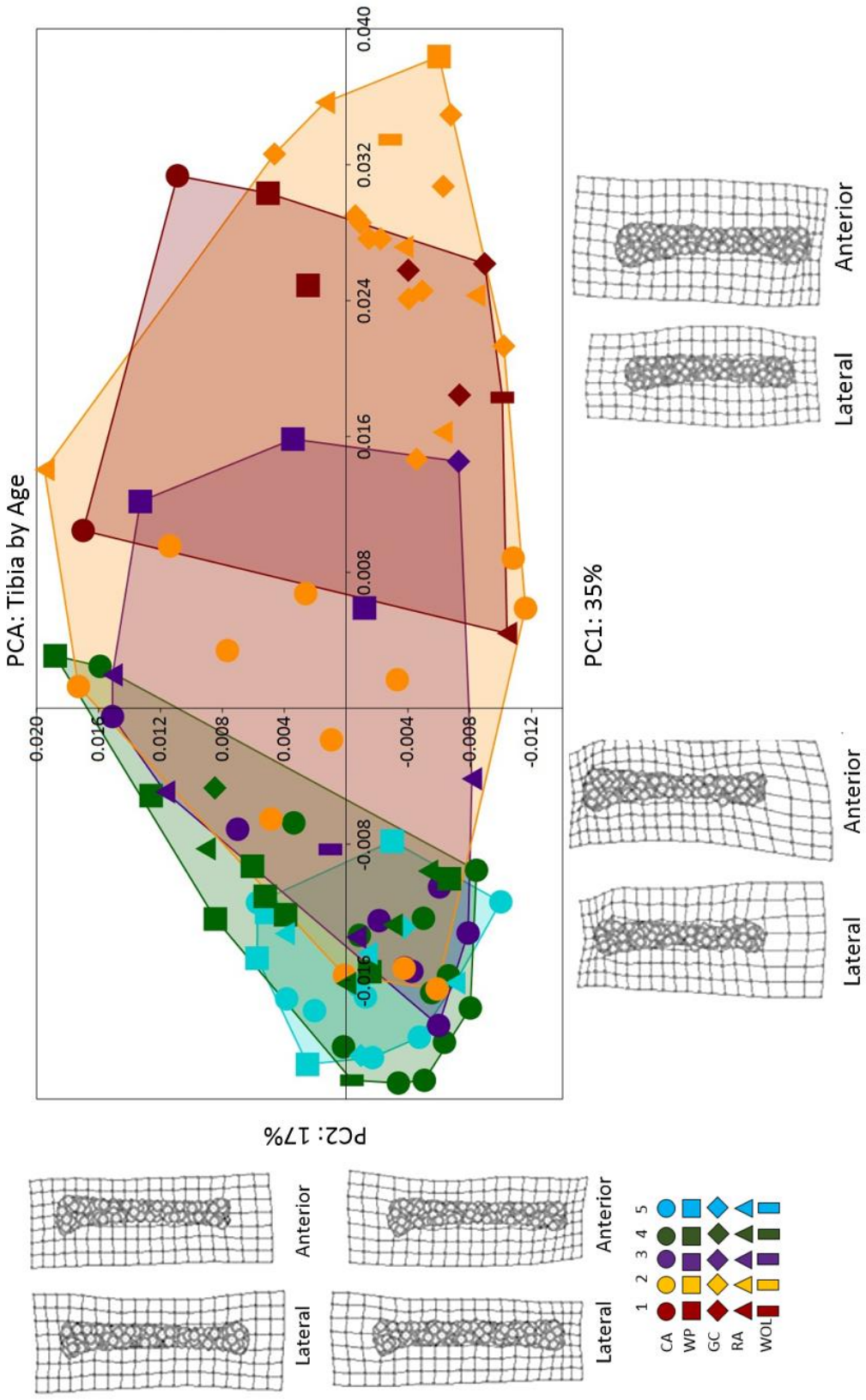

Figure 7.10: Principal Component Analysis for Group 1 (foetal: red), Group 2 (infant to 2 years old: orange), Group 3 (3 to 5 years old: purble), Group 4 (6 to 8 years old: green), and Group 5 (9 to 12 years old: blue) Tibiae for Canterbury (circle), Wharram Percy (square), Great Chesterford (dimond), Raunds (triangle), and Wolverhampton (bar).

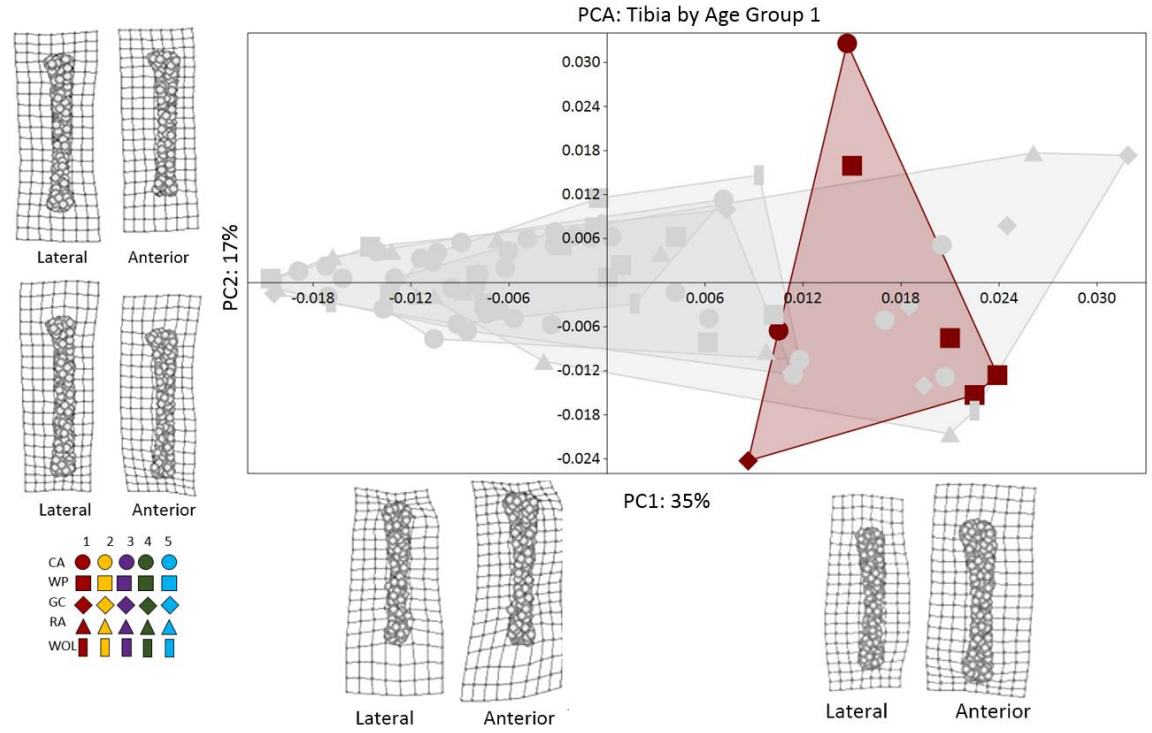

Figure 7.11: Group 1 (foetal) highlighted Principal Componenty Analysis of the Tibia.

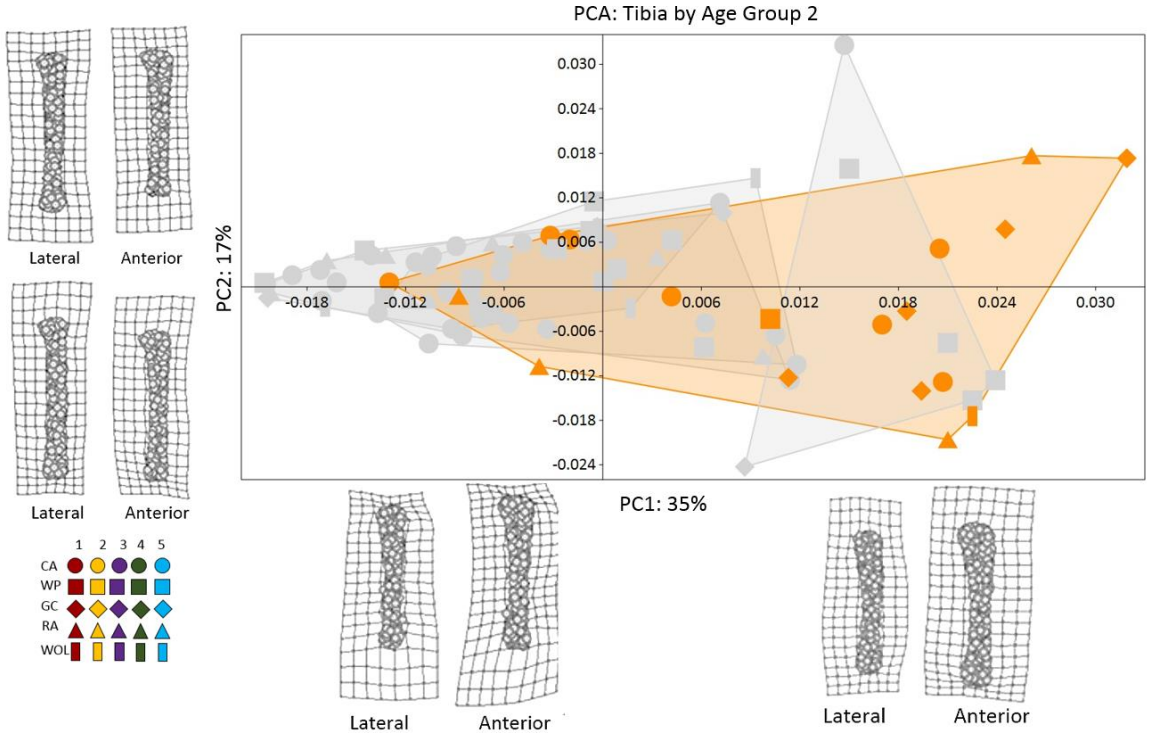

Figure 7.12 Group 2 (Infant to 2 years old) highlighted Principal Componenty Analysis of the Tibia.

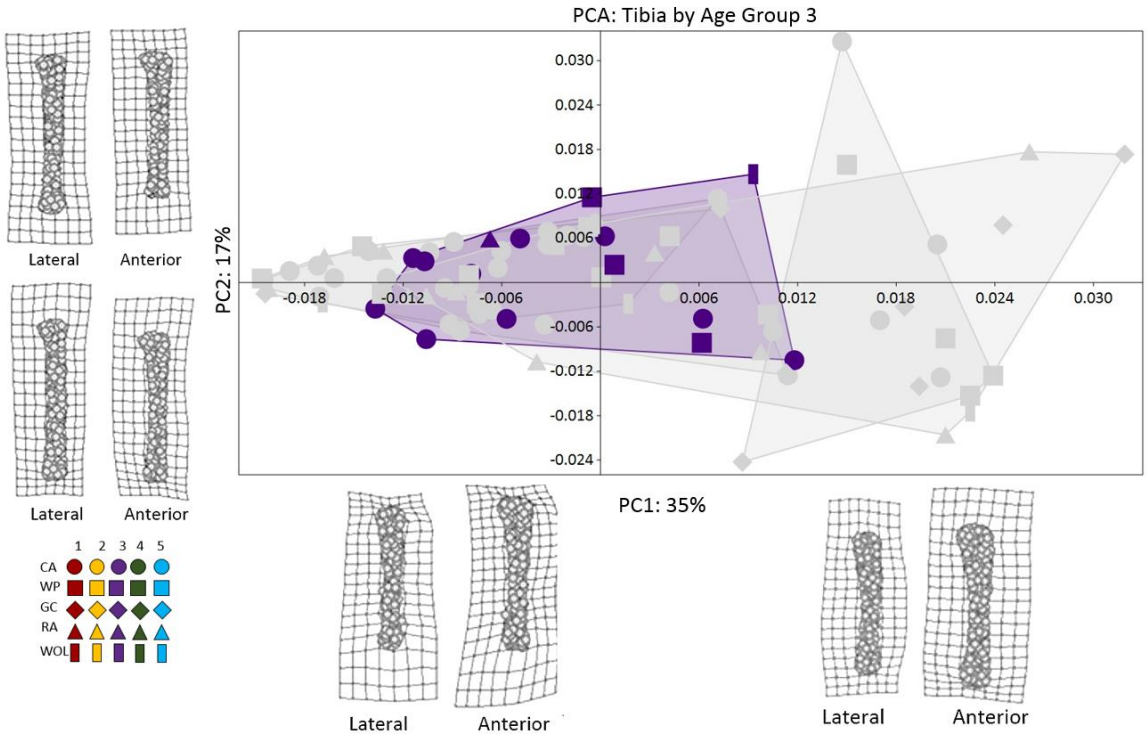

Figure 7.13: Group 3 (3 to 5 years old) highlighted Principal Componenty Analysis of the Tibia.

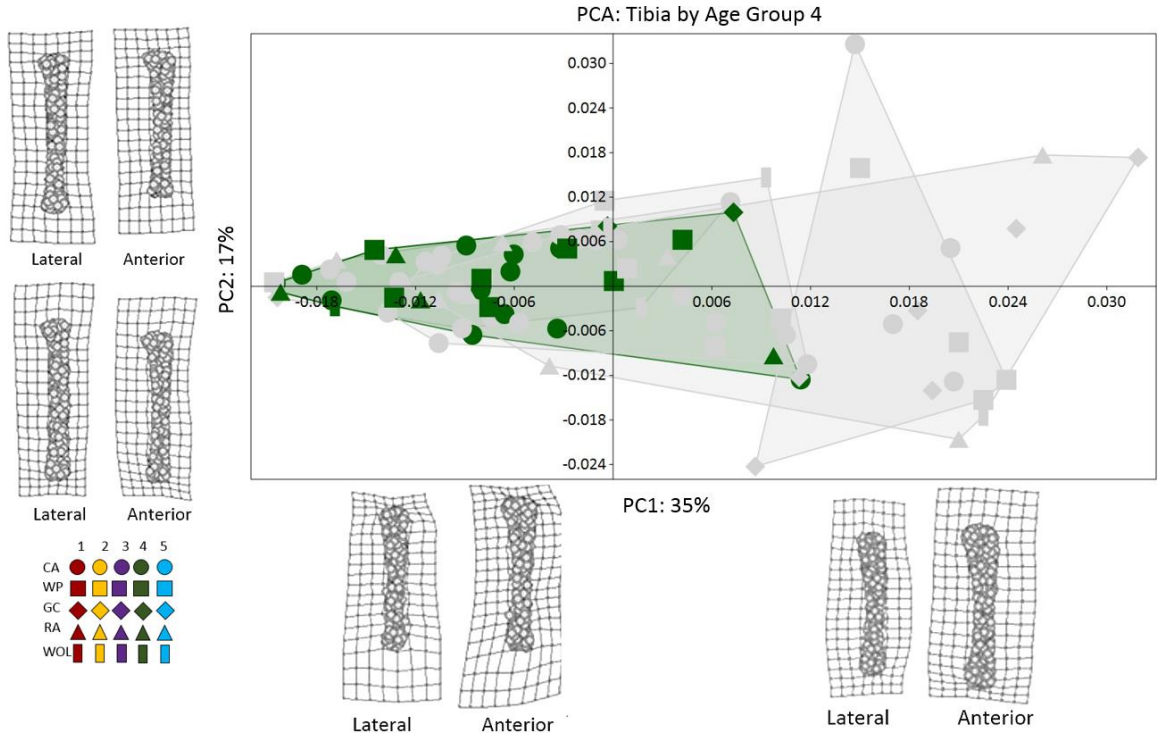

Figure 7.14: Group 4 (6 to 8 years old) highlighted Principal Componenty Analysis of the Tibia.

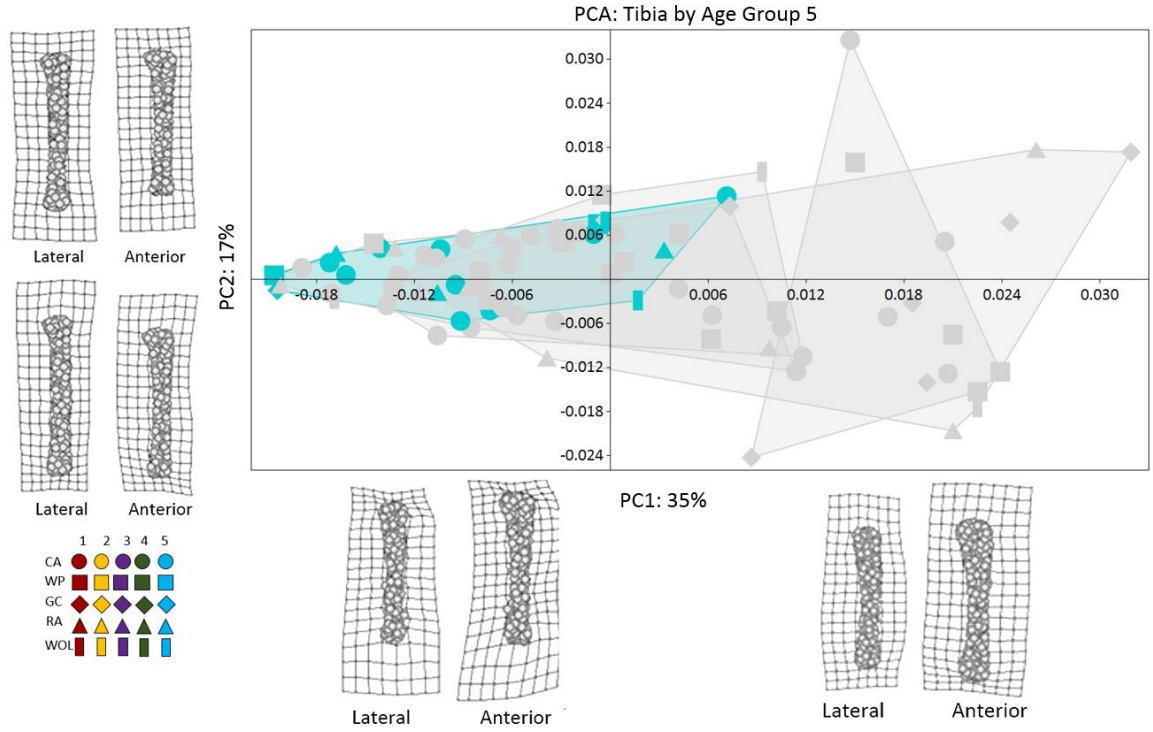

Figure 7.15: Group 5 (9 to 12 years old) highlighted Principal Componenty Analysis of the Tibia.

Statistically significant shape patterning of the tibiae is present by age group ($p>0.01$) and allometry ($p>0.01$), but not by site ($p>0.07$). The first principal component axis (35%) of the tibiae PCA (Figure 7.10-7.15) represents the angle of the proximal metaphyses while the second principal component axis (17%) represents the curvature of the diaphyses. Similarly to the femora, the younger tibiae (Group 1 and 2) are plotted in positive PC1 which represents a more convex proximal metaphyses. The older juveniles (Groups 3 to 5) cluster in negative PC1 and have a more concave proximal metaphyses which may reflect loading patterns. Positive PC2 represents a straighter diaphyses with negative PC2 showing slight curvature in the midshaft. There was no statistical significance of tibiae shape by site as they are heavily clustered together. Similarly to the femora, the Canterbury tibiae refelected similar shapes to the older groups from the other sites throughout all age groups. By Group 2 Great Chesterford reflected Wharram Percy tibiae shapes in Group 3. Additionally, by Group 3 Raunds reflecte Canterbury Group 4 tibaie. However, there is considerable clustering occurring in the older age groups which may be an effect of the small and unequal sample sizes. Therefore, teasing apart these groups will provide more insight into the developing tibiae morphology.

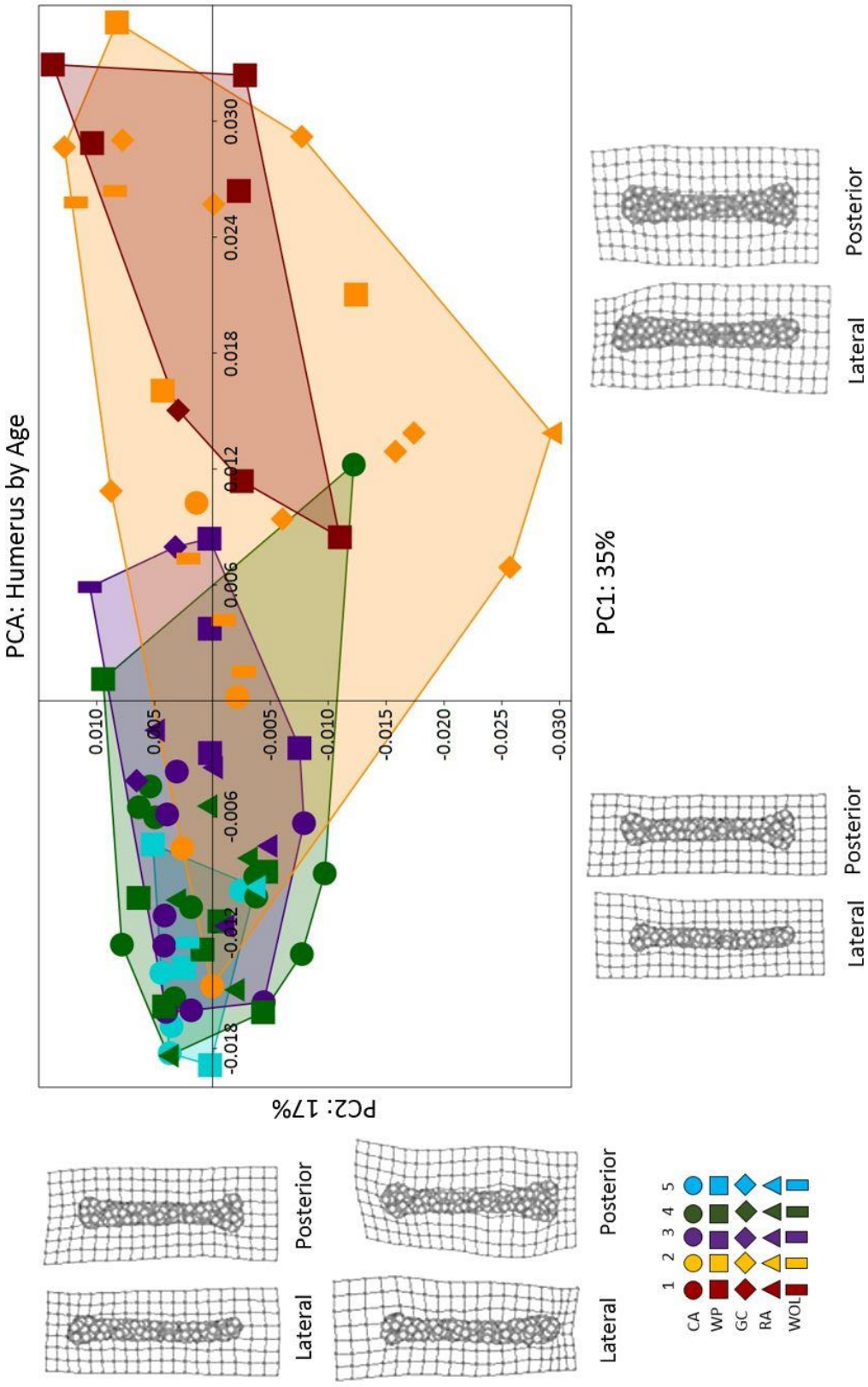

Figure 7.16: Principal Component Analysis for Group 1 (foetal: red), Group 2 (infant to 2 years old: orange), Group 3 (3 to 5 years old: purble), Group 4 (6 to 8 years old: green), and Group 5 (9 to 12 years old: blue) Humeri for Canterbury (circle), Wharram Percy (square), Great Chesterford (dimond), Raunds (triangle), and Wolverhampton (bar).

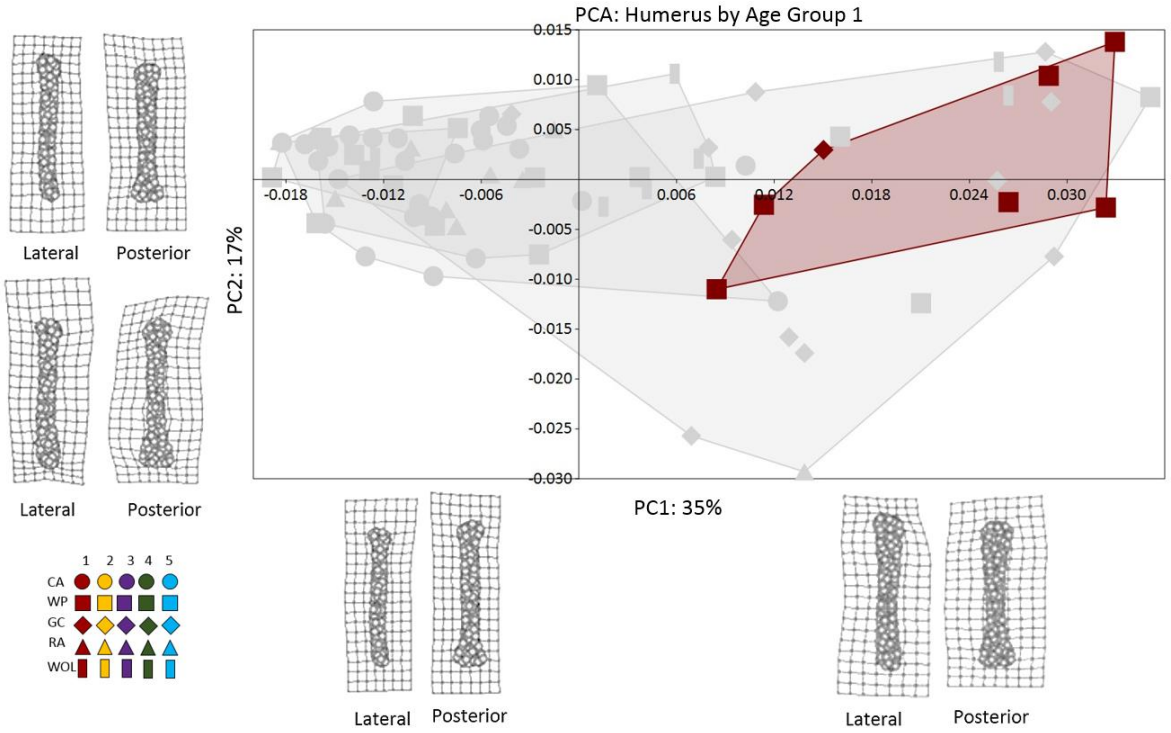

Figure 7.17: Group 1 (foetal) highlighted Principal Componenty Analysis of the Humerus.

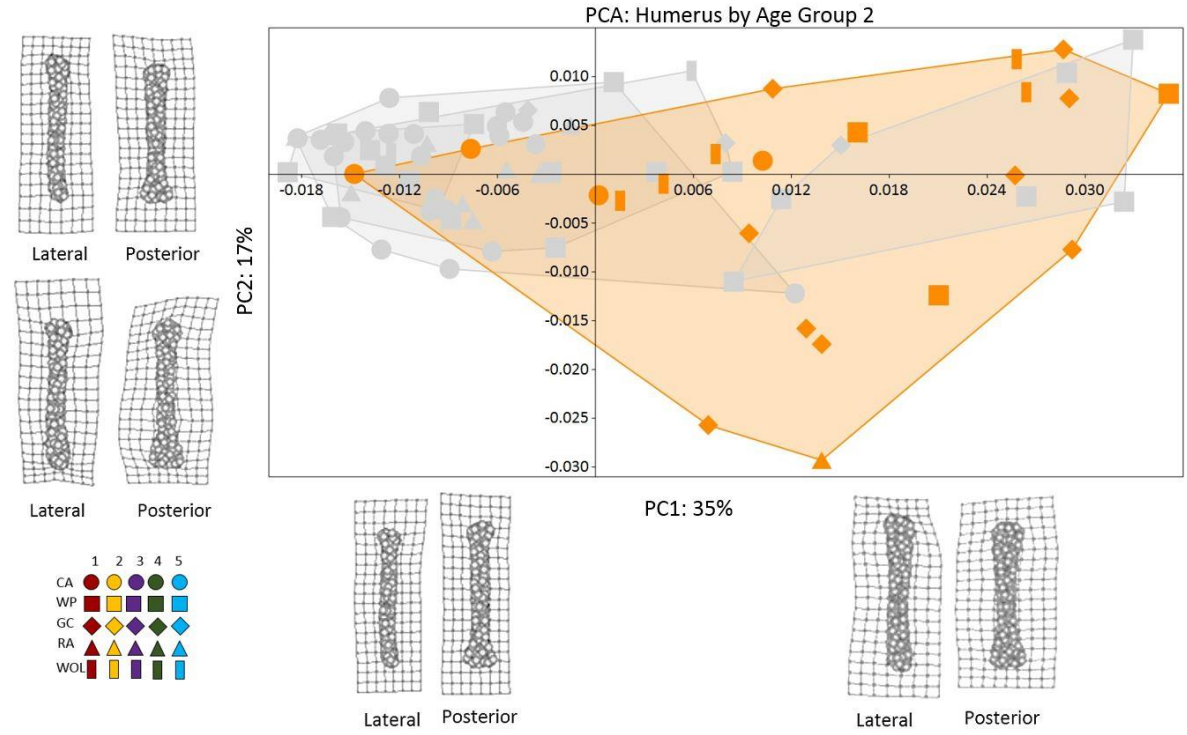

Figure 7.18: Group 2 (Infant to 2 years old) highlighted Principal Componenty Analysis of the Humerus.

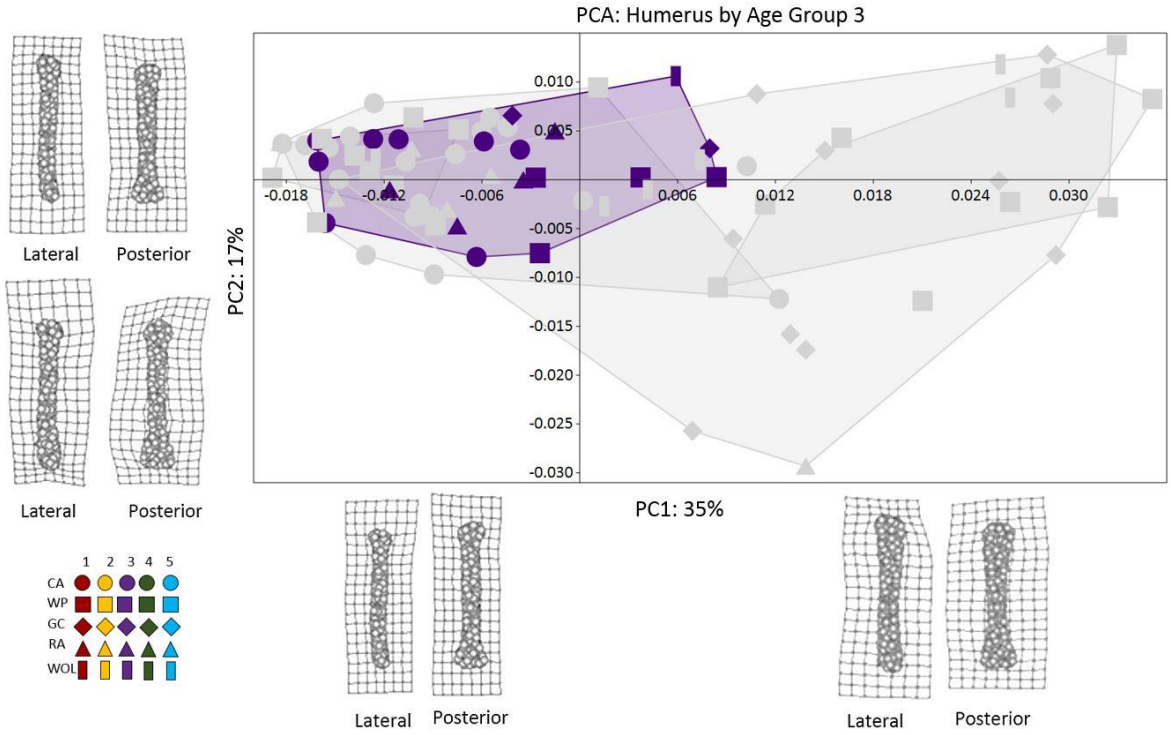

Figure 7.19: Group 3 (3 to 5 years old) highlighted Principal Componenty Analysis of the Humerus.

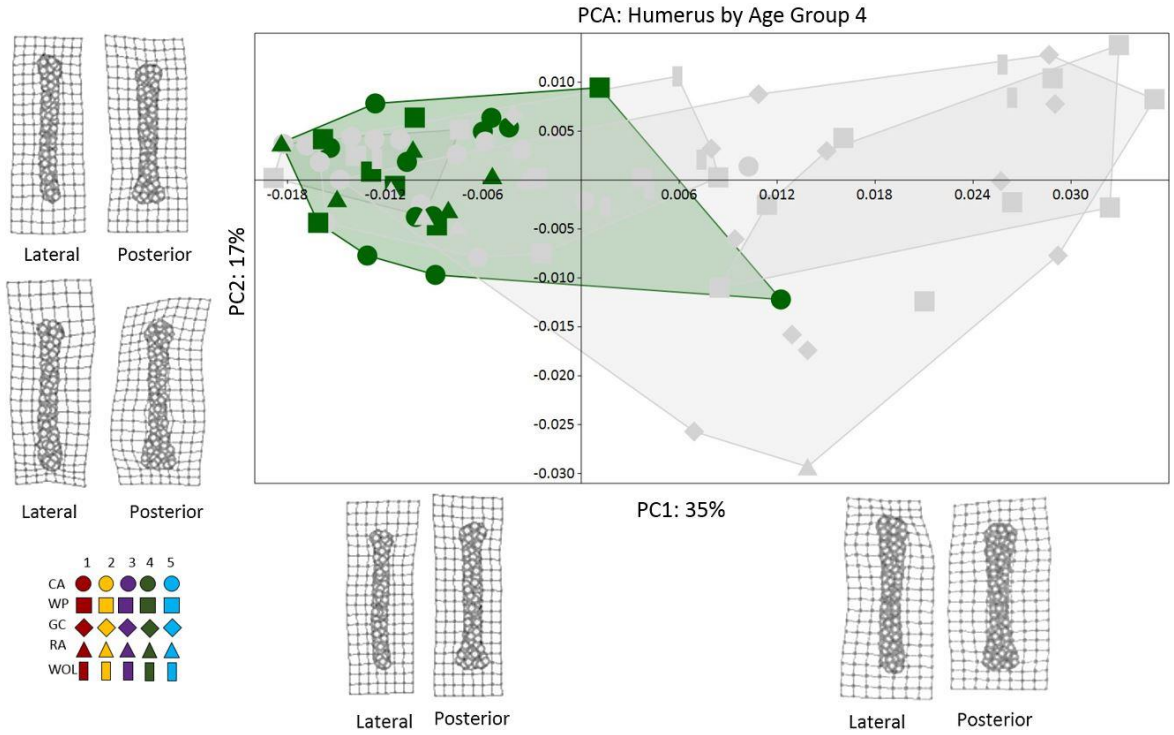

Figure 7.20: Group 4 (6 to 8 years old) highlighted Principal Componenty Analysis of the Humerus.

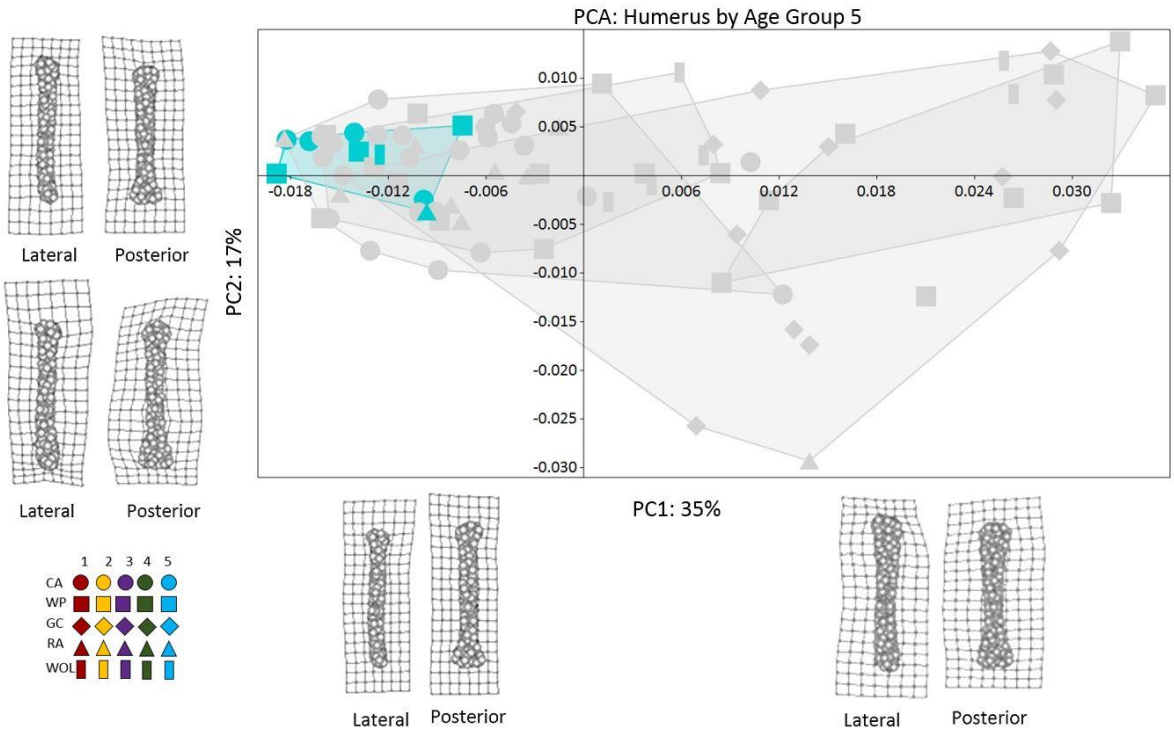

Figure 7.21: Group 5 (9 to 12 years old) highlighted Principal Componenty Analysis of the Humerus.

The PCA of the humeri (Figure 7.16-7.21) found statistically significant shape patterning by site ($p>0.01$), age group ($p>0.01$), and allometry ($p>0.01$). The first principal component axis (35%) represents the length and curvature of the proximal metaphyses while the second principal component axis (17%) reflects the width and curvature of the distal metaphyses. Positive PC1 represents a wider and shorter proximal metaphyses with a convex curvature in the anterior plane of the proximal diaphyses. The younger age groups from foetal (Group 1) to 5 years old (Group 2 and 3) fall within this shape space. Negative PC1 has a longer and narrower proximal metaphyses with more curvature in the anterior plane of the proximal diaphyses. Positive values for PC2 (17%) represent a convex distal metaphyses and narrower diaphyses, while negative values have a concave distal metaphyses and wider diaphyses. Similarly to the femora and tibiae, positive PC1 represents the younger age groups from foetal (Group 1) to 5 years old (Group 2 and 3). These age ranges also fall into both positive and negative PC2 shape spaces. The older age groups of 5 (Group 3) to 12 (Group 4 to 5) years old are clustered in negative PC1 and the centre of PC2. Similarly to the femora and tibiae, the Canterbury humeri reflect older shapes from Raunds and Wharram Percy throughout the age groups. By Group 2, Wolverhampton humeri reflect similar shapes to Group 3 Great Chesterford. Group 4 Raunds reflects similar shapes to Group 5 Canterbury and Wharram Percy reflects similar shapes to Group 5 Wolverhampton. As seen with the femora and tibiae, there is a substantial amount of clustering by site and age group which may be a result of unequal sample sizes in the age groups.

7.1.3 Allometry of Femora, Tibiae, and Humeri for Anglo-Saxon to Post-Medieval Juveniles

The allometric plots illustrate the relationship of size and shape for all elements. The allometric regression follows the same procedure described in Chapter 4 and its statistical significance by allometry is found in Table 7.6.

The allometric regression for the femora (Figure 7.22) found statistical significance ($p>0.01$) of size against shape. The first group (foetuses) reflects a range of variation in size and shape among sites. Similarly to the growth trajectories, Canterbury femora shape regression scores have a large degree of variation and therefore reflect the most and least robust shapes in terms of torsioin, curvature, and defined architecture for this age group. The remaining sites (Wharram Percy, Raunds, Great Chesterford, and Wolverhampton) fall within shape range. Group 2 (infant to 2 years old) has the largest variation of size and shape out of all age groups. This would be expected as there is a growth spurt (Bogin 1999), and a sudden range of movements occurring from crawling to walking during this age range. Canterbury is the most robust shape, followed by Raunds. Great Chesterford covers the lower half of this age group and Wharram Percy and Wolverhampton fall into the lower ends of more gracile shapes and smaller sized femora. Group 3 (3 to 5 years old) has a less varied range of shape and increase in size. Canterbury continues as the largest and most robust shape followed by Wharram Percy, Raunds, Wolverhampton and Great Chesterford. The last two age groups (4: 6-8 years old, 5: 9-12 years old) show a slowing down in shape variation. Canterbury continues as the largest and most robust shaped femora followed by Wharram Percy, Raunds, and Great Chesterford. This slowed progression of increasing shape and size variation may be a result of a conservative period in growth and development in preparation for the pubertal growth spurt which occurs at 14 years old (Gosman *et al.* 2013).

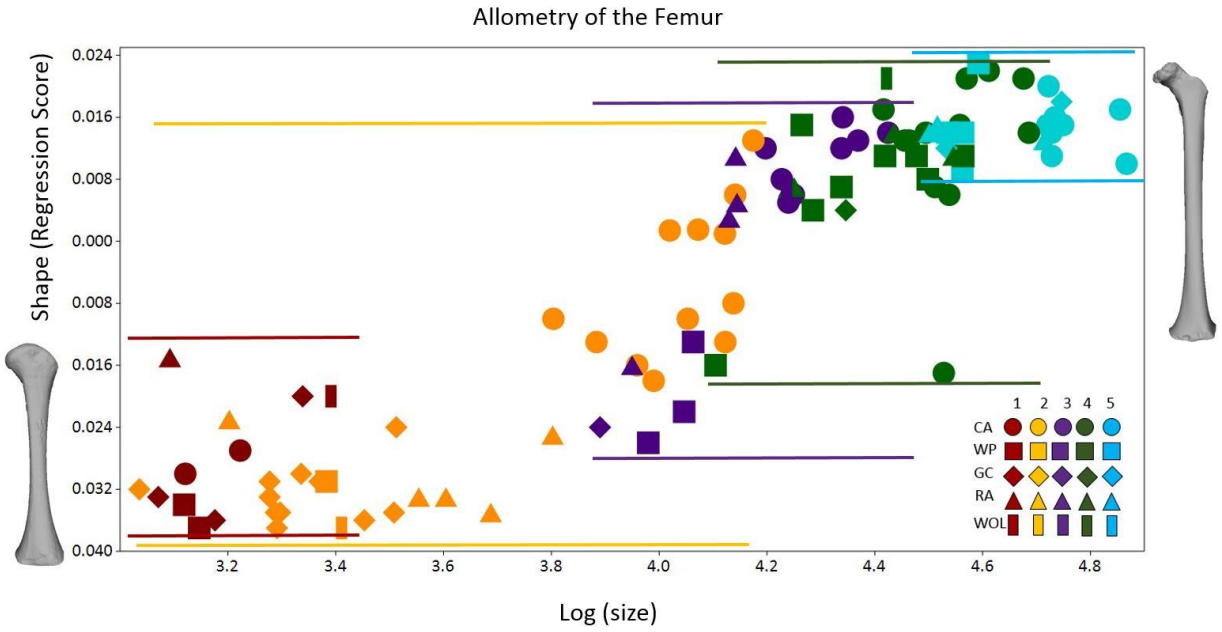

Figure 7.22 Allometric plot for Group 1 (foetal: red), Group 2 (infant to 2 years old: orange), Group 3 (3 to 5 years old: purble), Group 4 (6 to 8 years old: green), and Group 5 (9 to 12 years old: blue) Femora for Canterbury (circle), Wharram Percy (square), Great Chesterford (dimond), Raunds (triangle), and Wolverhampton (bar).

Similarly to the femora, the allometric trajectory of the tibiae (Figure 7.23) found statistical significance when regressing shape against size ($p>0.01$). The Canterbury tibiae for Group 1 represents the entire breadth of shape variation while the other sites fall within this range. Group 2 (infant to 2 years old) shows a large increase of shape variation, echoing that of the femora, with Canterbury representing the more architectually robust shapes followed by Raunds, Wharram Percy, Great Chesterford, and Wolverhampton. Group 3 (3 to 5 years old) shows an increase in size and shape, with Canterbury continuing as the most robust shape and largest size followed by Wharram Percy, Raunds, and Wolverhampton. Group 4 (6 to 8 years old) experiences a slight pause in size and shape of the tibiae, while Group 5 (8 to 12 years old) slows down at the end of the developmental trajectory.

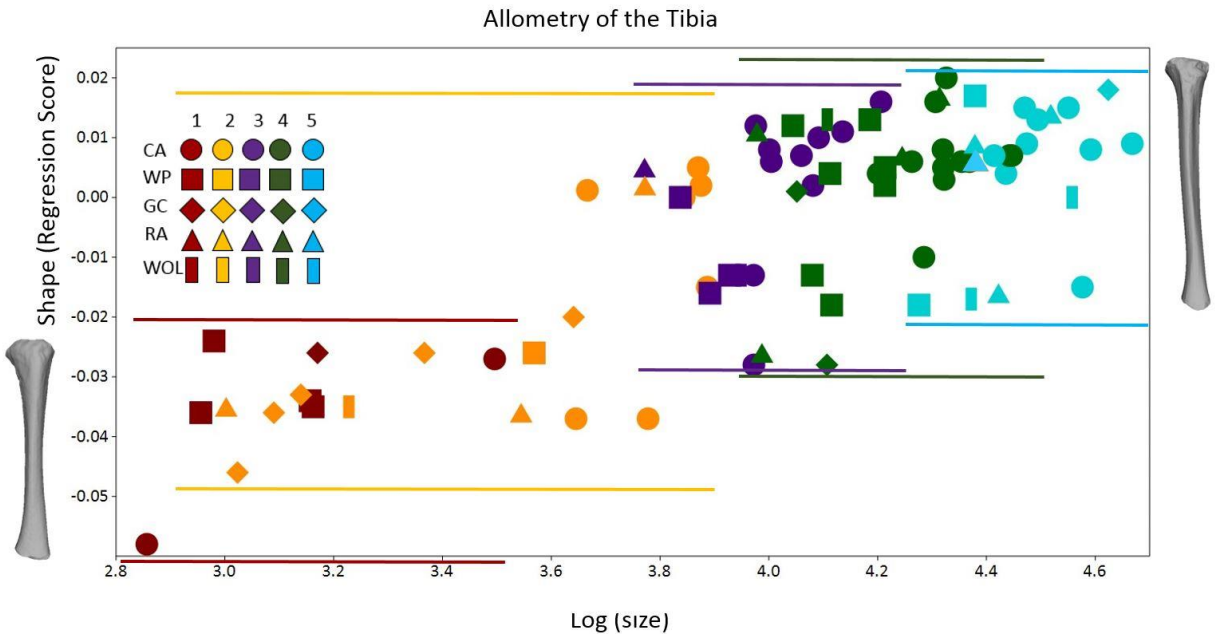

Figure 7.23: Allometric plot for Group 1 (foetal: red), Group 2 (infant to 2 years old: orange), Group 3 (3 to 5 years old: purble), Group 4 (6 to 8 years old: green), and Group 5 (9 to 12 years old: blue) Tibiae for Canterbury (circle), Wharram Percy (square), Great Chesterford (dimond), Raunds (triangle), and Wolverhampton (bar).

The allometry of the humeri (Figure 7.24) indicates statistically significant patterning for regressing humeral shape onto humeral size and represents a proxy for expected growth and development (Mays 2007). The humeri allometric trajectory follows similar patterns in timing of size and shape variation as the femora and tibiae trajectories. Group 1 (foetus) shows a range of size and shape with Wharram Percy representing the most and least developed shapes and Great Chesterford plotted within this range. Group 2 (infant to 2 years old) experiences a large shift in size and shape development. Interestingly, it is expected that the lower limbs will have extreme shape variation during the crawling to walking phase while the humeri demonstrates “reserved” growth (Mays 2007). However, this allometric regression may have picked up individuals who are in the crawling phase and therefore demonstrating more load bearing behaviour than is expected. Group 3 (3 to 5 years old) continues to show a range of shapes with Canterbury in the more robust shape region followed by Raunds, Great Chesterford, Wharram Percy, and Wolverhampton. Group 4 (6 to 8 years old) has a much more varied shape range compared to the lower limbs which may reflect differences in activity, for instance more manual labour on the farms or workshops as children in this age range begin work-related tasks. Group 5 (9-12 years old) shows a similar period of less varied size and shape as the lower limbs and may reflect a conserved pre-pubertal growth spurt phase.

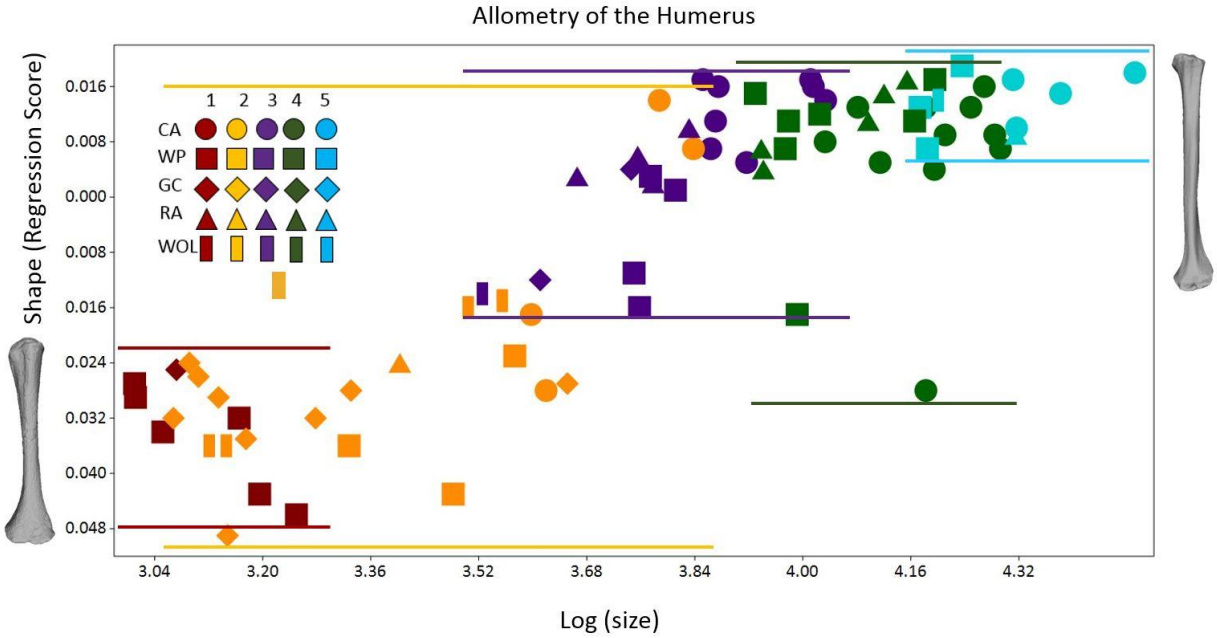

Figure 7.24: Allometric plot for Group 1 (foetal: red), Group 2 (infant to 2 years old: orange), Group 3 (3 to 5 years old: purble), Group 4 (6 to 8 years old: green), and Group 5 (9 to 12 years old: blue) Humeri for Canterbury (circle), Wharram Percy (square), Great Chesterford (dimond), Raunds (triangle), and Wolverhampton (bar).

7.1.4 Discussion: Growth, Development, and Allometry

The linear growth trajectories illustrate how the archaeological populations (apart from Canterbury) diverge from the known modern collection. From 2 years old and onwards, the trajectories begin to alter course as the Wharram Percy, Raunds, Great Chesterford, and Wolverhampton juveniles become shorter than the Canterbury and modern group. These findings are supported by Mays (2007: 96-99) study of femur length versus dental development for Wharram Percy, Poundbury, Mikulčice, Ensay, and Belleville collections. The archaeological populations revealed that despite the past 1500 years, the results are similar to one another and suggest that patterns in diaphyseal growth have changed very little over the past several centuries (Mays 2007: 96-99). The difference with the modern trajectory is likely to be a combination of factors such as increased nutrition and lessened disease burdens (Mays 2007: 99). Although the plotting of diaphyseal length against dental development shows interesting trends of increasing size of each element, it is difficult to determine how these changes in size affect the overall morphology of the long bones and how these changes occur from foetal to 12 years old.

The PCA and allometric plots did find statistical shape patterning for site, age, allometry (femora, tibiae, and humeri) and in some cases, period (femora). The first two age groups (foetal to 2 years old) showed the most varied range of shape and size for all elements and then varying rhythms of shape for the remaining age groups. The PCA plots illustrating the different age groups for the femora (Figure7.5-7.9), tibiae (Figure 7.11- 7.15) and humeri (Figure 7.17-7.21) revealed that some

sites, mainly Canterbury, reflected similar long bone shapes to older age groups of Wharram Percy, Raunds, and Great Chesterford. Wharram Percy, Great Chesterford, Raunds, and Wolverhampton varied between age group and element and overlapping shape spaces with older or younger age groups. These delayed or accelerated developmental patterns suggest that there are many variables that contribute to the developmental trajectory of juvenile long bones. Therefore, a more detailed look at each element by age group was carried out below, in order to tease apart these variables of size, shape, age, and how they relate to one another by site, period, and allometry. Each age group will have a null hypothesis to test the morphological variation (PCA) for each element by site and period, followed by a discussion on the possible interpretations of the statistical findings for the developmental and allometric trajectories.

7.2 Foetal Developmental and Allometric Trajectories

The null hypothesis for the Group 1 foetal long bones is based on the allometric trajectories (7.22-7.24) which found a large range of size and shape for all three elements during for this age group. Despite this variation, it is hypothesised that there are no statistically significant changes in long bone morphology as a result of shape changes by site, as the growth (Figure 7.1-7.3) and allometric (Figure 7.22-7.24) trajectories begin at the same starting point for all sites. Changes in mechanical loadings would increase the PC scores positively along PC1 with an increase of width and curvature of the metaphyses and diaphyses.

Null Hypothesis: There are no statistically significant changes in bone shape by site for the upper or lower limbs during the foetal stage.

Numerous studies on postnatal growth have explored the effects of external forces on shape and growth of the skeleton (Ruff *et al.* 1994; Sumner & Andriacchi 1996; Ruff 2003; Cowgill *et al.* 2010, Bonneau *et al.* 2011). These studies found a strong correlation between changes in bone during postnatal growth, both in shape and microarchitecture, and weight-bearing behaviour (Bonneau *et al.* 2011). Authors such as Bonneau and colleagues (2011) have only recently explored gravity as a crucial influence during post-natal growth and its mechanical impacts on foetal morphology.

Table 7.7 describes the skeletal material used for the foetal (Group 1) morphometric analysis, with Table 7.8 representing the results. Figures 7.25-7.27 shows the principal component analysis (PCA) and allometric trajectories for the femora, tibiae, and humeri for this age group.

Group 1: Foetal Skeletal Materials				
Site	Period	Femur (n)	Tibia (n)	Humerus (n)
Great Chesterford	Anglo-Saxon	3	1	1
Raunds	Anglo-Saxon	1	0	0
Canterbury	Medieval	0	1	0
Wharram Percy	Medieval	1	4	6
Wolverhampton	Post-Medieval	1	0	0

Table 7.7: Skeletal Sample Size for Group 1.

Group 1: ANOVA Results (p-values)			
Variables	Femur	Tibia	Humerus
Site	**0.03**	0.12	0.12
Period	**0.02**	**0.04**	0.13
Allometry	0.13	0.37	0.13

Table 7.8 Statistical Results for Development and Allometry of the Group 1 sample.

7.2.1 Femur

The Group 1 femora are statistically significant for shape between site and period. The first PC axis (45%) reflects differences in curvature of the diaphyses and width of the distal metaphyses. Positive values (Wharram Percy, Wolverhampton, and Great Chesterford) represent curvature from the medial diaphyses into a wider distal metaphyses. Negative values (Raunds and Great Chesterford) represent curvature in the medial-distal diaphyses into narrower distal metaphyses. PC2 (30%) reflects the width of the metaphyses and the projection of the diaphyseal curvature. Positive values (Great Chesterford, Raunds, and Wharram Percy) reflect wider, shorter, and straighter proximal metaphyses. Negative values (Wolverhampton) represent narrower and longer proximal metaphyses, with more curvature into the proximal diaphyses and angled distal metaphyses.

The allometric plot did not find a statistically significant correlation with femoral shape regressing onto femoral size. It can be seen however, that Wharram Percy and Wolverhampton have the largest in size and more robust femora. Femora from Great Chesterford and Raunds are smaller in size and more gracile in shape. These patterns confirm the findings in the PCA, as Wharram Percy and Wolverhampton have more robust shapes, curved midshafts, and wider metaphyses. The Anglo-Saxon collections of Great Chesterford and Raunds have more curvature in the medial-distal diaphyses and had narrower metaphyses.

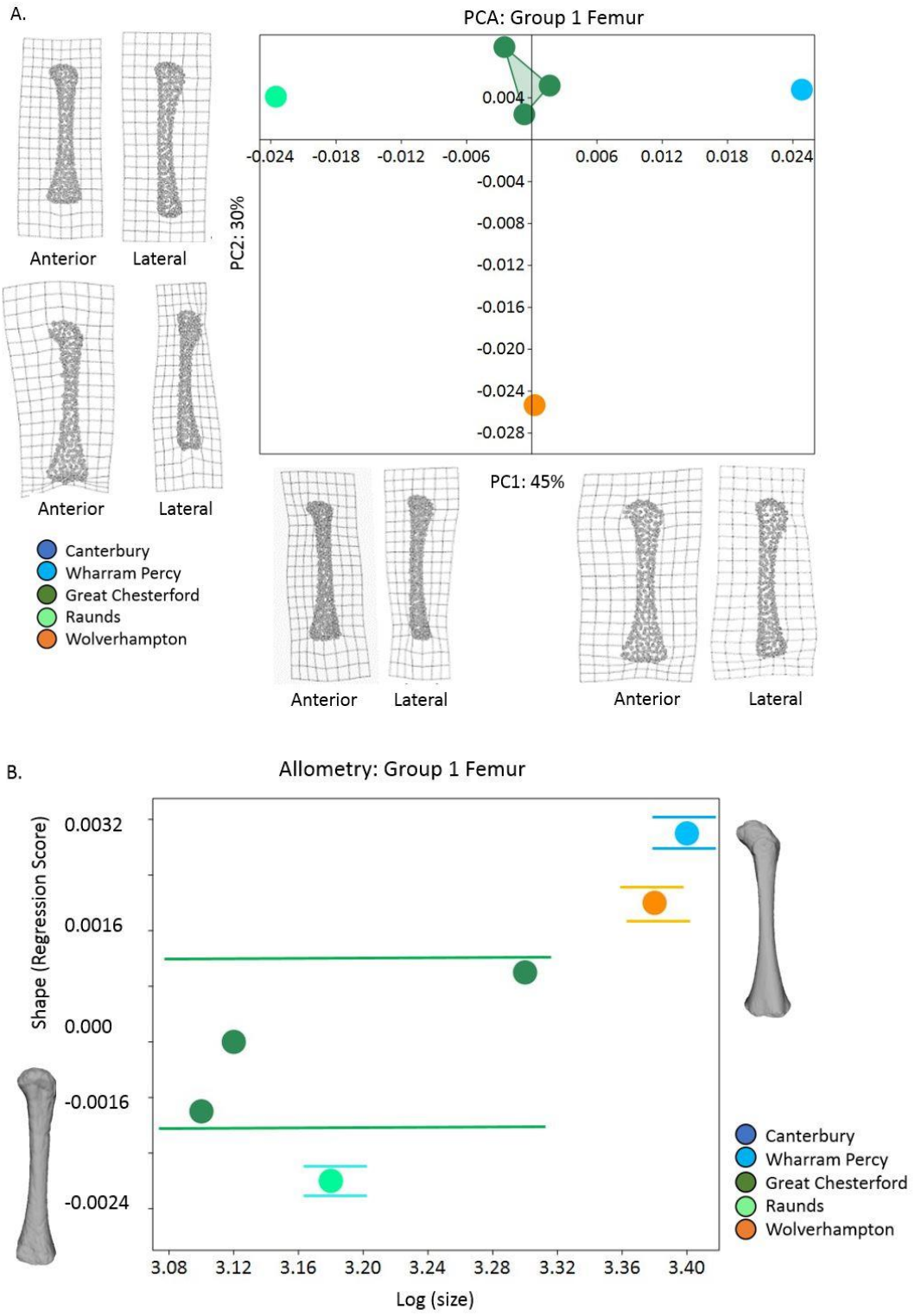

Figure 7.25: Principal Component Analysis (PCA: Left) and Allometric Plot (Right) for Group 1 (Foetal) Femora. A: Principal Component 1: anterior view. Positive values have more femoral head development and negative values show less femoral head development. Principal Component 2: anterior view. Negative values have more femoral neck and midshaft curvature and positive values have less. B: Allometric Plot: Positive Linear Regression with the foetal femora. Wolverhampton (Post-Medieval) and Wharram Percy (Medieval) have the largest and most developed femora. Great Chesterford (Anglo-Saxon) shows a large range of variation of shapes and Raunds (Anglo-Saxon) has the smallest and least developed femora.

7.2.2 Tibia

The foetal tibiae are statistically significant between shape and period. The first PC (45%) of the tibiae, reflects differences in the width of the proximal metaphyses and the curvature of the diaphyses. Positive values (Wharram Percy and Canterbury) represent wider proximal metaphyses with more curvature in the midshaft of the diaphyses. Negative values (Great Chesterford) signify a narrower proximal metaphyses and more curvature starting in the proximal diaphyses. PC2 (22%) reflects differences in the width of the diaphyses. Positive values (Wharram Percy) reflect a straighter and wider anterior diaphyses while negative values (Wharram Percy, Raunds, Canterbury) have a narrower and more curved anterior diaphyses.

There is no statistical significance in size regressed against shape for the foetal tibiae. The Canterbury tibia are the largest, while Great Chesterford and Wharram Percy are clustered together according to size. All foetal tibiae, however, are within the same shape range.

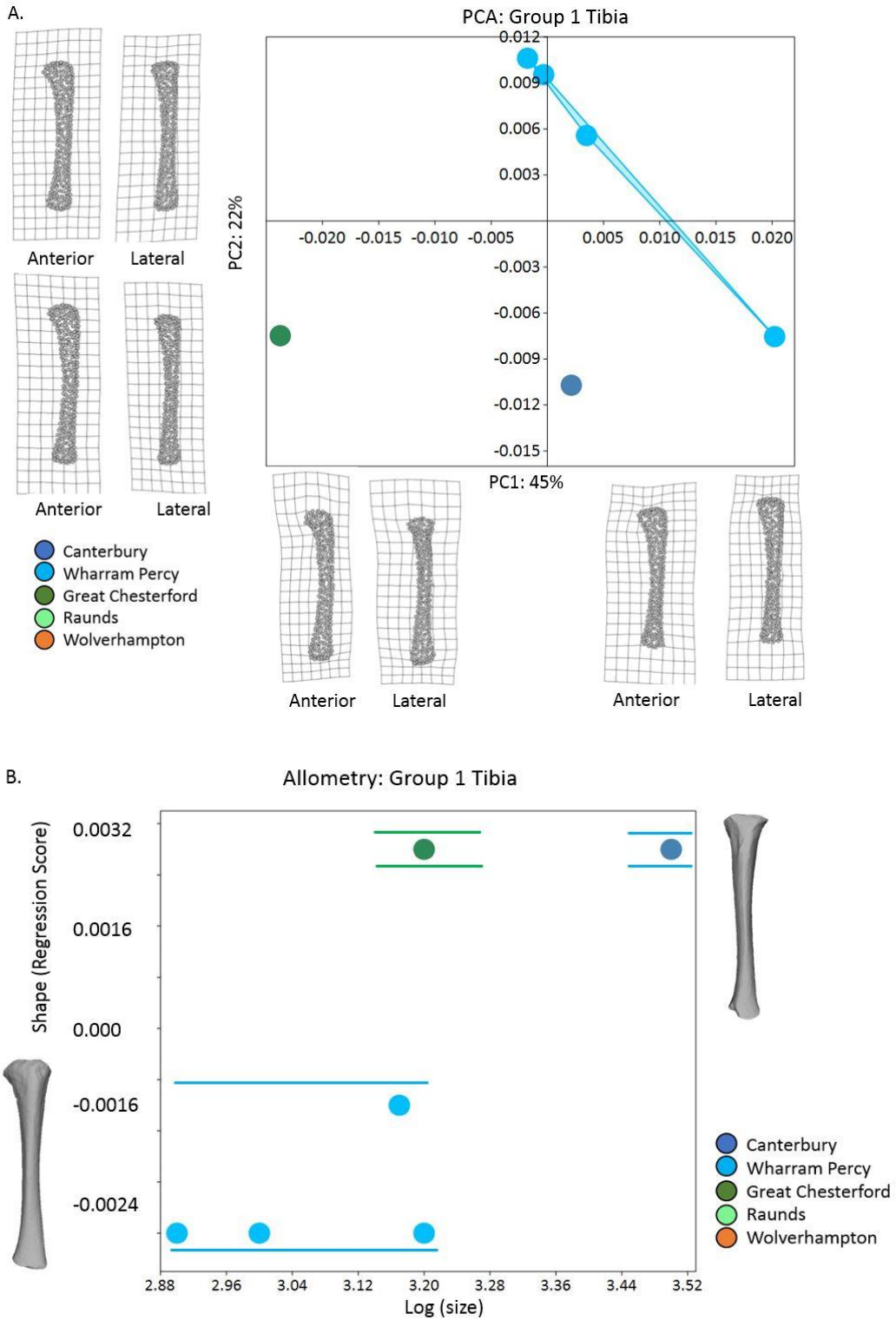

Figure 7. 26: Principal Component Analysis (PCA: Left) and Allometric Plot (Right) of Group 1 (Foetal) Tibia A: Principal Component 1: anterior view. Positive values reflect more development in the proximal medial metaphysis and negative values show more development in the proximal metaphysis and midshaft. Principal Component 2: anterior view. Positive values show more development in the proximal diaphysis and tibial tuberosity. Negative values show little shape development. B: Allometric Plot: Positive Linear Regression with Canterbury (Medieval) as the largest specimen and Great Chesterford (Anglo-Saxon) and Wharram Percy (Medieval) clustered within smaller sized tibia but overlapping shape with Canterbury.

7.2.3 Humerus

There is no statistical significance for foetal humeri between site or period. The first PC (55%) axis of the humeri represents differences in the width and angle of the proximal metaphyses. Positive values (Wharram Percy) represent wider and concave proximal metaphyses while negative values (Wharram Percy and Great Chesterford) have narrower and convex proximal metaphyses. PC2 (18%) represents the width and curvature of the diaphyses. Positive values (Wharram Percy) have narrower and more curved diaphyses while negative values (Wharram Percy and Great Chesterford) have wider and straighter diaphyses. Similarly to the femora and tibiae, there is no statistical significance in size regressed against shape for the humeri, as Great Chesterford falls within size and shape range of Wharram Percy.

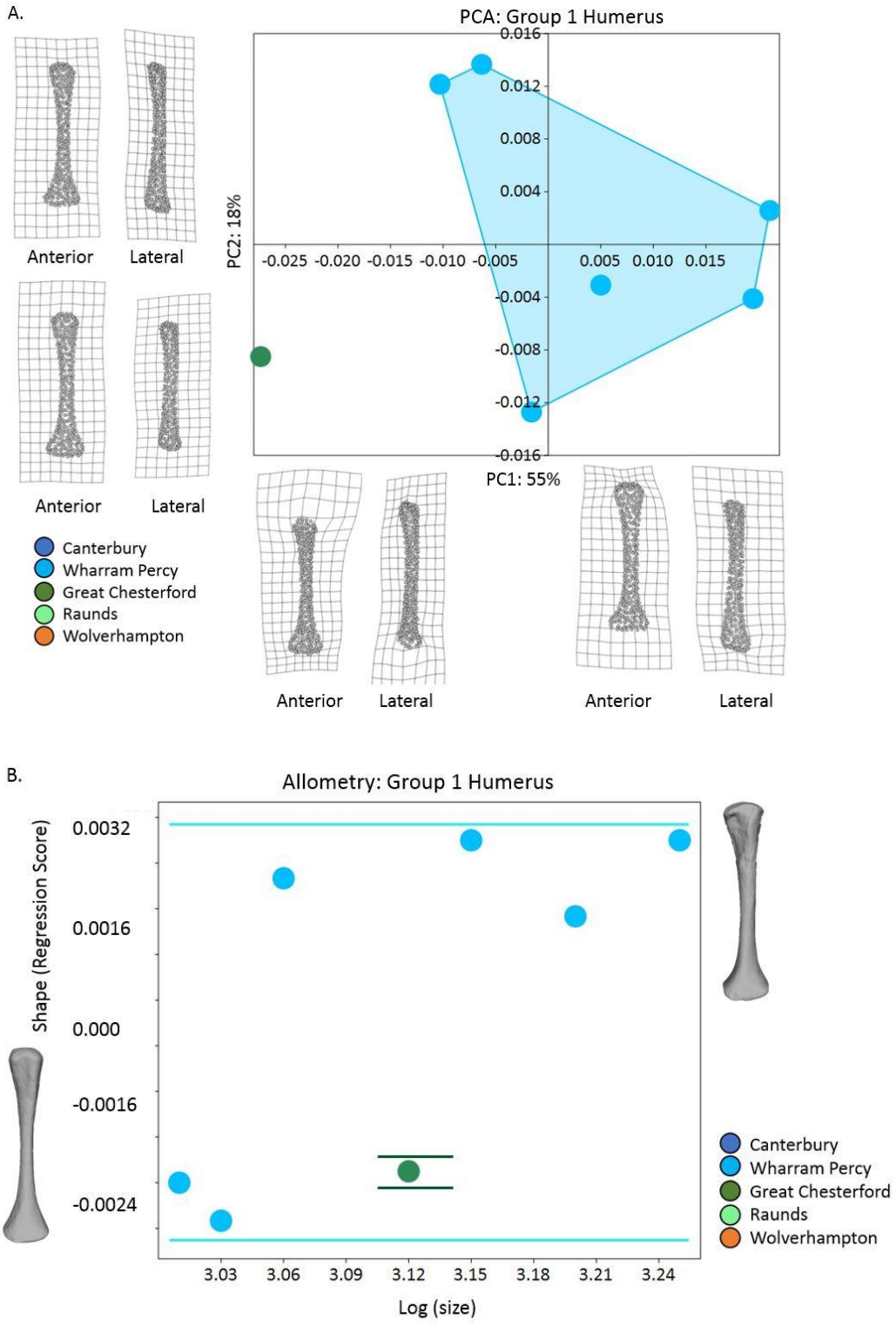

Figure 7.27: Principal Component Analysis (PCA: Left) and Allometric Plot (Right) of Group 1 (Foetal) Humerus A: Principal Component 1: anterior view. Positive values reflect more development in the distal metaphyses and negative values show more development in the lateral metaphyseal condyle and humeral head. Principal Component 2: anterior view. Positive values show more development in the coronid fossa (distal metaphysis) and negative values show little shape development. B: Allometric Plot: Positive Linear Regression with Great Chesterford (Anglo-Saxon) within range of Wharram Percy (Medieval) humeral shapes.

7.2.4 Discussion

Bioarchaeological studies use foetal long bones as a starting point for growth trajectories, however very few studies have focused on foetal morphology, partly as a result of a lack of methodologies that can be used to analyse and visualize these remains. Although the foetal femora, tibiae, and humeri have small and unequal sample sizes, this study indicates some interesting trends that have been highlighted by GM. Although the size of the elements were similar in the growth (Figure 7.1-7.3) and allometric (Figure 7.25-7.27) trajectories, the morphology was statistically significant for the femora (period and site) and tibiae (period). Therefore, the null hypothesis was rejected for the lower limbs. The humeri showed no statistical difference for shape between site and period and therefore the null hypothesis was accepted. In the lower limbs (Figure 7.25-7.27) it was found that the Medieval and Post-Medieval sites have wider proximal metaphyses with more curvature in the midshaft, while the Anglo-Saxon samples had shorter and narrower proximal metaphyses and straighter diaphyses. The humeri showed Medieval sites had wider and concave proximal metaphyses compared to the narrower and straighter Anglo-Saxon sites.

The femora showed clear patterning by period, as Anglo-Saxon (Raunds and Great Chesterford) juveniles were smaller in size and both sites displayed more curvature in the medial-distal diaphyses and narrower metaphyses compared to Medieval Wharram Percy and Post-Medieval Wolverhampton. It is difficult to make substantial claims as to why these differences occur. However, a possibility for these foetal long bone shapes is proposed by Bonneau *et al.* (2011), who found that variation in maternal parameters determines the intensity of the biomechanical constraints on the foetus and may result in two foetuses of similar femoral shaft length differing in their degree of shaft torsion. Although foetuses adapt several positions in utero, they all display cases of flexion followed by hyperflexion of the femur on the pelvis (Bonneau *et al.* 2011). This hyperflexion is caused by the increasing compression constraints during pregnancy and creates a mechanical force on the femur that can be seen as a first degree lever (Bonneau *et al.* 2011). When hyperflexion appears because of the compression of the foetus in the uterus, (Figure 7.28) the femoral shaft touches the anterior superior iliac spine through soft tissues, thus creating a fulcrum (Bonneau *et al.* 2011). Consequently, a resistive force occurs on the proximal femur and the femoral neck, which locks the femur into the acetabulum (Bonneau *et al*. 2011). The femoral neck, therefore, creates a lever arm and increases the movement of resistive force, resulting in torsion (Bonneau *et al.* 2011). The present study observed changes in morphological shape along the diaphyses for both femoral and tibial shapes (Figure 7.25-7.26). Bonneau *et al*. (2011) observed changes in femoral shaft torsion as a result of intrauterine constraints, which may explain more robust shapes occurring in the proximal regions of the long bones in the current study. Although genetic and epigenetic mechanisms may regulate timing of foetal development, Bonneau *et al.*

(2011) findings suggest that the foetal skeleton has an intrauterine mechanical history through adaptive bone plasticity (Bonneau *et al*. 2011: 438). It is possible that the differences seen in the foetal long bones of the current study are therefore a result of different forces applied to the proximal and distal metaphyses in addition to sample variation. The PCA plot in Figure 7.25 shows that the most robust shape occurs in the proximal metaphyses of the femur, specifically in the more robust femora from Wharram Percy and Wolverhampton.

Figure 7.28 Foetus position where hyperflexion can occur (Image by author)

Another possibility for the differences in foetal morphology may be a result of maternal hormonal or nutritional factors influencing growth of the foetus (Benson-Martin *et al.* 2006; Bonneau *et al.* 2011). It was previously thought that foetuses were 'buffered' from changes in their mother's health, however a strong body of evidence now suggests that the morphology of infants is affected by the nutritional state of the mother (Barker *et al.* 1989; Barker *et al.* 2002). The "Barker hypothesis", suggests that poor nutrition during pregnancy can alter "foetal programming" and change the course of the developing body's structure, function or metabolism (Barker *et al*. 1989). It is possible that development involves an induction of set patterns of development based on cues that prepare the foetus for the type of environment that they are likely to live in. Individuals adversely affected may have reacted to the environmental prediction from their mother (Bateson 2001). The effects of being small, which in the short term include higher death rates and childhood illness, are usually treated as an inevitable consequence of adverse environmental conditions that may derive from before conception to infancy (Eriksson *et al.* 1999). Gluckman and Hanson (2004), found that conditions such as poor nutrition during pregnancy results in a 'predictive adaptive response' in the foetus and therefore, developmental pathways are altered to what is perceived to be better suited to the postnatal environment (Gluckman & Hanson 2004; Low *et al*. 2012). This observation has been called the 'thrifty phenotype' model (Hales & Barker 2001) (see Chapter 2).

The functional and evolutionary approach suggests that pregnant woman in poor nutritional conditions may unknowingly signal to their unborn baby that it is about to enter a harsh world. This 'weather forecast' as Bateson and colleagues (2004: 420) refer to, is a result of the mother's body signalling to her unborn child to have a smaller phenotype (or bone morphology) and modified metabolism to cope with possible food shortages later in life. If the environmental circumstances change and high levels of nutrients are available after the development of a small phenotype has been initiated, rapid growth may occur as the 'catch-up' phase (Metcalfe & Monaghan 2001), but can trigger health problems arising in later life.

The Anglo-Saxon foetal femora were the smallest in size and the most gracile in shape with narrower and shorter metaphyses and straighter diaphyses. This may be linked to Anglo-Saxon women having difficult pregnancies as they tended to die during child bearing years. At the late Anglo-Saxon rural church cemetery of Raunds, Northamptonshire, 44% of all adult females died between the ages of 17 and 25 years old (Crawford 1999: 63). At Great Chesterford, Essex, a site with high numbers of infant burials (5 foetuses, 12 still born and 26 neonates- birth to 2 months) compared to most Anglo-Saxon cemeteries, two of the women died from complications during childbirth (Crawford 1999: 63).

As mentioned previously, it is difficult to make substantial interpretations to these patterns of small samples, however, it is interesting that Wharram Percy, a northern population shows more robust bone morphology compared to southern populations with more gracile bone morphologies for smaller sized bones. Wharram Percy is known to be a harsh geographical region and underwent periods of famine and stress (Mays 2007). These stressful events may be a combination of maternal health and how far along the foetus is in the gestational period. Although the results in the current study are limited, it does reveal interesting morphological patterns that occur much earlier than previously thought. Investigations of foetal and maternal skeletal morphology would be an interesting avenue of research (which is currently underexplored) to better understand their relationship for foetal skeletal morphology as this is the true starting point of an individual's developmental history.

7.3 Infant to 2 Year Olds: Developmental and Allometric Trajectories

The null hypothesis for the second age group is based on the allometric trajectories for all elements, age groups, and sites at the beginning of the Chapter (Figure 7.22-7.24). These analyses found that the second age group of infant to two years old has the most morphological variation. It is expected that the PCA for Group 2 reveals the lower limbs increasing positively on the PC axes during the transition of crawling to walking as the juveniles become more load bearing. Upper limbs however,

will show an increase in positive scores along the PC axes during the crawling phase as they are loadbearing. It is expected that the Medieval sites (Canterbury and Wharram Percy) will show changes in shape as a result of walking while the Anglo-Saxon (Raunds and Great Chesterford) and the Post-Medieval (Wolverhampton) sites will show less mechanical changes as historical contexts (Heywood 2014) refer to the prevention of these children from crawling.

Null Hypothesis: There will be no statistically significant differences in bone shape on the upper and lower limbs as increased positive scores on the PC axes will reflect the transition from crawling to walking in the lower limbs and crawling in the upper limbs.

The postnatal period is known to experience rapid growth following uterine constraints during gestational growth (Tanner 1994). Additionally, the child becomes exposed to many environmental challenges. Like all children in the past, the first stage of the child's life was occupied with problems of feeding warmth and attention (Hanawalt 1977:14). Providing infants with sufficient sustenance is a common problem for parents today, and keeping them warm is an even further challenge (Hanawalt 1977: 15). Children in the Anglo-Saxon period were wrapped in clothes once they were born (Crawford 1999: 68). Often babies were wrapped with their arms held straight at their side and legs extended together with additional support to hold the head steady. After a few months, the arms and head were left free. Historical texts such as coroner rolls indicate that in addition to disease, another danger to children during this age was fires. Most children in the past spent their first years of life in a cradle near the fire (Hanawalt 1977: 7). During the day the open door provided light and children and animals wandered through freely. At night candles were used which may have been left to burn all night, sometimes catching the houses on fire (Hanawalt 1977: 7). As described in the coroners rolls, a typical case showed a child lying in its cradle next to the hearth when a chicken or pig came in and knocked burring straw or an ember into the cradle. Since infants were wrapped in linen or wool, the smell of burning cloth or cry of the child would call attention to the accident if an adult were present (Hanawalt 1977: 14-15). By the end of the first year of swaddling, children became mobile enough to get into trouble. They wandered around courtyards and fell into wells, ponds, and ditches on their parents property. They also got into accidents in the house, the most common was pulling pots off trivets and falling (Hanawalt 1977: 14-15).

In addition to the changes in behaviour for this age group, drastic changes in biological and mechanical factors during growth have been reflected in the cross-sectional geometry (Ruff *et al.* 2013) of the long bones. Detailed longitudinal analysis of juvenile growth has revealed complex changes in human femora to humeri proportions that vary depending on the skeletal characteristic and age range examined (Ruff *et al.* 2013). The function and morphology of the human femur and

humerus have very distinct and separate roles and morphologies in terms of biomechanics (Sumner & Andriacchi 1996; 14, 15).

Table 7.9 describes the skeletal elements for Group 2 (infant to 2 years old) morphological analyses and the results in Table 7.10. Figure 7.29-7.31 shows the PCA and allometric trajectory for the femora, tibiae, and humeri.

Group 2: Infant to 2 Years Old Skeletal Materials				
Site	Period	Femur (n)	Tibia (n)	Humerus (n)
Great Chesterford	Anglo-Saxon	11	5	9
Raunds	Anglo-Saxon	5	4	1
Canterbury	Medieval	12	7	4
Wharram Percy	Medieval	1	1	3
Wolverhampton	Post-Medieval	1	1	6

Table 7.9: Skeletal Sample Size for Group 2.

Group 2: ANOVA Results (p-values)			
Variables	Femur	Tibia	Humerus
Site	**0.01**	0.15	**0.02**
Period	**0.01**	**0.07**	0.30
Allometry	**0.01**	**0.01**	**0.01**

Table 7.10: Statistical Results for Development and Allometry of the Group 2 Sample.

7.3.1 Femur

The shape of the infant to 2 year old femora are statistically significant between site and period. The first PC (38%) axis reflects differences in width and length of the proximal metaphyses and curvature in the diaphyses. Postive values (Great Chesterford, Raunds, Wharram Percy and Wolverhampton) reflect wider and shorter proximal metaphyses and more curvature in the midshaft. Negative values (Canterbury) suggest longer and narrower proximal diaphyses with more curvature in the proximal metaphyses. PC2 (20%) reflects differences in width and angulation of the metaphyses. Positive values represent convex proximal metaphyses with a concave angle in the distal metaphyses (inter-metaphyseal angle). Negative values reflect a concave angle in the proximal metaphyses with a convex angle in the distal metaphyses (inter-metaphyseal angle).

There is a statistically significant difference when regressing shape onto femoral size. Canterbury has the largest sized and most robust shaped femora. Great Chesterford, Raunds, and Wolverhampton have smaller size and more gracile femora. Interestingly, Wharram Percy is in the same size range as the Canterbury femora but is in the shape range of the more gracile sites.

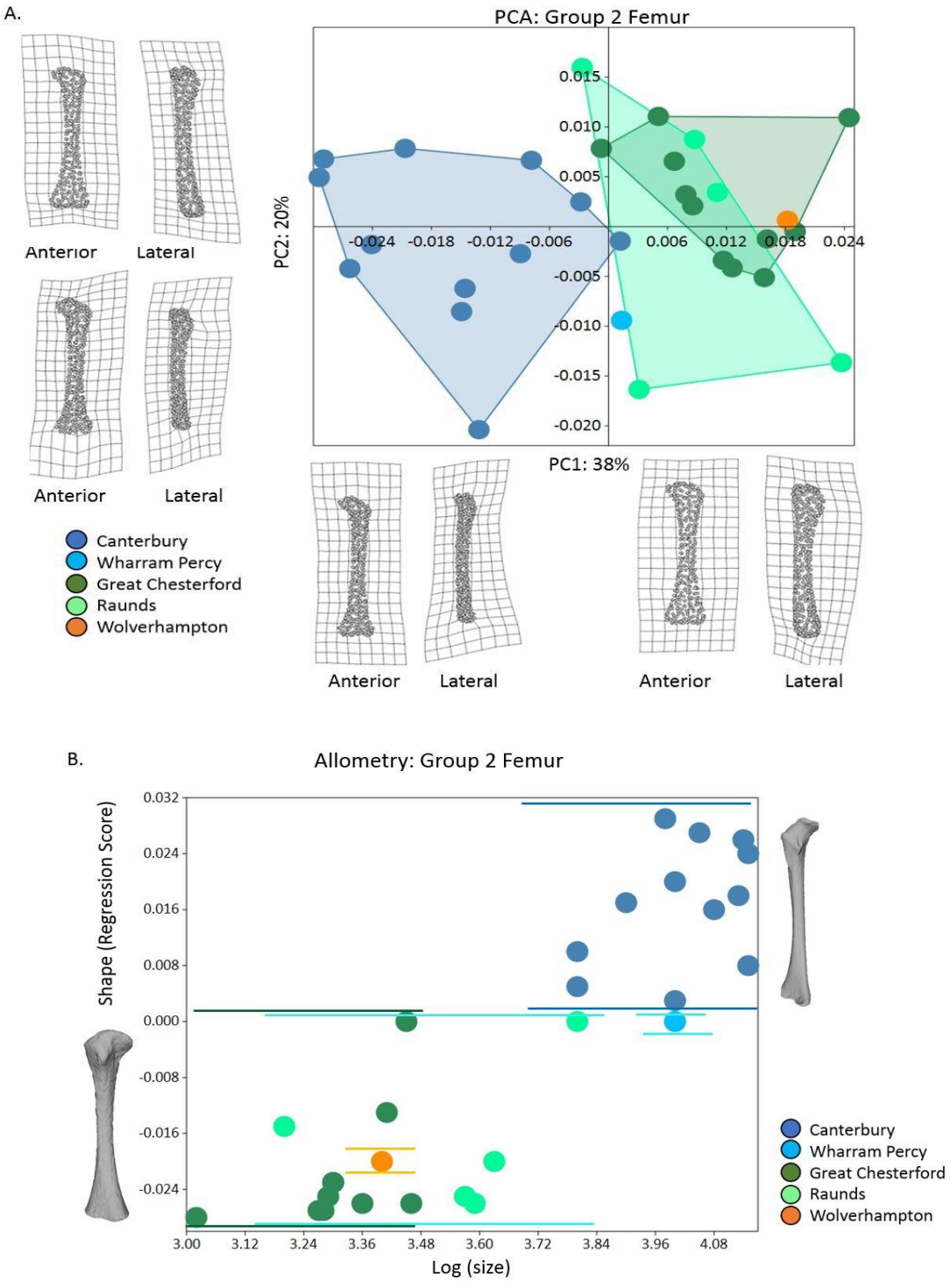

Figure 7.29: Principal Component Analysis (PCA: Left) and Allometric Plot (Right) of Group 2 (Infant to 2 years old) Femur A: Principal Component 1: anterior view. Negative values reflect more development in the metaphyses. Principal Component 2: anterior view. Positive values show more development in the femoral head and negative values represent more development in the midshaft. B: Allometric Plot: Positive Linear Regression with Canterbury (Medieval) as the largest femora in size and shape development. Great Chesterford (Anglo-Saxon) has the smaller size and shaped femora with Wolverhampton (Post-Medieval) falling within range of Great Chesterford. Raunds (Anglo-Saxon) shows the largest variation of shape which falls between that of Canterbury and Great Chesterford. Wharram Percy (Medieval) has similar size femora to those from Canterbury, but they are similar in shape to the other sites.

7.3.2 Tibia

The tibiae are statistically significant between shape and period. Principal Component 1 (34%) reflects the width of the diaphyses (anterior-posterior). Positive values (Canterbury, Wharram Percy, and Raunds) reflect a narrower diaphyses while negative values reflect a wider diaphyses (Canterbury, Raunds, Wolverhampton, and Great Chesterford). PC2 (20%) reflects the width of the metaphyses. These patterns echo the femora as positive values (Wharram Percy, Canterbury, Wolverhampton, Raunds, and Great Chesterford) represent a concave proximal metaphyses with a convex distal metaphyses. Negative values (Great Chesterford, Raunds, and Canterbury) represent a concave proximal metaphyses and a convex distal metaphyses.

There is a statistical significance when regressing shape onto tibiae size. Canterbury has larger and more robust tibiae with Wharram Percy falling within size and shape range of Canterbury. Great Chesterford has smaller size and more gracile shaped tibiae with Wolverhampton falling within the size and shape range of Great Chesterford. Raunds has the largest variation in tibiae size and shape and all sites fall within its size and shape variation.

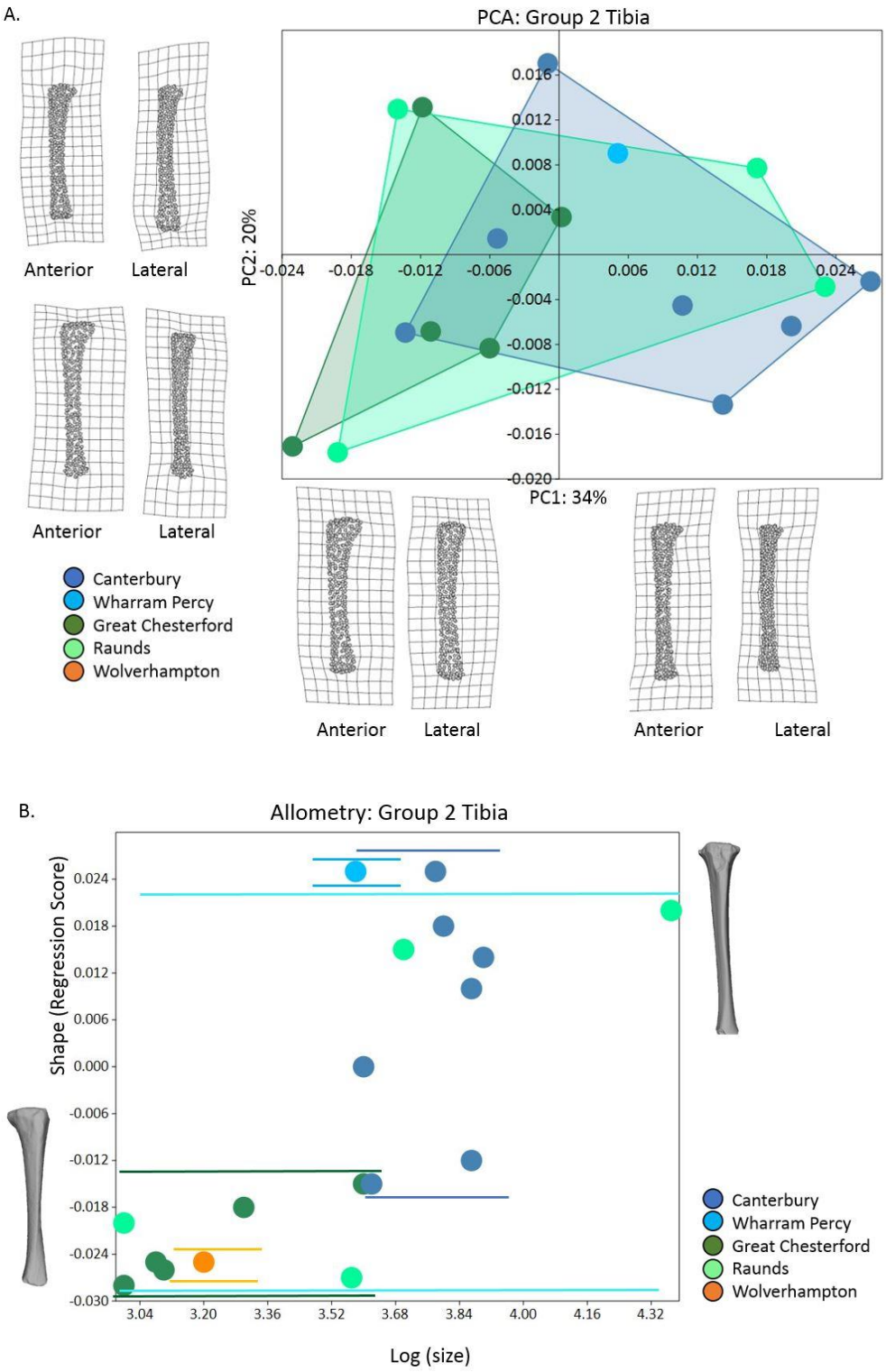

Figure 7.30: Principal Component Analysis (PCA: Left) and Allometric Plot (Right) of Group 2 (Infant to 2 years old) Tibiae A: Principal Component 1: anterior view. Positive values reflect more development in the metaphyses and negative values show more change in the midshaft. Principal Component 2: anterior view. Negative values show more development in the proximal metaphyses and midshaft. B: Allometric Plot: Positive Linear Regression with Raunds (Anglo-Saxon) representing the entire range of size and shape variation. Canterbury (Medieval) represents the larger and more developed tibiae, while Wharram Percy (Medieval) falls within the Canterbury developmental range. Great Chesterford (Anglo-Saxon) and Wolverhampton (Post-Medieval) have smaller sized and less developed tibiae.

7.3.3 Humerus

The infant to 2 year old humeri are statistically significant between shape and site. The first PC axis (33%) reflects the width of the distal metaphyses and the length of the proximal metaphyses. Positive values (Great Chesterford, Wolverhampton, and Wharram Percy) represent a wider distal metaphyses and a shorter proximal metaphyses. Negative values (Canterbury, Great Chesterford, Raunds, and Wolverhampton) represent narrower distal metaphyses and longer proximal metaphyses. PC2 (18%) represents the width and angle of the distal metaphyses. Positive values (Raunds, Great Chesterford, and Wharram Percy) represent more curvature in the distal metaphyses while negative values (Canterbury, Wolverhampton, Great Chesterford, and Wharram Percy) have a straighter angle in the lateral plane to the distal metaphyses.

There is a statistical significance in the results for regressing humeri size against shape. Similarly to the other elements, Canterbury has the largest and more robust humeri with a narrower distal and longer proximal metaphyses, and a straighter diaphyses. Wolverhampton and Great Chesterford have the largest range of size and shape with Raunds and Wharram Percy having smaller size and more gracile humeri.

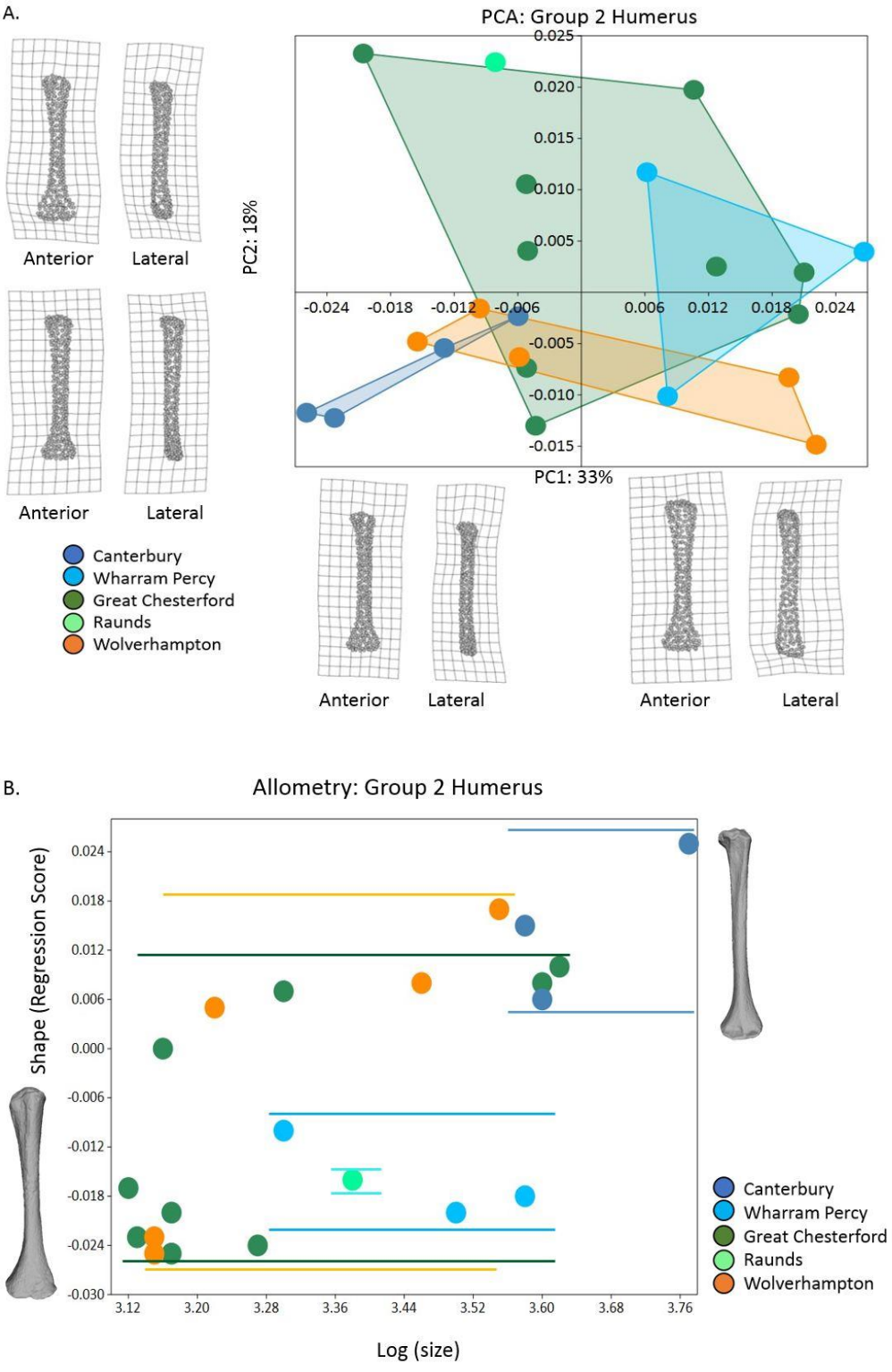

Figure 7.31: Principal Component Analysis (PCA: Left) and Allometric Plot (Right) of Group 2 (Infant to 2 years old) Humerus. A: Principal Component 1: anterior view. Negative values represent more development in the humeral head. Principal Component 2: anterior view. Negative values represent more changes in the curvature of the midshaft. B: Allometric Plot: There is no statically significant linear regression for humeral size against shape as all humeri are within the same shape range. The Canterbury (Medieval) humeri are the largest with Great Chesterford, Raunds (Anglo-Saxon), Wharram Percy (Medieval) and Wolverhampton (Post-Medieval) having smaller humeri.

7.3.4 Discussion

The infant to 2 year old group shows large variation in morphology, which is to be expected as there is a dramatic shift in the growth trajectories for femoral and humeral strength at 1 year of age, corresponding to the adaptation to bipedalism (Ruff *et al.* 2013). The null hypothesis was rejected as there was statistically significant changes in the bone shape for the upper and lower limbs as increased positive scores on the PC axes reflect the transition of crawling to walking. The femora were statistically significant for site, period, and allometry. The negative PC1 values represent the larger sized femora of Canterbury which reflect narrower proximal metaphyses with a mid-to-lower diaphyseal curvature. The positive values had shorter and wider proximal metaphyses with a curvature in the midshaft of the diaphyses. The positive PC1 shape quadrant consisted of Great Chesterford, Raunds, Wharram Percy and Wolverhampton, which are the smaller sized femora. Statistical significance of the tibiae was found for allometry and the first principal component axis represented the width of the diaphyses for which similar patterns were found to the femora. Canterbury and some of the Wharram Percy individuals reflected a range of shape with most development occurring in the angle of the proximal metaphyses into the diaphyses. This reflects a higher level of activity (De Groote *et al.* 2010). The data from Great Chesterford, Wolverhampton, and Raunds reflect more force in the knee as a concave proximal (tibiae) and convex distal (femora) pattern was seen. Lastly, statistical significance of the humeri for site and allometry was found, with positive PC1 values representing wider distal and shorter proximal metaphyses (Wolverhampton, Wharram Percy, and Great Chesterford) which may be a result of biomechanical loadings during crawling. The negative values indicate narrow distal and longer proximal metaphyses (Canterbury, Great Chesterford, Raunds, and Wolverhampton), which represents individuals that were not weight bearing in the upper limbs.

The morphological changes in shape seen in the current study reflect strength involved in the elbow flexors and knee extensors which increase at different rates during growth (Sumner & Andriacchi 1996; 23). As illustrated in Figure 7.32 there is a range of movements that occur in Group 2. Cameron and Demerath (2002) found a rapid increase in the cross-sectional geometric properties of the femora as a function of increasing bone length. The observations of this thesis are consistent with experimental studies which showed increased robusticity (diameter to length) in response to higher loads during postnatal development (Cameron & Demerath 2002) and decreased long bone robusticity when loads are then removed (Cameron & Demerath 2002). These changes in robusticity are followed by a two year period of rapid modification of the femora, tibiae, and humeri

to their new mechanical environments (femoral strength increasing much faster than humeral strength), during which the child acquires a mature gait pattern (Ruff 2003: 342).

The variation in long bone morphology for all sites in the current study confirms these mechanical changes. The juvenile long bones for infant to 2 year olds (Group 2), shows unique developmental patterns between sites (Great Chesterford, Raunds, Wharram Percy, Canterbury, and Wolverhampton) and period (Anglo-Saxon, Medieval, Post-Medieval). These sites show significantly different developmental pathways which likely result from environmental and biomechanical influences.

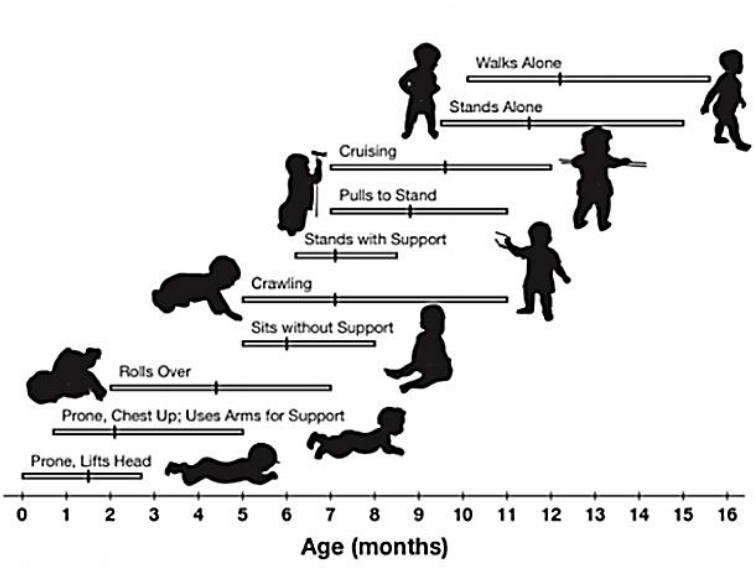

Figure 7.32: Developmental Milestones (Adolph & Robinson 2013: Figure 1.B).

Similar to a study by Gosman *et al.* (2013), and the Great Chesterford femora described in Chapter 4, the femora and tibiae midshafts for all sites are conserved during growth as the proximal and distal metaphyses are more sensitive to developmental changes and mechanical loads. Gosman *et al.* (2013) found accelerated growth from 0 to 0.19 and 2 to 5 year olds. The allometric trajectories (Figure 7.29, Figure 7.30) of the femora and tibiae show a large range of morphological variation for all sites in this age range, likely reflecting accelerated growth. Both Gosman *et al.* (2013) and the current study found that the medio-lateral proximal femur and anterior-posterior tibiae expanded with more robusticity during the accelerated periods, consistent with changes in locomotor loading patterns. Canterbury has the most robust morphology for all three elements. The majority of Canterbury femora shape changes occur in the proximal metaphyses followed by distal metaphyses. Additionally, the proximal tibiae and midshaft curvature all show early signs of

standing and walking. The Wharram Percy, Great Chesterford and Raunds femora and tibiae show similar patterns in morphological shape, however, there is slightly less robusticity occurring in the proximal tibiae. These sites therefore, appear to show variations in movement such as crawling and pulling to stand (as discussed in Chapter 2). Changes in the hamstrings occur in the distal femora and proximal tibiae as the hip and knee joint becomes more developed. Long bones tend to be stockier when the musculoskeletal system is not fully developed, which is seen with the Wharram Percy and Great Chesterford femora and tibiae. Apart from Wolverhampton, which has very little change occurring in the proximal femur and distal tibiae, the changes in hamstring development may cause some of the shape differences in lower limb morphology for this age group.

Children from around 2 years old have considerable motor skills and a lively interest in their environment which is seen in the long bone morphology of the current study. Although cradle fires continued to be a hazard in the early stages of this period, the accident pattern indicates that the process of exploring reached out to the world around them, and imitating adults intensified. According to the Coroners rolls (Hanawalt 1977: 15), the accidents show that children were exploring beyond the household. Wells (25% of deaths) were the most dangerous obstacle of the child's new lives as wanders, followed by ditches (20%), ponds (8%), streams and rivers (93%) (Hanawallt 1997: 15). Greater physical mobility without sufficient motor control caused many of the accidents for this group. For instance, one report in the Coroners rolls noted a child was playing with a duck and holding it in her arms. She wanted to put it into the river but fell in herself (Hanwallt 1977: 16).

It is no surprise that parents were often anxious when teaching their children to walk, given the large numbers of adults who ended up lame or rickety (Heywood 2014: 89). They discouraged infants from crawling on all fours, partly for the practical reason that floors were cold and damp (Heywood 2014: 89), and experts warned that it was dangerous to try and force a child to walk before it was naturally ready. Bartholomew the Englishman's advice insisted on waiting until at least the age of 1 and trying the earliest steps on a smooth, soft surface to avoid asymmetry in leg strength (Heywood 2014: 90). Parents attached leading strings to clothes and used little frames to encourage children to remain upright as soon as possible (Figure 7.33). Medieval iconography shows a familiar scene of a child being encouraged to walk in a wooden framed walker.

Figure 7.33 Jesus in a baby walker, The Hours of Catherine of Cleves, C. 1440

Interestingly, despite advice of discouraging infants from crawling, this seems to be represented in the morphology of the long bones for Medieval Wharram Percy and possibly early stages at both Anglo Saxon sites. At Wharram Percy, eight juveniles from 2 to 18 months showed evidence of rickets (Ortner & Mays 1998). Most mechanical deformities were seen in the arm rather than leg bones. This reflects the greater proportion of body weight born by the upper limbs in the crawling infant. In infant skeletons which had both leg and arms present, those with only arm bone deformation were aged between three and twelve months. Only one case which was eighteen months old showed both arm and leg deformities. Infants tend to walk by the end of their first year. The pattern of limb bone deformity in the rickets cases may be consistent with these findings. The restriction of leg bone deformity to the eighteen month old may indicate that this individual had begun to walk before death (Mays 2007: 177). Wolverhampton also showed a case of rickets from a 1 to 2 year old with bowing of the femur (Adams & Colls 2007). Although crawling was discouraged it does appear to have happened as evidence from the high number of rickets occurring in the upper and lower limbs at Wharram Percy and Wolverhampton and the shape patterns in this thesis.

The humeri (Figures 7.31) shows that Wharram Percy, Great Chesterford, and Raunds exhibit more robusticity in width than the other sites. Although the shape development occurs at different regions of the humeri for these three sites it is likely a result of different movements being used and therefore creating different morphological shapes in relation to loadings. Wharram Percy shows most shape development in the proximal and distal region of the humeri and has the broadest and most robust shape out of these three sites. It is likely that the mean shape of Wharram Percy is capturing crawling, as the shoulder and elbow joint is where most development is found thereby creating a more robust shape.

Great Chesterford and Raunds have slightly less robusticity (compared to Wharram Percy), and more deformation is found in the diaphyses of these sites. This could be the result of more loadings occurring in the humeri diaphyses as a result of propping up or pulling to stand (Adolph 2008: 215). Wolverhampton and Canterbury exhibit less robusticity, however, they capture the extreme shapes of Group 2 humeri variation. Wolverhampton has the most gracile humeri with changes occurring in the proximal and distal metaphyses. This may be the result of slight movement of propping up on the stomach. Canterbury, however, represents less loading perhaps because the individuals are already bipedal. The Canterbury humeri do reflect shape changes in the diaphyses and lateral metaphyses, but the humeri have become more slender compared to the Anglo-Saxon and Wharram Percy load bearing bones. These different functional demands of the humeri could explain how the trajectories differ after bipedal locomotion. The humeri show less development during the post-walking phase as the upper body 'reboots' to a different function of stabilizing the torso rather than a load bearing element.

It should be noted that some infants skip the crawling phase altogether (Adolph & Robinson 2013: 2-3) and it could be that the Canterbury juveniles skipped this phase while the Wharram Percy, Great Chesterford and Raunds juveniles were crawlers, thereby explaining the more robust morphology. Possible crawling was seen in the Wharram Percy humeri as they have more robusticity in the elbow and shoulder joint and development of the knee in the distal femur and proximal tibia. The Anglo-Saxon sites showed more diaphyseal development in the humeri, while Great Chesterford exhibited more robusticity in the hip and knee joint, and Raunds reflected most changes in the proximal and distal metaphyses of the femora. Therefore, Great Chesterford may be showing more standing compared to the crawlers of Wharram Percy and Raunds. Wolverhampton showed the most gracile shape in the long bones which may be the beginning stages of support on the stomach or propelling forward. As indicated in Chapter 6, the children's employment commission report of 1843 attributed the high death rate in infants to the custom of administering Godfrey's Cordial to infants and young children to keep them quiet or 'sleeping them' while their parents were out at work (Adams & Colls 2007). The desire to keep young infants 'asleep' may be reflected in the allometric and PCA plots for this group as they closely resemble morphologies found in foetal shapes (Group 1). The average age of the Wolverhampton Group 2 individuals in the younger age range of this group (4 months). It is possible that these individuals were not only tightly bound with a constricting environment (much like the intrauterine constraints in foetal morphology) but less 'active' as many children died during this age from induced sleep. The end of this age group also marks the beginning of diverging growth trajectories (Figure 7.1-7.3) as nutritional stress and diet begin impacting growth and developmental trajectories which may manifest in the older age groups of 3 to 12 years old.

7.4 Three to Five Year Olds: Developmental and allometric Trajectories

The allometric trajectories (Figure 7.22-7.24) show that Group 3 (3-5 years old) has a small growth spurt. It is expected that there will be no statistically significant changes in the metaphyseal morphology as a result of shape changes during 3 to 5 years old. It is suggested that there is a lack of statically significant changes in shape for this age range as this group reflects the transition to more refined adult gait patterns. Refined gait patterns are reflected in the positive values of the PC scores for the lower limbs. It is expected that slight changes in the hip and knee joints will occur but they will not be statistically different by site or period in their morphology. The upper limbs will undergo a catch up growth during this age range but it is expected that non-significant changes in shape will occur during this period as the humeri is a non-loadbearing element.

Null Hypothesis: There will be no statistically significant changes in shape for the upper and lower limbs as increased positive scores on the PC axes will reflect width and curvature of the metaphyses (hip and knee joints).

After 3 years old, childhood and early adolescence is characterized by a more gradual increase in femoral relative to humeral strength, with femoral strength paralleling growth in body size and humeral strength progressively declining relative to body size (Gosman *et al*. 2011). In Anglo-Saxon, Medieval, and Post-Medieval children, age 3 marked the emergence from 'infancy' to the next phase of childhood (Crawford 1999: 37). By the third year of the child's life cradle deaths were no longer common and children entered into the second phase of social development, reception to outside stimulus (Hanawalt 1977: 15). Although 3 year olds suffered many accidents similar to the earlier toddler years (Group 2), as a result of their advancing motor skills and lively interest in their environment, their mobility was still unrefined and caused many accidents while imitating roles of their parents (Hanawalt 1977: 15).

The frequency for this age group and morphometric results are found in Table 7.11 and 7.12. The PCA and allometric trajectories are found in Figure 7.34 to 7.36 for the femora, tibiae, and humeri.

Group 3: 3 to 5 Years Old Skeletal Materials				
Site	Period	Femur (n)	Tibia (n)	Humerus (n)
Great Chesterford	Anglo-Saxon	1	5	2
Raunds	Anglo-Saxon	4	1	4
Canterbury	Medieval	8	10	8
Wharram Percy	Medieval	3	3	4
Wolverhampton	Post-Medieval	1	1	1

Table 7.11: Skeletal Sample Size for Group 3.

Group 3: ANOVA Results (p-values)			
Variables	Femur	Tibia	Humerus
Site	**0.01**	0.16	**0.01**
Period	0.77	0.17	**0.03**
Allometry	**0.01**	0.25	**0.01**

Table 7.12: Statistical Results for Development and Allometry of the Group 3 Samples.

7.4.1 Femur

The Group 3 femora (Figure 7.34) showed statistical differences between sites. The first PC (35%) reflects differences in the width and angle of the proximal metaphyses into the proximal diaphyses (the femoral head angle). Positive values (Canterbury, Raunds, and Wolverhampton) suggest more medial curvature from the lateral plane into the proximal diaphyses from the metaphyses. Negative values (Raunds, Canterbury, Great Chesterford, and Wharram Percy) represent anterior curvature from the lateral plane of the proximal metaphyses in to the diaphyses. PC2 (20%) reflects the angle of the proximal and distal metaphyses (the hip and knee joint). Positive values (Canterbury, Wharram Percy, Raunds, and Wolverhampton) have more convex proximal metaphyses and a concave distal metaphyses (inter-metaphyseal angle). Negative values (Canterbury, Wharram Percy, Raunds, and Great Chesterford) indicate a flatter proximal metaphyses and a convex distal metaphyses (inter-metaphyseal angle).

There is a statistical significance in femoral shape when regressing onto size. Canterbury has the largest sized and most robust shaped femora, with Wolverhampton falling within shape range of Canterbury. Raunds has a larger variation in size and shape, which overlaps with Canterbury and Wolverhampton. Wharram Percy and Great Chesterford have the smaller sized and more gracile shaped femora.

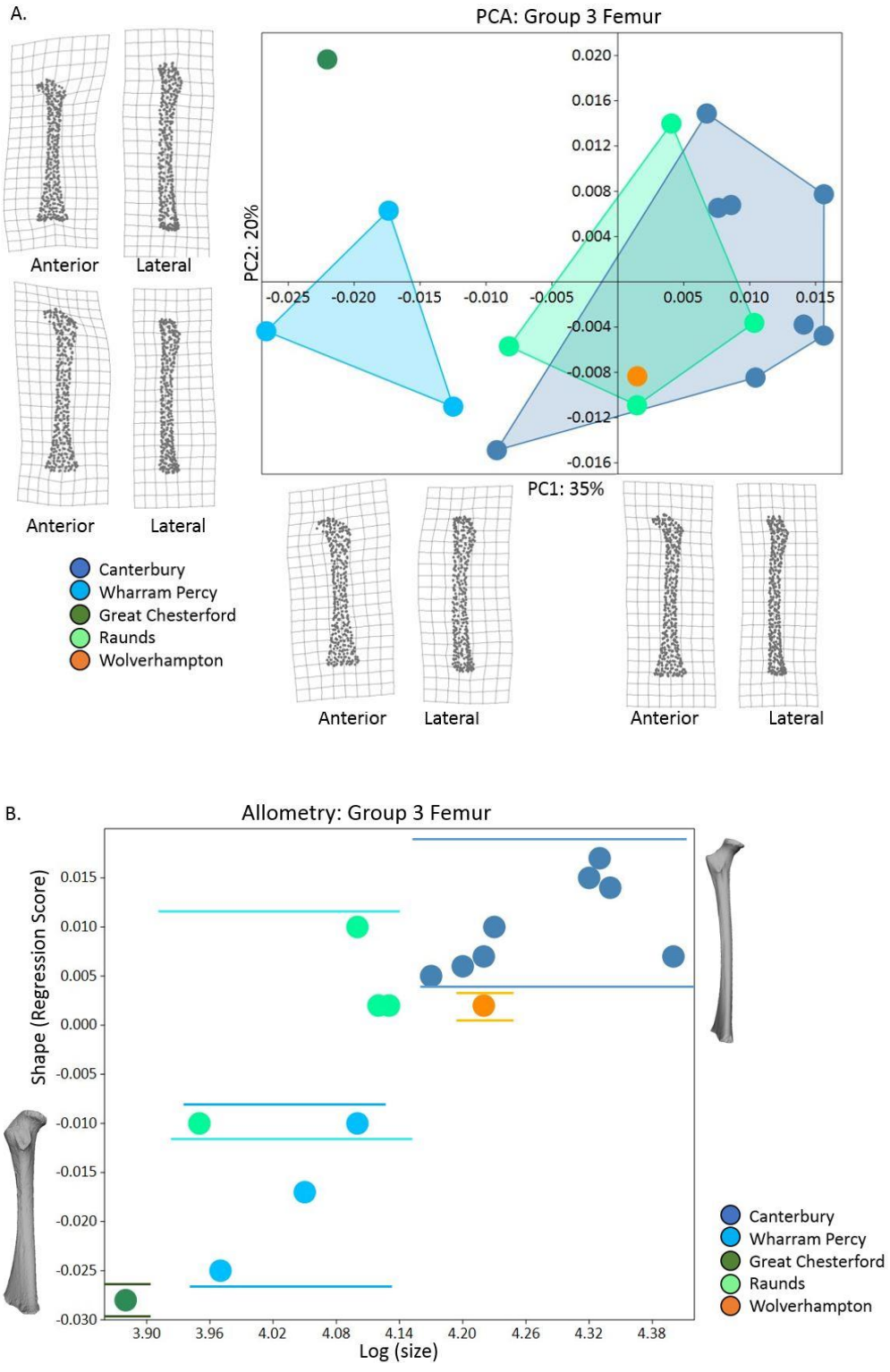

Figure 7.34: Principal Component Analysis (PCA: Left) and Allometric Plot (Right) of Group 3 (3 to 5 years old) Femur A: Principal Component 1: anterior view. Positive values reflect more development in the metaphyses. Principal Component 2: anterior view. Positive values show more development in the midshaft. B: Allometric Plot: There is no linear regression femoral size against shape as all sites are within the same shape range. Canterbury (Medieval) femora are the largest size and shape development while Wolverhampton (Post-Medieval) falls within range of Canterbury. Great Chesterford (Anglo-Saxon), Raunds (Anglo-Saxon), and Wharram Percy (Medieval) represent the smaller size and shaped femora.

7.4.2 Tibia

The Group 3 tibiae (Figure 7.35) do not show any statistical significance for PCA against site or period. Nonetheless, PC1 (33%) does represent some changes in the width and angle of the diaphyses into the proximal metaphyses. Positive values have a wider proximal metaphyses into the diaphyses with curvature at the anterior side of this junction (Canterbury, Wharram Percy, and Wolverhampton). Negative values (Canterbury and Raunds) have a narrower and straighter diaphyses. PC2 (18%) reflects some differences in the direction of curvature of the diaphyses. Positive values (Canterbury and Wharram Percy) have wider diaphyses and more lateral curvature from the distal metaphyses. Negative values (Canterbury, Raunds, Wharram Percy, and Wolverhampton) have narrower and straighter diaphyses.

There is no statistical significance in the allometric trajectory for regressing shape onto size. Canterbury is the largest sample and therefore has the largest range of size and shape variation. Wolverhampton, Great Chesterford, and Raunds are smaller in bone size but fall within Canterbury's shape range.

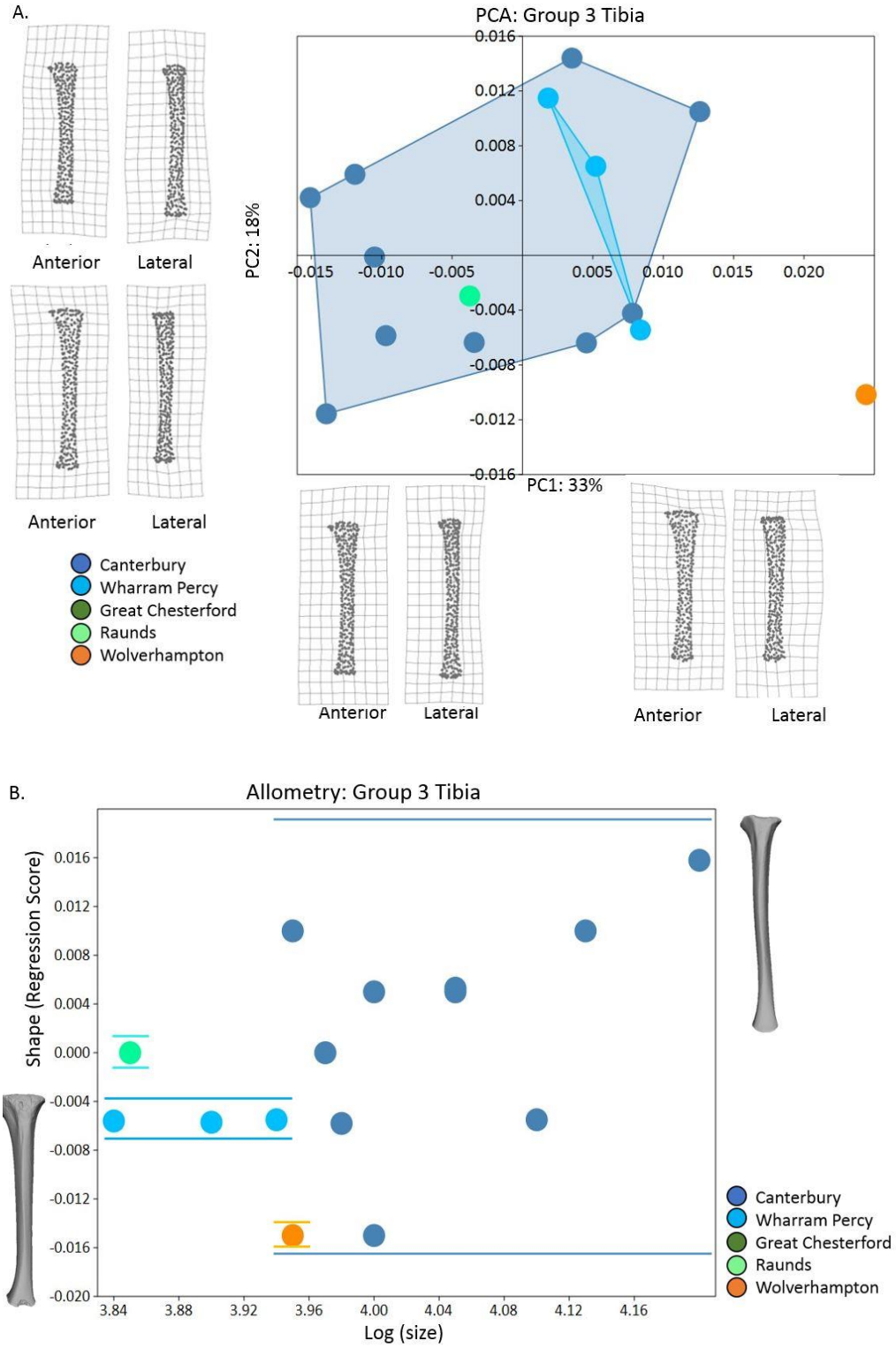

Figure 7.35 Principal Component Analysis (PCA: Left) and Allometric Plot (Right) of Group 3 (3 to 5 year old) Tibia. A: Principal Component 1: anterior view. Negative values reflect more development in the proximal metaphyses. Principal Component 2: anterior view. Negative values represent more development in the midshaft. B: Allometric Plot: There is no linear regression with tibial size against shape as all tibiae are within the same shape range. Canterbury (Medieval) are the largest and most varied shape for tibia. Wolverhampton (Post-Medieval) and Wharram Percy (Medieval) fall in the least developed shape range followed by Raunds (Anglo-Saxon).

7.4.3 Humerus

The humeri for Group 3 (Figure 7.36) shows statistically significant patterning for shape against site and period. PC1 (33%) represents the curvature of the anterior diaphyses into the proximal metaphyses. Positive values (Wolverhampton, Wharram Percy, Raunds, and Canterbury) reflect rounder convex proximal metaphyses with a wider diaphyses and torsion of the diaphyses from the anterior plane. Negative values (Canterbury, Great Chesterford, and Raunds) reflect narrower and flatter proximal metaphyses with more curvature and torsion at the midshaft from the posterior to anterior plane. PC2 (15%) represents the curvature of the distal diaphyses into the metaphyses. Positive values (Raunds, Wharram Percy, Great Chesterford, and Raunds) reflect wider distal diaphyses into the metaphyses. Negative values (Canterbury, Great Chesterford, Raunds, and Wolverhampton) have a narrower anterior curvature of the distal diaphyses into the metaphyses.

The allometric trajectory shows statistically significant patterns when regressing humeral shape onto size. Canterbury continues to have the largest size and more robust shapes. Great Chesterford, followed by Raunds and Wharram Percy have similar sized humeri with a large variation in shape. Wolverhampton has the smallest sized and most gracile shaped humeri.

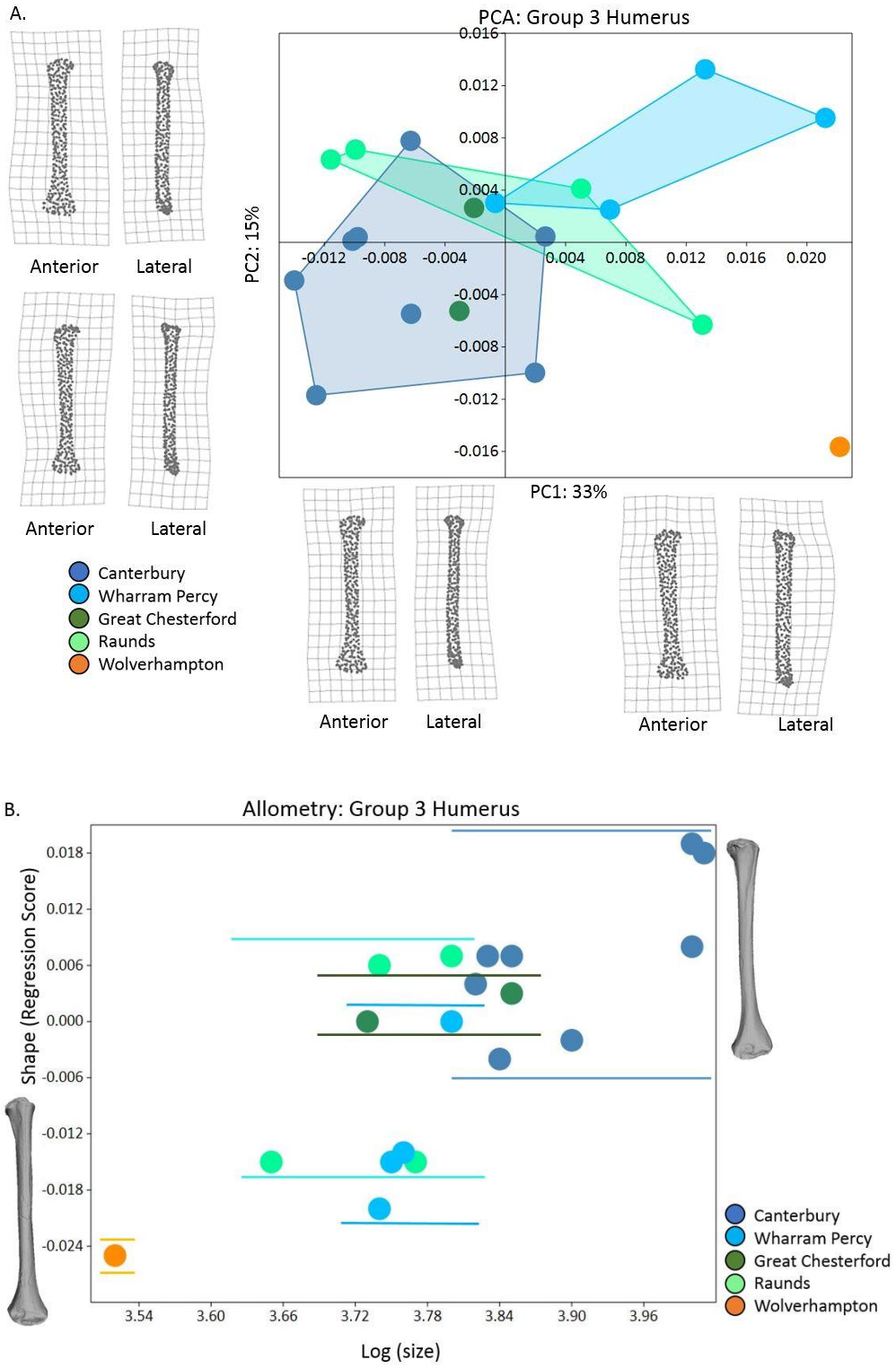

Figure 7.36: Principal Component Analysis (PCA: Left) and Allometric Plot (Right) of Group 3 (3 to 5 years old) Humerus A: Principal Component 1: anterior view. Positive values reflect more development in the midshaft and negative values more in the proximal metaphyses. Principal Component 2: anterior view. Negative values show more development in the distal metaphyses. B: Allometric Plot: Positive Linear Regression was found with Canterbury (Medieval) humeri as the largest in size and shape. Raunds (Anglo-Saxon) shows the largest variation of shape with Great Chesterford (Anglo-Saxon) and Wharram Percy (Mediaeval) falling with in size and shape range of Great Chesterford. Wolverhampton (Post-Medieval) has the smallest and least developed humeri.

7.4.4 Discussion

Once the lower limbs shift from quadrupedal to bipedal locomotion, there is a small growth spurt in developmental morphology as individuals refine adult-like gait patterns (Figure 7.1-7.3). Interestingly, there is an energy shift from a concentration of growth and development in the lower limbs and humeri between Group 2 and 3. The humeri experiences a conserved period of growth and development as the child transitions from quadrupedal to bipedal movement in Group 2, and then has a growth spurt in humeral size and shape during 3-5 years old (Group 3). Gosman *et al.* (2013) found accelerated growth from 0 to 0.19 and 2 to 5 year olds, while sites from the current study show similar patterns of acceleration.

The null hypothesis was rejected as there was statistical significance for the femora (site and allometry) and humeri (site, period, and allometry) but accepted for the tibiae as there was no statistical significance for shape between site, period, or allometry. For the femora increased positive scores on the PC axes reflect the angle of the proximal and distal metaphyses with the diaphyses. Canterbury, Raunds, and Wolverhampton had the positive shape scores and larger sized and more curved metaphyses while Wharram Percy, Raunds, and Great Chesterford had negative shape scores and smaller sized and straighter metaphyses. Positive scores are likely to reflect more refined gait patterns as the metaphyses (hip and knee joints) become more curved in these shape quadrants. The tibiae did not show any statistical significance as positive PC1 values reflected wider proximal diaphyses with an anterior curvature into the proximal metaphyses which represents the smaller tibiae of Canterbury, Wharram Percy, and Wolverhampton. The second PC axes represented the origin of curvature for the diaphyses and positive values had a wider curvature from the distal diaphyses into the metaphyses. The humeri did show statistically significant differences for all variables as positive values for the sites of Wolverhampton, Raunds, and Wharram Percy reflect smaller sized humeri with wider and rounder diaphyses and curvature at the anterior surface. Negative values (Canterbury, Raunds, and Great Chesterford) had a narrow and flatter diaphyses with curvature at the midshaft to distal end of the humeri which represented larger humeri.

The changes in more refined gait patterns reflected in the lower limbs width and curvature of the metaphyses, and a growth spurt occurred during a change in diet between the ages of four to six. The change in diet may be a factor for the growth spurt as childhood routines begin to change (Hanawalt 1977: 64). Greater mobility allowed children to accompany adults outside of their home and into the work place, leading to more time spent in adult company (Hanawalt 1977, 1988: 158). This may be seen in the Coroners Reports as children experienced fewer accidents from 4 years old

onwards, not necessarily because of their usefulness to society but because they were in the company of responsible adults and their parents had instilled some sense of caution and responsibility in them (Hanawalt 1977: 22). More time in adult company would have given more access to adult dietary staples, such as meat or vegetable pottage (Brears 2008).

Figure 7.37 Pieter Bruegel the Elder's Children's Games, 1560. Kunsthistorisches Museum, Vienna photo AKG London. (Heywood 2014: 113).

In addition to spending more time with adults, the this age range of 3-5 years old is also commonly represented as a period of play, such as in Pieter Bruegel the Elder's famous painting 'Children's Games' (Figure 7.37). The previous group of infant to 2 year olds experienced extreme changes in both form and function (crawling to walking) and diet (weaning). It is possible that the differences in lower limb morphology for Group 3 is a result of the juveniles adjusting to their new upright mobility, diet, and interaction with a larger environment. It is known that the weaning and post-weaning period can be problematic for juveniles (Mays 2003; 2002) as adequate nutritional supplements are not always achieved. This may be reflected in the tibiae and its lack of statistical shape patterning, as the tibiae are more sensitive to environmental changes (Roberts & Manchester 2005: 172).

7.5 Six to Eight Year Olds: Developmental and Allometric Trajectories

The allometric trajectories (Figure 7.22-7.24) showed that this age group of 6-8 years old had a conserved period of growth and development as it overlapped with Group 3 (3-5 years old) and Group 5 (9-12 years old). Therefore, the overlapping allometric trajectories of Group 4 with Groups 3 and 5 suggest that there will be no statistically significant change in the diaphyseal morphology as a result of shape change during the 6 to 8 year old age group. The previous age group reflected changes in refined gait patterns and demonstrated statistically significant changes in the shape and angle of the metaphyses. It would therefore seem likely that the positive values on the PC scores for this age group would reflect changes in torsion and loading of the diaphyses.

Null Hypothesis: There will be no statistically significant changes in shape or allometric trajectories for the upper and lower limbs and increased positive scores on the PC axes will reflect width and curvature of the diaphyses.

In theory, the age of 7 marked a significant turning point in the life of children in the past, although it may not have always been in practice (Heywood 2014: 103), as children became part of the productive economy of the household (Bogin 1999: 179). Gender differences became more pronounced as fathers took over the prime responsibility for sons and were expected to take a more prominent role in child-rearing at this stage (Heyword 2014: 103). Mothers would continue to teach daughters to spin, sew, and manage a household. Light work around the farm such as shepherding geese, minding pigs, or workshop apprenticeships would begin at 6-7 years old (Heywood 2014: 103).

The skeletal material for Group 4 is found in Table 7.13 and the morphometric results in Table 7.14. The PCA and allometric trajectories for the femora, tibiae, and humeri are found in Figure 7.38-7.40.

Group 4: 6-8 Years Old Skeletal Materials				
Site	Period	Femur (n)	Tibia (n)	Humerus (n)
Great Chesterford	Anglo-Saxon	1	2	0
Raunds	Anglo-Saxon	4	4	5
Canterbury	Medieval	12	11	11
Wharram Percy	Medieval	8	7	7
Wolverhampton	Post-Medieval	1	1	0

Table 7.13: Skeletal Sample Size for Group 4.

Group 4 : ANOVA Results (p-values)			
Variables	Femur	Tibia	Humerus
Site	0.17	0.12	0.51
Period	0.56	0.24	0.55
Allometry	0.05	0.08	0.57

Table 7.14: Statistical Results for Development and Allometry of the Group 4 Sample.

7.5.1 Femur

The Group 4 femora (Figure 7.38) did not show any statistical significance for site or period. The first PC axis (35%) reflects differences in the angle of the proximal metaphyses into the posterior curvature of the diaphyses. Positive values (Wharram Percy, Raunds, Great Chesterford, Raunds, and Canterbury) which represent smaller sized femora indicate a straighter angle of the proximal metaphyses into the midshaft curvature. Negative values (Canterbury, Wharram Percy, Raunds, and Wolverhampton) reflect a steeper curve from the posterior proximal metaphyses into the proximal diaphyses. PC2 (22%) reflects changes in the anterior curvature of the midshaft. Positive values (Canterbury, Wharram Percy, Raunds, and Wolverhampton) which represent larger sized femora have a concave curvature from the anterior plane of the proximal metaphyses into the proximal diaphyses. Negative values (Canterbury, Raunds, Great Chesterford, and Wharram Percy) have a concave proximal curvature from the anterior metaphyses and a concave anterior midshaft.

There is no statistical significance when regressing femoral shape onto size for 6 to 8 year olds. Canterbury continues to have the largest sized and most varied shape femora, while Raunds and Wharram Percy fall within Canterbury shape range. Great Chesterford remains in the smaller sized and more gracile shaped range for this group. Wolverhampton juveniles however, experience a growth spurt as they now fall in the larger size and more robust shaped range of femora from Canterbury and Raunds; in Groups 1 to 3 Wolverhampton was in the smaller sized and more gracile shape range.

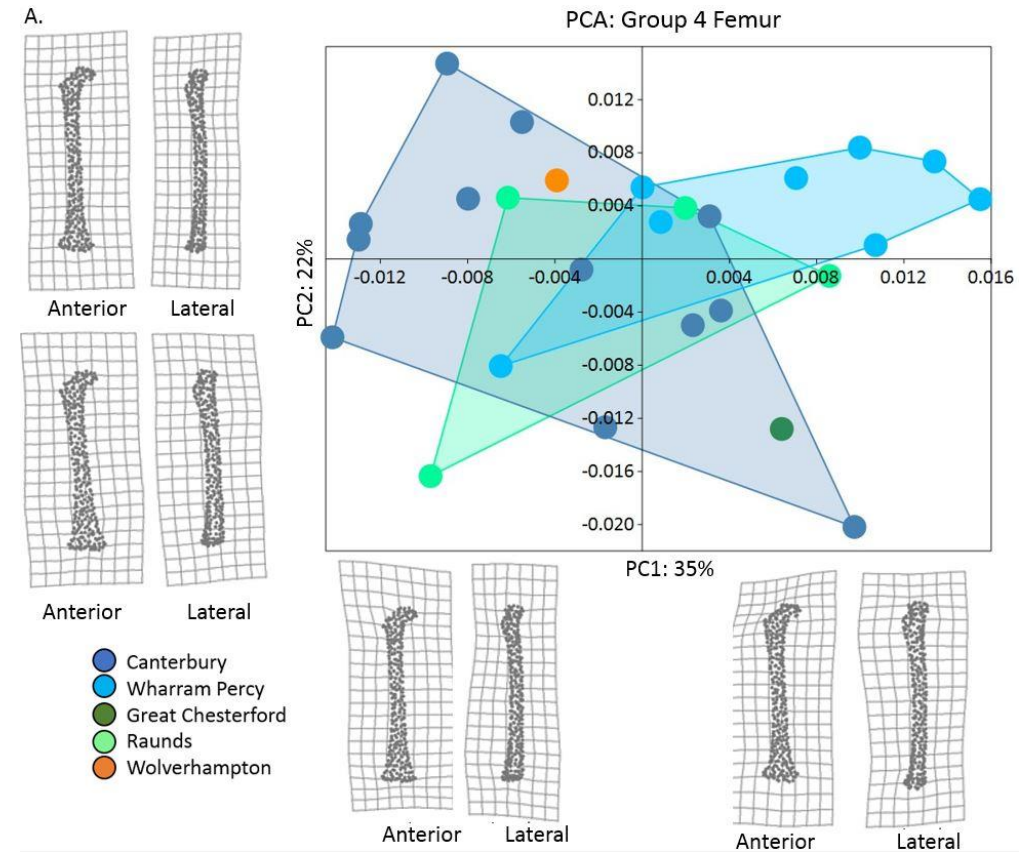

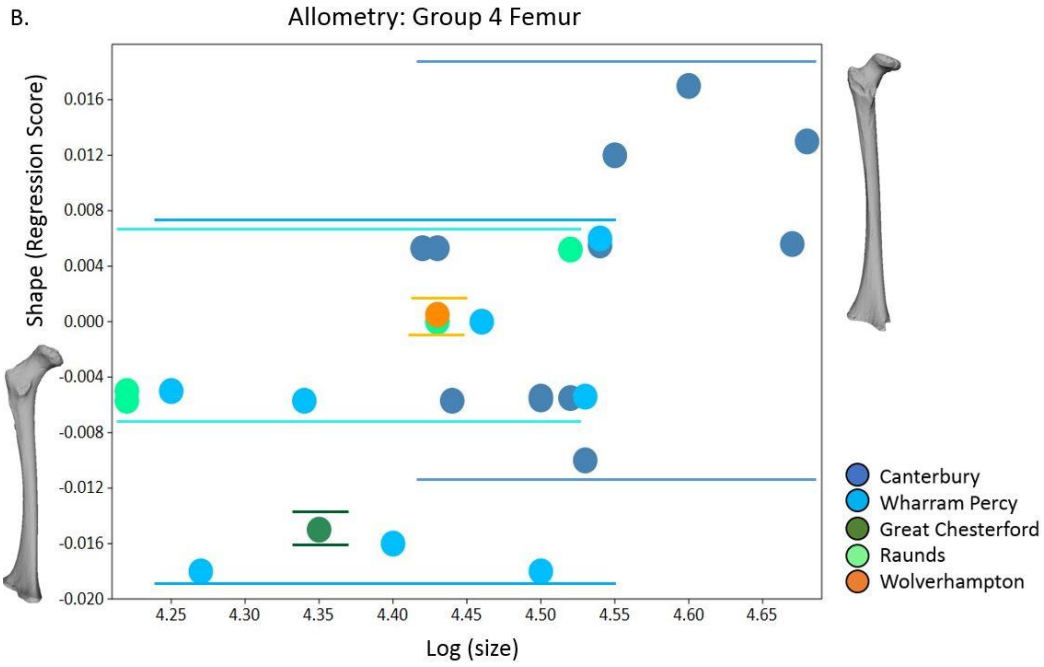

Figure 7.38: Principal Component Analysis (PCA: Left) and Allometric Plot (Right) of Group 4 (6 to 8 years old) Femur. A: Principal Component 1: anterior view. Positive values reflect more development in the second trochanter and medial metaphysis. Principal Component 2: anterior view. Positive values represent more development in the diaphysis. B: Allometric Plot: There is no linear regression as all femora fall within the same shape range. Canterbury (Medieval) shows the largest size and shape femora. Raunds (Anglo-Saxon), Wharram Percy (Medieval) Great Chesterford (Anglo-Saxon), and Wolverhampton (Post-Medieval) fall within Canterbury's shape range.

7.5.2 Tibia

The Group 4 tibia (Figure 7.39) were also not statistically significant for site or period. The first PC axis (33%) reflects the width of the diaphysis and curvature of the distal metaphyses. Positive values represent the smaller sized tibiae (Great Chesterford, Wharram Percy, Raunds, and Canterbury) and have a wider diaphyses with a convex curvature from the distal metaphyses into the diaphyses. Negative values (Canterbury, Raunds, Wharram Percy, and Wolverhampton) have a narrower diaphyses with a concave curvature from the distal metaphyses into the diaphyses. PC2 (20%) reflects the angle of the proximal metaphyses and lateral diaphyses. Positive values represent larger sized tibiae (Canterbury, Raunds, Wharram Percy, and Wolverhampton) which have a rounder proximal medial metaphyses. Negative values (Canterbury, Wharram Percy, Raunds, and Great Chesterford) have flatter and broader proximal metaphyses. The allometric trajectory follows similar patterning to the femora as Canterbury and Raunds which have the largest size and shape variation, with Wolverhampton and Wharram Percy falling within this range. Great Chesterford continues to have the smallest sized and more gracile shaped tibiae.

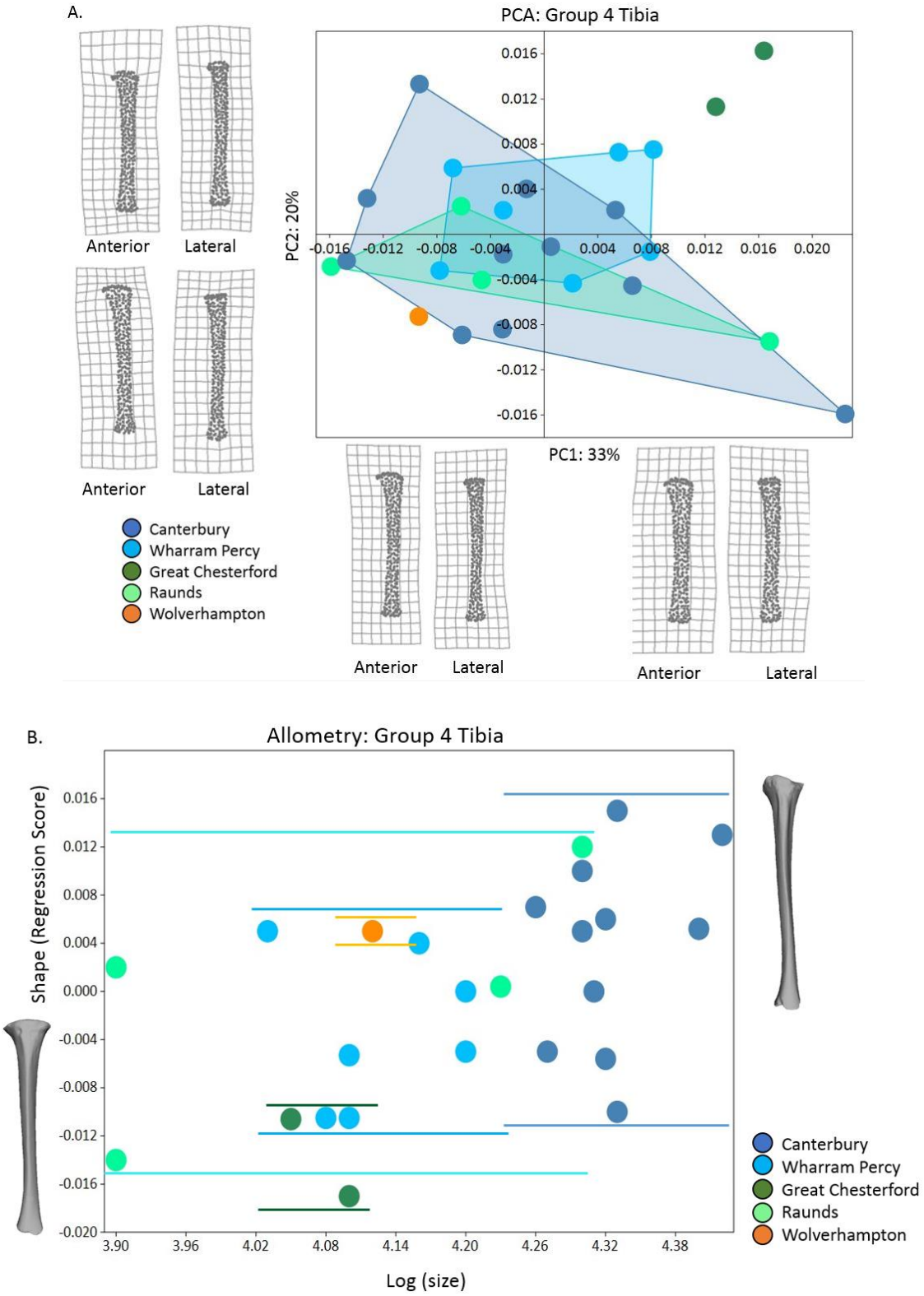

Figure 7.39: Principal Component Analysis (PCA: Left) and Allometric Plot (Right) of Group 4 (6 to 8 years old) Tibia. A: Principal Component 1: anterior view. Positive values reflect more development in the midshaft and negative values more in the proximal metaphyses. Principal Component 2: anterior view. Positive values represent more development in the proximal metaphysis. B: Allometric Plot: There is no linear regression as all tibiae fall within shape range. Canterbury (Medieval) represents the largest size and shaped tibiae. Wharram Percy (Medieval), Great Chesterford (Anglo-Saxon), and Wolverhampton (Post-Medieval) fall within the range of Raunds (Anglo-Saxon) for size and shape.

7.5.3 Humerus

The Group 4 humeri (7.40) were also not statistically significant for site or period. The first PC axis (28%) reflects differences in the width and curvature of the diaphyses. Positive values (Canterbury, Wharram Percy, and Raunds) reflect a wider diaphyses and more anterior torsion and surface curvature. Negative values (Canterbury, Wharram Percy, and Raunds) have a narrower diaphysis with a more S-shaped curvature. PC2 (18%) reflects changes in the angle of the proximal metaphyses into the diaphyses. Positive values (Canterbury, Wharram Percy, and Raunds) reflect a sloping proximal metaphyses from the medial side into a posterior curvature into the diaphyses. Negative values (Canterbury, Wharram Percy, and Raunds) have straighter diaphyses and a rounder proximal metaphyses. The allometric trajectory follows the femora and tibiae for this group as Canterbury has the largest humeri size and shape range followed by Raunds and Wharram Percy.

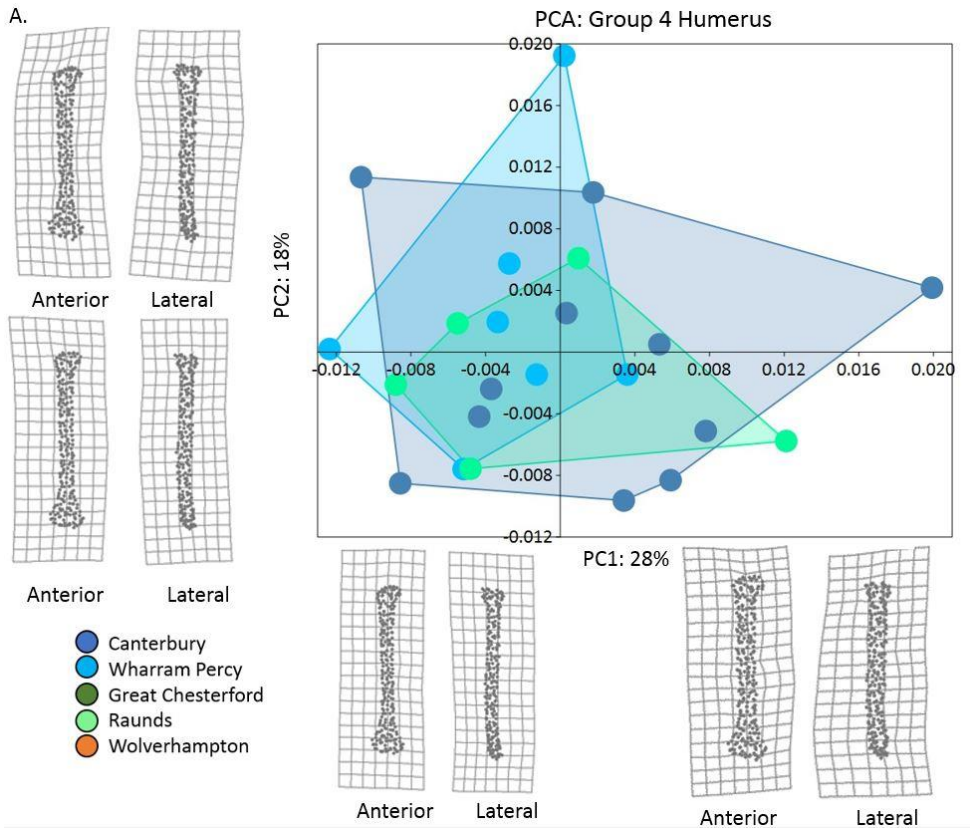

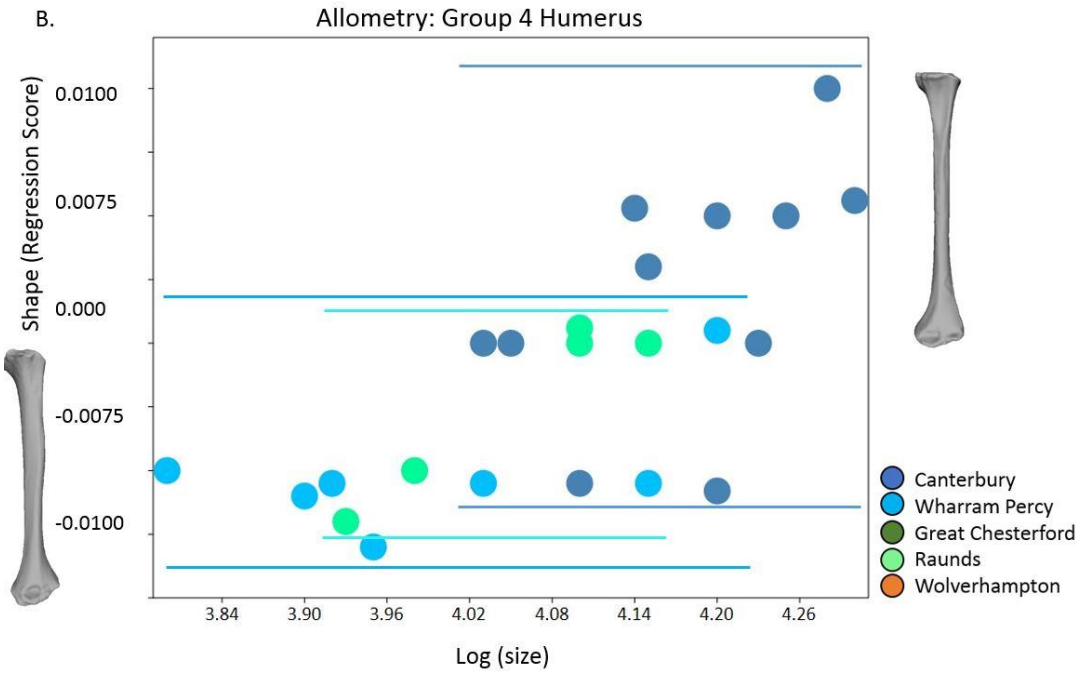

Figure 7.40: Principal Component Analysis (PCA: Left) and Allometric Plot (Right) of Group 4 (6 to 8 years old) Humerus A: Principal Component 1: anterior view. Positive values reflect more development in the proximal and distal metaphyses. Principal Component 2: anterior view. Negative values show more development in the diaphyses. B: Allometric Plot: There is no linear regression for humeral size against shape as all humeri are within the same shape range. Canterbury (Medieval) has the largest size and shaped humeri while Raunds (Anglo-Saxon) and Wharram Percy (Medieval) fall within Canterbury's shape range.

7.5.4 Discussion

Although this group marks an important time in the social life of the child, there is no statistical significance in shape patterning and variation for all elements, sites, periods, and allometry. Therefore, the null hypothesis was accepted as there is no statistical significance for any element. The PCA found that the femora with increased positive scores have a straighter angle from the proximal metaphyses into the midshaft curvature. These specimens were the smaller sized elements of Wharram Percy, Raunds, Great Chesterford, and Canterbury. Negative values had a steeper curve into the hip from the posterior proximal metaphyses into the diaphyses and reflected the larger sized individuals from Canterbury, Wharram Percy, Raunds, and Wolverhampton. These morphological changes are likely a result of increased loading and the torsion of the diaphyses. Similar patterns were found for the tibiae as positive PC1 values reflect wider and rounder distal metaphyses into the diaphyses. These also reflect the smaller tibiae of Great Chesterford, Wharram Percy, Raunds, and Canterbury. The second PC axes represent the angle of the proximal metaphyses and lateral diaphyses as positive values indicate a rounder proximal metaphyses while the negative values indicate an angled metaphyses. The first PC of the humeri represents the width and curvature of the diaphyses as positive values suggest wider anterior torsion to the diaphyses while negative values indicate narrower humeri with an S-shaped curvature. The second PC axes reflect differences in the angle of the proximal metaphyses into the diaphyses as positive values have a medial slope in the proximal metaphyses and a posterior curvature to the midshaft, while negative values indicate a straighter diaphyses and rounder metaphyses.

Another possibility for the lack of statistical significance is the diet of the juveniles during this age range. Recent morphological and mathematical investigations show that the brain growth in weight is complete at a mean age of seven years old (Cabana *et al*. 1993; Bogin 1999: 179). Coupled with dental development of the first permanent molars and brain maturation, the child becomes more capable of processing adult types of diet (Smith 1991; Bogin 1999: 179) and needs less nutrient requirements for maintenance and growth of the brain and body, which may lead to less variation between sites for this group. The growth trajectories (Figure 7.1-7.3) did reveal differences between sites in growth tempos for the 7 year old range, for instance, Wharram Percy shows slowed growth for all elements. Interestingly, the social life of a 7 year old child singled an important milestone known as the “end of human childhood” and is associated with an endocrine event called adrenarche (Bogin 1999: 179). This is the progressive increase in the secretion of adrenal androgen hormones which produce the mid-growth spurt in height and accelerated bone maturation. However, this ‘mid growth spurt’ appears to occur more in the Group 3 individuals of 3 to 5 years

old as there was no statistically significant changes in shape for the current Group of 6 to 8 years old. As discussed previously (section 7.1), archaeological children deviate from modern growth trajectories after 2 years old, so it is no surprise that the 'mid growth spurt' could occur at a slightly earlier or later age range for the archaeological children.

Figure 7.41: Post-Medieval children in the workhouse (BBC 2014).

In terms of activities, children began to mimic their parent's work, and performed small tasks around the home, farm, and/or workshops. Children's contribution was also seasonally, and peaking with intensive work around the harvest period as younger children would take food out to labourers in the fields. Apprenticeships in towns could start as early as 7 or 8 years old when children were placed with a farmer or craftsman by the Poor Law authorities (Heywood 2007: 127) (Figure 7.41).

7.6 Nine to Twelve Year Olds: Developmental and Allometric Trajectories

The allometric trajectory (Figure 7.22-7.24) shows that the 9 to 12 year old size and shape range overlaps with Group 4 (6-8 year olds). It is therefore expected that there will be no statistically significant change in the metaphyseal morphology as a result of changes in shape during the 9 to 12 year old age group. The pubertal growth spurt begins at the end of this age range (11 to 12 years old) and it is likely to reflect in the joint morphology of the proximal and distal metaphyses in the upper and lower limbs.

Null Hypothesis: There will be no statistically significant change in biomechanical forces and shape robusticity for the upper and lower limbs and increased positive scores on the PC axes will reflect curvature and width of the metaphases.

The final age group of 9-12 years old is the pre-puberty stage. Gosman and colleagues (2013) found this age range to show a second phase of accelerated growth. Children from all periods begin more specific work related activities such as farming, household chores, and even apprenticeships. Dietary shifts occur in this age Group as children begin consuming more meat and overall varied diet compared to the plant-based intake of the younger age Groups (Mays *et al.* 2002; Mays 2003).

The skeletal material for Group 5 is found in Table 7.15 and the morphological results in Table 7.16. The PCA and allometric trajectories are found in Figure 7.42-7.44.

Group 5: 9-12 Years Old Skeletal Materials				
Site	Period	Femur (n)	Tibia (n)	Humerus (n)
Great Chesterford	Anglo-Saxon	2	1	0
Raunds	Anglo-Saxon	2	3	1
Canterbury	Medieval	8	9	4
Wharram Percy	Medieval	3	2	3
Wolverhampton	Post-Medieval	0	1	1

Table: 7.15: Skeletal Sample Size for Group 5.

Group 5: ANOVA Results (p-values)			
Variables	Femur	Tibia	Humerus
Site	0.88	0.59	0.23
Period	0.75	0.53	**0.07**
Allometry	0.23	0.14	0.1

Table 7.16: Statistical Results for Development and Allometry of the Group 5 sample.

7.6.1 Femur

There is no statistical significance in shape for site or period for the Group 5 femora. The first PC axis (30%) for the Group 5 femora (Figure 7.42) reflects the width and curvature of the distal metaphyses. Positive values (Canterbury, Great Chesterford, Raunds, and Wharram Percy) reflect straighter distal metaphyses with a wider and more concave inter-metaphyseal angle. The negative values (Canterbury, Wharram Percy, and Great Chesterford) reflect rounder distal metaphyses with a narrower and more convex inter-metaphyseal angle. The second PC axes (15%) reflect the curvature of the proximal metaphyses. Positive values (Wharram Percy, Canterbury, Raunds, and Great Chesterford) represent straighter proximal metaphyses on the anterior plane. Negative values (Canterbury, Great Chesterford, and Wharram Percy) reflect an S-shaped curvature from the anterior proximal metaphyses into the diaphyses.

There is no statistical significance when regressing shape onto femoral size. The allometric trajectory follows similar patterning for all age groups with Canterbury as the largest size and most robust femora. Great Chesterford juveniles are the next largest size and shaped femora with Wharram Percy and Raunds falling within Great Chesterford range.

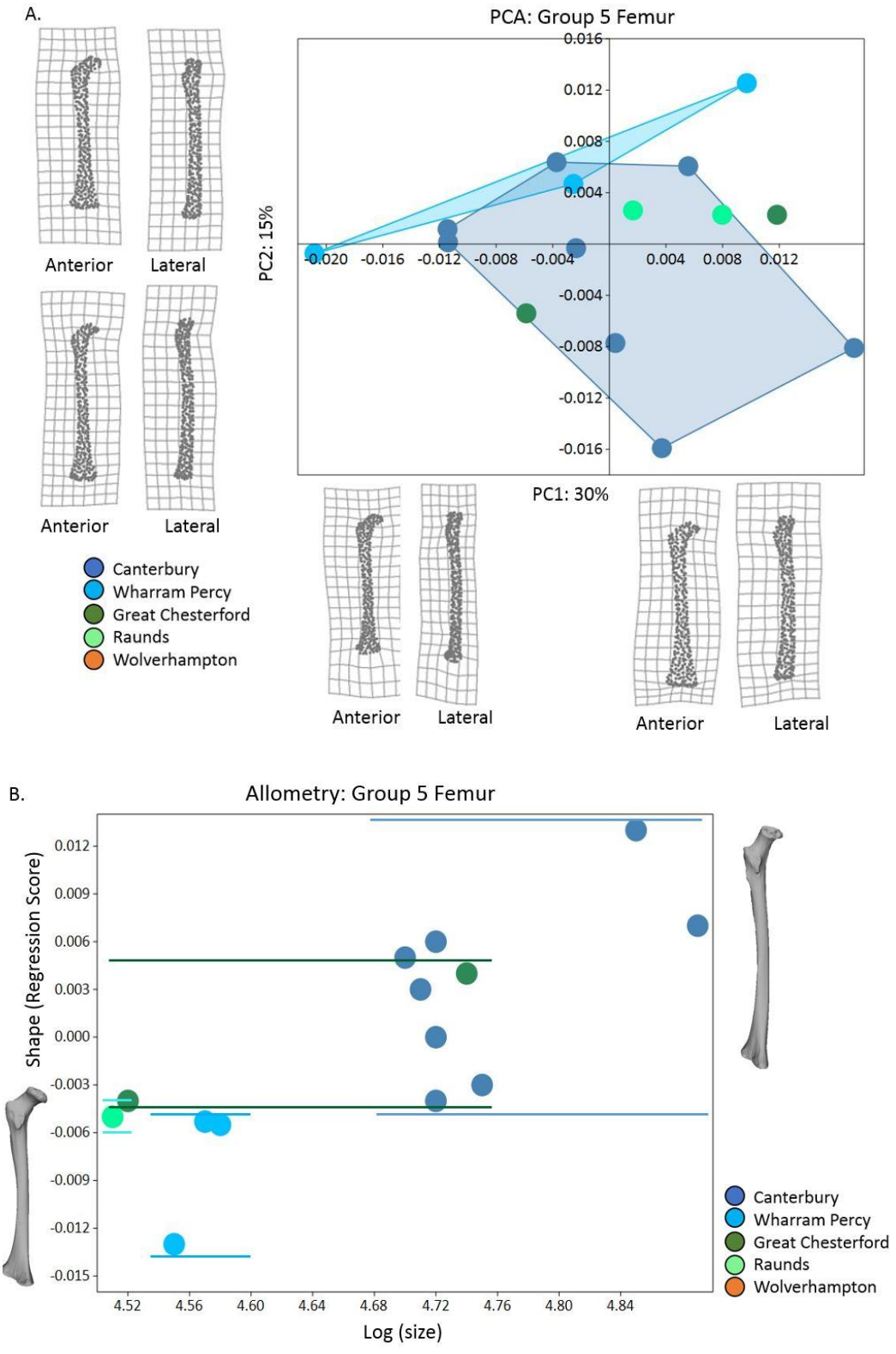

Figure 7.42: Principal Component Analysis (PCA: Left) and Allometric Plot (Right) for Group 5 (9 to 12 years old) Femur. A: Principal Component 1: anterior view. Negative values represent more development in the midshaft and femoral head. Principal Component 2: anterior view. Negative values show more development in the diaphyses. B: Allometric Plot: There is no linear regression for femoral size against shape as all femora are within the same shape range. Canterbury (Medieval) has the largest and more developed femora while Raunds (Anglo-Saxon), Wharram Percy (Medieval), and Great Chesterford (Anglo-Saxon) fall within Canterbury's shape range.

7.6.2 Tibia

Similarly to the femora, there is no statistical significance in shape for site or period in the tibiae for Group 5. The first PC axis (Figure 7.43: 33%) reflects the width and proximal medial curvature of the diaphyses. Positive values (Canterbury, Raunds, Wharram Percy, and Wolverhampton) reflect a wider and medial curvature in the proximal metaphyses and posterior diaphyses. Negative values (Canterbury, Raunds, Great Chesterford, and Wharram Percy) have a straighter diaphyses into the metaphyses. PC 2 (18%) reflects the curvature and torsion of the diaphyses. Positive values (Canterbury, Raunds, and Great Chesterford) have a more medial posterior curvature of the diaphyses while negative values (Canterbury, Raunds, Wharram Percy, and Wolverhampton) have a medial anterior curve of the diaphyses.

The allometric plot is not statistically significant for regressing tibiae size against shape. The allometric plot shows similar patterns to the femora as Great Chesterford and Canterbury have the largest size and shaped tibiae. Raunds, Wolverhampton, and Wharram Percy are in the smaller size and shaped range for the Group 5 tibiae.

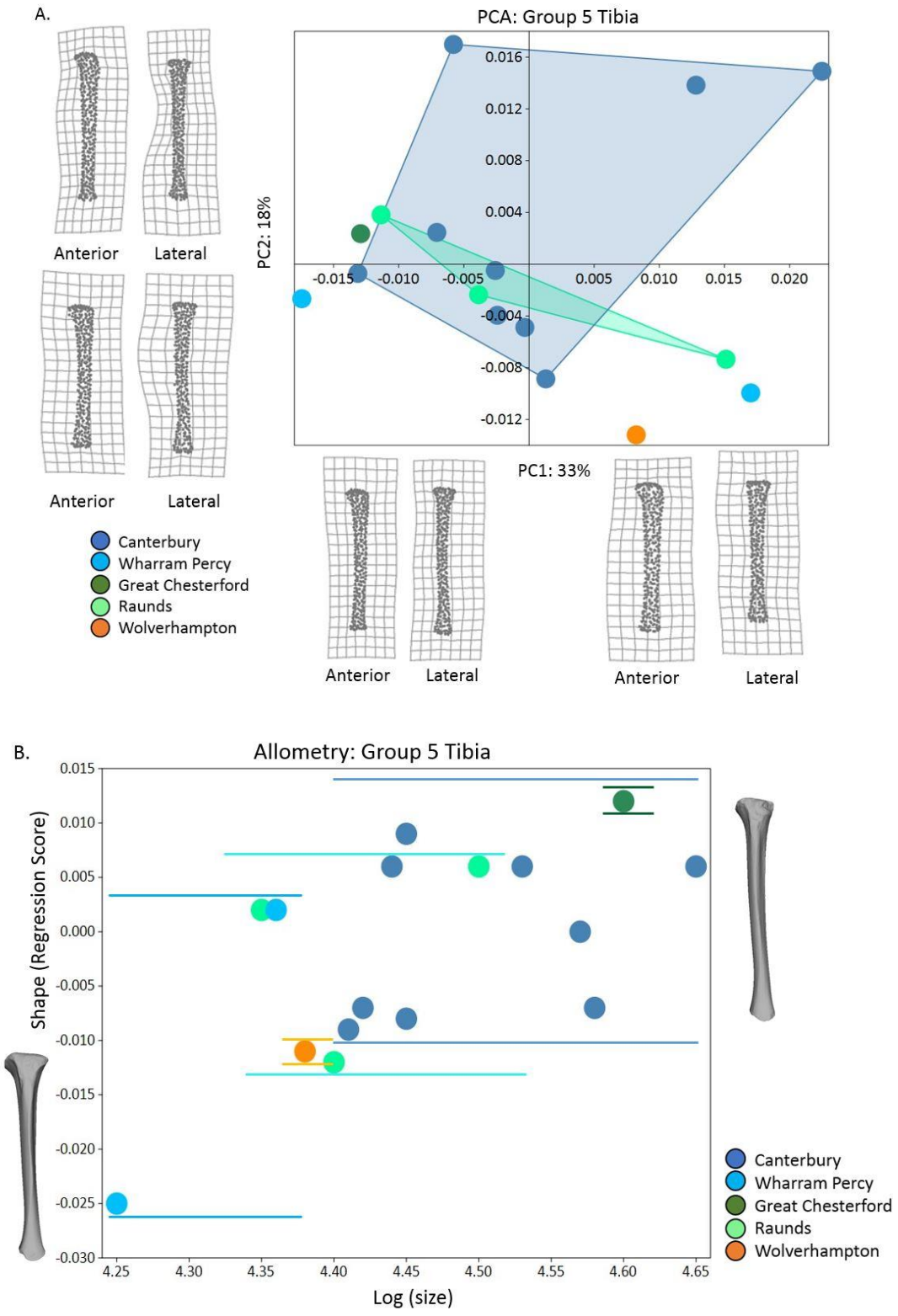

Figure 7.43: Principal Component Analysis (PCA: Left) and Allometric Plot (Right) of Group 5 (9 to 12years old) Tibiae. A: Principal Component 1: anterior view. Positive values reflect more development in the proximal and distal metaphyses. Principal Component 2: anterior view. Positive values show more development in the diaphyses. B: Allometric Plot: There is no linear regression for tibial size against shape as all sites are within the same shape range. Great Chesterford (Anglo-Saxon) and Canterbury (Medieval) are the largest size and shaped tibiae. Raunds (Anglo-Saxon), Wharram Percy (Medieval), and Wolverhampton (Post-Medieval) are in a smaller size and shaped range.

7.6.3 Humerus

The humeri are not statistically significant between shape, period, or site. The first PC axis (35%) for the humeri (Figure 7.44) reflects the curvature of the distal diaphyses into the metaphyses. Positive values (Wharram Percy and Canterbury) have more curvature form the posterior midshaft into the anterior metaphyses while negative values (Canterbury, Wharram Percy, Wolverhampton, and Raunds) have straighter humeri. PC2 (18%) reflects the proximal curvature of the metaphyses into the diaphyses. Positive values (Canterbury, Wharram Percy, and Wolverhampton) reflect more curvature from the posterior proximal metaphyses into the anterior diaphyses. Negative values (Canterbury, Wharram Percy, and Raunds) reflect more curvature from the proximal metaphyses into the diaphyses.

The allometric regression is not statistically significant when regressing humeri shape onto size. The allometric regression follows similar patterns to the lower limbs as Canterbury continues to have the largest size and shape variation with Raunds, Wolverhampton, and Wharram Percy falling within Canterbury's shape range.

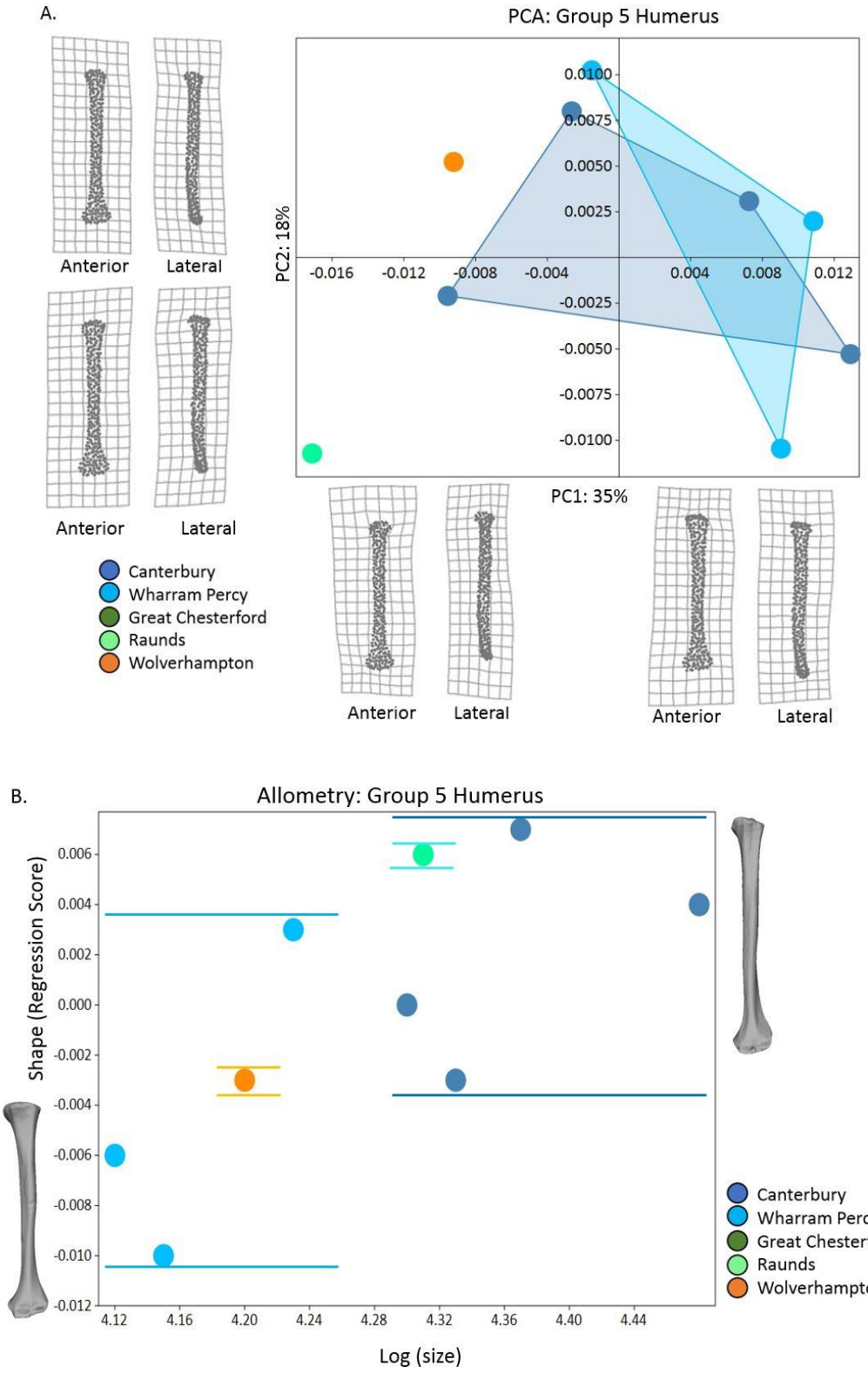

Figure 7.44: Principal Component Analysis (PCA: Left) and Allometric Plot (Right) of Group 5 (9 to 12 years old) Humeri. A: Principal Component 1: anterior view. Negative values reflect more development in the proximal metaphyses (humeral head). Principal Component 2: anterior view. Negative values show more development in the diaphyses. B: Allometric Plot: There is no linear regression for humeral size against shape as all sites are within shape range. Canterbury (Medieval) has the largest and more developed humeri while Raunds (Anglo-Saxon), Wharram Percy (Medieval), and Wolverhampton (Post-Medieval) fall within Canterbury's shape range.

7.6.4 Discussion

The age group of 9- 12 year olds, did not show any statistically significant patterning between site, period, or allometry. The hypothesis of statistical changes in the joint morphologies and allometric trajectories is accepted for all elements. The PCA found that the femora with positive scores had a straighter distal metaphyses and concave inter-metaphyseal angle, while negative scores had a rounder distal metaphyses and convex inter-metaphyseal angle. The increased positive scores for tibiae reflect a medial curve in the proximal metaphyses and posterior diaphysis, while negative values reflect a straighter curvature in the diaphyses. The higher positive scores represented the Canterbury and Great Chesterford sites which have larger sized elements, Wharram Percy, Raunds, and Wolverhampton had negative values which consisted of smaller sized elements. These morphological changes in the lower limbs are likely a result of the changes in the breadth of the hip and the knee joints which occurs as a result of increased locomotor loadings (Gosman *et al.* 2013). Increased values for humeri represent more curvature from the posterior midshaft to the anterior metaphyses while negative values had a straighter diaphyses. These changes are likely to represent the development of the triceps brachii (Aiello & Dean 1990: 309).

Similar to Gosman and colleagues (2013), there are changes in robusticity and development of the lower and upper limbs as the joints (proximal and distal metaphyses) and shaft (diaphysis) undergo different shape developments. These changes, although insignificant in statistically significant sense, are likely to reflect changes in activities.

It was common for children from the Anglo-Saxon to Post-Medieval period to leave home from 10 to 14 years of age (Heywood 2014: 116). More skilled training during the Anglo-Saxon and Medieval periods began at the earliest of age 10, such helping with cowherds or lambs. This transition into early teen years moved juveniles from childhood to youth, and gender differences among young farm workers became more pronounced. Daughters would continue to help their mothers around the house, garden, and dairy, while sons worked beside their fathers in the fields and stables (Heywood 2014: 123).

In the 19th century, children typically entered full time work when they got closer to 12 years old (Heywood 2014: 127). They began with light work such as making clothes or 'trimmings' for furniture, street selling, or making deliveries. Even without full time jobs they could help with household chores and domestic trade as many children learned to craft informally by watching their parents work. Girls in particular looked after younger children for their mothers (Heywood 2014:127).

During the eighteenth and early nineteenth centuries, the authorities in many regions were keen to provide a reliable source of employment for women and children living in poverty (Heywood 2014: 129). A common assumption is that industrialization did draw young children to the labour force, although it is not clear whether the peak in Britain was during the proto-industrial phase of the eighteenth and early ninetieth century or the alter factory based phase of the 1830s and 1840s (Heywood 2014). Most historians believe that industrialization brought a more intensive work regime for child workers in certain occupations (Heywood 2014: 129).

In the 1840s most working class children over the age of eight worked full time. Children from Wolverhampton in particular provided cheap labour and were often used to do the jobs that adults could not do, such as crawling underneath machines in factories or staying underground in mines to open and close the ventilation doors. It was normal for children to work up to 13 hours a day (Heywood 2014: 131).

Figure 7.45: Post-Medieval children in the coal mines (BBC 2014).

It is possible that the differences, although not statistically significant, in the mean shapes (Figure 7.45) in this age group are a result of timing of pubertal growth spurts and very early signs of sexual dimorphism. Although these pubertal growth spurts are believed to occur after this age group, they may be a reason for the visual (although not statistically significant) differences in the long bones. Analysis of juveniles in Group 4: 6-8 years old showed that individuals at some sites had accelerated growth while others were delayed. Therefore, it is likely that differences in diet and stress impacted the developmental timings of robust shape and delayed pubertal growth spurts. For instance, it is known that Wharram Percy juveniles had an extended growth period as growth ceased at 25 years old. Therefore, it is possible that the people of these archaeological sites are experiencing extended growth periods and the acceleration expected in this age range of 9 to 12 year olds, may be seen in the mid-teens to early 20's from the current studies sites.

7.7 Discussion: Ontogenetic Trajectories from Anglo-Saxon to Post-Medieval Infants to 12 Years Old

This discussion will summarize the application of GM to the archaeological material presented in this chapter. First, a look at the developmental trajectories for each element and the bone regions of where shape occurred from foetal to 12 years old will be presented. Second, the potential and extent of the developmental trajectory for each age group and the activities that children were likely to engage in will be examined. Lastly, the impact of developmental pathways, such as stress and diet from each archaeological site and their possible effects on long bone morphology will be assessed. Table 7.17 summarizes the hypotheses tested for each age group and the statistical significance of each element by morphological shape, site, period, and allometry.

Group Hypothesis and Statistical Results (p-values)		
Group 1 (Foetal) Null Hypothesis: There are no statistically significant changes in bone shape by site for the upper or lower limbs during the foetal stage.		
Femur	Accept: Allometry (0.13)	Reject: Site (0.03), Period (0.02)
Tibia	Accept: Site (0.12) and Allometry (0.37)	Reject: Period (0.04)
Humerus	Accept: Site (0.12), Period (0.3), Allometry (0.13)	Reject: None
Group 2 (Infant to 2 years old) Null Hypothesis :There will be no statistically significant changes in bone shape on the upper and lower limbs as increased positive scores on the PC axes will reflect the transition from crawling to walking in the lower limbs and crawling in the upper.		
Femur	Accept: None	Reject: Site (0.01), Period (0.01), and Allometry (0.01)
Tibia	Accept: Site (0.15) and Period (0.07)	Reject: Allometry (0.01)
Humerus	Accept: Period (0.30)	Reject: Site (0.02) and Allometry (0.01)
Group 3 (3 to 5 year olds) Null Hypothesis: There will be no statistically significant changes in shape for the upper and lower limbs and increased positive scores on the PC axes will reflect width and curvature of the metaphyses (hip and knee joints).		
Femur	Accept: Period (0.77)	Reject: Site(0.01) and Allometry (0.01)
Tibia	Accept: Site (0.16), Period (0.17), and Allometry (0.5)	Reject: None
Humerus	Accept: None	Reject: Site (0.01), Period (0.03), and Allometry 0.01)
Group 4: (6 to 8 year olds) Null Hypothesis: There will be no statistically significant changes in shape or allometric trajectories for the upper and lower limbs and increased positive scores on the PC axes will reflect width and curvature of the diaphyses.		
Femur	Accept: Site (0.17), Period (0.56), and Allometry (0.05)	Reject: None
Tibia	Accept: Site (0.12), Period (0.24), and Allometry (0.08)	Reject: None
Humerus	Accept: Site (0.51), Period (0.550, and Allometry (0.57)	Reject: None
Group 5 (9 to 12 year olds) Null Hypothesis: There will be no statistically significant change in biomechanical forces and shape robusticity for the upper and lower limbs and increased positive scores on the PC axes will reflect curvature and width of the metaphases.		
Femur	Accept: Site (0.88), Period (0.75), and Allometry (0.23)	Reject: None
Tibia	Accept: Site (0.59), Period (0.53), and Allometry (0.14)	Reject: None
Humerus	Accept: Site (0.23), Period (0.07), and Allometry (0.10)	Reject: None

Table 7.17: All Statistical Results for all Element, Age Group, Site, Period, and Allometry.

7.7.1 Morphological and Developmental Patterns of the Femora, Tibiae, and Humeri

This chapter demonstrated unique patterns of shape development for each element from foetal to 12 years old. The developmental pattern for all long bones can be characterized as a trajectory from a cylindrical morphological shape along the entire diaphyses to a highly variable asymmetric morphology in later adolescence (Gosman *et al.* 2013: 781). All three bone element studies in this thesis have unique developmental trajectories with a range of shape variation along the diaphyses and metaphyses. Mechanisms for this dynamic developmental process includes the reshaping of the proximal and distal metaphyses and diaphyses. The age groups that are statistically significant in shape between site and period are from Group 1 (foetal), Group 2 (infant to 2 years old), and Group 3 (3 to 5 years old). During these age groups, the size and shape of the femora, tibiae, and humeri undergo the most statistically significant change between site and/or period. The timing of these changes is suggested to have occurred as a result of the acquisition of different forms of movement from intrauterine pressures, quadrupedal to bipedal walking, and refined gait patterns. These changes in locomotion that occur from foetal to 5 years old are associated with changes in load type and magnitude on the lower limb (Ruff 2003; Ryan & Krovitz 2006; Gosman & Ketcham 2009; Gosman *et al*. 2013: 783). Gosman *et al.* (2013: 783) found a second period of notable change for juvenile's age 9-14 years as a reflection of the pre-pubertal growth spurt. This age group was not statistically significant in the current study between shape, site, period or allometry, and instead represented a possible conserved period of growth before the pre-pubertal growth spurt.

The most notable change in the limbs was in the proximal and distal metaphyses of the femora, proximal metaphyses and midshaft of the tibiae, and proximal and distal metaphyses of the humeri (Figure 7.4, 7.10, 7.16). The distal femora showed asymmetric shapes in later childhood compared to a more cylindrical shape during early life (Figure 7.4). This shape change in the femora reflects bone expansion in the anterior-posterior axis which is likely to relate to developmental kinematics and bending forces of the hip and knee during walking and running (Pauwels 1980). The midshaft of the femora diaphyses maintains a more circular shape, with few asymmetrical sections along the shaft (Ruff *et al*. 1994; Cowgill *et al.* 2010; Gosman *et al*. 2013: 781).

The tibiae diaphyses developed from a more uniformly rounded shape along the whole diaphyses to a highly asymmetric shape in later adolescence (Figure 7.10). This pattern was more clearly seen in the proximal half of the tibia. This growth trajectory reflects the progressive development of the characteristic triangular cross sectional shape of the tibia with more growth in the anterior-posterior plane (Gosman *et al.* 2013). The distal tibiae reflected a more conserved cylindrical shape throughout the growth period under study.

Lastly, the humeri began cylindrical like the lower limbs and developed into an asymmetrical shape in the proximal metaphyses and flatter shape in the medio-lateral plane of the distal metaphyses (Figure 7.16). This growth trajectory reflects the progressive development of the flattened oval region in the distal diaphyses as more growth occurs in the medio-lateral plane. The proximal humeri maintains a rounded shape with some asymmetrical sections along the diaphyses.

The current study demonstrated that the midshaft of the femora and humeri remain the most consistent throughout development compared to the highly variable proximal and distal regions of the femora and humeri diaphyses and metaphyses (Figure 7.4 and Figure 7.16). The tibia displayed a different pattern, as more shape variation occurred in the proximal diaphyses and metaphyses with less change in the distal tibiae during development (Figure 7.10). According to Frost (1997), the developmental bone strength and mass begin to increase when bone strains exceed a threshold range. The midshaft of the long bones may represent 'high threshold' regions which requires relatively more strain to trigger modelling responses. It is possible that the midshaft strains remain low in the current samples. This would allow the hip, knee, shoulder, and elbow joint morphologies to dominate during the growth and developmental trajectories, with little change evident in the mechanically adequate midshaft.

7.7.2 Developmental Trajectories from Foetal to 12 Years Old

In addition to the unique regions of development that have occurred for all three bones from foetal to 12 years old, this thesis found variations in the extent of developmental trajectories and levels of activities that can occur for each age group. As only the first three age groups are statistically significant for shape between site and period, it is possible that the age groups or stages in this thesis are not equivalent in terms of the potential of shape that can be achieved at each stage. For instance, Group 1 foetal long bones are the starting point of the trajectory and are the most cylindrical and gracile shaped bones. This Chapter has demonstrated that there is statistical significance in the amount of variability that can occur in this age group. The variation and potential of shape for Group 1 is likely to be affected by the intrauterine constraints on the lower limbs, as the larger foetal individuals undergo hyperflexion which results in an increased robusticity and shape for the Wolverhampton and Wharram Percy femora and Canterbury tibiae.

The statistical results for Group 2 (infant to 2 years old) revealed the most distinctive morphological differences between sites and periods as juveniles from infant to 2 years old engaged in a variety of movements such as crawling to walking which leads to a highly varied age range for movement and potential shape development. GM highlighted the morphological transition from quadrupedal

to bipedal loadings in the femora, tibiae, and humeri. By incorporating the developmental patterns all three elements, it could be suggested that Canterbury juveniles were walking, Wharram Percy, Great Chesterford, and Raunds were in transition of crawling to standing, and Wolverhampton juveniles were stationary and near crawling.

The last age group that was statistically significant for shape between site and period was the Group 3, 3 to 5 year olds. This age range reflected refined gait patterns as individuals had the potential to achieve the 'archetype' adult walking gait which was seen at Canterbury. It is likely that the variation of shapes that occurred in this group between site and period are a reflection of the different stages of early to refined walkers. Another possibility is the types of activities that occur during this age group. As discussed in Chapter 6 and earlier in this Chapter, this age group is were play occurs. Play comes in the form of many types of activities. For instance, urban juveniles from Post-Medieval Wolverhampton lived in a densely populated community and are likely to have been more limited to stationary play as they were confined by their demographic settings (Heywood 2014: 127). Rural children such as Wharram Percy, Raunds, and Great Chesterford are more likely to have played outside, from climbing trees, running in fields, or chasing animals (Hanawalt 1977: 64). There is more space and freedom in types of activities for rural juveniles compared to juveniles in urban and densely populated settings. Canterbury juveniles however, are unique for an urban site as the demographic of this population was ecclesiastic and sedentary compared to the Industrial Wolverhampton population. It is possible that Canterbury juveniles didn't have as much freedom as the rural communities of Wharram Percy, Great Chesterford, and Raunds but more range of activity compared to the overpopulated Wolverhampton community.

GM did not produce any statistical significance of long bone shape between site and/or period for 6 to 12 year olds. It is possible that the remaining age groups reflect a lower potential for statistically significant shape as there is less variation in movement and activity that is found after the adult walking pattern is achieved at 5 years old. This is not to say that the last two age groups are not changing in morphology but perhaps they are more region specific, such as femoral head curvature, while the younger individuals from foetal to 5 years old are significant for whole bone morphology. In terms of the social life of the child, play is likely to have continued from 6 to 12 years old, however, juveniles also begin work related tasks and chores during this age range. It is possible that the differences in these activities such as working around the home, fields, or workshops are subtle in terms of bone shape and GM was not able to determine any statistical significance for site or period. Thus, activity in children from 6 to 12 is similar according to long bone shape between all sites and time periods while play encompasses a more varied range of activities that is seen in the long bone morphology.

7.7.3 Developmental Pathways and Archaeological Interpretations of the Juvenile Long Bones

In addition to specific regions of where development occurs in the long bones and the potential shape variation for age groups, the trajectory can also change during development. The application of GM to the archaeological material in this Chapter revealed that plasticity and the direction of the developmental trajectory varies between sites. The morphological trends from the PCA plots of the Great Chesterford femora (Figures 7.25, 7.29, 7.34, 7.38, 7.42) reflect shorter and wider proximal metaphyses with a shorter proximal neck angle. The diaphyses reflect more curvature in the distal midshaft and have a convex inter-metaphyseal angle. The tibiae reflect a narrower and more slender midshaft curvature in the diaphyses and lateral angle at the proximal metaphyses. The humeri displays a robust morphology with a wider diaphyses and shorter proximal metaphyses and a robust medial distal metaphyses (epicondyle). These morphological patterns suggest that juveniles from Great Chesterford had a moderate level of activity (De Groote *et al.* 2010). This site was an agricultural community so it would be expected that juveniles would work in fields and attend to animal husbandry. For a site with a large proportion of juveniles, there is a relatively low frequency of stress markers in the juvenile remains. The recorded cases of cribra orbitalia and hypoplasia are likely to be a result of malnutrition (Inskip 2008) and rather a fast-acting infection as there is a low frequency of lesions in the collection.

In contrast to the juveniles from Great Chesterford, Raunds has a high prevalence of stress. Out of 361 individuals recorded, 85 out of 286 with orbits had skeletal evidence of cribra orbitalia (3-29.7%), 46 out of 187 with at least one canine had linear enamel hypoplasia (24.6%) and 109 out of 316 with at least one tibia present had tibial periostitis (34.5%). Several correlations between stress markers and grave elaborations produced statistically significant results (Boddington 1996) as nearly half of the adolescents at Raunds displayed signs of stress (cribra orbitalia, enamel hypoplasia, and tibial periostitis) (Boddington 1996). Similarly to Great Chesterford, the morphological patterns of the femora (Figures 7.25, 7.29, 7.34, 7.38, 7.42) reflect a long and robust proximal metaphyses with a steep curvature into the midshaft, and a concave inter-metaphyseal angle. The tibiae have a slender and straighter diaphyses compared to Great Chesterford and flatter proximal metaphyses. Lastly, the humeri reflect a straighter and more slender diaphyses with a narrower proximal metaphyses compared to Great Chesterford. The patterning found at Raunds represents moderate activity consistent with juveniles played and worked at small subsistence agricultural tasks (Lewis 2002: 212). Interestingly, despite the higher prevalence of stress seen at Raunds compared to Great Chesterford, juveniles at Raunds had larger and more robust shaped

elements for all age groups (Figures 7.4, 7.10, 7.16). Wood *et al.* (1992) have suggested that it may be the advantaged groups in society that are more likely to survive an episode of stress long enough for a skeletal lesion to become visible. It is possible that the most stressed individuals died relatively quickly at Great Chesterford when a stressful assault occurred, thereby not surviving long enough for the skeletal manifestations like those at Raunds to be seen. Hadyock *et al.* (2013: 609), investigated the stable-isotope ratios from Raunds which confirmed archaeological and documentary evidence that suggests weaning and a change of status took place between 2 and 3 years old (Crawford 1999: 70-73; Haydock *et al.* 2013: 609). The developmental, allometric, and growth trajectories for all ages and elements at Raunds fell in the middle of the other sites trajectories while Great Chesterford was in the more gracile shape range until the end of the trajectory. Thus, the juveniles at Raunds experienced more pathological stress but had larger sized and more variation in shape than Great Chesterford. This may suggest that the Raunds juveniles were better adapted to stress, including dietary change during the weaning process.

The Medieval Canterbury juveniles have a similar growth trajectory to the Modern Denver growth study (Figure 7.1-7.3) and the GM results show that this site has the most robust shapes for all elements in all age groups (Figures 7.4, 7.10, 7.16). The morphological trends (Figures 7.25, 7.29, 7.34, 7.38, 7.42) show that the femora have a wide and short proximal metaphyses and higher curvature into the diaphyses which forms a concave inter-metaphyseal angle. The tibiae reflects a robust blade-like morphology in the diaphyses with a flatter proximal metaphyses. Lastly, the humeri are slender with asymmetrical robusticity in the proximal metaphyses. These morphological patterns are likely to reflect moderate to higher levels of activity (De Groote *et al.* 2010). Hicks and Hicks (2001) found both Canterbury juveniles and adults have a tall mean stature which suggests an overall high standard of health and growth during childhood, at least for those who survived to adulthood. There are little signs of recorded pathological stress compared to other southern Medieval English sites (Dawson 2014). Thus, as stated by Wood *et al.* (1992), those being buried at Canterbury may be dying before the bone formation associated with stress had time to manifest (Hicks & Hicks 2001) and disrupt the growth and developmental trajectories for the juveniles at this site.

In stark contrast, Wharram Percy is known for the high prevalence of stress among the juvenile population (Mays 2007). The morphological trends (Figures 7.4, 7.10, 7.16) found at Wharram Percy reflect shorter, robust proximal metaphyses with a steep femoral head curve. The curvature of diaphyseal midshaft displays a concave inter-metaphyseal angle. The tibiae display a robust midshaft curvature and slight angle into the medial proximal metaphyses. The humeri reflect slender diaphyses and proximal metaphyses with robust distal metaphyses in the medial plane. These trends are likely to reflect a moderate activity group (De Groote *et al.* 2010; De Groote 2011).

Wharram Percy was a lower status settlement in a very hierarchical society and the juveniles at Wharram Percy might have been more vulnerable to disease and nutritional stress. Documentary sources indicate that dietary shortages were common in peasant communities in the Medieval period (Gies 1990, 96-8). The current study found that juveniles from Wharram Percy fell in the small to mid-shaped trajectories for all ages and elements. Although there are robust regions of the long bones reflecting moderate activity levels, it is likely that the juvenile's experienced stunted growth in size and therefore, more gracile shaped long bones compared to the other sites, specifically at the age of 7 when the developmental trajectories plateaued for all elements. These findings of smaller sized and less robust shapes coincide with previous findings by Mays (1995) on the formation of Harris lines in the juveniles of Wharram Percy. Mays (1995) found that the long bones were deficient in length and cortical thickness, which would then affect the developmental trajectory and morphology as seen in this study. The juveniles from Wharram Percy also experienced high rates of active cribra orbitalia and porotic hyperostosis in infants and small children (73.7% of all juveniles at Wharram Percy); the latter was active at time of death (Mays 2007). This could reflect differences in the natural environment between the skeletal samples as the soils at Wharram Percy are thin and prone to nutritional exhaustion (Hayfield 1988: 25-6). The harsher climate at Wharram Percy may have led to higher rates of crop failures and food shortages relative to lowland southern England sites. The growth stunting found at Wharram Percy reflects a population that likely experienced chronic stress (Ortner & Mays 1998) which was reflected in the development of size and shape. Unlike Great Chesterford, which was able to recover from stressful events and demonstrated accelerated growth and development, Wharram Percy had a steady trajectory of lower rates of size and shape for all ages and elements (Ortner & Mays 1998).

As discussed in Chapter 6, isotopic studies at Wharram Percy found that breast-feeding ceased between one and two years old, which is consistent with Medieval documentary sources (Fildes 1986). Mays (2007) plotted isotopic results in the older juveniles and adults and found that during middle childhood, ages 4 -8 years old, had smaller proportions of marine foods and/or meat than those of later childhood and adulthood (Mays 2003; Mays *et al.* 2002). This is also the age range that Wharram Percy plateaued in shape and size for the femora and tibiae (Figure 7.4-7.9) and may suggest that the lack of a high protein and meat based diet would affect the development and robusticity of the lower limbs.

Post-Medieval Wolverhampton juveniles represented the smallest size and most gracile shaped elements for all ages (Figures 7.4, 7.10, 7.16). The morphological trends for the Wolverhampton femora (Figures 7.25, 7.29, 7.34, 7.38, 7.42) reflect long and narrow proximal metaphyses with a straight curvature into the diaphyses and a distal curvature of the midshaft. The tibiae are more robust and rounded with an angled proximal metaphyses from the medial to lateral plane. The humeri display a robust proximal metaphyses and an S-shaped curvature in the diaphyses along the biceps and triceps. The Wolverhampton juveniles lived in an urban city and adolescents likely spent more time in workshops rather than fields. This would explain for the low to moderate morphology of the lower limbs and robust regions of the humeri. Additionally, of all the sites examined in this study Wolverhampton has the highest level of infant mortality, with 40% of all juveniles dying from foetal to 2 years old. The evidence of cribra orbitalia was also high which could be a result of the poor diet that infants received (Roberts & Cox 2003; 307). As discussed in Chapter 6, Wolverhampton juveniles suffered from poor health and harsh working conditions which is likely to have influenced the small size and shape trajectories found in this thesis.

The developmental trajectories presented in this chapter are likely to have been influenced by the intensity and duration of environmental stress for the juveniles in the study sites. The growth stunting that occurred at Wolverhampton, Raunds, Great Chesterford, and Wharram Percy, is often greater in later childhood than immediately following the post-weaning period (Mays 2007). It appears that both longitudinal bone growth and morphological shape are affected by the conclusion of breast-feeding at one to two years old. This marks the start of a general pattern of deficient growth (Mays 2007) at Wharram Percy, Raunds, Wolverhampton, and Great Chesterford, while Canterbury continued to grow and develop at a faster rate. However, despite the disruptions in the developmental growth trajectories, the post-weaning phase of 6 to 12 years old was not statistically significant for long bone shape between site and/or period. Therefore, it is possible that all individuals from all sites were affected by the loss of the nutritional benefits from breast milk and all became more susceptible to environmental stresses as all juveniles and long bone morphologies are within the same shape range after 6 years old.

7.7.4 Concluding Remarks

Growth of increasing bone size is a continuous process until the cessation of growth. Development, or changes in shape, are not a linear progression of continuously larger shapes but rather fluctuating rhythms of shape. As seen in this Chapter, the trajectory of shapes vary depending on the potential of shape development that can occur at each age group. Differences in activity or movement are other variables that are likely to impact long bone morphology. From intrauterine constraints seen in the foetal age group, crawling to walking from infant to 2 years old, and refined

gait patterns from 3 to 5 years old. Trajectories can also alter course depending on the environment surrounding the individual during the growth process. Interestingly, similar sized bones for the same age range do not necessarily represent similar morphological shapes during growth and development, an aspect of juvenile growth that is often overlooked, to which this thesis has made an important contribution.

8. Conclusion

This thesis has sought to apply a methodological framework (GM), to archaeological juveniles, and to explore how biological processes affect bone shape during ontogeny. Using Anglo-Saxon to Post-Medieval foetal to 12 year olds, this research integrated GM with traditional bioarchaeological methodologies of growth and development to determine if long bone plasticity was influenced by archaeological sites (sample variation), and/or time period.

For this thesis, both a methodological and bioarchaeological component was essential for analysing and visualising ontogenetic trajectories from Anglo-Saxon to Post-Medieval juvenile long bones. By venturing to answer '*What makes up bone shape and what do shape trajectories tell us?*' the following methodological and bioarchaeological questions were put forward:

1. How effectively can GM be used on small cylindrically shaped bones?
2. Do the visible differences in morphological shape change by scanning technique?
3. Is plasticity influenced by site and/or time period?

In order to answer these questions a series of methodological validation studies were produced (Chapter 4 and 5) and bioarchaeologoical applications were examined (Chapter 7). This conclusion will discuss the findings of the methodological and bioarchaeolgoical contributions this thesis made, followed by an assessment of its limitations and future prospects for the GM study of juvenile development.

8.1 Methodological Contribution: Analysing and Visualising Juvenile Long Bones

The methodological aim of this thesis was to develop a reproducible methodology that captures the torsion, curvature, and whole bone growth and development of the long bones. To test the methodological applicability of 3D GM on juvenile long bones, the first validation study examined traditional linear measurements, 3D GM (landmark and semi-landmark), and auto3dgm analyses on juvenile femora (Chapter 4). This validation study sought to determine if GM could be used on juvenile long bones and asked: '*Is there an effect on size and shape?'* and *'what is the effect on femur morphology in response to mechanical loading?'* By answering these questions through three different methodological analyses, it was found that auto3dgm was the best-suited method for analysing the shape of juvenile long bones. Auto3dgm was the only method that could remove user subjectivity and bias as to what points on the bone are morphologically important. This is a key difference between the linear ratio and traditional GM analyses which were difficult to define and

locate suitable measurement points that could be found on all specimens in the sample and capture the entire shape of the bone. Additionally, auto3dgm removes measurement error which is found when manually collecting and/or digitizing measurement points. The last essential difference that was found with this study was that auto3dgm aligns specimen by surfaces such as curvature and torsion, rather than points along the bone surface which was seen in the linear and traditional GM analyses. This validation study demonstrated that difficult to capture shapes, such as juvenile long bones, can be used in GM analyses to explore developmental variation and allometric trajectories.

The second validation study in this thesis was immediately posed to test '*do the visible differences in morphological shape change by scanning technique?'* This validation study revealed that by scanning five femora (one representing each age group) through photogrammetry, structured-light-scanning, and laser scanning, revealed differences in the logistics of each method and mesh quality. Structured-light-scanning was found to be the most reasonable method in terms of the logistics of travelling, affordability, and user demands. Although the features of the younger juveniles (foetal to 5 month olds) were not captured as well as with laser scanning, auto3dgm found no statistical significance is shape between scanning techniques. The findings of this chapter demonstrated that through the rigorous testing of different methodologies, any morphological variation found in Chapter 7, was a result of bone shape rather than artificial shape from scanning method.

The validation studies in thesis determined that GM can work on juvenile long bones and scanning methods do not impact shape. This thesis has shown that insights on developmental morphology can be acquired without expensive equipment such as CT scans. Auto3dgm can quantify shape and illustrate where shape changes occur and is not affected by scanning methods. Thus, the analyses used in this thesis are not exclusive and can be applied to multiple morphological studies and varied data sets. The data collection of different scanning methods and analysis of auto3dgm allows for more varied research potential. As digitising collections are becoming more common through open access repositories, such as morphosource or ADS, these digital databases expand research potential for morphological studies. For instance, working with digital collections that derive from remote locations that researchers may not have been able to reach initially, or instances where there is limited access to the physical specimens. The methods in this thesis are reproducible and can be applied to further bioarchaeological or archaeological studies.

8.2 Bioarchaeological Contribution: Developmental Trajectories of Anglo-Saxon to Post-Medieval Juveniles

The second aim of this thesis was to apply the power of GM analysis with human juvenile long bones by examining whether plasticity is influenced by archaeological sites and or time period (Chapter 7). By using the multivariate concept of shape and teasing apart growth, development, and allometry of the long bones, this thesis found: 1) regions of where most shape occurred for each element from foetal to 12 years old, 2) the extent and direction of the developmental trajectory for each age group, and 3) morphological patterns by site and period.

The first morphological pattern that GM revealed for the long bones was were robusticity and shape change occurred for each element from foetal to 12 years old. The medio-lateral proximal femur, anterio-posterior tibiae, and distal medial-lateral humeri expansions are likely the result of the effects of hip breadth and locomotor loads for the lower limbs and shoulder breadth effects for the humeral morphology. The significance of this study is the quantitative aspect of whole bone shape along the diaphyses and metaphsyes and the complexity of these changes. Interestingly, the results in this thesis and Gosman *et al.* (2013) found only a small variation in diaphyses shape during the foetal to 12 years old age range as it is possible that there is not enough mechanical stimulus to result in significant morphological changes in this region. The whole diaphyseal perspective supports the established concepts that developmental heterogeneity in bone morphology is a reflection of dynamically changing patterns of growth (Gosman *et al.* 2013), spatially specific bone-muscle interactions (Carpenter and Carter 2008), complicated locomotor biomechanical forces (Lieberman et al 2004), and anatomically differentiated growth rates (Bass et al, 2002).

The second finding in this thesis was that each age group was not equivalent for the amount of variation that could occur in the long bone morphologies. Therefore, developmental trajectories had different levels of shape potential for each age group. The first three age groups of foetal to 5 years old indicate more potential shape variation and development as the juveniles experience intrauterine constraints (Group 1),the transition from limited mobility to upright walking (Group 2), and refined adult walking (Group 3). After the archetype adult shape was reached at 5 years old, the remaining age groups of 6 to 12 years old had limited potential for statistically significant shapes within their groups. This is a unique finding suggesting that growth or long bone size is fairly consistent in the potential size that can be achieved at different age groups until the cessation of growth. Shape however, is constrained to the level of activity that can be achieved for different ages. This is not to suggest that shape reaches an ‘end shape’, but rather more regional differences

in shape are likely to occur in older juveniles and adults while statistically significant differences in whole bone shape occurs in younger juveniles.

The third finding in this thesis was that in addition to developmental trajectories having different levels of potential for different age groups, they could also change directions as a result of developmental pathways. The incorporation of bioarchaeological recordings of stress and diet, and historical documentation of activities, provided context for the interpretation of fluctuation in long bone shapes. Raunds and Wharram Percy juveniles displayed a moderate to high level of stress throughout the age ranges in this thesis. Their developmental trajectories were consistently in the middle of the shape variation for sites and elements. Canterbury and Wolverhampton trajectories were fairly consistent with Canterbury juveniles as the largest and most robust for all age groups and elements. Wolverhampton however, reflected the smallest and most gracile shapes for all ages and experienced the harshest living conditions with extreme dietary stress, infectious diseases, and poor sanitation which are likely to have impacted the developmental trajectory for this site. Although the juveniles in the current study did not make it to adulthood, it is possible that the developmental pathways that affect juvenile shape are a combination of sample variation and the reflection of overall exposures and intensities to environmental stress. Weaning is a problematic period for all archaeological children, which is no different to the current study's findings. All sties went into an immediate conserved period of growth and development while stress manifestations such as cribra orbitalia, linear enamel hypoplasia, and periostitis affected juveniles from almost all of the sites from infant to 7 years old. Although individuals with stress lesions were not included in the current study sample, these individuals with stress represent the overall population health for these skeletal sites and contexts. Thus, this thesis suggests that developmental pathways reflect the duration and intensity of environmental stress which further constrains the potential juvenile long bone shape.

This thesis found that by marrying qualitative and quantitative data, developmental patterns were identified for all three long bone elements from foetal to 12 years old. Through the graphical outputs of complex vectors of shape change, this thesis found where regions of robust or gracile development occurred for the long bones by site and period. The graphical visualisations allowed for long bone comparisons to be made between sites and inferred possible activities levels from moderate to highly active juveniles. This thesis also identified that shape is not a linear progression of increasingly larger shapes but rather fluctuations in the changes of shape. The trajectories of shape found that each age group had differences in the potential and extent of shape that could occur for each group. In addition, the direction of the shape trajectory could change as a result of developmental pathways such as nutritional or environmental stress that occurred during growth.

8.3 Moving Forward: Limitations and Future Juvenile Studies

It must be acknowledged that certain limitations were encountered during this research, however, these issues provide interesting future research topics. The first limitation to this research was the skeletal material and sample parameters. The unevenness of sample sizes in some of the age groups dictates caution in the interpretation of the data set. The parameters of the age groups themselves may have skewed the results in this thesis and the extent of interpretations that could be made. Thus, the age classes have potential variation due to age within the groups that is not controlled for in the PCA. For instance, the second age group which had the most variability in shape (infant to 2 years old) has a large range of biomechanical and nutritional factors that occur between an individual aged at the lower end of this age range compared to the individuals in the upper range of this group. These age distributions may vary within the group and between sites which could compromise the comparisons. For instance, a 2 year old weaned walker from Canterbury compared to a 6 month old Raunds infant not yet crawling and feeding on breast milk may have statistically significant long bone morphologies. As the first three age groups (foetal to 5 years old) were statistically significant for shape between site and period, it would be useful to focus on whole bone shape by each age from foetal through 5 years old, rather than splitting juveniles into age groups. This thesis demonstrated that after 5 years old there was no statistical significance for shape between site or period and it is possible that the older juveniles would benefit from analysis of region-specific shape change rather than whole bone shape change. For instance, FEA (Finite Element Analysis) would be an interesting approach to analysing the 6 to 12 year old longs bones in order to determine if there is statistical significance between age and loading patterns between sites and periods. Another possibility for the auto3dgm analyses would be to use multiple types of elements for each permutation. This would be a useful study to assess how elements, such as the femur and tibiae, relate to one another during growth and development. For instance, the relationship of the proximal femur curvature and the proximal distal metaphyses in the older individuals for 6 to 12 years old.

In addition to the limitations in the sample parameters, another includes the issue of pooling sex together in this thesis. Pooling of sexes only allows for associations to be developed as these data sets cannot establish sex-related tasks and difference in the rate and tempo of bone development and growth. The gross morphology of the long bones are likely to be influenced to some degree by the inherent developmental variability of the sample, including slight sexual dimorphism (Frelatt & Mitteroecker 2011). Nonetheless, limiting this study to pre-puberty does restrict some of the sexual dimorphism and activities that may affect bone morphology as this is expected to occur in the teen

years. In addition, the growth trajectories in Chapter 7 (Figures 7.1-7.3) demonstrated that male and female femora, tibiae, and humeri were plotted together by age and did not reflect any significant changes in size, age, or sex.

Another drawback to this research is the use of cross-sectional versus longitudinal growth data. As discussed throughout this research, reference populations are used as a proxy of 'normal growth' which derives from modern healthy children (e.g. Denver Growth Study) over long periods of time. These growth trajectories are known as 'longitudinal' data as the same study population is sampled at differing ages during the growth trajectory. Archaeological samples however, are only taken once, at time of death, which are referred to as 'cross-sectional' data (Hoppa & FitzGerald 1999: 7-9). One of the main challenges of comparing longitudinal versus cross-sectional growth trajectories is that the latter does not allow observations of individual variability in the rate or velocity of growth or the timing of the adolescent growth spurt. Researchers have attempted to remedy this issue by constructing skeletal growth profiles as a percentage of mean adult long bone length or mean adult stature for individual populations (Lovejoy *et al*. 1990; Wall 1991; Hoppa 1992; Goode *et al*. 1993). By using the mean adult long bone length it can take into account the variation in limb proportions and differences in the regression equations that are used to reconstruct mean stature (Hoppa & Saunders 1994).

Unfortunately for the current study, there is no geometric morphometric data for the adults from the sampling populations or a living modern sample. Therefore, there is no workaround for creating 'shape' comparisons between the adults or even living children. This will present a limitation in the analysis and interpretation of this work as a true 'growth or developmental trajectory' can never truly be determined as the children are measured at only one particular time; the time of their death. However, this would be a promsing avenue for future resreach regarding GM growth and developmental trajectoreis.

Another limitation with this thesis was perhaps the skeletal collections were not varied enough in terms of site, region, and period. Expanding the study parameters past Anglo-Saxon to Post-Medieval sites in the UK to include juveniles from hunter-gatherer communities and other geographical regions would provide more variables to study shape. For instance, differences in subsistence patterns, mobility, and regional variation could further explore patterns of long bone plasticity from foetal to 12 years old.

The final limitation was not directly analysing the relationship between pathological stress and shape. This thesis has demonstrated that nutritional stress may impact the developmental trajectories of the juvenile long bones. By incorporating nutritionally and paleopathologically stressed individuals versus their 'non-stressed' cohorts from the same site could be used in an

attempt to group pathologies by shape. This would indicate which environmental stresses causes the most severe disruption to development and at what ages the developmental trajectory changes direction. Weaning is another developmental pathway that could be analysed in more detail. This thesis identified a post-weaning phase which is likely to have altered the developmental trajectory for all juveniles in the study sample. Thus, regressing isotopic data of ð13C and ð15N values against the shape regression score of each element (computed through the Generalized Procrustes Analysis) could indicate correlations between bone morphology and dietary changes.

Despite these limitations, this thesis has demonstrated that shape is a complex concept in both theory and practice. This thesis has demonstrated that GM offers a unique approach to juvenile remains when combined with bioarchaeological methods of recording stress and diet, and incorporating historical context to the study samples. The variation of development that occurs from foetal to 12 years old is substantial and not necessarily a linear trajectory. GM was able to capture these rapid changes in morphology and the subtle rhythms of development that are often overlooked with traditional growth studies. Long bone morphology is a combination of closely knit variables where the duration and intensity of environmental impacts continuously shape and reshape developmental pathways.

Appendix A: Chapter 4 Validation Study Error Test

A.1 Linear Measurements Intra-Observer Error Test

To gauge the reliability of the linear measurements used in the Chapter 4 validation study, all 18 femora were measured two times over two consecutive days by the same investigator using digital callipers. An interclass correlation coefficient (ICC) was used to quantify the measurement error through PAST (Shrout & Fleiss 1979; Hammer et al. 2001: 77). The second model was used as it represents the same rate for all measurements and all measurements. As all confidence intervals and the Interclass Correlations are close to 1, the measurement reliability is considered good (Hammer et al. 2001: 77).

Measurement	Interclass Correlation	95% Confidence Interval
FL	0.99	0.9782, 0.9999
CCD	0.9997	0.9993,0.9999
BW	0.99	0.998,0.999
LC	0.9998	0.9995,0.9999
MC	0.978	0.9435,0.9917
IN	0.9996	0.9999,0.9999
AP	0.995	0.9987,0.9998
ML	0.9997	0.9992,0.9999
FHL	0.99	0.9998,0.999
FHW	0.99	0.9782, 0.9999

Table A.1: Measurement Error of Great Chesterford Femora.

A.2 GM Landmark Intra-Observer Error Test

In order to test the repeatability of the 3D landmarks, a small subset of femora were selected from each age group (Group 1:3; Group 2: 3; Group 3:1; Group 4:1; Group 5: 2) and analysed three times. A Procrustes ANOVA comparing variation in landmark location (Klingenberg & McIntyre 1998) was used to determine whether there was significance based on landmark placement. It is expected that floating landmarks, those found on the middle of a surface or the individual curves, would vary most. Although there was the same statistical significance for each test ($p>0.01$), it can be seen that there is some variation in the PCA. The first two groups (infant to 2 years old) and the last Group (9-12 year olds) have slight differences in their specimen plots. Group 3 (3-5 years old) and Group 4 (6-8 years old) however, vary along the second principal component axis. Although the statistical significance remained the same for all three analyses, the interpretations are skewed as two groups varied along the second principal component axis.

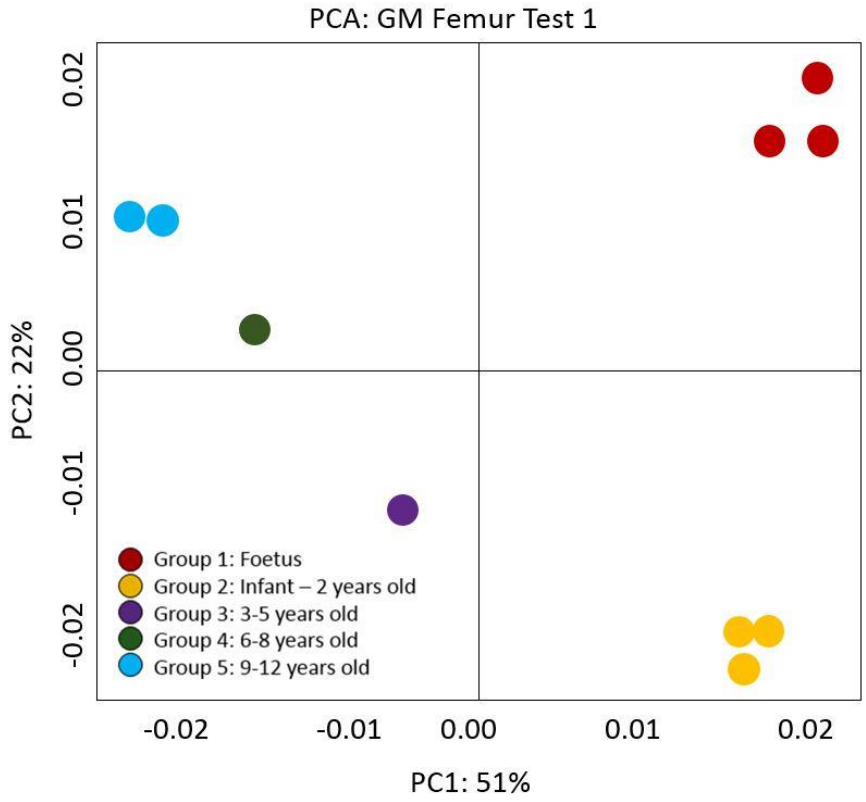

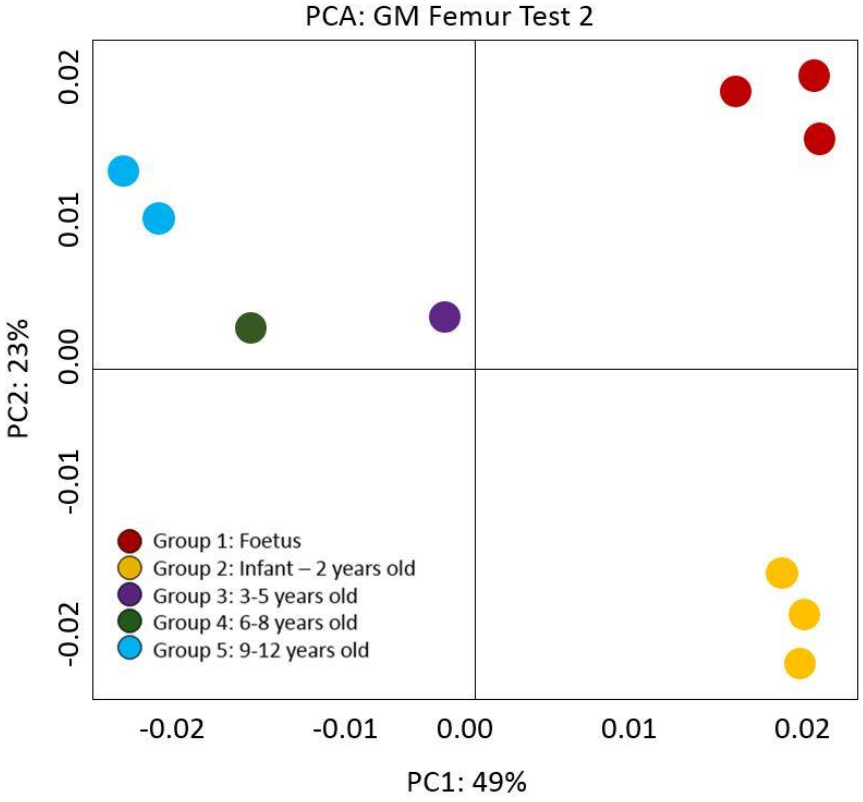
PCA: GM Femur Test 2
PC2: 23%
PC1: 49%
0.02
0.01
0.00
-0.01
-0.02
-0.02
-0.01
0.00
0.01
0.02
Group 1: Foetus
Group 2: Infant – 2 years old
Group 3: 3-5 years old
Group 4: 6-8 years old
Group 5: 9-12 years old

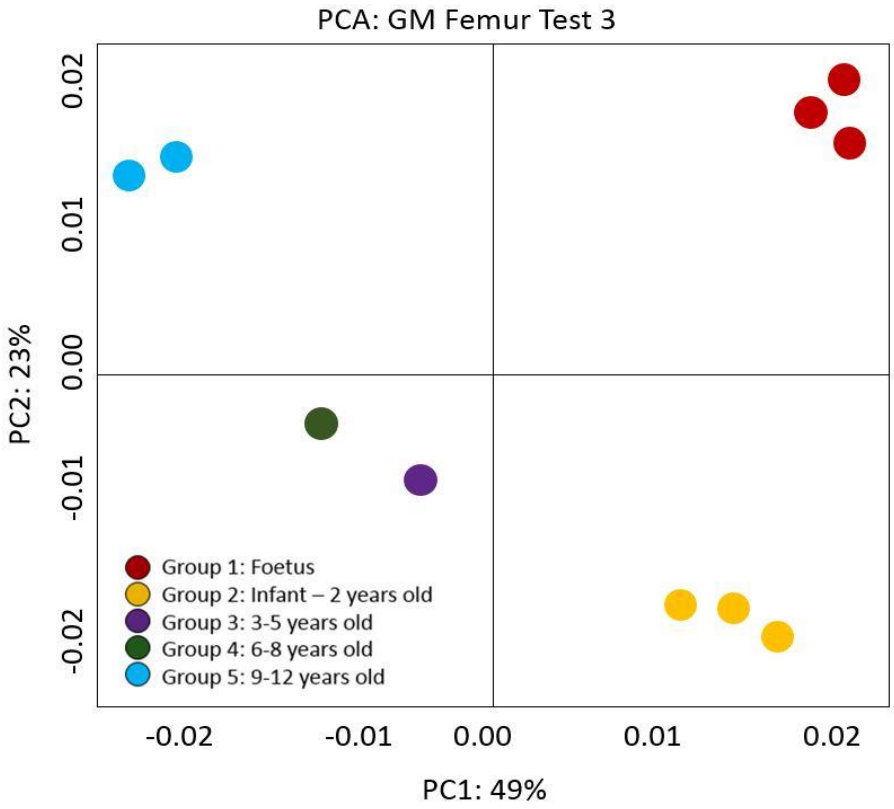
PCA: GM Femur Test 3
PC2: 23%
PC1: 49%
0.02
0.01
0.00
-0.01
-0.02
-0.02
-0.01
0.00
0.01
0.02
Group 1: Foetus
Group 2: Infant – 2 years old
Group 3: 3-5 years old
Group 4: 6-8 years old
Group 5: 9-12 years old

A.3 Auto3dGM Inter-Observer Error Test

In order to asses the automated error the same skeletal materials (Group 1:3; Group 2: 3; Group 3:1; Group 4:1; Group 5: 2) and Principal Component Analysis from A.2 was run three times. It is seen that there are no differences in the plotting of specimens for each PCA analysis when using auto3dgm.

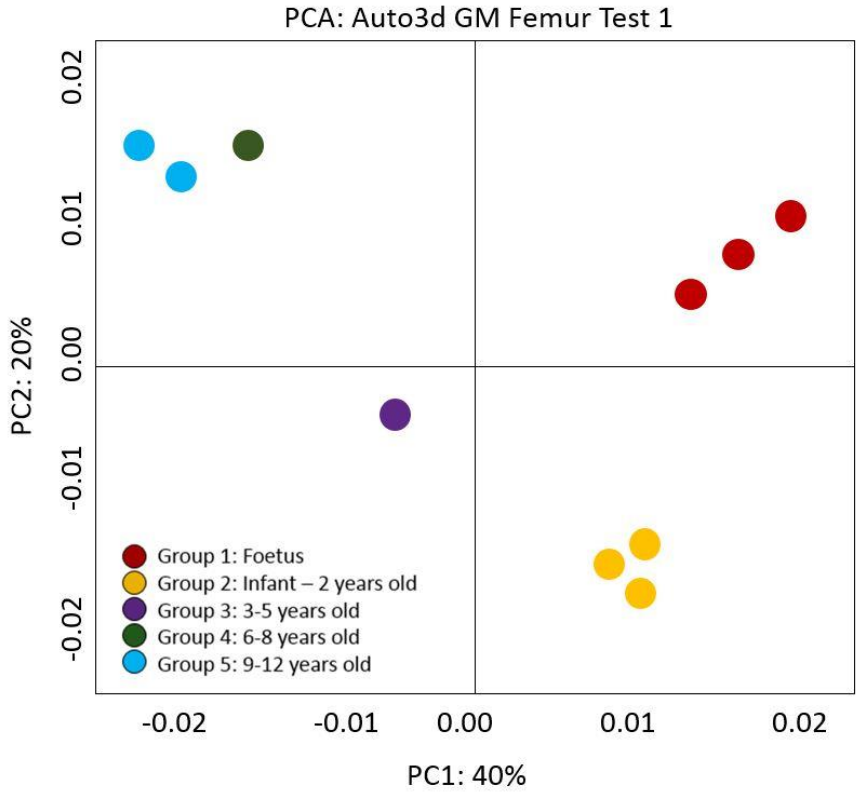

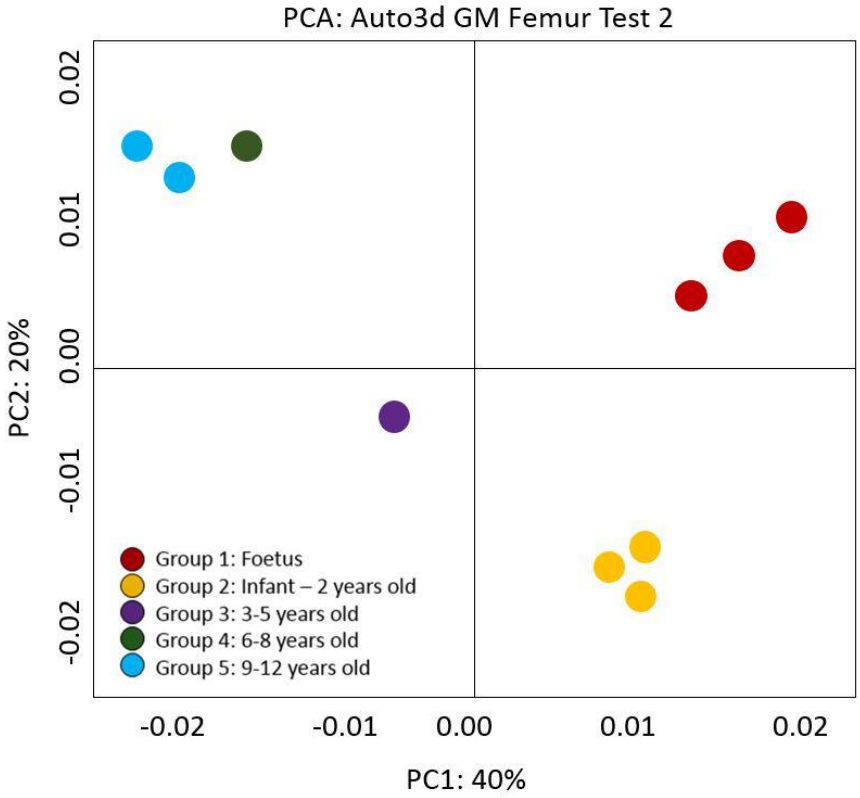
PCA: Auto3d GM Femur Test 2
PC2: 20%
0.02
0.01
0.00
-0.01
-0.02
Group 1: Foetus
Group 2: Infant – 2 years old
Group 3: 3-5 years old
Group 4: 6-8 years old
Group 5: 9-12 years old
-0.02
-0.01
0.00
0.01
0.02
PC1: 40%

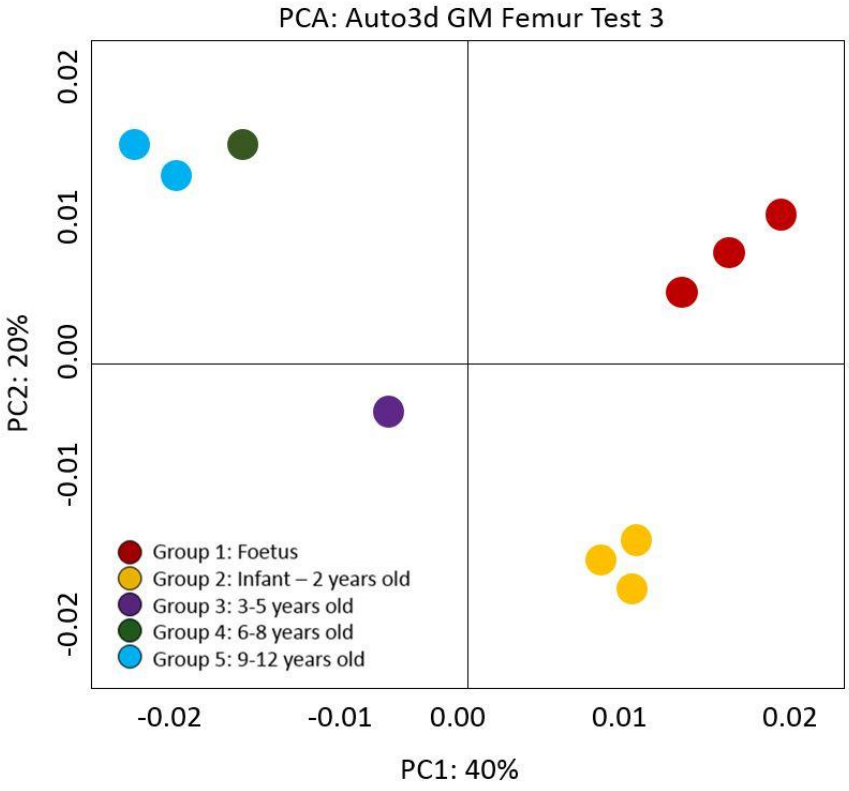
PCA: Auto3d GM Femur Test 3
PC2: 20%
0.02
0.01
0.00
-0.01
-0.02
Group 1: Foetus
Group 2: Infant – 2 years old
Group 3: 3-5 years old
Group 4: 6-8 years old
Group 5: 9-12 years old
-0.02
-0.01
0.00
0.01
0.02
PC1: 40%

Appendix B: Great Chesterford

The following table provides the frequencies for skeletal element by age group for the Great Chesterford juveniles. The results of the PCA ANOVA for element by group and the allometric regression of shape onto size are also found in the table. A detailed description of the PCA and allometric trajectories are discussed below by element. The femora is found in Chapter 4 as the GM validation study.

Great Chesterford Juveniles			
Variables	Femur (n=18)	Tibia (n=9)	Humerus (n=12)
Group 1: Foetus	3	1	1
Group 2: Infant to 2 years old	11	5	9
Group 3: 3 to 5 years old	1	0	2
Group 4: 6 to 8 years old	1	2	0
Group 5: 9 to 12 years old	2	1	0
PCA ANOVA (p-value)	0.01	0.02	0.03
Allometry (p-value)	0.02	0.01	0.01

B.1 Great Chesterford Tibia

The first principal component (40%) represents changes in the curvature of the diaphyses. Positive values (Groups 1 and 2) of the lateral view show changes in the midshaft curvature while negative values (Groups 4 and 5) represent changes of curvature in the proximal and distal midshaft. The anterior view shows positive values have a straighter diaphysis while negative values curve in the lateral plane. The second principal component (30%) represents the width of the proximal metaphyses and midshaft curvature. Positive values (Group1, 2, 5) in the lateral view show more curvature in the midshaft of the diaphysis with a wider flare in the distal metaphyses. The negative values (Group 2, 4) represent a straighter distal diaphysis. The anterior view shows positive values represent a narrower proximal diaphysis into a wider metaphyses while negative values show a wider diaphysis to metaphyses. The second principal component axis shows changes in the remodelling processes as the clustering is not by increasing age but fluctuating shape.

The allometric plot found a statistically significant difference when regressing shape onto size. Group 2 (infant to 2 years old) shows a large range of size and shape variation, with the individual from Group 1 (foetal) falling within range. There is a large increase in size for Group 4 (6-8 years old) and another increase to Group 5 (9-12 years old).

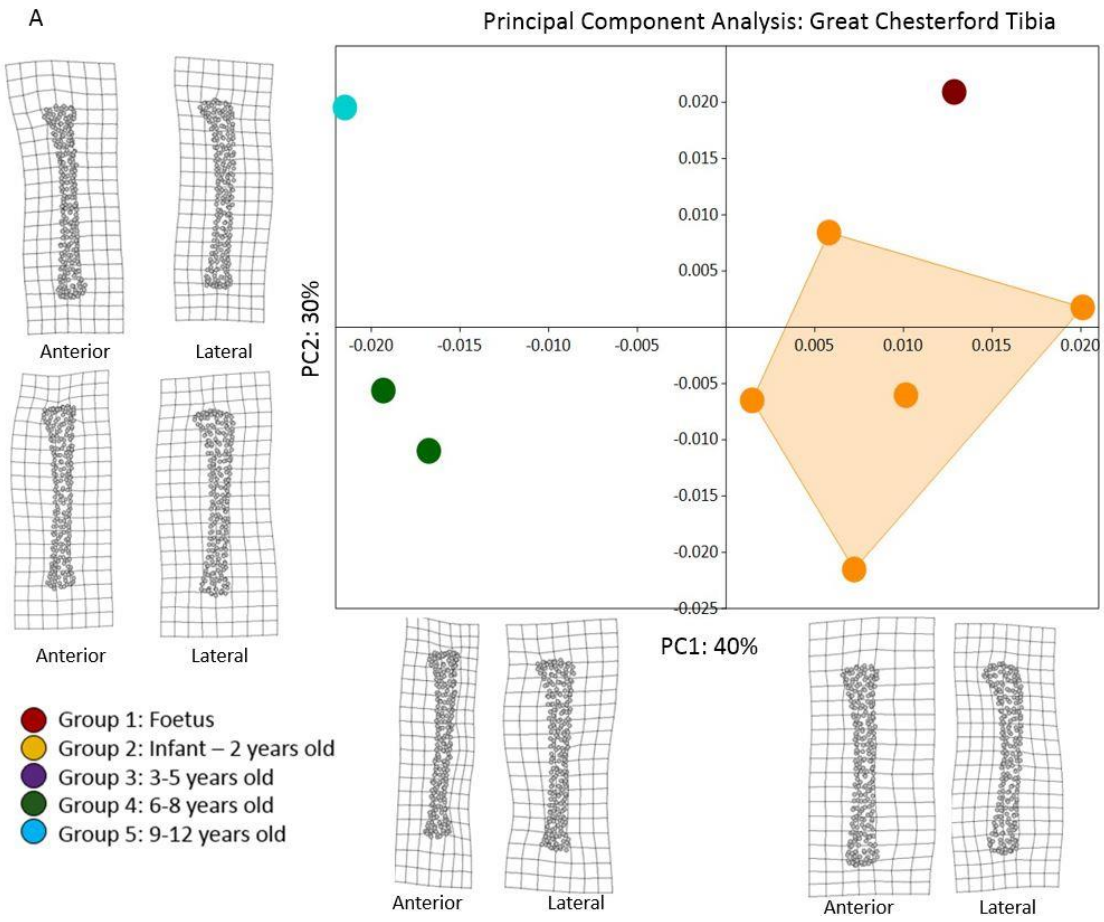
A
Principal Component Analysis: Great Chesterford Tibia
PC2: 30%
PC1: 40%
0.020
0.015
0.010
0.005
-0.005
-0.010
-0.015
-0.020
-0.025
-0.020
-0.015
-0.010
-0.005
0.005
0.010
0.015
0.020
Anterior
Lateral
Anterior
Lateral
Anterior
Lateral
Anterior
Lateral
Group 1: Foetus
Group 2: Infant – 2 years old
Group 3: 3-5 years old
Group 4: 6-8 years old
Group 5: 9-12 years old

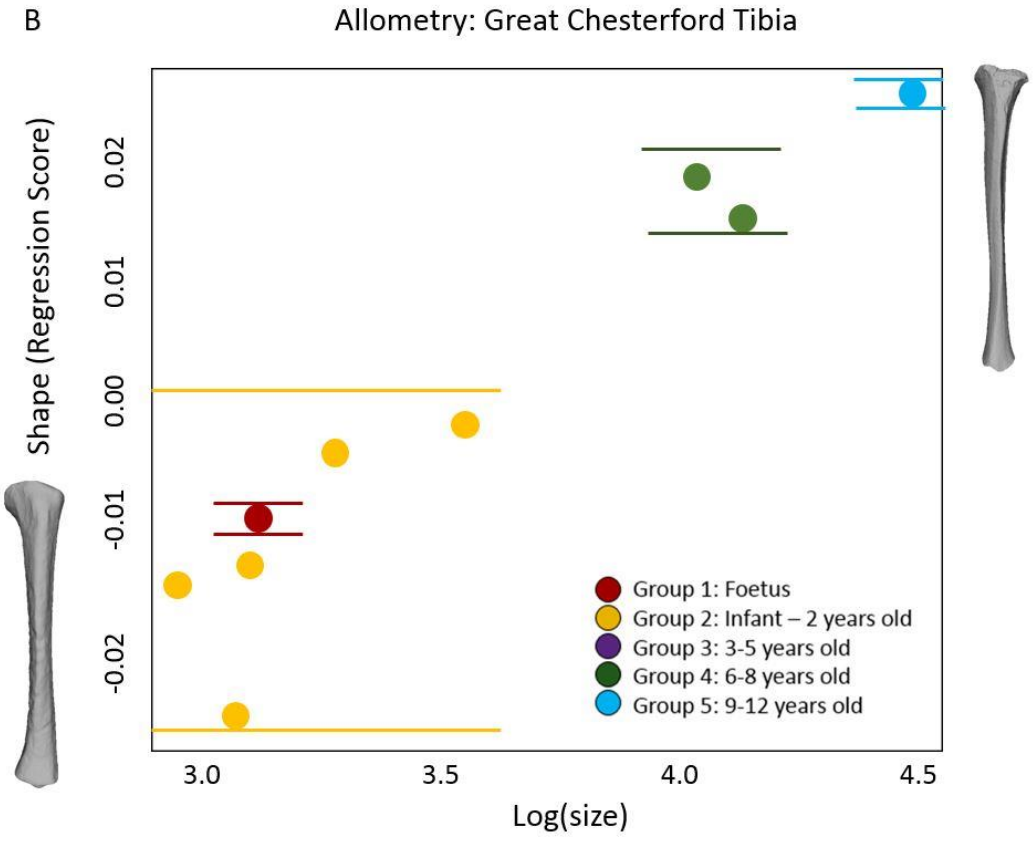
B
Allometry: Great Chesterford Tibia
Shape (Regression Score)
0.02
0.01
0.00
-0.01
-0.02
3.0
3.5
4.0
4.5
Log(size)
Group 1: Foetus
Group 2: Infant – 2 years old
Group 3: 3-5 years old
Group 4: 6-8 years old
Group 5: 9-12 years old

B.2 Great Chesterford Humerus

The first principal component axis (38%) represents the width of the proximal metaphyses and curvature of the diaphysis. Positive values (Group 2) from the lateral view show more curvature in the anterior distal diaphysis and width of the proximal metaphyses. Negative values (Group 1 and 3) have narrower metaphyses and a straighter diaphysis. The second principal component axis (28%) represents the width of the distal metaphyses. The lateral view shows an s-shaped curve in the positive values (Groups 2 and 3) and a straighter curvature in the negative values (Group 1 and 2). The anterior view shows negative values (Group 1 and 2) have a wider distal diaphysis and metaphyses compared to a narrower positive values (Group 2 and 3).

The allometric plot of the humeri shows a large variation of size and shape for Group 2 with an overlap of Group 1. The Group 3, 3-5 year old age Groups shows a clear distinction of increasing shape and size. The overall allometry of the humeri shows a linear regression of increasing size and increasing shape of the humeri.

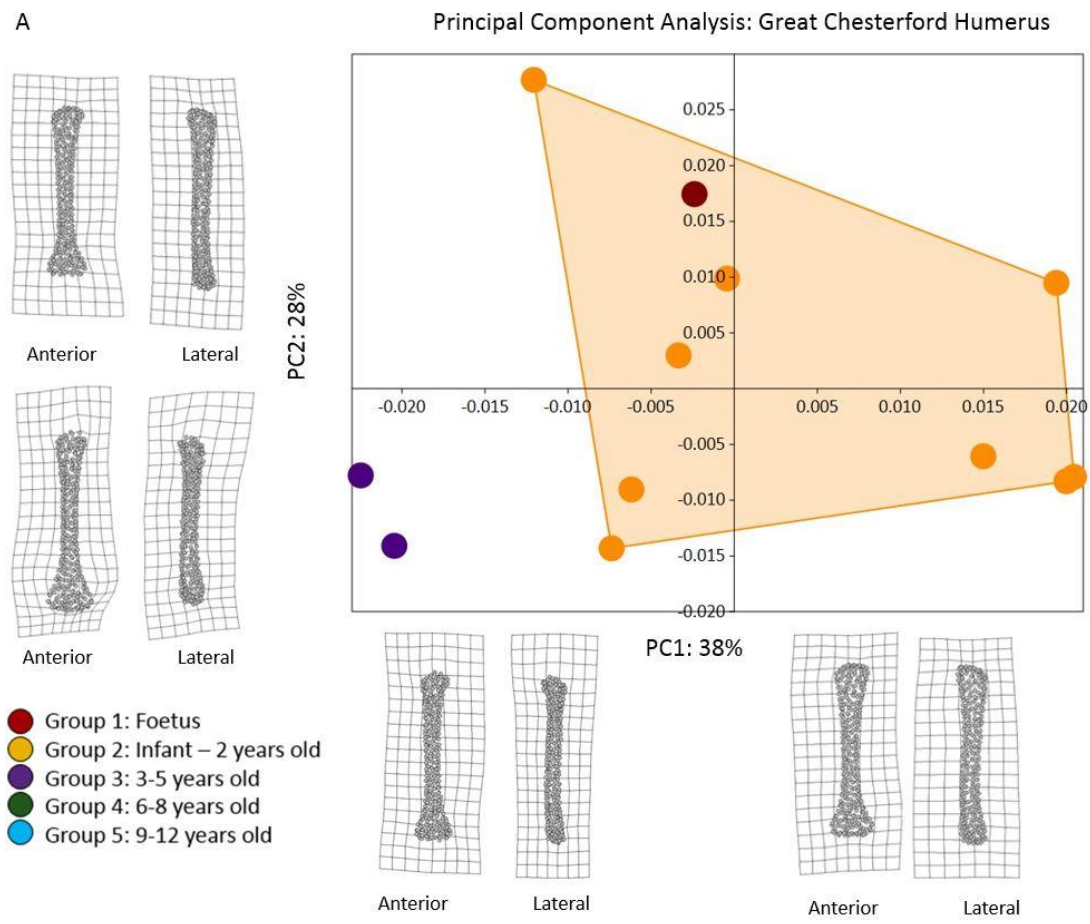
A
Principal Component Analysis: Great Chesterford Humerus
Anterior
Lateral
Anterior
Lateral
PC2: 28%
0.025
0.020
0.015
0.010
0.005
-0.020
-0.015
-0.010
-0.005
0.005
0.010
0.015
0.020
-0.005
-0.010
-0.015
-0.020
PC1: 38%
Anterior
Lateral
Anterior
Lateral
Group 1: Foetus
Group 2: Infant – 2 years old
Group 3: 3-5 years old
Group 4: 6-8 years old
Group 5: 9-12 years old

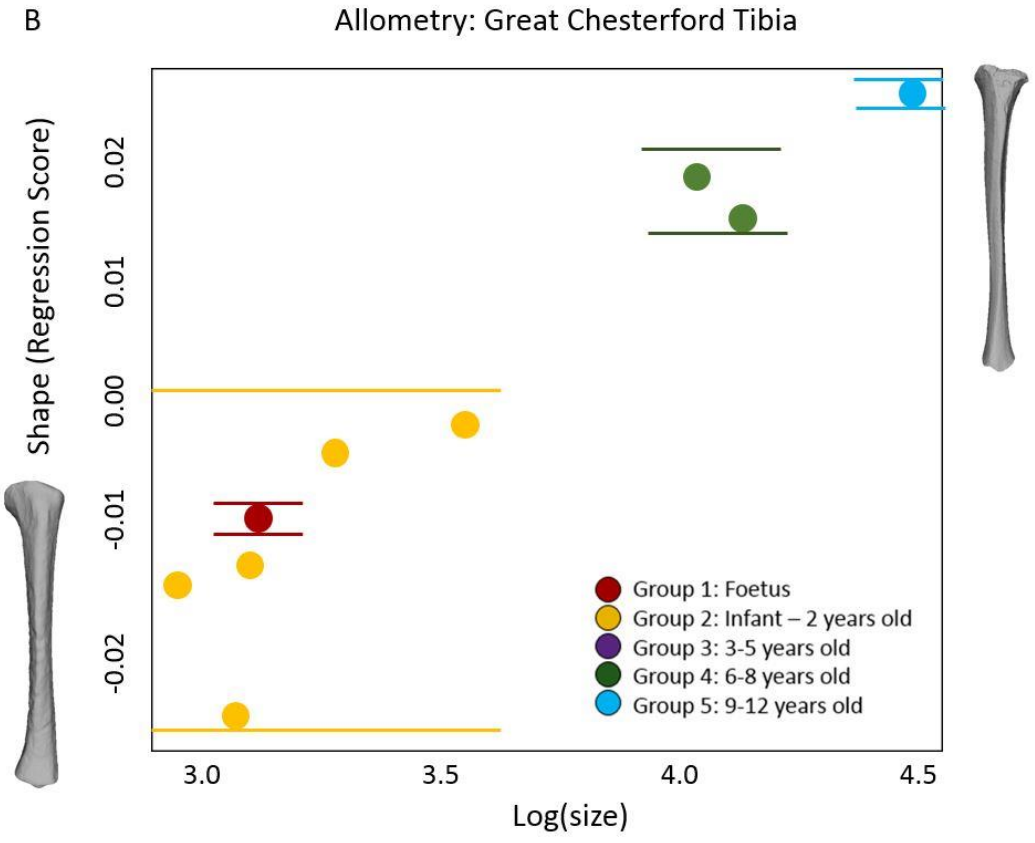
B
Allometry: Great Chesterford Tibia
Shape (Regression Score)
0.02
0.01
0.00
-0.01
-0.02
3.0
3.5
4.0
4.5
Log(size)
Group 1: Foetus
Group 2: Infant – 2 years old
Group 3: 3-5 years old
Group 4: 6-8 years old
Group 5: 9-12 years old

Appendix C: Raunds

The following table provides the frequencies for skeletal element by age group for the Raunds juveniles. The results of the PCA ANOVA for element by group and the allometric regression of shape onto size are also found in the table. A detailed description of the PCA and allometric trajectories are discussed below by element.

Raunds Juveniles			
Variables	Femur (n=17)	Tibia (n=12)	Humerus (n=11)
Group 1: Foetus	1	0	0
Group 2: Infant to 2 years old	5	4	1
Group 3: 3 to 5 years old	4	1	4
Group 4: 6 to 8 years old	4	4	5
Group 5: 9 to 12 years old	3	3	1
PCA ANOVA (p-value)	0.01	0.07	0.03
Allometry (p-value)	0.01	0.02	0.01

C.1 Raunds Femur

The first principal component axis (49%) represents the width of the metaphyses and curvature of diaphysis. The lateral view shows the positive values (Group 1 and 2) have wider metaphyses and a straighter angle into the anterior diaphysis. Negative values (3-5) have a narrower and longer proximal and distal metaphyses and deeper curvature into the diaphysis. The second principal component axis (15%) represents the angle of curvature in the metaphyses. Negative values (Group 2-4) of the lateral view show a broader and flatter proximal metaphyses with a deeper curve in the midpoint of the diaphysis. Positive values have a rounder proximal metaphyses with curvature occurring in the distal diaphyses. Negative values of the anterior view reflect more concave angling in the proximal metaphyses and convex shape in the distal metaphyses while the positive values reflect the opposite curvature.

The allometric plot shows a large variation of shape in the second Group (infant to 2 years old) for both size and shape. There is a large increase in shape and size variation for Group 3 (3 to 5 years old) and a slower tempo of overlapping size and shape for Group 4 (6 to 8 year olds) and 5 (9 to 12 year olds).

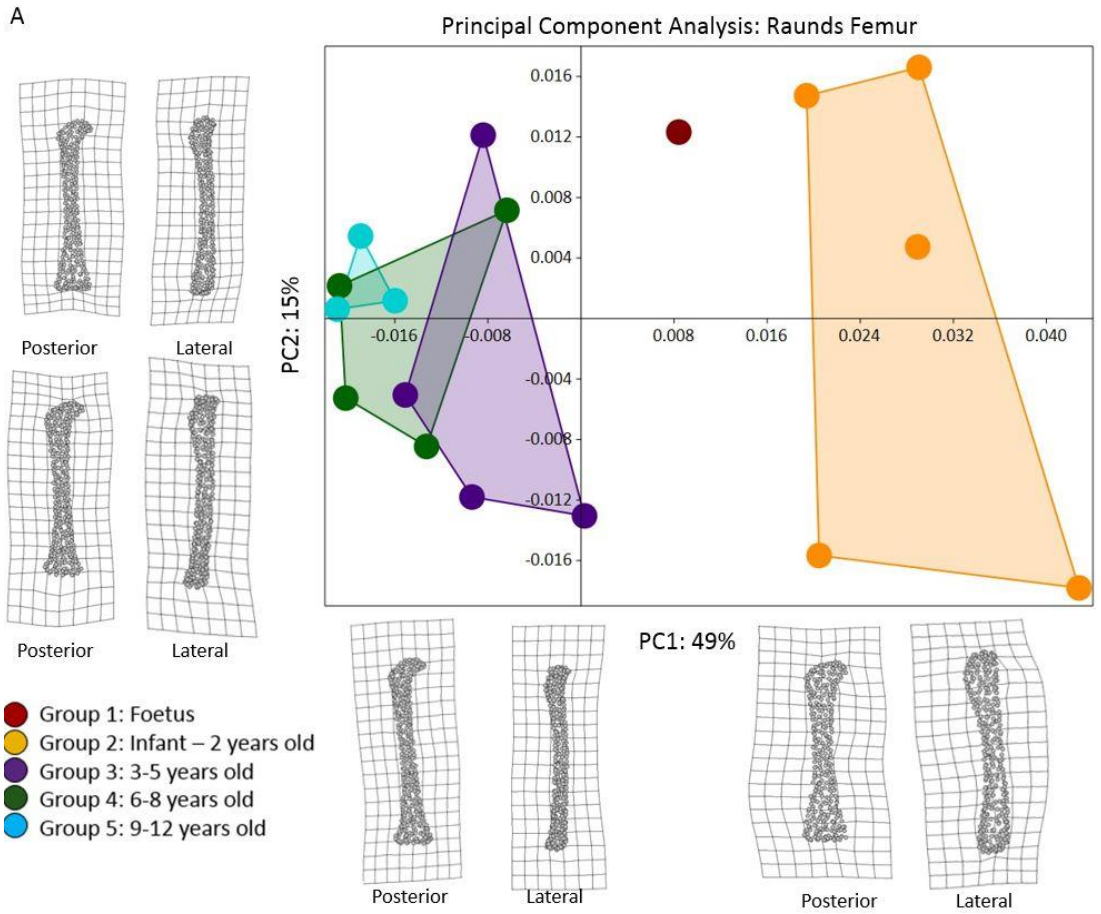
A
Principal Component Analysis: Raunds Femur
PC2: 15%
PC1: 49%
0.016
0.012
0.008
0.004
-0.004
-0.008
-0.012
-0.016
-0.016
-0.008
0.008
0.016
0.024
0.032
0.040
Posterior
Lateral
Posterior
Lateral
Posterior
Lateral
Posterior
Lateral
Group 1: Foetus
Group 2: Infant – 2 years old
Group 3: 3-5 years old
Group 4: 6-8 years old
Group 5: 9-12 years old

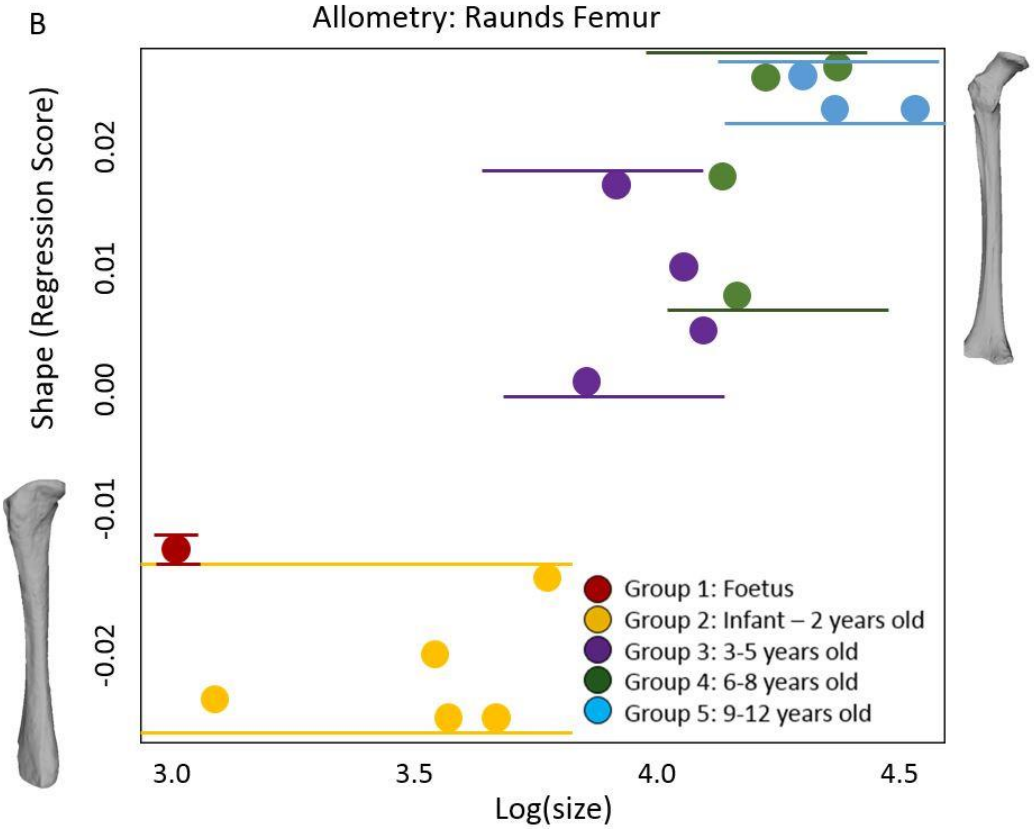
B
Allometry: Raunds Femur
Shape (Regression Score)
0.02
0.01
0.00
-0.01
-0.02
3.0
3.5
4.0
4.5
Log(size)
Group 1: Foetus
Group 2: Infant – 2 years old
Group 3: 3-5 years old
Group 4: 6-8 years old
Group 5: 9-12 years old

C.2 Raunds Tibia

The first principal component (46%) represents the width of the proximal and distal metaphyses to diaphysis. Positive values of the lateral view (Groups 2, 4, 5) show a wider diaphyses and curvature to the proximal midshaft. Negative values (Groups 2, 3, 4, 5) represent a narrower and straighter diaphysis. The anterior view shows negative values have wider metaphyses which curve into a narrower diaphysis while positive values have less curvature into the diaphysis. The second principal component (20%) represents the angle of the proximal metaphyses. The lateral view shows positive values represent a concave angle of the proximal metaphyses while negative values are more convex. Positive values from the anterior view show an s-shaped curvature of the metaphyses into the diaphysis while negative values show some curvature in the lateral metaphyses and a straighter diaphysis.

The allometric regression shows a similar pattern of large variation of size and shape for Group 2 (infant to 2 years old). There is a large increase in size and shape for Group 3 (3 to 5 years old) which is within shape range of Group 4 (6-8 years old). Group 5 (9 to 12 years old) slows in tempo of size and shape and falls within range of Group 4.

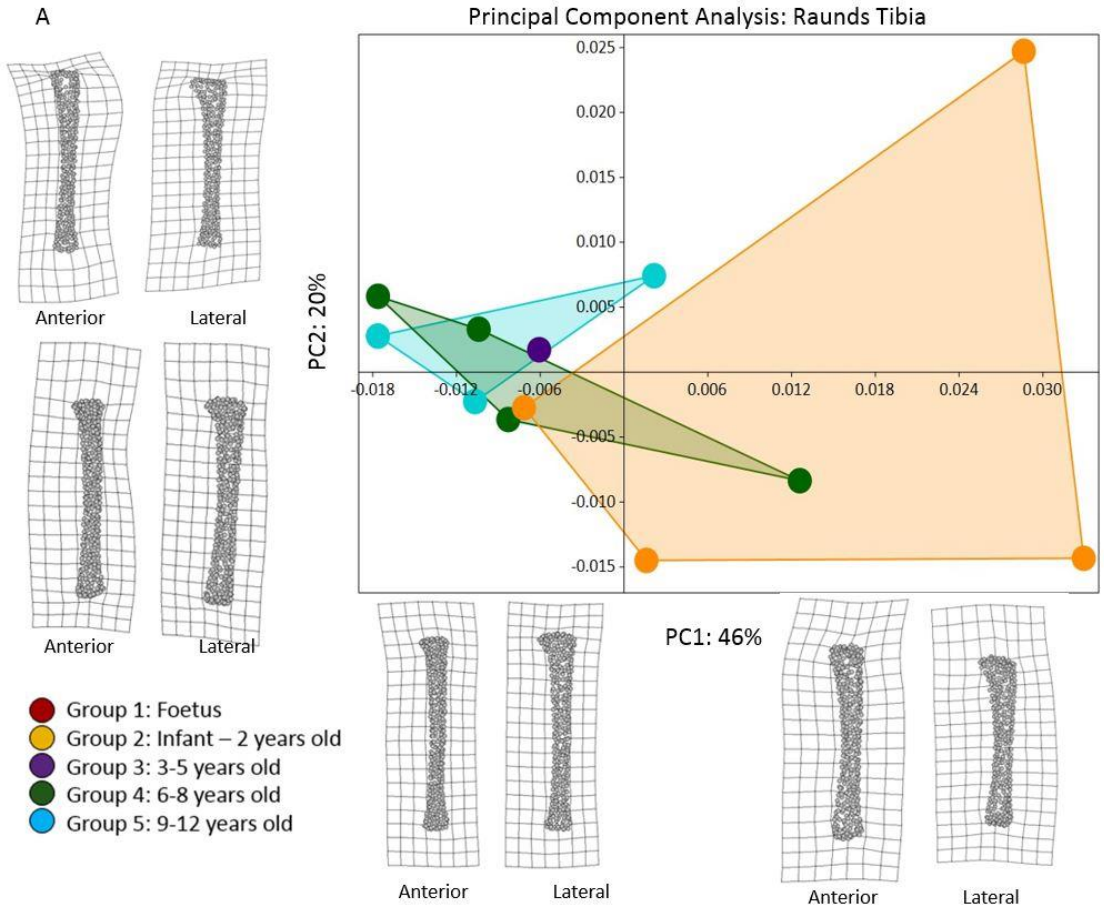
A
Principal Component Analysis: Raunds Tibia
PC2: 20%
PC1: 46%
0.025
0.020
0.015
0.010
0.005
-0.005
-0.010
-0.015
-0.018
-0.012
-0.006
0.006
0.012
0.018
0.024
0.030
Anterior
Lateral
Anterior
Lateral
Anterior
Lateral
Anterior
Lateral
Group 1: Foetus
Group 2: Infant – 2 years old
Group 3: 3-5 years old
Group 4: 6-8 years old
Group 5: 9-12 years old

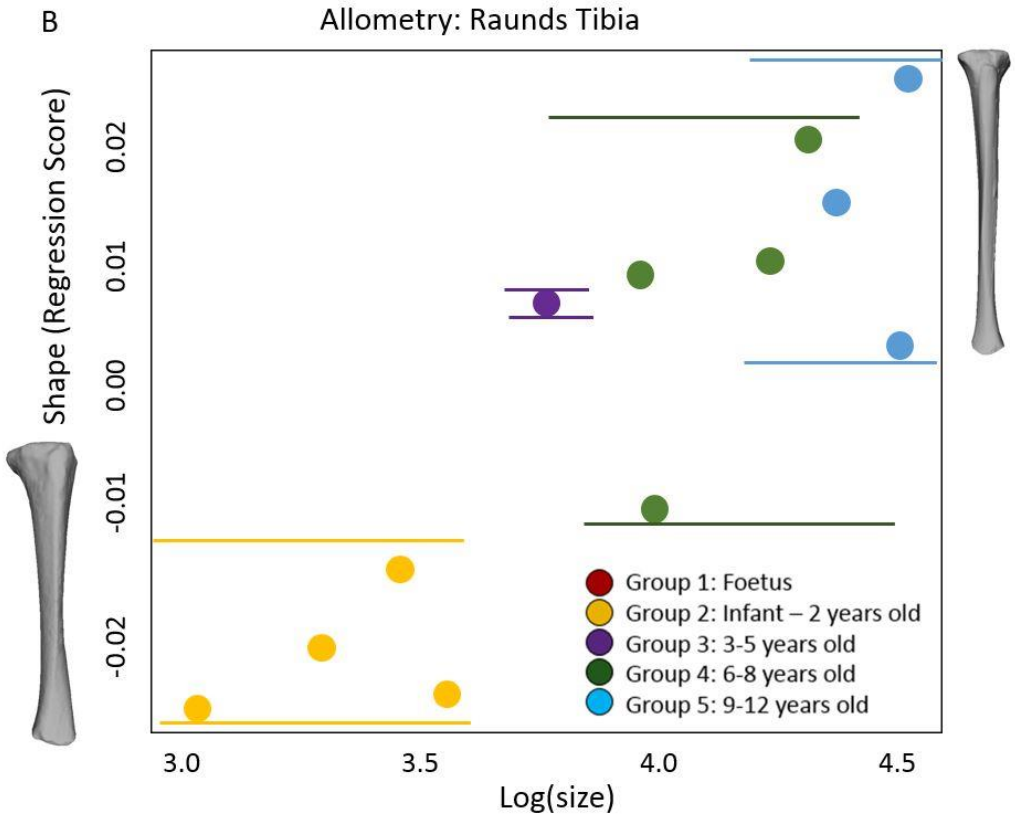
B
Allometry: Raunds Tibia
Shape (Regression Score)
0.02
0.01
0.00
-0.01
-0.02
3.0
3.5
4.0
4.5
Log(size)
Group 1: Foetus
Group 2: Infant – 2 years old
Group 3: 3-5 years old
Group 4: 6-8 years old
Group 5: 9-12 years old

C.3 Raunds Humerus

The first principal component (40%) represents the changes in the width and curvature of the metaphyses and diaphyses. Positive values show the lateral view (Groups 1, 3, 4) are wider and longer in the distal metaphyses and into the diaphyses. Negative values (Groups 3, 4, 5) are narrow in the distal metaphyses with more curvature from the anterior metaphyses. The anterior view shows positive values have a wider distal metaphyses into the diaphysis while negative values have a narrower curvature from the diaphysis to metaphyses. The second principal component (23%) represents the curvature angle of proximal metaphyses. Negative values (Group 3 and 4) have a concave metaphyses from the lateral view while positive values are more convex. The anterior view reveals negative values have a convex metaphyses compared to the concave positive values.

The allometric plot shows a large increase in size and shape from Group 2 (infant to 2 years old) to Group 3 (3 to 5 years old). Another increase in size and shape occurs in Group 4 (6 to 8 years old) and a slower tempo of size and shape for Group 5 (9 to 12 years old) which falls within range of Group 4.

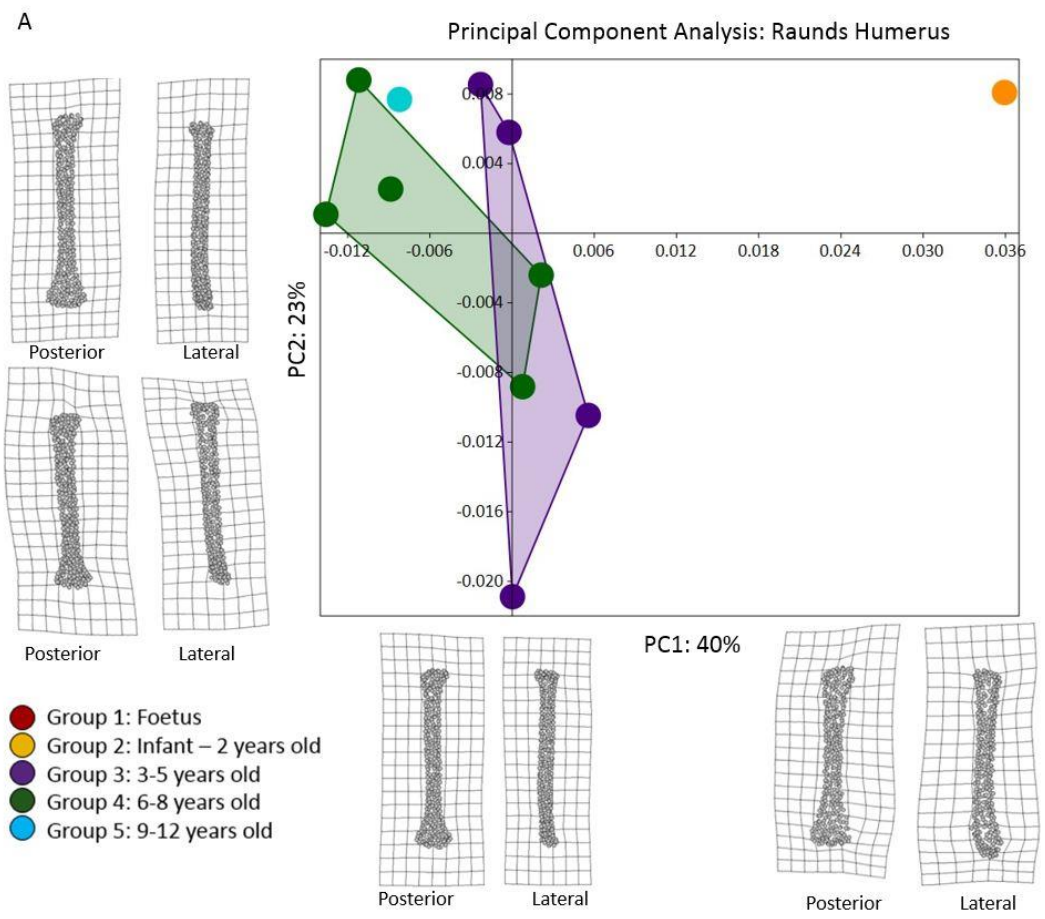
A
Principal Component Analysis: Raunds Humerus
PC2: 23%
PC1: 40%
0.008
0.004
-0.004
-0.008
-0.012
-0.016
-0.020
-0.012
-0.006
0.006
0.012
0.018
0.024
0.030
0.036
Posterior
Lateral
Posterior
Lateral
Posterior
Lateral
Posterior
Lateral
Group 1: Foetus
Group 2: Infant – 2 years old
Group 3: 3-5 years old
Group 4: 6-8 years old
Group 5: 9-12 years old

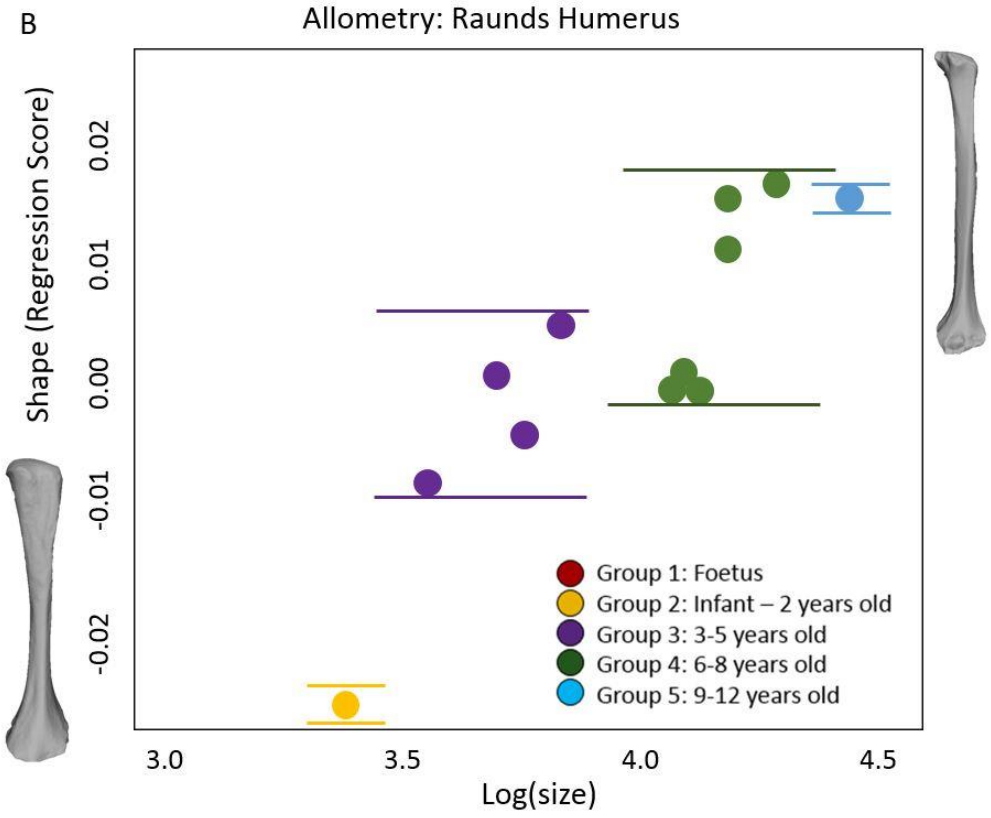
B
Allometry: Raunds Humerus
Shape (Regression Score)
0.02
0.01
0.00
-0.01
-0.02
3.0
3.5
4.0
4.5
Log(size)
Group 1: Foetus
Group 2: Infant – 2 years old
Group 3: 3-5 years old
Group 4: 6-8 years old
Group 5: 9-12 years old

Appendix D: Wharram Percy

The following table provides the frequencies for skeletal element by age Group for the Wharram Percy juveniles. The results of the PCA ANOVA for element by Group and the allometry of regressing shape onto size are also found in the table. A detailed description of the PCA and allometric trajectories are discussed below by element.

Wharram Percy Juveniles			
Variables	Femur (n=18)	Tibia (n=17)	Humerus (n=23)
Group 1: Foetus	3	4	6
Group 2: Infant to 2 years old	1	1	3
Group 3: 3 to 5 years old	3	3	4
Group 4: 6 to 8 years old	8	7	7
Group 5: 9 to 12 years old	3	2	3
PCA ANOVA (p-value)	0.01	0.01	0.01
Allometry (p-value)	0.01	0.01	0.01

D.1 Wharram Percy Femur

PC1 (54%) reflects differences in width of metaphyses and midshaft curvature. Positive values of PC1 (54%) have a higher degree of curvature in the diaphysis and are made up of the first 3 age Groups (foetal to 5 years old). Negative values have lower degree of curvature and are made up of the last two age Groups of 6 to 12 year olds. The anterior view represents the differences in width of the distal metaphyses and diaphysis. Positive values have a wider distal metaphyses and diaphysis and less curvature compared to the negative values. PC2 (15%) represents differences in the diaphyseal curvature. Negative values of the anterior view of PC2 (15%) have a lower apex of curvature and more anterior orientation of the proximal curvature compared to the positive values which have a higher apex of curvature and a posteriorly oriented proximal curve. Negative values of the anterior view represent femora with wider proximal metaphyses and more curvature in the proximal diaphysis and metaphyses than positive values.

The PCA plot shows clustering of age Groups with only Group 5 (9-12 year olds) falling within range of Group 4 (6-8 year olds). The allometric plot shows some overlapping shapes among the age Groups. There is statistical significance when regression shape onto size ($p>0.01$). The femur shows an hourglass effect as there is similar variation in Group 1 (foetus) with more variation in size and then shape-although this is only a small sample in Group 2. Growth spurts in Group 3 (3-5) there is much less variation in shape. A larger range of shape is found in Groups 4 and 5 (6-12 years old) which could be a catch-up phase where the danger of weaning has passed (Group 3:3-5 years old) and there is more energy for shape development.

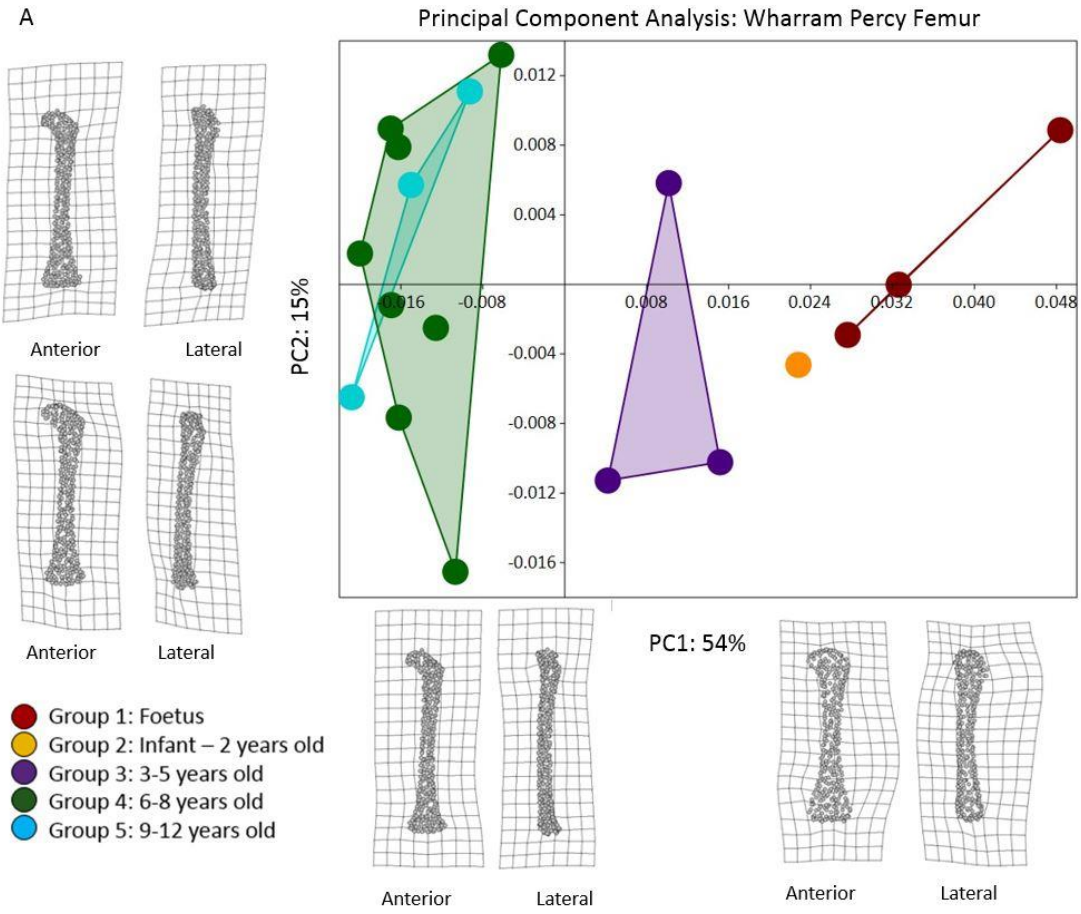
A
Principal Component Analysis: Wharram Percy Femur
PC2: 15%
PC1: 54%
0.012
0.008
0.004
-0.004
-0.008
-0.012
-0.016
-0.016
-0.008
0.008
0.016
0.024
0.032
0.040
0.048
Anterior
Lateral
Anterior
Lateral
Anterior
Lateral
Anterior
Lateral
Group 1: Foetus
Group 2: Infant – 2 years old
Group 3: 3-5 years old
Group 4: 6-8 years old
Group 5: 9-12 years old

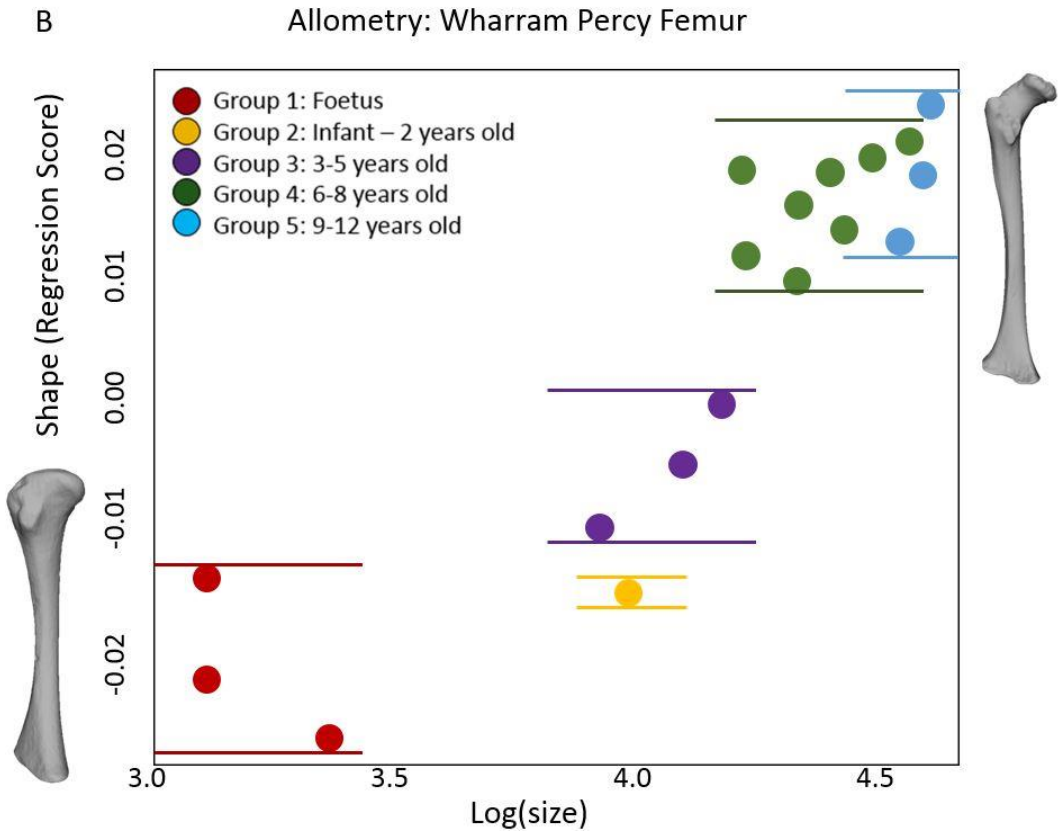
B
Allometry: Wharram Percy Femur
Shape (Regression Score)
0.02
0.01
0.00
-0.01
-0.02
3.0
3.5
4.0
4.5
Log(size)
Group 1: Foetus
Group 2: Infant – 2 years old
Group 3: 3-5 years old
Group 4: 6-8 years old
Group 5: 9-12 years old

D.2 Wharram Percy Tibia

PC1 (44%) reflects the variation of the width of the midshaft. Negative values for the lateral view represent more of a blade-like shape as the midshaft widens. Positive values represent more curvature in the posterior curvature of the midshaft. The anterior view represents more change in the flaring of the distal metaphyses as negative values have wider distal metaphyses than positive values. The positive values are made up of the first 3 age Groups (foetal to 5 years old) while the older Groups (6-12 years old) are in the negative values. PC2 (14%) represents changes in the proximal and distal metaphyses. The lateral view shows negative values are represented by more concave distal diaphysis into the metaphyses while positive values are more convex. The anterior negative values show more curvature in the lateral diaphysis with a wider proximal metaphyses while positive values have a narrower proximal mataphyses and straighter diaphysis. The age Groups are evenly split between the positive and negative values of this axis and it is likely that these developmental differences are capturing the remodelling process of the tibiae as it grows in size and follows in shape.

Similarly to the femora, Group 1 (foetus), the allometric plot reveals more variation in size and shape. Group 2 (infant to 2 years old) and 3 (3 to 5 years old) shows an increase in both size and shape. There is a large burst of increasing tibial size and shape variation for the last two age Groups (6 to 12 years old).

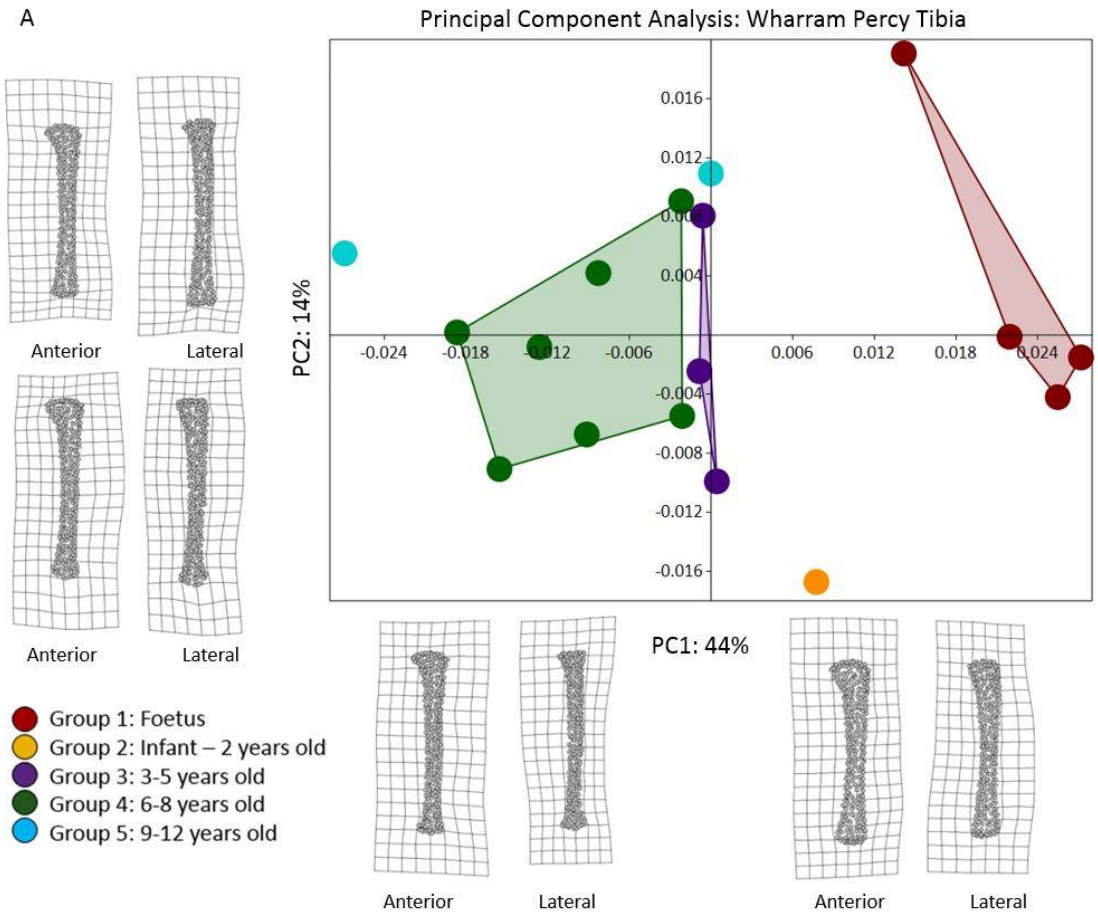
A
Principal Component Analysis: Wharram Percy Tibia
PC2: 14%
PC1: 44%
0.016
0.012
0.004
-0.004
-0.008
-0.012
-0.016
-0.024
-0.018
-0.006
0.006
0.012
0.018
0.024
Anterior
Lateral
Anterior
Lateral
Anterior
Lateral
Anterior
Lateral
Group 1: Foetus
Group 2: Infant – 2 years old
Group 3: 3-5 years old
Group 4: 6-8 years old
Group 5: 9-12 years old

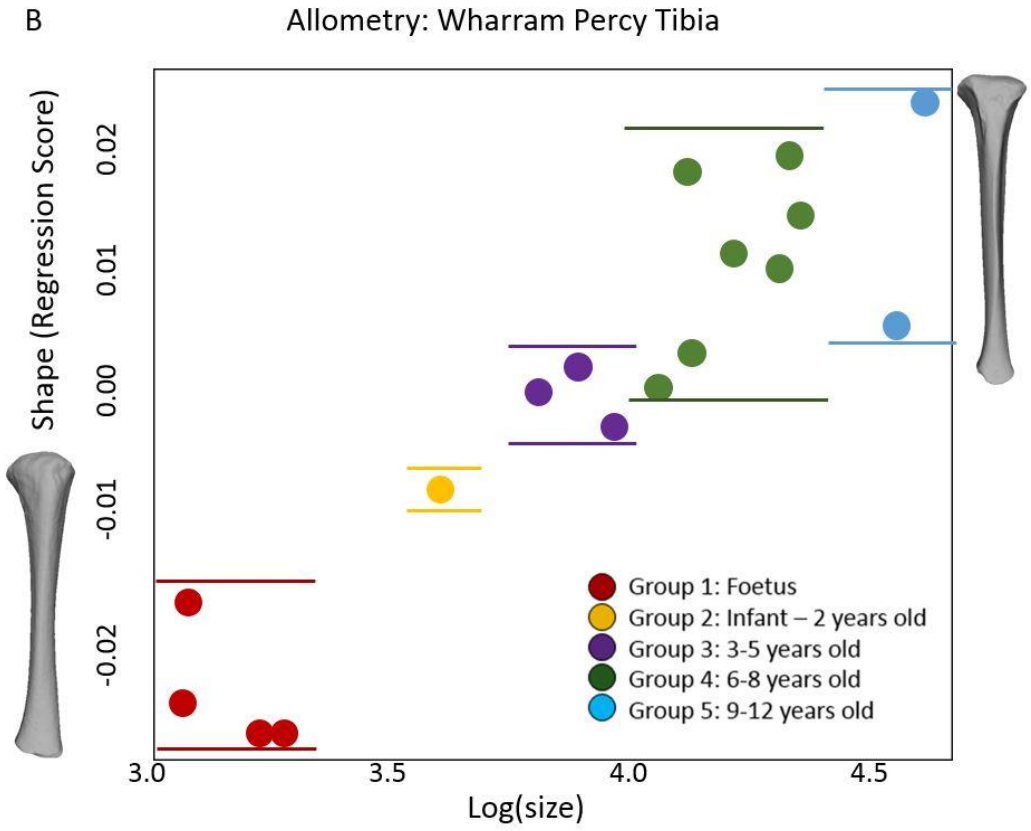
B
Allometry: Wharram Percy Tibia
Shape (Regression Score)
0.02
0.01
0.00
-0.01
-0.02
3.0
3.5
4.0
4.5
Log(size)
Group 1: Foetus
Group 2: Infant – 2 years old
Group 3: 3-5 years old
Group 4: 6-8 years old
Group 5: 9-12 years old

D.3 Wharram Percy Humerus

The first principal component axis (51%) represents changes in the distal metaphyses and curvature of the diaphysis. The lateral and anterior view shows positive values have a wider distal metaphyses and straighter diaphyses (Groups 1 to 3) while negative values have a narrower and curved distal metaphyses with an s-shaped curve from the proximal metaphyses into metaphyses (Groups 3-5). The second principal component axis (10%) represents elongation of the proximal metaphyses. Negative values represent more elongation in the proximal metaphyses while negative values have a shorter and wider proximal metaphyses. Similarly to the tibiae, some individuals from Group 1, 2, 4, and 5 fall in the negative values with the other individuals (including Group 3) fall into the positive values. This may reflect the remodelling process of the humeri.

The foetal humeri (Group 1) have a large range of size and shape variation. Interestingly, there is a conserved period in Group 2 (infant to 2 years old) followed by accelerated size and shape for the last three age Groups (3 to 12 years old). This trend is likely to show that the Group 2 humeri undergo a conservative period when the lower limbs are transition from quadrupedal to bipedal movement.

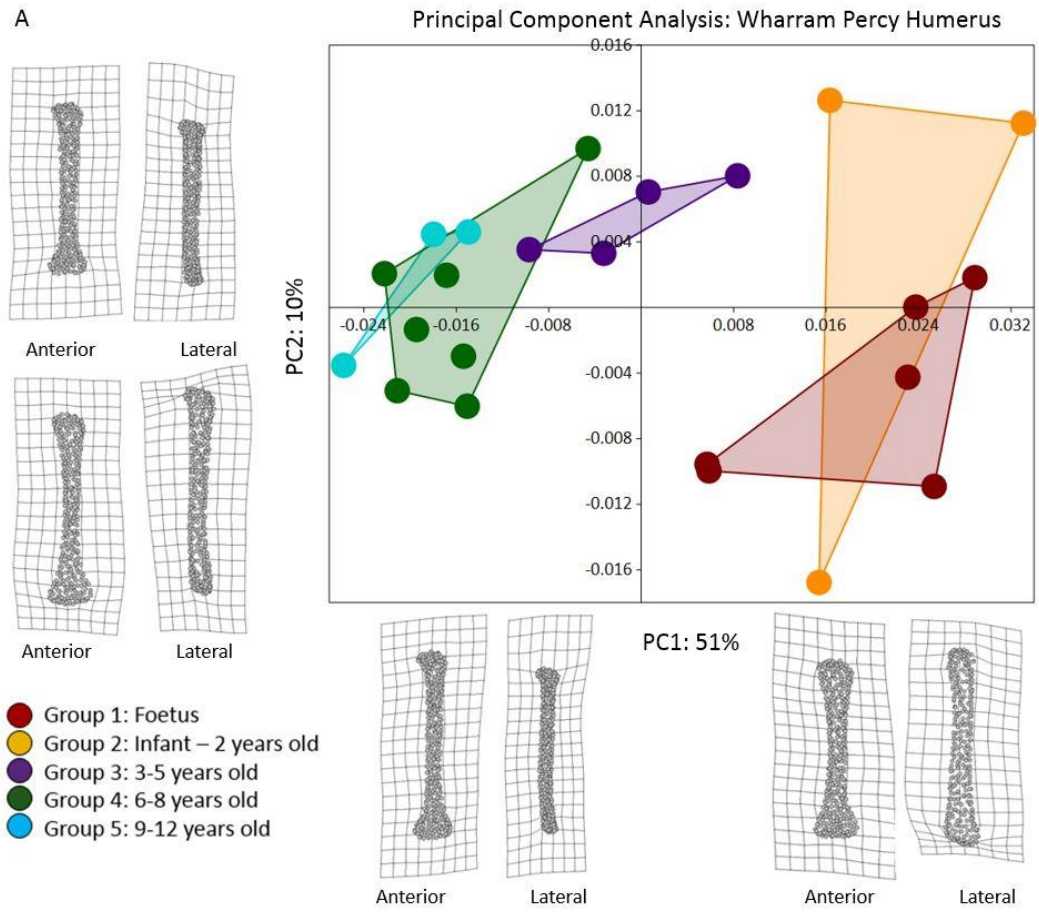
A
Principal Component Analysis: Wharram Percy Humerus
PC2: 10%
PC1: 51%
0.016
0.012
0.008
0.004
-0.004
-0.008
-0.012
-0.016
-0.024
-0.016
-0.008
0.008
0.016
0.024
0.032
Anterior
Lateral
Anterior
Lateral
Anterior
Lateral
Anterior
Lateral
Group 1: Foetus
Group 2: Infant – 2 years old
Group 3: 3-5 years old
Group 4: 6-8 years old
Group 5: 9-12 years old

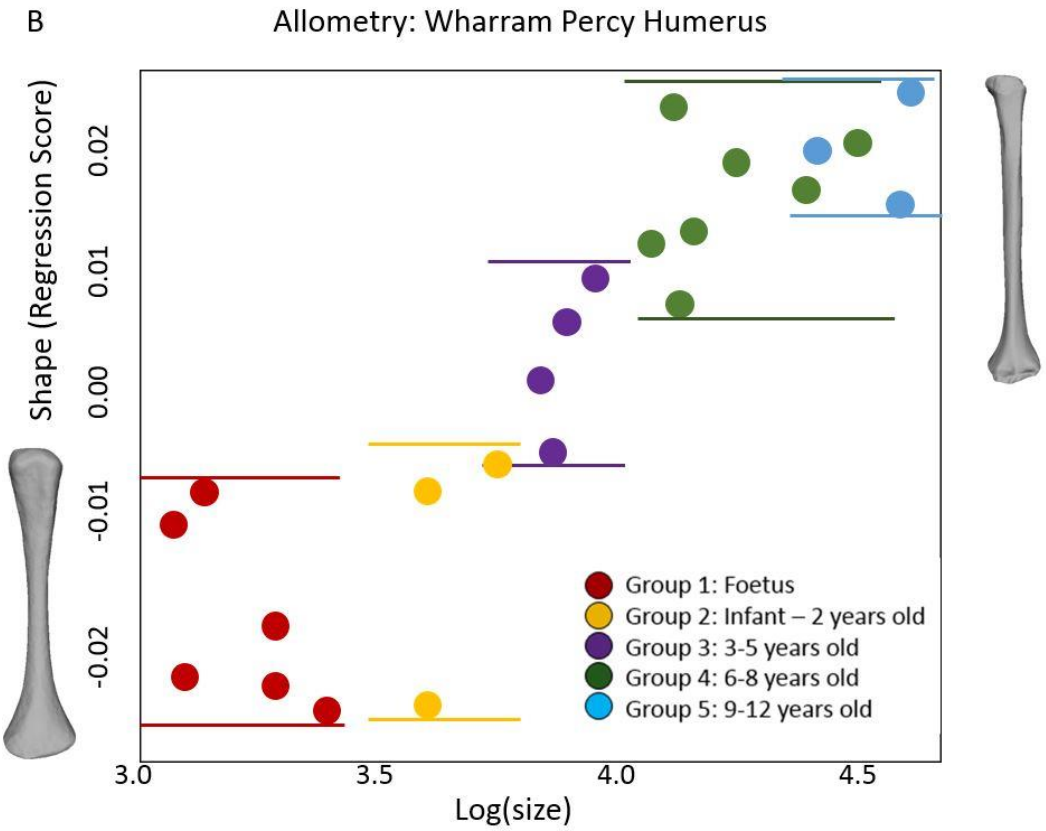
B
Allometry: Wharram Percy Humerus
Shape (Regression Score)
0.02
0.01
0.00
-0.01
-0.02
3.0
3.5
4.0
4.5
Log(size)
Group 1: Foetus
Group 2: Infant – 2 years old
Group 3: 3-5 years old
Group 4: 6-8 years old
Group 5: 9-12 years old

Appendix E: Canterbury

The following table provides the frequencies for skeletal element by age group for the Canterbury juveniles. The results of the PCA ANOVA for element by group and the allometry of regressing shape onto size are also found in the table. A detailed description of the PCA and allometric trajectories are discussed below by element.

Canterbury Juveniles			
Variables	Femur (n=42)	Tibia (n=40)	Humerus (n=27)
Group 1: Foetus	2	2	0
Group 2: Infant to 2 years old	12	7	4
Group 3: 3 to 5 years old	8	10	8
Group 4: 6 to 8 years old	12	12	11
Group 5: 9 to 12 years old	8	9	4
PCA ANOVA (p-value)	0.01	0.01	0.05
Allometry (p-value)	0.01	0.01	0.02

E.1 Canterbury Femur

The first principal component axis (39%) represents changes in the width and curvature of the proximal metaphyses. Positive values (Groups 1-3) from the lateral view represent wider, shorter, and straighter proximal metaphyses. The anterior view shows a wider proximal metaphyses into the metaphyses. The second principal component axis (15%) represents the curvature of the distal metaphyses. The anterior and lateral view shows that positive values (Groups 2-5) have a concave distal metaphyses while negative values (Groups 1-5) have a convex distal metaphyses. The allometric plot shows that there is statistical significance when regressing shape onto size. There is an acceleration of shape and size variation from Group 1 (foetal) to Group 2 (infant to 2 years old). There is a gradual slowing down in size and shape from Group 3 (3 to 5 years old) to Group 5 (9 to 12 years old) with overlapping size and shape.

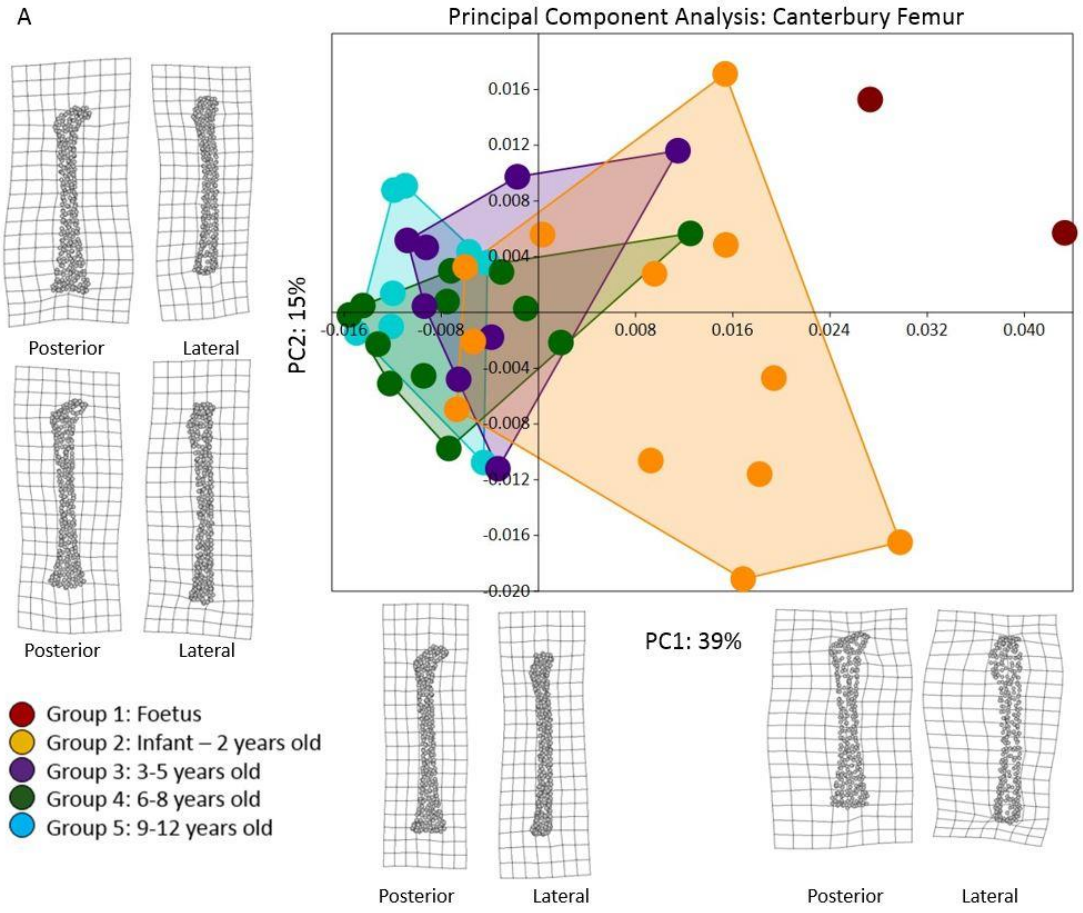
A
Principal Component Analysis: Canterbury Femur
PC2: 15%
PC1: 39%
0.016
0.012
0.008
0.004
-0.004
-0.008
-0.012
-0.016
-0.020
-0.016
-0.008
0.008
0.016
0.024
0.032
0.040
Posterior
Lateral
Posterior
Lateral
Posterior
Lateral
Posterior
Lateral
Group 1: Foetus
Group 2: Infant – 2 years old
Group 3: 3-5 years old
Group 4: 6-8 years old
Group 5: 9-12 years old

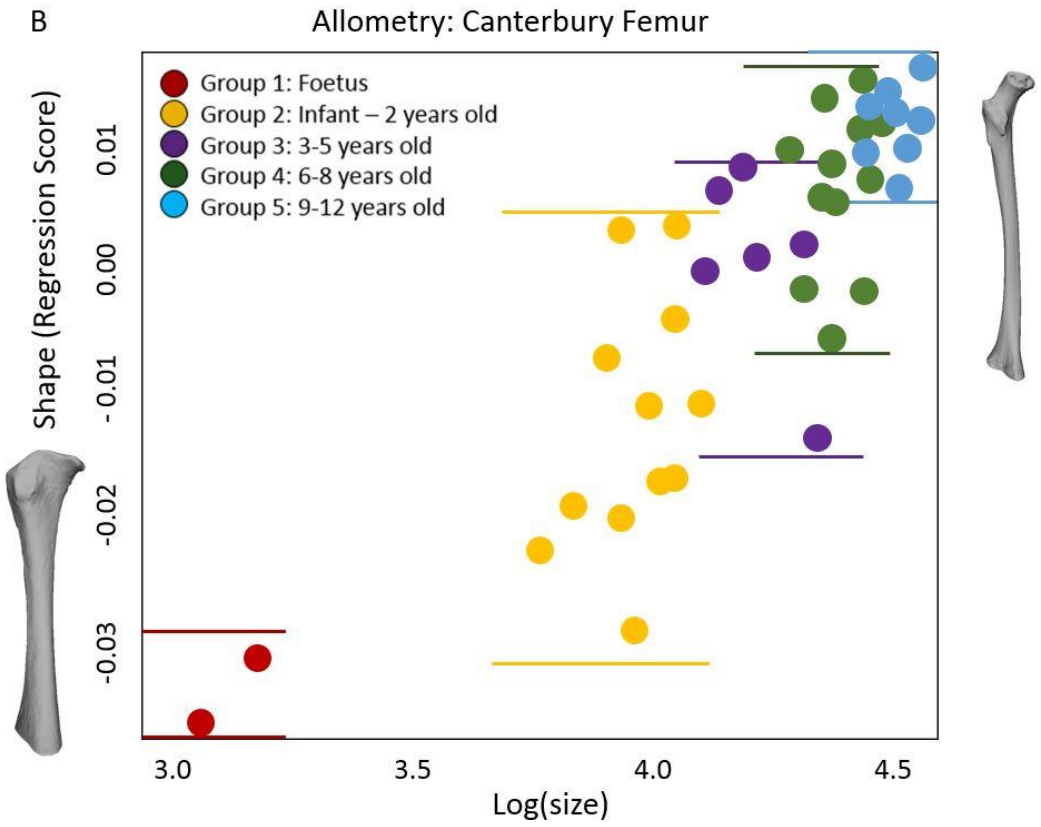
B
Allometry: Canterbury Femur
Shape (Regression Score)
0.01
0.00
- 0.01
-0.02
-0.03
3.0
3.5
4.0
4.5
Log(size)
Group 1: Foetus
Group 2: Infant – 2 years old
Group 3: 3-5 years old
Group 4: 6-8 years old
Group 5: 9-12 years old

E. 2 Canterbury Tibia

The first principal component axis (32%) represents the curvature of the diaphysis. Positive values (Groups 1 to 3) reflect broader diaphysis from the lateral and anterior view, with a slight curvature. Negative values (Groups 3 to 5) reflect a slender and straighter diaphysis. The second principal component axis (11%) represents the angle of the proximal metaphyses. Positive values show more curvature from the lateral proximal metaphyses and more depth in the distal metaphyses. Negative values show more curvature in the medial proximal metaphyses and diaphysis. The allometric plot shows a similar pattern to the femora. There is statistical significance of increasing size followed by increasing shape. There is a large range of variation of size and shape in Group 1 (foetus) and a gradual decrease in size and shape variation for the remaining age Groups.

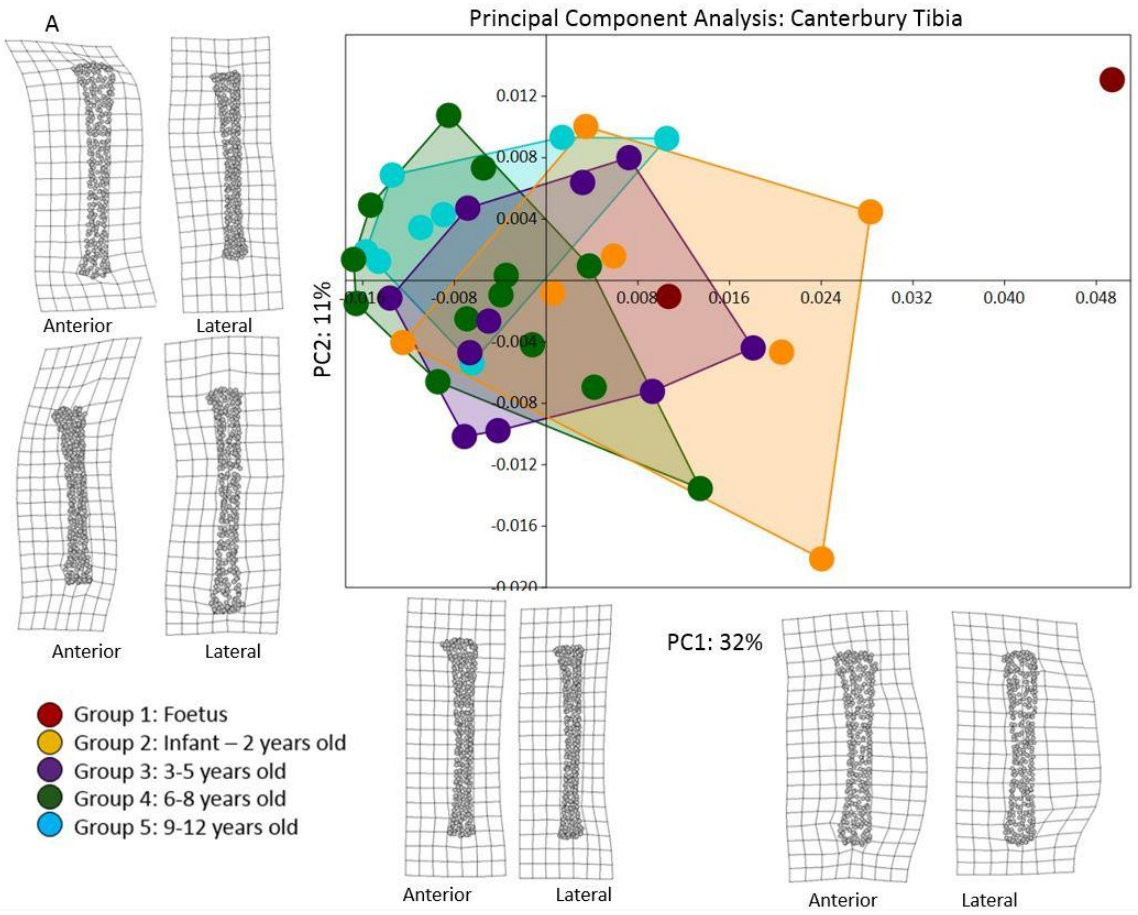
A
Principal Component Analysis: Canterbury Tibia
Anterior
Lateral
Anterior
Lateral
PC2: 11%
0.012
0.008
0.004
-0.004
-0.008
-0.012
-0.016
-0.020
-0.008
0.008
0.016
0.024
0.032
0.040
0.048
PC1: 32%
Anterior
Lateral
Anterior
Lateral
Group 1: Foetus
Group 2: Infant – 2 years old
Group 3: 3-5 years old
Group 4: 6-8 years old
Group 5: 9-12 years old

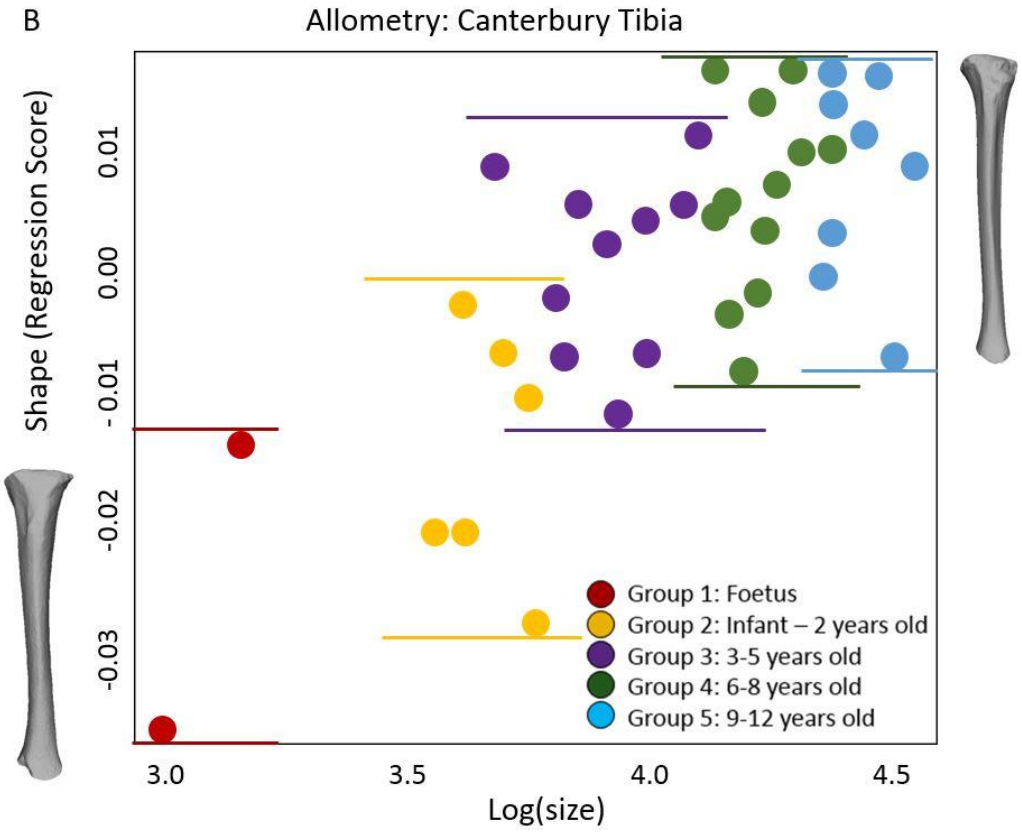
B
Allometry: Canterbury Tibia
Shape (Regression Score)
0.01
0.00
- 0.01
-0.02
-0.03
3.0
3.5
4.0
4.5
Log(size)
Group 1: Foetus
Group 2: Infant – 2 years old
Group 3: 3-5 years old
Group 4: 6-8 years old
Group 5: 9-12 years old

E. 3 Canterbury Humerus

The first principal component axis (32%) represents the width and curvature of the distal metaphyses. Positive values (Group 2-4) represent wider and straighter distal metaphysis. The negative values represent a narrower and more curved distal metaphyses. The second principal component axis (11%) represents the width and curvature of the proximal metaphyses and diaphysis. Positive values have a more convex proximal metaphyses and straighter proximal metaphyses. Negative values have a convex proximal metaphyses and a more curved proximal metaphyses. The allometric plot has a large range of size and shape variation in Group 2 (infant to 2 years old). Group 3 (3 to 5 years old) has a slower range of shape and size while Group 4 (6-8 year olds) and Group 5 (9-12 year olds) represent accelerated growth.

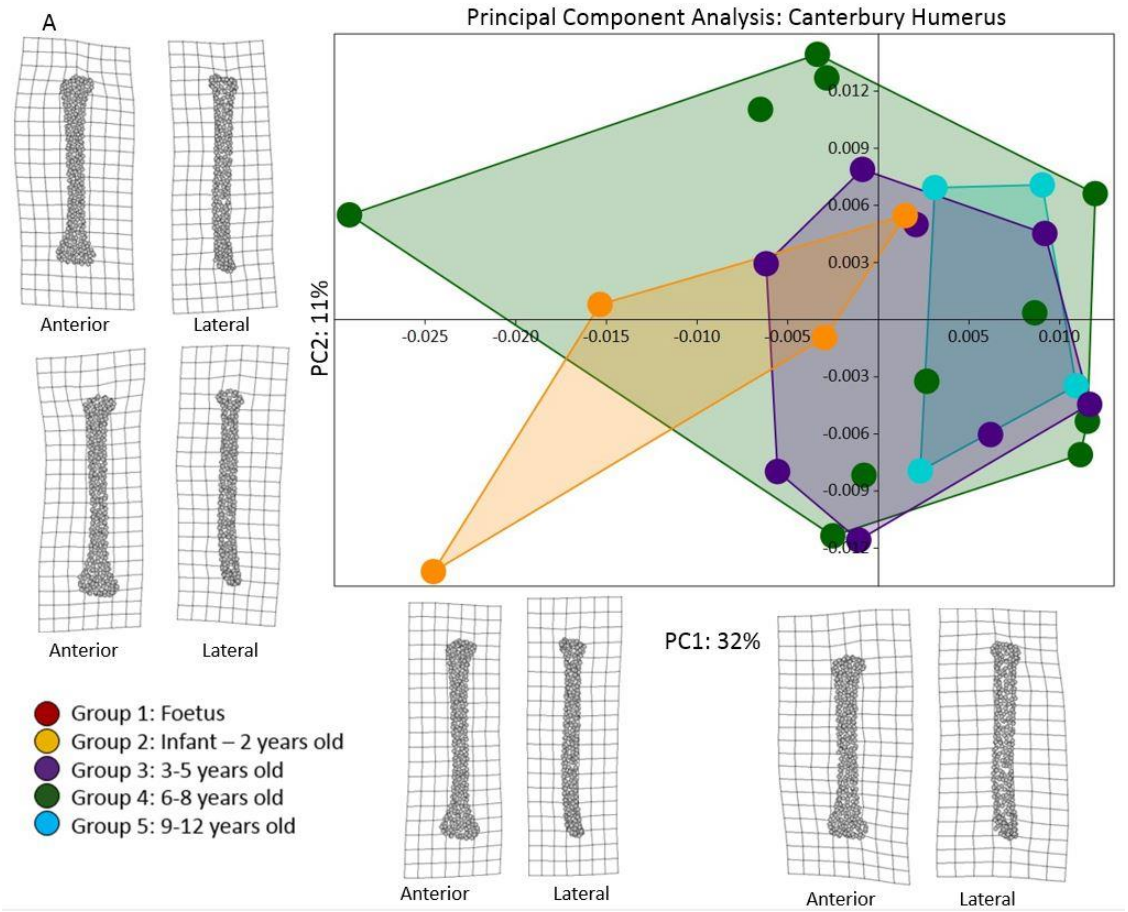
A
Principal Component Analysis: Canterbury Humerus
Anterior
Lateral
Anterior
Lateral
PC2: 11%
0.012
0.009
0.006
0.003
-0.025
-0.020
-0.015
-0.010
-0.005
0.005
0.010
-0.003
-0.006
-0.009
PC1: 32%
Anterior
Lateral
Anterior
Lateral
Group 1: Foetus
Group 2: Infant – 2 years old
Group 3: 3-5 years old
Group 4: 6-8 years old
Group 5: 9-12 years old

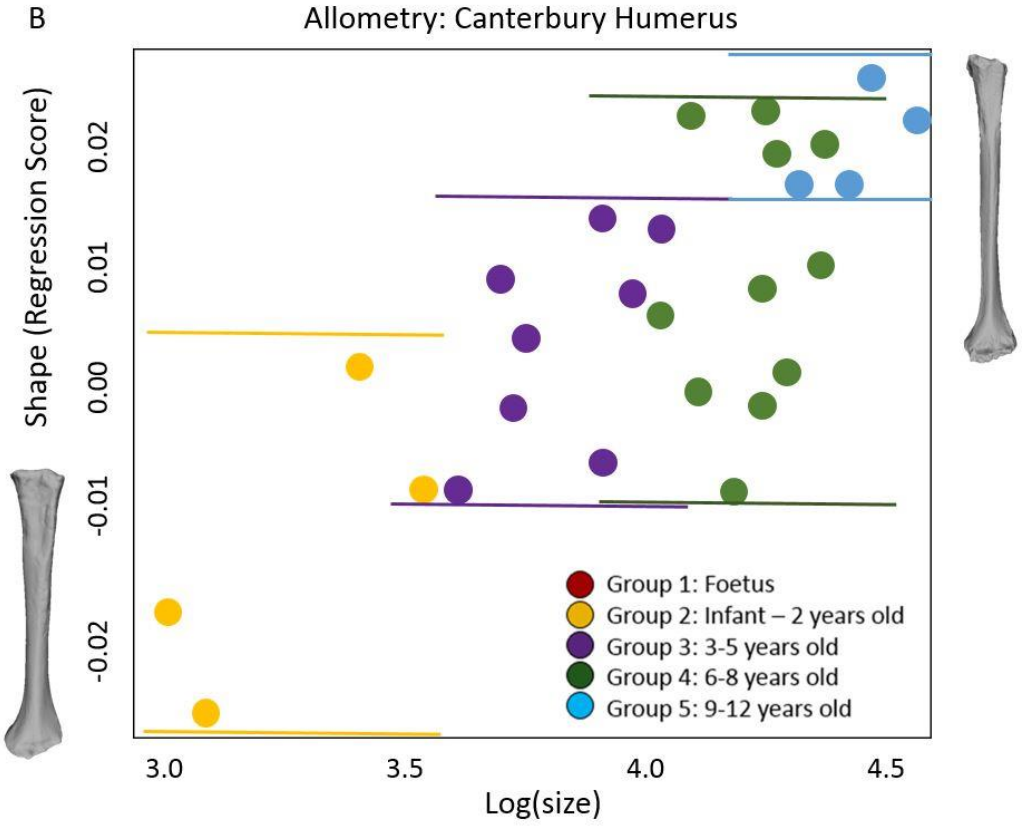
B
Allometry: Canterbury Humerus
Shape (Regression Score)
0.02
0.01
0.00
-0.01
-0.02
3.0
3.5
4.0
4.5
Log(size)
Group 1: Foetus
Group 2: Infant – 2 years old
Group 3: 3-5 years old
Group 4: 6-8 years old
Group 5: 9-12 years old

Appendix F: Wolverhampton

The following table provides the frequencies for skeletal element by age group for the Wolverhampton juveniles. The results of the PCA ANOVA for element by group and the allometry of regressing shape onto size are also found in the table. A detailed description of the PCA and allometric trajectories are discussed below by element.

Wolverhampton Juveniles			
Variables	Femur (n=4)	Tibia (n=5)	Humerus (n=7)
Group 1: Foetus	1	0	0
Group 2: Infant to 2 years old	1	1	5
Group 3: 3 to 5 years old	1	1	1
Group 4: 6 to 8 years old	1	1	0
Group 5: 9 to 12 years old	0	2	1
PCA ANOVA (p-value)	0.08	0.26	0.12
Allometry (p-value)	0.08	0.30	0.05

F.1 Wolverhampton Femur

The first principal component represents (68%) curvature of the midshaft. Positive values (Groups 1 and 2) represent wider and straighter proximal metaphyses with more curvature in the midshaft. Negative values (Groups 3 and 4) represent narrower and more curved proximal metaphyses with more curvature in the proximal metaphyses. The second principal component (22%) represents differences in the angle of the metaphyses. Positive values represent a more convex proximal and distal metaphyses (Groups 2 and 4). Negative values represent a more concave proximal and distal metaphyses. The allometric plot shows a slowed rate of increasing size and shape for Group 1 (foetal) and 2 (infant to 2 years old) followed by accelerated size and shape for Group 3 (3 to 5 years old) and Group 4 (6-8 years old).

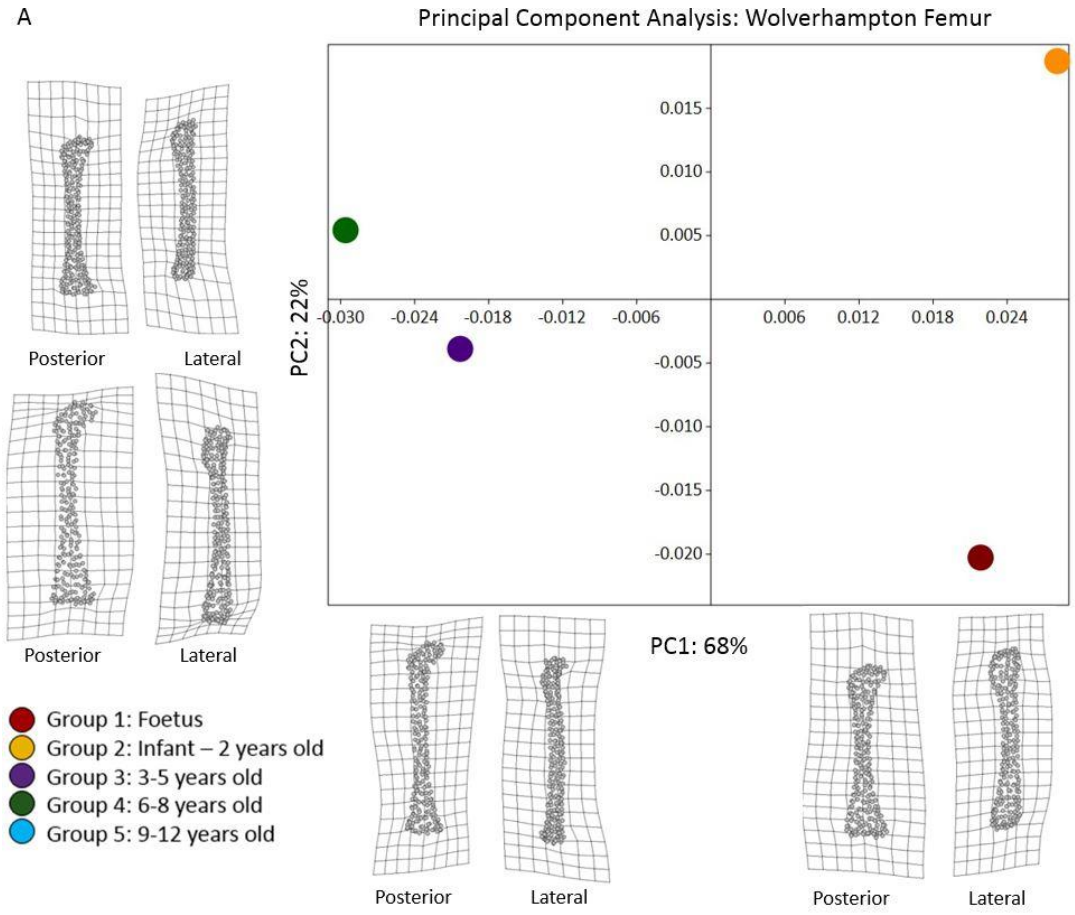
A
Principal Component Analysis: Wolverhampton Femur
PC2: 22%
PC1: 68%
0.015
0.010
0.005
-0.005
-0.010
-0.015
-0.020
-0.030
-0.024
-0.018
-0.012
-0.006
0.006
0.012
0.018
0.024
Posterior
Lateral
Posterior
Lateral
Posterior
Lateral
Posterior
Lateral
Group 1: Foetus
Group 2: Infant – 2 years old
Group 3: 3-5 years old
Group 4: 6-8 years old
Group 5: 9-12 years old

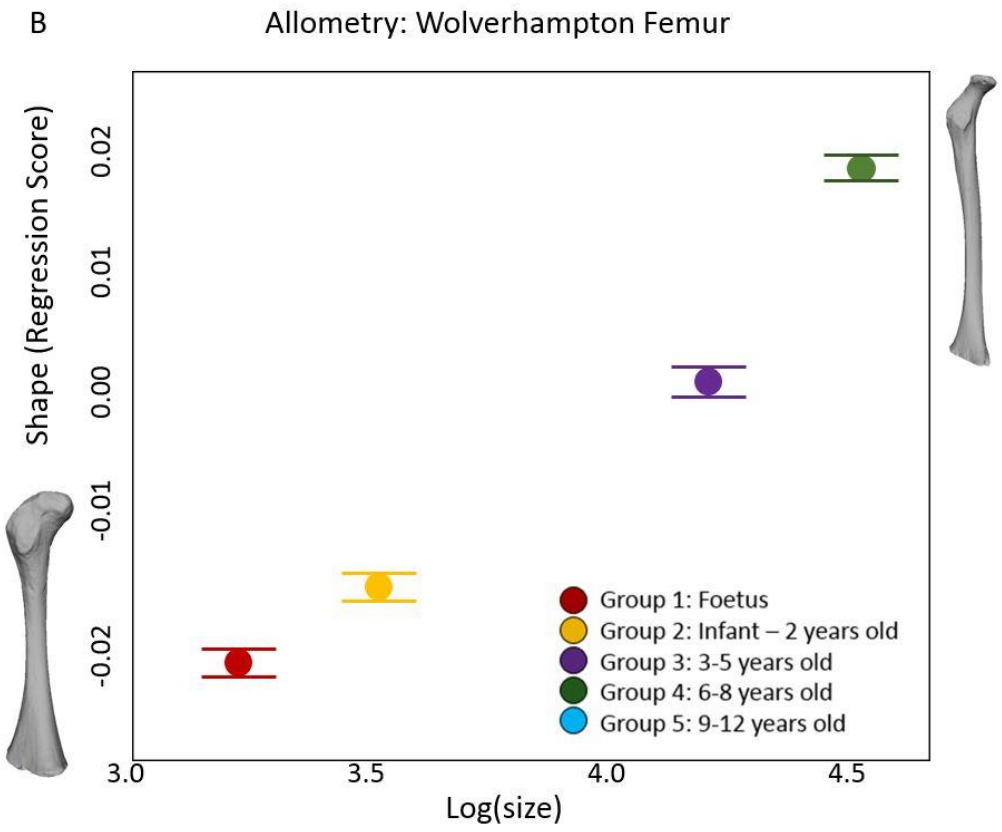
B
Allometry: Wolverhampton Femur
Shape (Regression Score)
0.02
0.01
0.00
-0.01
-0.02
3.0
3.5
4.0
4.5
Log(size)
Group 1: Foetus
Group 2: Infant – 2 years old
Group 3: 3-5 years old
Group 4: 6-8 years old
Group 5: 9-12 years old

F.2 Wolverhampton Tibia

The first principal component (48%) represents curvature of the diaphysis. Positive values (Group 2) represent a wider diaphysis with more curvature in the midshaft. Negative values (Group 3 to 5) represents a narrower diaphysis with more curvature in the proximal metaphyses. The second principal component (32%) represents differences in the proximal metaphyses. Negative values (Group 2, 3, 5) represents more curvature in the lateral condyle. The allometric plot shows an increase in size with little increase in shape from Group 2 (infant to 2 years old) to Group 3 (3 to 5 years old). There is an acceleration in size and shape from Group 4 (6 to 8 years old) and 5 (9 to 12 years old).

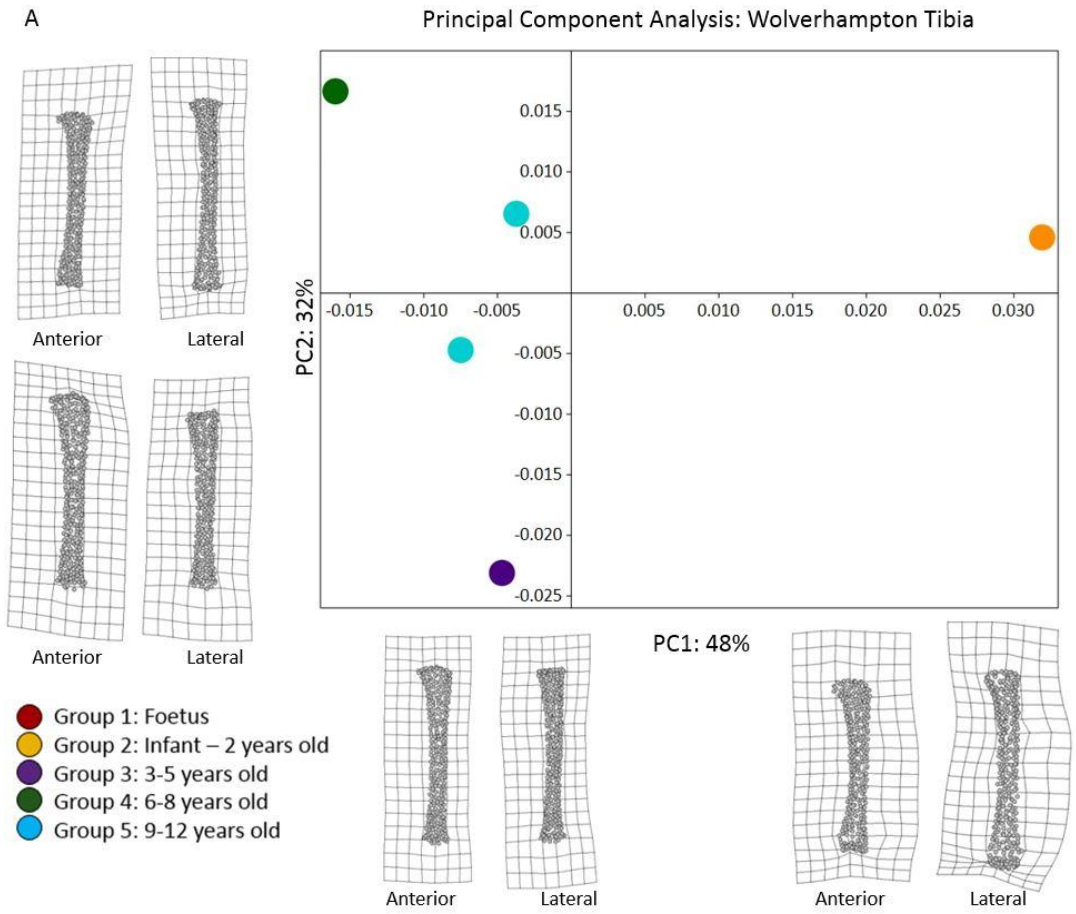
A
Principal Component Analysis: Wolverhampton Tibia
Anterior
Lateral
Anterior
Lateral
PC2: 32%
0.015
0.010
0.005
-0.015
-0.010
-0.005
0.005
0.010
0.015
0.020
0.025
0.030
-0.005
-0.010
-0.015
-0.020
-0.025
PC1: 48%
Anterior
Lateral
Anterior
Lateral
Group 1: Foetus
Group 2: Infant – 2 years old
Group 3: 3-5 years old
Group 4: 6-8 years old
Group 5: 9-12 years old

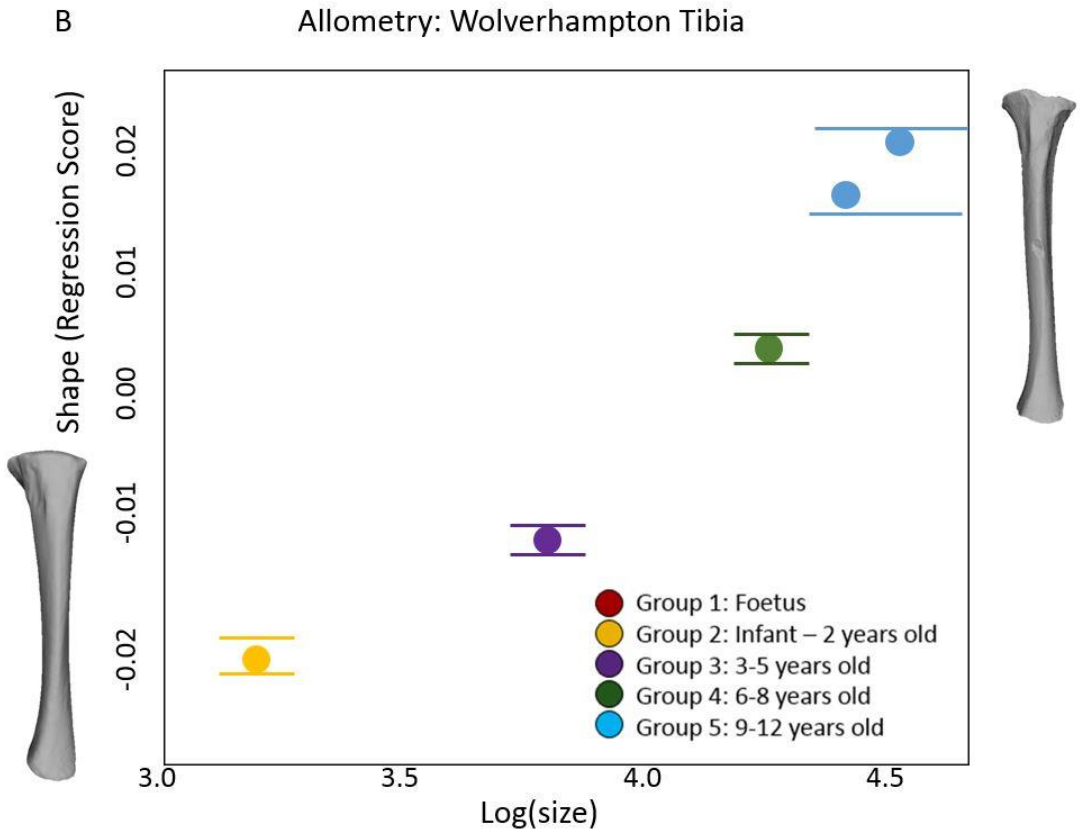
B
Allometry: Wolverhampton Tibia
Shape (Regression Score)
0.02
0.01
0.00
-0.01
-0.02
3.0
3.5
4.0
4.5
Log(size)
Group 1: Foetus
Group 2: Infant – 2 years old
Group 3: 3-5 years old
Group 4: 6-8 years old
Group 5: 9-12 years old

F.3 Wolverhampton Humerus

The first principal component (50%) represents changes in the proximal metaphyses. Positive values (Group 2 and 3) show a more concave proximal metaphyses on the lateral side. Negative values (Group 2 and 5) have a more convex proximal metaphyses and narrower proximal diaphysis. The second principal component (18%) represents changes in the diaphyses. Positive values have a straighter diaphysis (Group 2) and negative values (Group 2, 3, 5) have a more s-shaped curvature from the metaphyses to diaphysis. There is a small range of size and shape variation for Group 2 (infant to 2 years old) and a small increase in size and shape to Group 3 (3 to 5 years old). Group 5 (9 to 12 years old) has an accelerated size and shape, which is likely because of the lack of a Group 4 (6 to 8 year old) specimen.

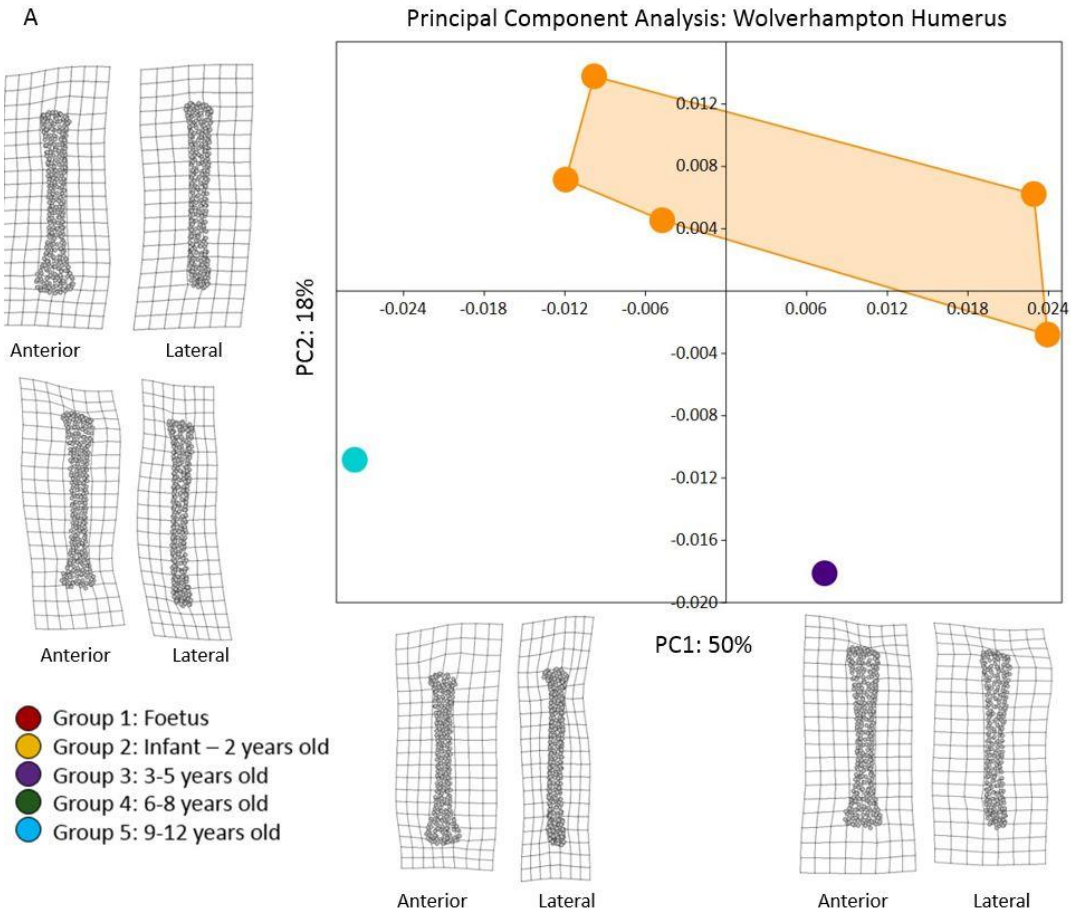
A
Principal Component Analysis: Wolverhampton Humerus
Anterior
Lateral
Anterior
Lateral
PC2: 18%
0.012
0.008
0.004
-0.024
-0.018
-0.012
-0.006
0.006
0.012
0.018
0.024
-0.004
-0.008
-0.012
-0.016
-0.020
PC1: 50%
Anterior
Lateral
Anterior
Lateral
Group 1: Foetus
Group 2: Infant – 2 years old
Group 3: 3-5 years old
Group 4: 6-8 years old
Group 5: 9-12 years old

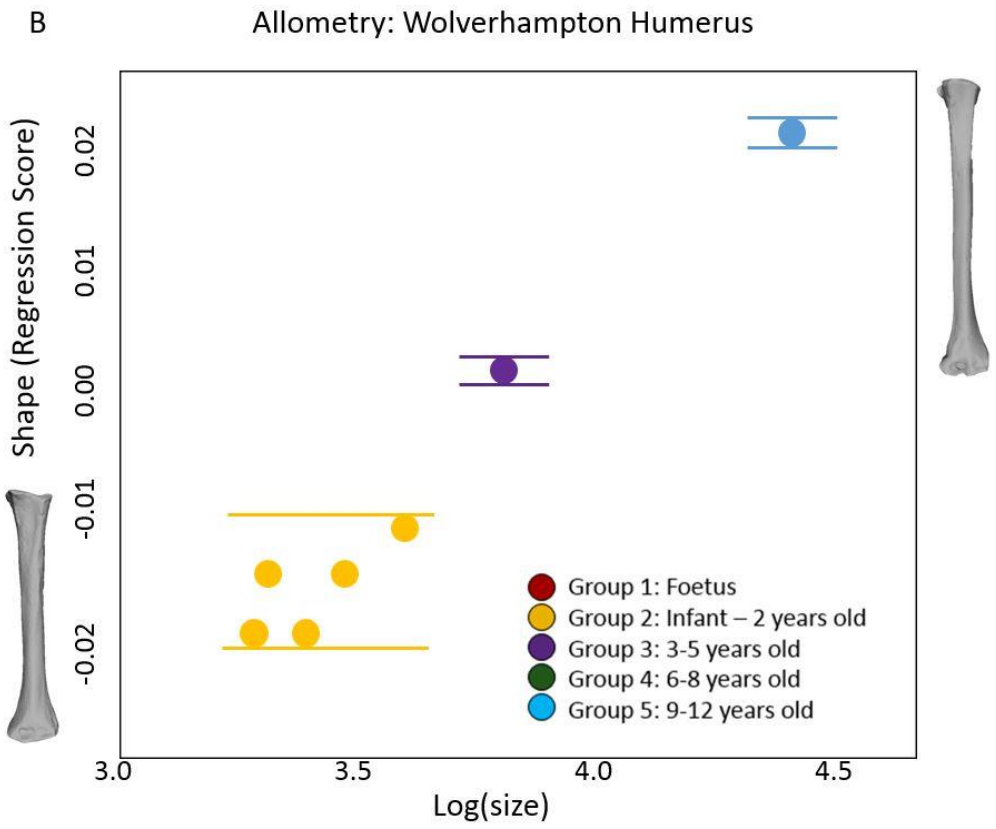
B
Allometry: Wolverhampton Humerus
Shape (Regression Score)
0.02
0.01
0.00
-0.01
-0.02
3.0
3.5
4.0
4.5
Log(size)
Group 1: Foetus
Group 2: Infant – 2 years old
Group 3: 3-5 years old
Group 4: 6-8 years old
Group 5: 9-12 years old

Appendix G: Skeletal Materials

Collection	Period	Urban/ Rural	Skeleton	Age	Group	Femur File	Femur Length (mm)	Tibia File	Tibia Length (mm)	Humerus File	Humerus Length (mm)
Canterbury	Medieval	Urban/ Rural	GR624F	12	5	SGF1	382	SGT1	323	o	o
Canterbury	Medieval	Urban/ Rural	GR5F	12	5	SGF2	374	SGT2	296	o	o
Canterbury	Medieval	Urban/ Rural	GR1014	12	5	o	o	SGT3	294	o	o
Canterbury	Medieval	Urban/ Rural	GR123	12	5	o	o	SGT4	288	o	o
Canterbury	Medieval	Urban/ Rural	GR10	12	5	o	o	o	o	SGH1	264
Canterbury	Medieval	Urban/ Rural	GR860F	11	5	SGF3	338	SGT5	269	o	o
Canterbury	Medieval	Urban /Rural	GR804F	10	5	SGF4	333	SGT6	267	o	o
Canterbury	Medieval	Urban/ Rural	GR97F	10	5	SGF5	331	SGT7	258	o	o
Canterbury	Medieval	Urban/ Rural	GR364F	10	5	SGF6	327	o	o	SGH2	239
Canterbury	Medieval	Urban/ Rural	GR42	9	5	o	o	SGT8	256	SGH4	218
Canterbury	Medieval	Urban/ Rural	GR253F	9	5	SGF7	325	SGT11	243	o	o
Canterbury	Medieval	Urban/ Rural	GR760F	9	5	SGF8	322		o	SGH5	216
Canterbury	Medieval	Urban/ Rural	GR620F	8	4	SGF9	312		o	SGH3	224
Canterbury	Medieval	Urban/ Rural	GR389F	8	4	SGF10	306	SGT9	255	o	o
Canterbury	Medieval	Urban/ Rural	GR90	8	4	o	o	SGT10	251	o	o
Canterbury	Medieval	Urban/ Rural	GR339F	7	4	SGF11	288	SGT16	223	SGH9	196
Canterbury	Medieval	Urban/Rural	GR269F	7	4	SGF12	276	SGT12	235	o	o
Canterbury	Medieval	Urban/Rural	GR607	7	4	o	o	SGT13	231	SGH11	187
Canterbury	Medieval	Urban/ Rural	GR127	7	4	o	o	SGT14	229	SGH6	214
Canterbury	Medieval	Urban/ Rural	GR78	7	4	o	o	SGT15	228	SGH8	200
Canterbury	Medieval	Urban/ Rural	GR859F	7	4	SGF13	276	SGT17	223	SGH10	191
Canterbury	Medieval	Urban/ Rural	GR481F	7	4	SGF14	268	o	o	o	o
Canterbury	Medieval	Urban/ Rural	GR27F	7	4	SGF15	267	SGT18	221	SGH12	187
Canterbury	Medieval	Urban/ Rural	GR650	7	4	o	o	o	o	SGH7	212
Canterbury	Medieval	Urban/ Rural	GR261F	6	4	SGF16	266	o	o	o	o
Canterbury	Medieval	Urban/ Rural	GR82	6	4	o	o	SGT19	218		
Canterbury	Medieval	Urban/ Rural	GR779F	6	4	SGF17	259	o	o	o	o
Canterbury	Medieval	Urban/ Rural	GR286F	6	4	SGF18	254	SGT20	208	o	o
Canterbury	Medieval	Urban/ Rural	GR797F	6	4	SGF19	254	o	o	o	o
Canterbury	Medieval	Urban/ Rural	GR184F	6	4	SGF20	251	SGT21	201	o	o
Canterbury	Medieval	Urban/ Rural	GR1029	6	4	o	o	o	o	SGH13	178
Canterbury	Medieval	Urban/ Rural	GR258	6	4	o	o	o	o	SGH14	167
Canterbury	Medieval	Urban/ Rural	GR782	6	4	o	o	o	o	SGH15	167
Canterbury	Medieval	Urban/ Rural	GR800F	5	3	SGF21	244	o	o	o	o
Canterbury	Medieval	Urban/ Rural	GR801	5	3	o	o	SGT22	197	o	o

Canterbury	Medieval	Urban/ Rural	GR759F	5	3	SGF22	230		o	o	o
Canterbury	Medieval	Urban/ Rural	GR21	5	3	o	o	SGT23	186	SGH17	164
Canterbury	Medieval	Urban/ Rural	GR46	5	3	o	o	SGT24	177	o	o
Canterbury	Medieval	Urban /Rural	GR107	5	3	o	o	o	o	SGH16	166
Canterbury	Medieval	Urban/ Rural	GR161F	4	3	SGF23	227	o	o	o	o
Canterbury	Medieval	Urban/ Rural	GR232F	4	3	SGF24	221	SGT25	176	SGH18	162
Canterbury	Medieval	Urban/ Rural	GR17F	4	3	SGF25	206	SGT27	166	o	o
Canterbury	Medieval	Urban/ Rural	GR83	4	3	o	o	SGT26	167	o	o
Canterbury	Medieval	Urban/ Rural	GR40	4	3	o	o	o	o	SGH19	149
Canterbury	Medieval	Urban/ Rural	GR325	4	3	o	o	o	o	SGH20	143
Canterbury	Medieval	Urban/ Rural	GR753	4	3	o	o	o	o	SGH21	140
Canterbury	Medieval	Urban/ Rural	GR374F	3	3	SGF26	202	SGT28	161	o	o
Canterbury	Medieval	Urban/ Rural	GR1141F	3	3	SGF27	201	o	o	o	o
Canterbury	Medieval	Urban/ Rural	GR823F	3	3	SGF28	194	SGT31	156	o	o
Canterbury	Medieval	Urban/ Rural	GR1009	3	3	o	o	SGT29	159	o	o
Canterbury	Medieval	Urban/ Rural	GR631	3	3	o	o	SGT30	158	o	o
Canterbury	Medieval	Urban/ Rural	GR32	3	3	o	o	o	o	SGH22	138
Canterbury	Medieval	Urban/ Rural	GR26	3	3	o	o	o	o	SGH23	138
Canterbury	Medieval	Urban/ Rural	GR25F	2	2	SGF29	186	o	o	SGH24	135
Canterbury	Medieval	Urban/ Rural	GR373F	2	2	SGF30	185	o	o	o	o
Canterbury	Medieval	Urban/ Rural	GR781F	2	2	SGF31	182	o	o	o	o
Canterbury	Medieval	Urban/ Rural	GR284F	2	2	SGF32	180	SGT33	140	o	o
Canterbury	Medieval	Urban/ Rural	GR26F	2	2	SGF33	179	o	o	o	o
Canterbury	Medieval	Urban/ Rural	GR1179	2	2	o	o	SGT32	145	o	o
Canterbury	Medieval	Urban/ Rural	GR206	2	2	o	o	o	o	SGH25	131
Canterbury	Medieval	Urban/ Rural	GR126F	1	2	SGF34	168	SGT34	137	o	o
Canterbury	Medieval	Urban/ Rural	GR1236F	1	2	SGF35	165			o	o
Canterbury	Medieval	Urban/ Rural	GR755F	1	2	SGF36	164	SGT35	137	o	o
Canterbury	Medieval	Urban/ Rural	GR575F	1	2	SGF37	156	o	o	o	o
Canterbury	Medieval	Urban/ Rural	GR113F	1	2	SGF38	153	o	o	o	o
Canterbury	Medieval	Urban/ Rural	GR178F	1	2	SGF39	140	SGT37	114	o	o
Canterbury	Medieval	Urban/ Rural	GR46BF	1	2	SGF40	128	SGT38	110	o	o
Canterbury	Medieval	Urban/ Rural	GR802	1	2	o	o	SGT36	126	o	o
Canterbury	Medieval	Urban/ Rural	GR102	1	2	o	o	o	o	SGH26	108
Canterbury	Medieval	Urban/ Rural	GR665	1	2	o	o	o	o	SGH27	108
Canterbury	Medieval	Urban/ Rural	GR326F	0	1	SGF41	71	o	o	o	o
Canterbury	Medieval	Urban/ Rural	GR61F	0	1	SGF42	64	SGT40	52	o	o
Canterbury	Medieval	Urban/ Rural	GR95	0	1	o	o	SGT39	98	o	o
Wharram Percy	Medieval	Rural	NA089	10.5	5	WPF2	283	WPT1	219	WPH1	203
Wharram Percy	Medieval	Rural	NA095	9	5	WPF1	289	WPT2	238	WPH2	221
Wharram Percy	Medieval	Rural	NA063	9.5	5	WPF3	293	o	o	o	o

Wharram Percy	Medieval	Rural	NA182	8.5	4	WPF6	260	WPT4	200	o	o
Wharram Percy	Medieval	Rural	G280	8	4	WPF11	287	o	o	WPH3	203
Wharram Percy	Medieval	Rural	EE072	10	5	o	o	o	o	WPH4	200
Wharram Percy	Medieval	Rural	CN04	7	4	WPF5	271	WPT3	208	o	o
Wharram Percy	Medieval	Rural	NA023	7	4	o	o	WPT6	185	o	o
Wharram Percy	Medieval	Rural	NA065	6.5	4	WPF4	277	o	o	WPH5	197
Wharram Percy	Medieval	Rural	NA111	6.5	4	WPF7	249	WPT5	200	WPH6	173
Wharram Percy	Medieval	Rural	NA098	6	4	o	o	WPT9	171	o	o
Wharram Percy	Medieval	Rural	G542	5.5	4	WPF8	228	WPT8	179	WPH7	168
Wharram Percy	Medieval	Rural	NA025	5.5	4	o	o	WPT7	182	WPH8	164
Wharram Percy	Medieval	Rural	NA098	6	4	WPF9	210	o	o	WPH9	160
Wharram Percy	Medieval	Rural	NA120	6	4	WPF10	210	o	o	WPH10	155
Wharram Percy	Medieval	Rural	NA110	4	3	o	o	WPT10	151	o	o
Wharram Percy	Medieval	Rural	WC0163	4	3	WPF12	180	o	o	o	o
Wharram Percy	Medieval	Rural	NA079	3	3	o	o	WPT11	145	WPH11	140
Wharram Percy	Medieval	Rural	WC0100	2.5	3	WPF13	171	o	o	WPH12	134
Wharram Percy	Medieval	Rural	G367	3	3	o	o	WPT12	138	WPH13	133
Wharram Percy	Medieval	Rural	WC0108	2.5	3	WPF14	159	o	o	WPH14	132
Wharram Percy	Medieval	Rural	NA165	1.8	2	WPF15	162	o	o	o	o
Wharram Percy	Medieval	Rural	NA028	1.5	2	o	o	o	o	WPH15	111
Wharram Percy	Medieval	Rural	G522	1.3	2	o	o	WPT13	104	o	o
Wharram Percy	Medieval	Rural	NA203A	0.5	2	o	o	o	o	WPH16	99
Wharram Percy	Medieval	Rural	NA092	0.4	2	o	o	o	o	WPH17	84
Wharram Percy	Medieval	Rural	NA052	0	1	o	o	o	o	WPH18	77
Wharram Percy	Medieval	Rural	NA064	0	1	o	o	WPT15	72	WPH19	73
Wharram Percy	Medieval	Rural	NA193	0	1	o	o	WPT14	74	WPH20	72
Wharram Percy	Medieval	Rural	NA037A	0	1	o	o	o	o	WPH21	65
Wharram Percy	Medieval	Rural	EE088	0	1	o	o	o	o	WPH22	62
Wharram Percy	Medieval	Rural	V03	0	1	WPF17	68	o	o	WPH23	61
Wharram Percy	Medieval	Rural	EE034	0	1	o	o	WPT16	61	o	o
Wharram Percy	Medieval	Rural	NA099	0	1	o	o	WPT17	58	o	o
Wharram Percy	Medieval	Rural	NA170A	0	1	WPF16	86	o	o	o	o
Wharram Percy	Medieval	Rural	NA082	0	1	WPF18	66	o	o	o	o
Great Chesterford	Anglo-Saxon	Rural	121	12	5	o	o	GCT1	311	o	o
Great Chesterford	Anglo-Saxon	Rural	119	9	5	GCF1	336	o	o	o	o
Great Chesterford	Anglo-Saxon	Rural	17	9	5	GCF2	267	o	o	o	o
Great Chesterford	Anglo-Saxon	Rural	147	7	4	o	o	GCT2	187	o	o
Great Chesterford	Anglo-Saxon	Rural	118	5.5	4	GCF3	222	GCT3	175	o	o
Great Chesterford	Anglo-Saxon	Rural	111	1.5	3	GCF4	137.98	GCT4	111.96	o	o

Great Chesterford	Anglo-Saxon	Rural	141	3	3	o	o	o	o	GCH1	113.51
Great Chesterford	Anglo-Saxon	Rural	158	3	3	o	o	o	o	GCH9	146
Great Chesterford	Anglo-Saxon	Rural	136	1.5	2	o	o	o	o	GCH2	113.51
Great Chesterford	Anglo-Saxon	Rural	99	1.5	2	o	o	o	o	GCH3	112
Great Chesterford	Anglo-Saxon	Rural	107	0.8	2			GCT5	95	GCH4	85.41
Great Chesterford	Anglo-Saxon	Rural	105	0.3	2	GCF5	94.78	o	o	o	o
Great Chesterford	Anglo-Saxon	Rural	58	0.3	2	GCF6	93.05	o	o	GCH5	78.26
Great Chesterford	Anglo-Saxon	Rural	143	0.3	2	GCF7	88.4	o	o	GCH6	73.16
Great Chesterford	Anglo-Saxon	Rural	61	0.3	2	GCF8	81.42	o	o	o	o
Great Chesterford	Anglo-Saxon	Rural	32	0.3	2	o	o	o	o	GCH7	69.53
Great Chesterford	Anglo-Saxon	Rural	64	0.2	2	GCF9	78.34	o	o	o	o
Great Chesterford	Anglo-Saxon	Rural	83	0.2	2	GCF10	77	GCT8	66.05	o	o
Great Chesterford	Anglo-Saxon	Rural	83.1	0	1	GCF11	77.27	GCT7	68.05	GCH10	67.21
Great Chesterford	Anglo-Saxon	Rural	71	0.2	2	o	o	GCT6	69.93	GCH11	66.35
Great Chesterford	Anglo-Saxon	Rural	70	0.2	2	GCF12	77.82	o	o	GCH8	68.52
Great Chesterford	Anglo-Saxon	Rural	88	0.3	2	GCF13	75.25	o	o	GCH12	64.59
Great Chesterford	Anglo-Saxon	Rural	89	0.2	2	GCF14	74.69	o	o	o	o
Great Chesterford	Anglo-Saxon	Rural	95	0.2	2	GCF15	72.83	GCT9	62.2	o	o
Great Chesterford	Anglo-Saxon	Rural	43	0	1	GCF16	68.19	o	o	o	o
Great Chesterford	Anglo-Saxon	Rural	49	0.2	2	GCF17	75.89	o	o	o	o
Great Chesterford	Anglo-Saxon	Rural	104	0	1	GCF18	61.64	o	o	o	o
Raunds	Anglo-Saxon	Rural	5037	12	5	RAF1	322.24	o	o	o	o
Raunds	Anglo-Saxon	Rural	5265	12	5	RAF2	254.6	o	o	o	o
Raunds	Anglo-Saxon	Rural	5200	11	5	o	o	RAT1	279.43	o	o
Raunds	Anglo-Saxon	Rural	5168	11	5	o	o	RAT2	249.12	o	o
Raunds	Anglo-Saxon	Rural	5317	10	5	o	o	o	o	RAH1	223.63
Raunds	Anglo-Saxon	Rural	5014	9	4	o	o	RAT3	236.45		
Raunds	Anglo-Saxon	Rural	5041	8	4	RAF3	244.97	RAT6	207.43	RAH2	178.19
Raunds	Anglo-Saxon	Rural	5131	7	4	RAF4	202.51	o	o	o	o
Raunds	Anglo-Saxon	Rural	5281	8	4	RAF5	263.13	RAT5	222.11	RAH4	184.37
Raunds	Anglo-Saxon	Rural	5335	7	4	RAF6	203.68	RAT4	155.05	o	o
Raunds	Anglo-Saxon	Rural	5216	7	4	o	o	o	o	RAH3	183
Raunds	Anglo-Saxon	Rural	5032	6	4	o	o	RAT7	159.82	o	o
Raunds	Anglo-Saxon	Rural	5297	6	4	o	o	o	o	RAH5	151.52
Raunds	Anglo-Saxon	Rural	5335	6	4	o	o	o	o	RAH6	150.6
Raunds	Anglo-Saxon	Rural	5194	3	3	RAF7	182.91	o	o	o	o
Raunds	Anglo-Saxon	Rural	5208	5	3	RAF8	153.2	o	o	RAH8	113.76
Raunds	Anglo-Saxon	Rural	5199	5	3	o	o	o	o	RAH7	137.57
Raunds	Anglo-Saxon	Rural	5271	3	3	RAF9	182.81	o	o	o	o
Raunds	Anglo-Saxon	Rural	5274	3	3	RAF10	182.72	o	o	RAH9	127.13
Raunds	Anglo-Saxon	Rural	5345	3	3	o	o	RAT8	128.78	RAH10	125.91

Raunds	Anglo-Saxon	Rural	5096	0.6	2	RAF11	110.62	o	o	o	o
Raunds	Anglo-Saxon	Rural	5279	0.3	2	RAF12	68.37	RAT11	58.49	o	o
Raunds	Anglo-Saxon	Rural	5302	2	2	RAF13	125.59	o	o	o	o
Raunds	Anglo-Saxon	Rural	5310	2	2	o	o	RAT9	97.75	o	o
Raunds	Anglo-Saxon	Rural	5280	2	2	o	o	RAT10	131.04	o	o
Raunds	Anglo-Saxon	Rural	5304	0.6	2	RAF14	98.34	o	o	o	o
Raunds	Anglo-Saxon	Rural	5329	2	2	RAF15	103.36	o	o	o	o
Raunds	Anglo-Saxon	Rural	5305	0	1	RAF16	61.71	o	o	o	o
Raunds	Anglo-Saxon	Rural	5216	12	5	RAF17	259.45	o	o	o	o
Raunds	Anglo-Saxon	Rural	5185	0.6	2	o	o	RAT12	59	RAH11	86.7
Wolverhampton	Post-Medieval	Urban	Wol147T	12	5	o	o	Wol2T	284.8	o	o
Wolverhampton	Post-Medieval	Urban	Wol55T	10	5	o	o	Wol1T	228.31	o	o
Wolverhampton	Post-Medieval	Urban	Wol20H	9	5	o	o	o	o	WolH1	194.78
Wolverhampton	Post-Medieval	Urban	Wol48T	7	4	o	o	Wol4T	178.16	o	o
Wolverhampton	Post-Medieval	Urban	Wol 139F	7	4	Wol1F	245.24	o	o	o	o
Wolverhampton	Post-Medieval	Urban	Wol68T	4	3	Wol2F	194.57	Wol3T	153.52	o	o
Wolverhampton	Post-Medieval	Urban	Wol110H	3	3	o	o	o	o	WolH2	103.53
Wolverhampton	Post-Medieval	Urban	Wol50H	0.2	2	Wol3F	64.59	Wol5T	72.24	WolH3	70.43
Wolverhampton	Post-Medieval	Urban	Wol79bH	0.2	2	Wol4F	61.45	o	o	WolH4	66.7
Wolverhampton	Post-Medieval	Urban	Wol103H	1	2	o	o	o	o	WolH5	98.27
Wolverhampton	Post-Medieval	Urban	Wol64H	0.2	2	o	o	o	o	WolH6	64.14
Wolverhampton	Post-Medieval	Urban	Wol102H	1.5	2	o	o	o	o	WolH7	103.89
Denver Growth Study	Modern	Urban	Modern	0.125	1	MF1	86	MT1	70	MH1	71
Denver Growth Study	Modern	Urban	Modern	0.25	2	MF2	100	MT2	81	MH2	80
Denver Growth Study	Modern	Urban	Modern	0.5	2	MF3	111	MT3	90	MH3	87
Denver Growth Study	Modern	Urban	Modern	1	2	MF4	135	MT4	109	MH4	104
Denver Growth Study	Modern	Urban	Modern	1.5	2	MF5	154	MT5	125	MH5	118
Denver Growth Study	Modern	Urban	Modern	2	2	MF6	171	MT6	139	MH6	128
Denver Growth Study	Modern	Urban	Modern	2.5	3	MF7	186	MT7	151	MH7	137.5
Denver Growth Study	Modern	Urban	Modern	3	3	MF8	199	MT8	162	MH8	146
Denver Growth Study	Modern	Urban	Modern	3.5	3	MF9	211	MT9	172	MH9	154
Denver Growth Study	Modern	Urban	Modern	4	3	MF10	223	MT10	181	MH10	161
Denver Growth Study	Modern	Urban	Modern	4.5	3	MF11	235	MT11	191	MH11	169

Denver Growth Study	Modern	Urban	Modern	5	3	MF12	247	MT12	200	MH12	175
Denver Growth Study	Modern	Urban	Modern	5.5	4	MF13	258	MT13	209	MH13	183
Denver Growth Study	Modern	Urban	Modern	6	4	MF14	269	MT14	218	MH14	190
Denver Growth Study	Modern	Urban	Modern	6.5	4	MF15	280	MT15	226	MH15	196.5
Denver Growth Study	Modern	Urban	Modern	7	4	MF16	290	MT16	235	MH16	203
Denver Growth Study	Modern	Urban	Modern	7.5	4	MF17	300	MT17	243	MH17	210
Denver Growth Study	Modern	Urban	Modern	8	4	MF18	311	MT18	252	MH18	216
Denver Growth Study	Modern	Urban	Modern	8.5	5	MF19	320	MT19	260	MH19	222
Denver Growth Study	Modern	Urban	Modern	9	5	MF20	329	MT20	267	MH20	228
Denver Growth Study	Modern	Urban	Modern	9.5	5	MF21	339	MT21	276	MH21	235
Denver Growth Study	Modern	Urban	Modern	10	5	MF22	348	MT22	284	MH22	240
Denver Growth Study	Modern	Urban	Modern	10.5	5	MF23	357	MT23	292	MH23	245
Denver Growth Study	Modern	Urban	Modern	11	5	MF24	367	MT24	299	MH24	251
Denver Growth Study	Modern	Urban	Modern	11.5	5	MF25	377	MT25	208	MH25	258
Denver Growth Study	Modern	Urban	Modern	12	5	MF26	387	MT26	316	MH26	264

Glossary of Terms

Allometry: Changes in shape correlating to changes in size (Zelditch *et al.* 2012: 455).

Bending Energy: A measure of the amount of non-uniform force needed to bend an infinitely thing steel plate by a given amplitude between points (i.e. landmarks). This 'measure' provides a spatial scale as it takes more energy to bend the plate by a given amount between closely spaced landmarks than between more distantly spaced landmarks. For instance principal warps with large eigenvalues represent more localized components of deformation than principal warps with smaller eigenvalues (Zelditch *et al.,* 2012; 456).

Centroid Size: A measure of geometric scale that is calculated as the square root of the summed squared distances of each landmark from the centroid of the landmark configuration. This provides the size measure used in GM and is uncorrelated with shape in the absence of allomery (Zelditch *et al.* 2012; 457).

Deformation: A smooth and continuous mapping used in morphometrics, typically the transformation of one shape into another. The deformation refers to changes in landmark positions and interpolated changes in locations of unanalysed points between landmarks (Zelditch *et al.* 2012: 458).

Development: Is the pathways of biological milestones along the life cycle (Agarwal 2016: 132). This processes is analysed through the correlation of shape and age.

Generalized Procrustes Analysis: The superimposition of a set of specimens onto their mean. This can be done with two-dimensional or three-dimensional landmark coordinates. The analysis can be performed on fixed landmark points, semi-landmarks on curves, semi-landmarks on surfaces, or any combination. This is the primary means for shape variables to be obtained from landmark data. This method translates all specimens to the origin, scales them to unit-centroid size, and rotates them (using a least-squares criterion) until the coordinates of corresponding points align as closely as possible. The final aligned Procrustes coordinates represent the shape of each specimen and are found in a curved space related to Kendall's shape space (Kendall 1984). Any semi-landmarks on curves are slid along their tangent directions or planes during the superimposition (Zelditch *et al.* 2012; 460).

Growth: The process of enlarging tissues with chronological age (Agarwal 2016: 132). This process is described by the correlation of size and age of a specimen.

Homology: In biological terms, similarity due to common evolutionary origin. In morphometrics, the correspondences between landmarks (Zelditch *et al.* 2012; 460).

Landmark: In biology these are discrete and homologous anatomical loci. Mathematically, they are point of correspondence that match within and between populations (Zelditch *et al.* 2012; 461).

Ontogenetic Trajectory: Change in shape correlated with increasing size and age (Zelditch *et al.* 2012: 455). This process encompasses growth, development, and allometry for each individual.

Principal Component Analysis: This method of shape variation plots two dimensions of tangent space for a set of Procrustes-aligned specimens (commonly PC1 vs. PC2). The percent of variation along each PC-axis is presented and deformation grids display the shape of specimens at the ends of the range of variation along each PC axis (Zelditch *et al.* 2012; 464).

Semi-landmarks: A point on a geometric feature such as a curve, edge or surface. A sliding semi-landmark slides between two landmark points to capture the geometric information in that region.

Shape: In regards to geometric morphometrics, it is all geometric information remaining in a landmark configuration (series of landmarks) after location, rotation, and scale are removed (Zelditch *et al.* 2012; 466).

Size: Measures of size include lengths between landmarks, sums or differences of interlandmark distances, square roots of area, etc. GM size is referred to as the centroid size.

List of References

ADAMS, D.C., Rohlf, F.J. and Slice, D.E., 2004. Geometric morphometrics: ten years of progress following the 'revolution'. Italian Journal of Zoology, 71(1), pp.5-16.

ADAMS, J.C., Colls, K. 2007. Out of Darkness, Cometh Light: Life and death in Nineteenth-Century Wolverhampton: Excavation of the Overflow Burial Ground of St Peter's Collegiate Church, Wolverhampton 2001-2002. BAR British Series 442 Archeopress, Oxford

ADAMS, D.C., Otarola-Catillo, E., and Sherratt, E. 2014. *geomorph*: software for geometric morphometric analyses. R package version 2.0. http://cran.r-project.org/web/packages/*geomorph*?index.html

ADOLPH, K.E. and Robinson, S.R., 2013. The road to walking: What learning to walk tells us about development. *Oxford handbook of developmental psychology*, *1*, pp.403-443.

ADOLPH, K.E., 2008. Learning to move. *Current Directions in Psychological Science*, *17*(3), pp.213-218.

ADOLPH, K.E. and Robinson, S.R., 2013. The road to walking: What learning to walk tells us about development. *Oxford handbook of developmental psychology*, *1*, pp.403-443.

AGARWAL, S.C., 2016. Bone morphologies and histories: Life course approaches in bioarchaeology. *American journal of physical anthropology*, *159*(S61), pp.S130-S149.

AGARWAL, S.C. and Beauchesne, P., 2011. It is not Carved in Bone. *Social bioarchaeology*, pp.312-332.

AGISOFT., L.L..C. 2013. Agisoft PhotoScan Professional Edition Help.

AIELLO, L. and Dean, C., An introduction to human evolutionary anatomy, 1990.

ALBERCH, P., Gould, S.J., Oster, G.F. and Wake, D.B., 1979. Size and shape in ontogeny and phylogeny. *Paleobiology*, *5*(3), pp.296-317.

ALEXANDER, R.M., 1981. Factors of safety in the structure of animals. *Science Progress (1933-)*, pp.109-130.

ALLEN, H,L,. Estrada K., Lettre G., Berndt S.I., Weedon, M.N., Rivadeneira, F., Willer, C.J., Jackson, A.U., Vedantam, S., Raychaudhuri, S., *et al*. 2010. Hundreds of variants clustered in genomic loci and biological pathways affect human height. *Nature.* 467: 832-838.

ANDERSON, T. and Carter, A.R., 1994. Periosteal reaction in a new born child from Sheppey, Kent. *International Journal of Osteoarchaeology*, *4*(1), pp.47-48.

ANDERSON, T. and Carter, A.R., 1995. An unusual osteitic reaction in a young medieval child. *International Journal of Osteoarchaeology*, *5*(2), pp.192-195.

ANDERSON, J.Y. and Trinkaus, E., 1998. Patterns of sexual, bilateral and interpopulational variation in human femoral neck-shaft angles. *The Journal of Anatomy*, *192*(2), pp.279-285.

ANDERSON, T., and Andrews, J. 2001. The Human Remains. In: St Gregory's Priory Northgate Canterbury Excavations 1988-1991. Canterbury Archaeological Trust LTD, Canterbury. pp. 338-370.

ARMELAGOS, G.J., 2003. . Bioarchaeology as Anthropology. *Archeological Papers of the American Anthropological Association*, *13*(1), pp.27-40.

ARMELAGOS, G.J., Mielke, J.H., Owen, K.H., Van Gerven, D.P., Dewey, J.R. and Mahler, P.E., 1972. Bone growth and development in prehistoric populations from Sudanese Nubia. *Journal of Human Evolution*, *1*(1), pp.89-119.

AUERBACH, B.M., 2008. Human skeletal variation in the New World during the Holocene: Effects of climate and subsistence across geography and time-Part I. THE JOHNS HOPKINS UNIVERSITY.

BAILEY, R.C. and Byrnes, J., 1990. A new, old method for assessing measurement error in both univariate and multivariate morphometric studies. *Systematic Zoology*, *39*(2), pp.124-130.

BAKER, P.T., Hannah, M.J., Baker, T.S. 1986. The changing Samoans. Oxford Oxford Univeristy Press.

BARKER, DJP. 2012. Developmental origins of chronic disease. Public Health 126:185–189.

BARKER, D.J., Osmond, C., Winter, P.D., Margetts, B. and Simmonds, S.J., 1989. Weight in infancy and death from ischaemic heart disease. *The Lancet*, *334*(8663), pp.577-580.

BARKER, D.J., Eriksson, J.G., Forsén, T. and Osmond, C., 2002. Fetal origins of adult disease: strength of effects and biological basis. *International journal of epidemiology*, *31*(6), pp.1235-1239.

BASS, S., Delmas, P.D., Pearce, G., Hendrich, E., Tabensky, A. and Seeman, E. 1999. The differing tempo of growth in bone size, mass, and density in girls is region-specific. *The Journal of clinical investigation*, *104*(6), pp.795-804.

BASTIR, M., Martínez, D.G., Recheis, W., Barash, A., Coquerelle, M., Rios, L., Peña-Melián, Á., Río, F.G. and O'Higgins, P., 2013. Differential growth and development of the upper and lower human thorax. *PloS one*, *8*(9), p.e75128.

BATESON, P., 2001. Fetal experience and good adult design a. *International journal of epidemiology*, *30*(5), pp.928-934.

BATESON, P., Barker, D., Clutton-Brock, T., Deb, D., D'Udine, B., Foley, R.A., Gluckman, P., Godfrey, K., Kirkwood, T., Lahr, M.M. and McNamara, J., 2004. Developmental plasticity and human health. *Nature*, *430*(6998), pp.419-421.

BAXTER, J.H. 1875. Statistics, Medical and Anthropological, of Over a Million Recruits. Washington, DC: Government Printing Office.

BAXTER, J.E., 2008. The archaeology of childhood. *Annual Review of Anthropology*, *37*, pp.159-175.

BBC. 2014. Victorian Britain. http://www.bbc.co.uk/schools/primaryhistory/victorian_britain/victorian_children_at_work/teachers_resources.shtml. Accessed 27 September 2017.

BEAUMONT, J., Gledhill, A., Lee-Thorp, J. and Montgomery, J., 2013. Childhood diet: a closer examination of the evidence from dental tissues using stable isotope analysis of incremental human dentine. *Archaeometry*, *55*(2), pp.277-295.

BENNIKE, P., Lewis, M.E., Schutkowski, H. and Valentin, F., 2005. Comparison of child morbidity in two contrasting medieval cemeteries from Denmark. *American journal of physical anthropology*, *128*(4), pp.734-746.

BEN-SHLOMO, Y. and Kuh, D., 2002. A life course approach to chronic disease epidemiology: conceptual models, empirical challenges and interdisciplinary perspectives.

BENSON-MARTIN, J., Zammaretti, P., Bilic, G., Schweizer, T., Portmann-Lanz, B., Burkhardt, T., Zimmermann, R. and Ochsenbein-Kölble, N., 2006. The Young's modulus of fetal preterm and term

amniotic membranes. *European journal of obstetrics & gynecology and reproductive biology*, *128*(1), pp.103-107.

BERESFORD, M.W. 1987. 'The Documentary Evidence'. In: J.G. Hurst and P.A. Rahtz, *Wharram: A Study of Settlement on the Yorkshire Wolds, III: Wharram Percy: The church of St Martin.* London: The Society for Medieval Archaeology Monograph Series: No.11.

BERESFRORD, M. and Hurst, J. 1990. English Heritage Book of Wharram Percy Deserted Medieval Village. Batsford Ltd.

BERGE, C. and Penin, X., 2004. Ontogenetic allometry, heterochrony, and interspecific differences in the skull of African apes, using tridimensional Procrustes analysis. *American Journal of Physical Anthropology*, *124*(2), pp.124-138.

BERTRAM, J.E. and Biewener, A.A., 1988. Bone curvature: sacrificing strength for load predictability?. *Journal of Theoretical Biology*, *131*(1), pp.75-92.

BESL, P.J. and McKay, N.D., 1992. A method for registration of 3-D shapes. *IEEE Transactions on pattern analysis and machine intelligence*, *14*(2), pp.239-256.

BLACKITH, R.E. and Reyment, R.A., 1971. *Multivariate morphometrics*.

BLACKWELL, D.L., Hayward, M.D. and Crimmins, E.M., 2001. Does childhood health affect chronic morbidity in later life?. *Social science & medicine*, *52*(8), pp.1269-1284.

BLAKEY, M.L. and Armelagos, G.J., 1985. Deciduous enamel defects in prehistoric Americans from Dickson Mounds: prenatal and postnatal stress. *American Journal of Physical Anthropology*, *66*(4), pp.371-380.

BOAS, F., 1912. Changes in the bodily form of descendants of immigrants. *American Anthropologist*, *14*(3), pp.530-562.

BOAS, F., 1922. The measurement of differences between variable quantities. *Journal of the American Statistical Association*, *18*(140), pp.425-445.

BODDINGTON, A. 1996. *Raunds Furnells: the Anglo-Saxon church and churchyard* (Vol. 7). London: English Heritage.

BOGIN, B. 1988. *Patterns of Human Growth*. Second Edition. Cambridge University Press.

BOGIN, B., 1995. Plasticity in the growth of Mayan refugee children living in the United States. *Human variability and plasticity. Cambridge: Cambridge University Press. p*, pp.46-74.

BOGIN, B., 1999. Evolutionary perspective on human growth. *Annual Review of Anthropology*, pp.109-153.

BOGIN, B., Smith, P., Orden, A.B., Varela Silva, M.I. and Loucky, J., 2002. Rapid change in height and body proportions of Maya American children. *American Journal of Human Biology*, *14*(6), pp.753-761.

BONNEAU, N., Simonis, C., Seringe, R. and Tardieu, C., 2011. Study of femoral torsion during prenatal growth: interpretations associated with the effects of intrauterine pressure. *American journal of physical anthropology*, *145*(3), pp.438-445.

BOOKSTEIN, F.L., 1985. Morphometrics in evolutionary biology: the geometry of size and shape change, with examples from fishes. Academy of Natural Sciences.

BOOKSTIEN, F.L., 1989. Principal warps: Thin-plate splines and the decomposition of deformations. *IEEE Transactions on pattern analysis and machine intelligence*, *11*(6), pp.567-585.

BOOKSTEIN, F.L., 1998. A hundred years of morphometrics. *Acta Zoologica Academiae Scientiarum Hungaricae*, *44*(1-2), pp.7-59.

BOOKSTEIN, F.L. 1991. Thin-plate splines and the atlas problem of biomedical images. In *Biennial International Conference on Information Processing in Medical Imaging.* pp/ 326-342. Springer, Berlin, Heidelberg.

BOOKSTEIN, F.L. 1996. Biometrics, biomathematics and the morphometric synthesis. *Bulletin of mathematical biology*, *58*(2) 313-365.

BOOKSTEIN, F.L., 1997. Morphometric tools for landmark data: geometry and biology. Cambridge University Press.

BOOKSTEIN, F., Schäfer, K., Prossinger, H., Seidler, H., Fieder, M., Stringer, C., Weber, G.W., Arsuaga, J.L., Slice, D.E., Rohlf, F.J. and Recheis, W. 1999. Comparing frontal cranial profiles in archaic and modern Homo by morphometric analysis. *The Anatomical Record*, *257*(6), pp.217-224.

BOUCHER, B.J., 1957. Sex differences in the foetal pelvis. *American Journal of Physical Anthropology*, *15*(4), pp.581-600.

BOWDITCH, H.P., 1879. *The growth of children: A supplementary investigation*. Rand, Avery & Company.

BOWMAN, J.E., MacLaughlin, S.M., and Scheue, J.L. 1993. A study of documentary and skeletal evidence relating to 18th and 19th century crypt burials in the City of London: The St. Bride's Project, *American Journal of Physical Anthropology,* Suppl 16, 60.

BOYER, D.M., Lipman, Y., Clair, E.S., Puente, J., Patel, B.A., Funkhouser, T., Jernvall, J. and Daubechies, I., 2011. Algorithms to automatically quantify the geometric similarity of anatomical surfaces. *Proceedings of the National Academy of Sciences*, *108*(45), pp.18221-18226.

BOYER, D.M., Punente, J. Gladman, J.T., Glynn, C., Mukherjee, S., Yapuncich, G.S., and Daubechies, I. 2015. A new fully automated approach for aligning and comparing shapes. *The Anatomical Record,* 29(1), 249-276.

BRADNEY, M., Karlsson, M.K., Duan, Y., Stuckey, S., Bass, S. and Seeman, E. 2000. Heterogeneity in the growth of the axial and appendicular skeleton in boys: implications for the pathogenesis of bone fragility in men. *Journal of Bone and Mineral Research*, *15*(10), pp.1871-1878.

BREARS, P.C., 2008. *Cooking and dining in medieval England*. Prospect Books (UK).

BERQUIST, R.M., Gledhill, K.M., Peterson, M.W., Doan, A.H., Baxter, G.T., Yopak, K.E., Kang, N., Walker, H.J., Hastings, P.A. and Frank, L.R., 2012. The Digital Fish Library: using MRI to digitize, database, and document the morphological diversity of fish. *PLoS One*, *7*(4), p.e34499.

BRICKLEY, M. and Ives, R., 2006. Skeletal manifestations of infantile scurvy. *American Journal of Physical Anthropology*, *129*(2), pp.163-172.

BRONSTEIN, A.M., Bronstein, M.M. and Kimmel, R., 2006. Efficient computation of isometry-invariant distances between surfaces. *SIAM Journal on Scientific Computing*, *28*(5), pp.1812-1836.

BUCKBERRY, J., 2000. Missing, presumed buried? Bone diagenesis and the under-representation of Anglo-Saxon children.

BUIKSTRA, JE, Beck LA, editors. 2009. Bioarchaeology: the contextual analysis of human remains. Walnut Creek, CA: Left Coast Press.

BUIKSTRA, J.E. and Cook, D.C., 1980. Palaeopathology: an American account. *Annual Review of Anthropology*, pp.433-470.

BULYGINA, E., Mitteroecker, P. and Aiello, L., 2006. Ontogeny of facial dimorphism and patterns of individual development within one human population. *American Journal of Physical Anthropology*, *131*(3), pp.432-443.

CABANA, T., Jolicoeur, P. and Michaud, J., 1993. Prenatal and postnatal growth and allometry of stature, head circumference, and brain weight in Québec children. *American Journal of Human Biology*, *5*(1), pp.93-99

CADMAN, G., Foard, G. and Faull, M.L., 1984. Studies in Late Anglo-Saxon Settlement.

CAMERON, N. and Demerath, E.W., 2002. Critical periods in human growth and their relationship to diseases of aging. *American journal of physical anthropology*, *119*(S35), pp.159-184.

CAMPBELL, G. 1994. The preliminary archaeobotanical results from Anglo-Saxon West Cotton and Raunds, in Rackham (ed.), *Environment and Economy in Anglo-Saxon England,* 65-82.

CARPENTER, R.D. and Carter, D.R., 2008. The mechanobiological effects of periosteal surface loads. *Biomechanics and modeling in mechanobiology*, *7*(3), pp.227-242.

CARRANO, M.T., 1999. What, if anything, is a cursor? Categories versus continua for determining locomotor habit in mammals and dinosaurs. *Journal of Zoology*, *247*(1), 29-42.

CARRIER, D.R., 1996. Ontogenetic limits on locomotor performance. *Physiological zoology*, *69*(3), pp.467-488.

CARTER, D.R., Polefka, E.L. and Beaupré, G.S., 2000. Mechanical influences on skeletal regeneration. In *Human Biomechanics and Injury Prevention* (pp. 129-136). Springer, Tokyo.

CARTER, D.R. and Beaupré, G.S., 2001. *Skeletal function and form: mechanobiology of skeletal development, aging, and regeneration*. Cambridge University Press.

CHENERY, C., Müldner, G., Evans, J., Eckardt, H. and Lewis, M., 2010. Strontium and stable isotope evidence for diet and mobility in Roman Gloucester, UK. *Journal of archaeological Science*, *37*(1), pp.150-163.

CLAUSEN, J. 1985. The life course: a sociological perspective, 1ed. Englewood Cliffs, NJ: Pearson.

CLOUDCOMPARE. Version 2. 7, GPL software. 2016. Retrieved from http://www.cloudcompare.org/

COBB, S.N. and O'Higgins, P., 2004. Hominins do not share a common postnatal facial ontogenetic shape trajectory. *Journal of Experimental Zoology Part B: Molecular and Developmental Evolution*, *302*(3), pp.302-321.

COCKBURN, T.A., 1971. Infectious diseases in ancient populations. *Current Anthropology*, *12*(1), pp.45-62.

COHEN, M.N., 2009. Introduction: rethinking the origins of agriculture. *Current Anthropology*, *50*(5), pp.591-595.

COLLYER, M.L., Sekora, D.J. and Adams, D.C. 2015. A method for analysis of phenotypic change for phenotypes described by high-dimensional data. *Heredity*.

COQUERELLE, M., Bookstein, F.L., Braga, J., Halazonetis, D.J., Weber, G.W. and Mitteroecker, P., 2011. Sexual dimorphism of the human mandible and its association with dental development. *American journal of physical anthropology*, *145*(2), pp.192-202.

COWGILL, L.W., Warrener, A., Pontzer, H. and Ocobock, C., 2010. Waddling and toddling: the biomechanical effects of an immature gait. *American journal of physical anthropology*, *143*(1), pp.52-61.

CRAIG, E. and Buckberry, J., 2010. Investigating social status using evidence of biological status: a case study from Raunds Furnells.

CRAWFORD, S., 1991. When do Anglo-Saxon children count. *Journal of Theoretical Archaeology*, *2*, pp.17-24.

CRAWFORD, S., 1999. *Childhood in Anglo-Saxon England*. Sutton Publishing.

CURREY, J.D., 2003. The many adaptations of bone. *Journal of biomechanics*, *36*(10), pp.1487-1495.

DANIELL, C. 1997. *Death and burial in medieval England 1066–1550*. London: Routledge.

DAVENPORT, C.B., 1933. The crural index. *American Journal of Physical Anthropology*, *17*(3), pp.333-353.

DAVEY SMITH, G. 2011. Epidemiology, epigenetics and the 'gloomy prospect': embracing randomness in population health research and practice. Int J Epidemiol 40:537–562.

DAVIES, T.G., Rahman, I.A., Lautenschlager, S., Cunningham, J.A., Asher, R.J., Barrett, P.M., Bates, K.T., Bengtson, S., Benson, R.B., Boyer, D.M. and Braga, J., 2017, April. Open data and digital morphology. In *Proc. R. Soc. B* (Vol. 284, No. 1852, p. 20170194). The Royal Society.

DAWSON, H., 2014. Unearthing Late Medieval Children. *BAR British Series*, *593*.

DEAN, D., Hans, M.G., Bookstein, F.L. and Subramanyan, K., 2000. Three-dimensional Bolton–Brush Growth Study landmark data: ontogeny and sexual dimorphism of the Bolton standards cohort. *The Cleft palate-craniofacial journal*, *37*(2), pp.145-156.

DE GROOTE, I., 2008. A comprehensive analysis of long bone curvature in Neanderthals and Modern Humans using 3D morphometrics. Doctoral thesis. University of London.

DE GROOTE, I., 2011. Femoral curvature in Neanderthals and modern humans: a 3D geometric morphometric analysis. *Journal of human evolution*, *60*(5), pp.540-548.

DE GROOTE, I., Lockwood, C.A. and Aiello, L.C., 2010. A new method for measuring long bone curvature using 3D landmarks and semi-landmarks. *American journal of physical anthropology*, *141*(4), pp.658-664.

DE VITO, C. and Saunders, S.R., 1990. A discriminant function analysis of deciduous teeth to determine sex. *Journal of Forensic Science*, *35*(4), pp.845-858.

DEWITTE, S.N. and Wood, J.W., 2008. Selectivity of Black Death mortality with respect to preexisting health. *Proceedings of the National Academy of Sciences*, *105*(5), pp.1436-1441.

DMITRIEW, C.M., 2011. The evolution of growth trajectories: what limits growth rate?. *Biological Reviews*, *86*(1), pp.97-116.

DUDA, G.N., Schneider, E. and Chao, E.Y., 1997. Internal forces and moments in the femur during walking. *Journal of biomechanics*, *30*(9), pp.933-941.

DUPRAS, T.L. and Tocheri, M.W., 2007. Reconstructing infant weaning histories at Roman period Kellis, Egypt using stable isotope analysis of dentition. *American Journal of Physical Anthropology*, *134*(1), pp.63-74.

DURAY, S.M., 1996. Dental indicators of stress and reduced age at death in prehistoric Native Americans. *American Journal of Physical Anthropology*, *99*(2), pp.275-286.

DYER, C., 1989. *Standards of Living in the later Middle Ages: Social change in England c. 1200-1520*. Cambridge University Press.

ELDER, Jr G. 1995. The life course paradigm: Social change and individual development. In: Moen P, Elder Jr, Lüscher K, editors. Examining lives in context: perspectives on the ecology of human development. Washington, DC: *American Psychological Association*. pp. 101–139.

EMANUEL, I., 1986. Maternal health during childhood and later reproductive performance. *Annals of the New York Academy of Sciences*, *477*(1), pp.27-39.

ERIKSSON, J. G., Forsen, T., Tuomilehto, J., Winter, P. D., Osmond, C., & Barker, D. J. 1999. Catch-up growth in childhood and death from coronary heart disease: longitudinal study. *Bmj*, *318*(7181), 427-431.

EVANS, A.R., Wilson, G.P., Fortelius, M. and Jernvall, J. 2007. High-level similarity of dentitions in carnivorans and rodents. *Nature*, *445*(7123), 78-81.

EVELETH, P.B. and Tanner, J.M. 1990. *Worldwide variation in human growth.* Cambridge: Cambridge University Press.

EVISON, V. 1994. *An Anglo-Saxon Cemetery at Great Chesterford, Essex*. CBA Research Report 91. Council for British Archaeology: London.

FALKINGHAM, P.L. 2012. Acquisition of high resolution three-dimensional models using free, open-source, photogrammetric software. *Palaeontologia electronica*, *15*(1), p.15.

FILDES, V., 1986. *Breasts, bottles and babies-a history of infant feeding*. Edinburgh University Press.

FINK, B., Grammer, K., Mitteroecker, P., Gunz, P., Schaefer, K., Bookstein, F.L. and Manning, J.T., 2005. Second to fourth digit ratio and face shape. *Proceedings of the Royal Society of London B: Biological Sciences*, *272*(1576), pp.1995-2001.

FINUCANE, R.C., 2000. The Rescue of the Innocents: endangered children in medieval miracles. Macmillan.

FISHER, R.A., 1935. The logic of inductive inference. *Journal of the Royal Statistical Society*, *98*(1), pp.39-82.

FORTUN, M. 2009. Genes in our knot. In: Atkinson P, Glasner P, Lock M, editors. Handbook of Genetics and Society. Mapping the New Genomic Era. Oxford: Routledge. p 247–259.

FRELAT, M.A. and Mittereocker, P. 2011. Postnatal ontogeny of tibia and femur form in two human populations: a multivariate morphometric analysis. *American Journal of Human Biology*, *23*(6), pp.796-804.

FRELAT, M.A., Katina, S., Weber, G.W. and Bookstein, F.L. 2012. Technical note: a novel geometric morphometric approach to the study of long bone shape variation. *American journal of physical anthropology*, *149*(4), pp.628-638.

FRIESS, M., 2012. Scratching the surface? The use of surface scanning in physical and paleoanthropology. *Journal of Anthropological Sciences*, *90*, pp.1-25.

FROST, H.M., 1969. Tetracycline-based histological analysis of bone remodeling. *Calcified tissue international*, *3*(1), pp.211-237.

FROST, H.M., 1997. On our age-related bone loss: insights from a new paradigm. *Journal of Bone and Mineral Research*, *12*(10), pp.1539-1546.

FROST, H.M., 2003. Bone's mechanostat: a 2003 update. *The anatomical record*, *275*(2), pp.1081-1101.

FRUCIANO, C., Celik, M.A., Butler, K., Dooley, T., Weisbecker, V. and Phillips, M.J., 2017. Sharing is caring? Measurement error and the issues arising from combining 3D morphometric datasets. *Ecology and evolution*, *7*(17), pp.7034-7046.

GARCIA MARTINEZ, D., Recheis, W. and Bastir, M., 2016. Ontogeny of 3D rib curvature and its importance for the understanding of human thorax development. *American journal of physical anthropology*, *159*(3), pp.423-431.

GARN, S.M., Nagy, J.M., Sandusky, S.T. and Trowbridge, F., 1973. Economic impact on tooth emergence. *American journal of physical anthropology*, *39*(2), pp.233-237.

GERBER, J., 2014. Skeletal manifestations of stress in child victims of the Great Irish Famine (1845–1852): Prevalence of enamel hypoplasia, Harris lines, and growth retardation. *American journal of physical anthropology*, *155*(1), pp.149-161.

GERBER, S., Neige, P. and Eble, G.J., 2007. Combining ontogenetic and evolutionary scales of morphological disparity: a study of early Jurassic ammonites. *Evolution & development*, *9*(5), pp.472-482.

GIES, F., 1990. Joseph. Daily Life in Medieval Times.

GLENCROSS, B. and Stuart-Macadam, P., 2000. Childhood trauma in the archaeological record. *International Journal of Osteoarchaeology*, *10*(3), pp.198-209.

GLUCKMAN, P.D. and Hanson, M.A., 2004. Living with the past: evolution, development, and patterns of disease. *Science*, *305*(5691), pp.1733-1736.

GLUCKMAN, PD, Hanson MA, Low FM. 2011. The role of developmental plasticity and epigenetics in human health. Birth Defects Res 93:12–18

GOLDBERG, P.J.P., 2013. Female labour, service and marriage in the late medieval urban north. *Northern History*.

GOODALL, C., 1991. Procrustes methods in the statistical analysis of shape. *Journal of the Royal Statistical Society. Series B (Methodological)*, pp.285-339.

GOODE, H., Waldron, T. and Rogers, J. 1993. Bone growth in juveniles: a methodological note. *International Journal of Osteoarchaeology,* 3, 321-323.

GOODMAN, A.H., Armelagos, G.J. and Rose, J.C., 1980. Enamel hypoplasias as indicators of stress in three prehistoric populations from Illinois. *Human biology*, pp.515-528.

GOODMAN, A.H. and Armelagos, G.J., 1989. Infant and childhood morbidity and mortality risks in archaeological populations. *World Archaeology*, *21*(2), pp.225-243.

GORDON, E.C., 1991. Accidents among medieval children as seen from the miracles of six English saints and martyrs. *Medical history*, *35*(02), pp.145-163.

GOSMAN, J.H. and Ketcham, R.A., 2009. Patterns in ontogeny of human trabecular bone from SunWatch Village in the prehistoric Ohio Valley: general features of microarchitectural change. *American journal of physical anthropology*, *138*(3), pp.318-332.

GOSMAN, J. H., Stout, S. D., and Larsen, C. S. 2011. Skeletal biology over the life span: a view from the surfaces. *American journal of physical anthropology*, *146*(S53), 86-98.

GOSMAN, J.H., Hubbell, Z.R., Shaw, C.N. and Ryan, T.M. 2013. Development of cortical bone geometry in the human femoral and tibial diaphysis. *The Anatomical Record*, *296*(5),774-787.

GOULD, S.J., 1966. Allometry and size in ontogeny and phylogeny. *Biological Reviews*, *41*(4), pp.587-638.

GOULD, S.J., 1977. *Ontogeny and phylogeny*. Harvard University Press.

GOULD, F.D. 2014. To 3D or not to 3D, that is the question: do 3D surface analyses improve the ecomorphoogical power of the distal femur in placental mammals?. *PloS one,* 9(3), e91719.

GOWLAND, R.L. 2015. Entangled lives: Implications of the developmental origins of health and disease hypothesis for bioarchaeology and the life course. *American Journal of Physical Anthropology*, *158*(4), pp.530-540.

GOWLAND, R.L. and Chamberlain, A.T. 2002. A Bayesian approach to ageing perinatal skeletal material from archaeological sites: implications for the evidence for infanticide in Roman-Britain. *Journal of Archaeological Science*, *29*(6), pp.677-685.

GRAUER, A.L., 1993. Patterns of anemia and infection from medieval York, England. *American Journal of Physical Anthropology*, *91*(2), pp.203-213.

GUNZ, P., 2012. Evolutionary relationships among robust and gracile australopiths: an “evo-devo” perspective. *Evolutionary Biology*, *39*(4), pp.472-487.

GUNZ, P., Mitteroecker, P. and Bookstein, F.L., 2005. Semilandmarks in three dimensions. In *Modern morphometrics in physical anthropology* (pp. 73-98). Springer US.

HADLEY, D.M. and Hemer, K.A. eds., 2014. *Medieval Childhood: Archaeological Approaches* (Vol. 3). Oxbow Books.

HALES, C.N. and Barker, D.J., 2001. The thrifty phenotype hypothesis. *British medical bulletin*, *60*(1).

HALFON, N., Larson, K., Lu, M., Tullis, E. and Russ, S., 2014. Lifecourse health development: past, present and future. *Maternal and child health journal*, *18*(2), pp.344-365.

HALL, C., Figueroa, A., Fernhall, B.O. and Kanaley, J.A., 2004. Energy expenditure of walking and running: comparison with prediction equations. *Medicine and science in sports and exercise*, *36*, pp.2128-2134.

HALLGRIMSSON, B., Willmore, K. and Hall, B.K., 2002. Canalization, developmental stability, and morphological integration in primate limbs. *American journal of physical anthropology*, *119*(S35), pp.131-158.

HAMMER, Ø., Harper, D.A.T., and P. D. Ryan, 2001. PAST: Paleontological Statistics Software Package for Education and Data Analysis. Palaeontologia Electronica 4(1): 9pp.

HANAWALT, B.A., 1977. Childrearing among the lower classes of late medieval England. *The Journal of interdisciplinary history*, *8*(1), pp.1-22.

HANAWALT, B.A., 1988. Men's games, King's deer: poaching in Medieval England in Rewriting the Middle Ages. *The Journal of medieval and Renaissance studies*, *18*(2), pp.175-193.

HARRIS, L.J., Ray, S.N. and Ward, A., 1933. The excretion of vitamin C in human urine and its dependence on the dietary intake. *Biochemical Journal*, *27*(6), p.2011.

HARTMAN, S.E., 1989. Stereophotogrammetric analysis of occlusal morphology of extant hominoid molars: phenetics and function. *American Journal of Physical Anthropology*, *80*(2), pp.145-166.

HAYDOCK, H., Clarke, L., Craig-Atkins, E., Howcroft, R. and Buckberry, J., 2013. Weaning at Anglo-Saxon raunds: Implications for changing breastfeeding practice in britain over two millennia. *American journal of physical anthropology*, *151*(4), pp.604-612.

HAYFIELD, C., 1988. The Origins of the Roman Landscape around Wharram Percy. *East Yorkshire*, pp.99-122.

HEIGHWAY, C. 2007. Part Four: The Burials, The Attributes of Burials. In: S. Mays, C. Harding and C. Heighway, *Wharram: A Study of Settlement on the Yorkshire Wolds, XI: The Churchyard.* York University Archaeological Publications 13. English Heritage.

HELLIER, C.A. and Jeffery, N., 2006. Morphological plasticity in the juvenile talus. *Foot and Ankle surgery*, *12*(3), pp.139-147.

HERRING, D., Saunders, S.R. and Katzenberg, M.A., 1998. Investigating the weaning process in past populations. *American Journal of Physical Anthropology*, *105*(4), pp.425-439.

HEYWOOD, C., 2014. *A history of childhood*. John Wiley & Sons.

HICKS, M. and Hicks, A., 2001. *St Gregory's Priory, Northgate, Canterbury: Excavations 1988-1991* (Vol. 2). Canterbury Archaeological Trust Limited.

HILLSON, S., 2003. Wealth, health, diet and dental pathology. Wealth, health and human remains in archaeology. 25th Kroonlecture, Metz WH (ed). Amsterdam: Foundation for Anthropology and Prehistory in The Netherlands, pp.7-38.

HOCHBERG, Z, Feil R, Constance M, Fraga, M, Junien C, et al. 2011. Child health, developmental plasticity and epigenetic programming. Endocrine Rev 32:159–224.

HOPPA, R.D., 1992. Evaluating human skeletal growth: An Anglo-Saxon example. *International Journal of Osteoarchaeology*, *2*(4), pp.275-288.

HOPPA, R.D., and Saunders, S.R. 1994. The δ1 metho for examining bone growth in juveniles: a reply. *International Journal of Osteoarchaeology*, 10, 1-10.

HOPPA, R.D. and Fitzgerald, C.M., 1999. *Human growth in the past: studies from bones and teeth* (Vol. 25). Cambridge University Press.

HOTELLING, H. 1933. Analysis of a complex of statistical variables into principal components. *J. Educ. Psychol.*, 24: 417–441. 498–520.

HOWELLS, W.W., 1973. Cranial variation in man. A study by multivariate analysis of patterns of difference. Among recent human populations. *Papers of the Peabody Museum of Archaeology and Ethnology*, (67), pp.1-259.

HOWELLS, W.W., 1989. Skull shapes and the map: craniometric analyses in the dispersion of modern Homo (Vol. 79). Peabody Museum of Archaeology.

HUDA, T.F. and Bowman, J.E., 1995. Age determination from dental microstructure in juveniles. *American journal of physical anthropology*, *97*(2), pp.135-150.

HUMPHREY, L., 2000. Growth studies of past populations: an overview and an example. *Human Osteology in Archaeology and Forensic Science Greenwich Medical Media: London*, pp.23-38.

HUMPHREY, L.T. and King, T., 2000. Childhood stress: a lifetime legacy. *Anthropologie*, *38*(1), pp.33-49.

HUMAN ANATOMY LIBRARY. Anatomy of the Biceps Brachii. http://humananatomylibrary.com/anatomy-of-the-biceps-brachii/anatomy-of-the-biceps-brachii-the-brachialis-muscle-yoganatomy/. Accessed 30 September 2017

HUXLEY, J. S. 1932. *Problems of Relative Growth*, Methuen, London.

INGOLD, T., 1998. From complementarity to obviation: On dissolving the boundaries between social and biological anthropology, archaeology and psychology. *Zeitschrift für Ethnologie*, pp.21-52.

INSKIP, S., 2008. Great Chesterford: a catalogue of burials. *BAR INTERNATIONAL SERIES*, *1743*, p.57.

JAY, M., 2013. Breastfeeding and weaning behaviour in archaeological populations: evidence from the isotopic analysis of skeletal materials. *Childhood in the Past*.

JOHNSTON, F.E., 1962. Growth of the long bones of infants and young children at Indian Knoll. *American Journal of Physical Anthropology*, *20*(3), pp.249-254.

JOHNSTON, F.E., 1968. Growth of the skeleton in earlier peoples. *The skeletal biology of earlier human populations*, pp.57-66.

JOHNSTON, F.E. and Snow, C.E., 1961. The reassessment of the age and sex of the Indian Knoll skeletal population: demographic and methodological aspects. *American Journal of Physical Anthropology*, *19*(3), pp.237-244.

JOLICOEUR, P., 1963. 193. Note: the multivariate generalization of the allometry equation. *Biometrics*, *19*(3), pp.497-499.

JONKE, E., Schaefer, K., W Freudenthaler, J., Prossinger, H. and L Bookstein, F., 2003. A cephalometric comparison of skulls from different time periods–the Bronze Age, the 19th century and the present. *Collegium antropologicum*, *27*(2), pp.789-801.

KAATI, G, Bygren LO, Edvinsson S. 2002. Cardiovascular and diabetes mortality determined by nutrition during parents' and grandparents' slow growth period. Eur J Hum Genet 10: 682–688.

KAMP, K.A., 2001. Where have all the children gone?: the archaeology of childhood. *Journal of Archaeological Method and Theory*, *8*(1), pp.1-34.

KATZENBERG, M.A. and Pfeiffer, S., 1995. JL4 nitrogen isotope evidence for weaning age in a nineteenth century canadian skeletal sample. *Bodies of evidence: reconstructing history through skeletal analysis*, p.221.

KATZENBERG, M.A., Herring, D. and Saunders, S.R., 1996. Weaning and infant mortality: evaluating the skeletal evidence. *American Journal of Physical Anthropology*, *101*(S23), pp.177-199.

KEENE, D., 1983. The medieval urban environment in documentary records. *Archives*, *16*(70), p.137.

KEMKES-GOTTENTHALER, A. 2005. Sex determination by discriminant analysis: an evaluation of the reliability of patella measurements. *Forensic Science International* 147: 129–133.

KENDALL, D.G., 1977. The diffusion of shape. *Advances in applied probability*, *9*(3), pp.428-430.

KENDALL, D.G., 1984. Shape manifolds, procrustean metrics, and complex projective spaces. *Bulletin of the London Mathematical Society*, *16*(2), pp.81-121.

KENDALL, D.G. and Kendall, W.S., 1980. Alignments in two-dimensional random sets of points. *Advances in Applied probability*, pp.380-424.

KIMMERLE, E.H. and Jantz, R.L., 2005. Secular trends in craniofacial asymmetry studied by geometric morphometry and generalized Procrustes methods. In *Modern morphometrics in physical anthropology* (pp. 247-263). Springer, Boston, MA.

KING, S.E. and Ulijaszek, S.J., 1999. 7 lnvisible insults during growth and development. *Human growth in the past: Studies from bones and teeth*, *25*, p.161.

KLINGENBERG, C.P. and McIntyre, G.S., 1998. Geometric morphometrics of developmental instability: analyzing patterns of fluctuating asymmetry with Procrustes methods. *Evolution*, pp.1363-1375.

KNOWLES, D. and Hadcock, R.N., 1971. *Medieval religious houses, England and Wales*. Addison-Wesley Longman Ltd.

KOEHL, P. and Hass, J., 2015. Landmark-free geometric methods in biological shape analysis. *Journal of The Royal Society Interface*, *12*(113), p.20150795.

KUZAWA, C.W., 2005. Fetal origins of developmental plasticity: are fetal cues reliable predictors of future nutritional environments?. *American Journal of Human Biology*, *17*(1), pp.5-21.

LAMAR, Cyriaque. 23 October 2012. "Behold, the divine baby walker of Jesus Christ". https://io9.gizmodo.com/5953846/behold-the-divine-baby-walker-of-jesus-christ Accessed 24 September 2017.

LANKTREE, M.B., Guo, Y., Murtaza, M., Glessner, J.T., Bailey, S.D., Onland-Moret, N.C., Lettre, G., Ongen, H., Rajagopalan, R., Johnson, T. *et al.* 2011. Meta-analysis of dense genecentric association studies reveals common and uncommon variants associated with height. *The American Journal of Human Genetics* 88(1): 6-18.

LANYON, L.E. (1980) The influence of function on the development of bone curvature: An experimental study on the rat tibia. J Zool Lond *192:* 457–466.

LANYON, L.E., 1987. Functional strain in bone tissue as an objective, and controlling stimulus for adaptive bone remodelling. *Journal of biomechanics*, *20*(11-12), pp.1083-1093.

LANYON, L.E. and Bourn, S.H.E.I.L.A., 1979. The influence of mechanical function on the development and remodeling of the tibia. An experimental study in sheep. *JBJS*, *61*(2), pp.263-273.

LARSEN, C.S., 1995. Biological changes in human populations with agriculture. *Annual Review of Anthropology*, *24*(1), pp.185-213.

LARSEN, C.S., 2002. Bioarchaeology: the lives and lifestyles of past people. *Journal of Archaeological Research*, *10*(2), pp.119-166.

LARSEN, C.S., 2015. *Bioarchaeology: interpreting behavior from the human skeleton* (Vol. 69). Cambridge University Press.

LASKER, G.W., 1969. Human biological adaptability. *Science*, *166*(3912), pp.1480-1486.

LEIGH, S.R., 2006. Cranial ontogeny of Papio baboons (Papio hamadryas). *American Journal of Physical Anthropology*, *130*(1), pp.71-84.

LEONARD, W.R. and Robertson, M.L., 1992. Nutritional requirements and human evolution: a bioenergetics model. *American Journal of Human Biology*, *4*(2), pp.179-195.

LETTRE, G., Jackson, A.U., Gieger, C., Schumacher, F.R., Berndt, S.I., Sanna, S., Eyheramendy, S., Voight, B.F., Butler, J.L., Guiducci, C., et al. 2008. Identification of ten loci associated with height highlights new biological pathways in human growth. *Nature Genetics* 40(5): 584-91.

LEWIS, M.E., 2002. Impact of industrialization: comparative study of child health in four sites from medieval and postmedieval England (AD 850–1859). *American Journal of Physical Anthropology*, *119*(3), pp.211-223.

LEWIS, M.E., 2007. The bioarchaeology of children: perspectives from biological and forensic anthropology (Vol. 50). Cambridge University Press.

LEWIS, M.E., 2010. Life and death in a civitas capital: metabolic disease and trauma in the children from late Roman Dorchester, Dorset. *American Journal of Physical Anthropology*, *142*(3), pp.405-416.

LEWIS, M. 2011a. The osteology of infancy and childhood: misconceptions and potential.

LEWIS, M.E., 2011b. Tuberculosis in the non-adults from Romano-British Poundbury Camp, Dorset, England. *International Journal of Paleopathology*, *1*(1), pp.12-23.

LEWIS, A.B. and Garn, S.M., 1960. The relationship between tooth formation and other maturational factors. *The Angle Orthodontist*, *30*(2), pp.70-77.

LEWIS, M. and Roberts, C., 1997. Growing pains: the interpretation of stress indicators. *International Journal of Osteoarchaeology*, *7*(6), pp.581-586.

LIEBERMAN, D.E. and Pearson, O.M., 2001. Trade-Off Between Modeling and Remodeling Responses to Loading in the Mammalian Limb. *Museum of*, *156*(1), pp.269-282.

LIEBERMAN, D.E., O.M., Pearson, J.D. Polk. 2001. Growth versus repair responses to loading in mammalian limb bones. American Zoologist

LIEBERMAN, DE, Polk, JD & Demes, B 2004, 'Predicting Long Bone Loading from Cross-Sectional Geometry' *American Journal of Physical Anthropology*, vol 123, no. 2, pp. 156-171.

LIMP, F., Payne, A., Simon, K., Winters, S. and Cothren, J. 2011. Developing a 3-D digital heritage ecosystem: From object to representation and the role of a virtual museum in the 21st century. *Internet Archaeology*, *30*.

LIVERSIDGE, H.M., 1994. Accuracy of age estimation from developing teeth of a population of known age (0–5.4 years). *International Journal of Osteoarchaeology*, *4*(1), pp.37-45.

LOTH, S.R. and Henneberg, M., 2001. Sexually dimorphic mandibular morphology in the first few years of life. *American Journal of Physical Anthropology*, *115*(2), pp.179-186.

LOVEJOY, C, Russell, K.F., and Harrison, M.L. 1990. Long bone growth velocity in the Libben population. *American Journal of Human Biology.* 2, 533-541.

LOVEJOY, C.O., McCollum, M.A., Reno, P.L. and Rosenman, B.A., 2003. Developmental biology and human evolution. *Annual Review of Anthropology*, *32*(1), pp.85-109.

LOW, F.M., Gluckman, P.D. and Hanson, M.A., 2012. Developmental plasticity, epigenetics and human health. *Evolutionary Biology*, *39*(4), pp.650-665.

LUNDSTROM, U., Siimes, M.A. and Dallman, P.R., 1977. At what age does iron supplementation become necessary in low-birth-weight infants?. *The Journal of pediatrics*, *91*(6), pp.878-883.

MACINTOSH, A.A., Davies, T.G., Pinhasi, R. and Stock, J.T., 2015. Declining tibial curvature parallels ~ 6150 years of decreasing mobility in central European agriculturalists. *American journal of physical anthropology, 157* (2), pp.260-275.

MACINTOSH, A.A., Pinhasi, R., and Stock, J.T., 2017. Prehistoric women's manual labor exceeded that of athletes through the first 5500 years of farming in Central Europe. *Science advances,* 3(11), p. eaao3893.

MACLEOD, N.2002. Morphometrics. Encyclopaedia of evolution, pp. 768-771.

MACLEOD N.2008. Understanding morphology in systematic contexts: 3D specimen ordination and 3D specimen recognition. *The New Taxonomy. CRC Press, Taylor & Francis Group, London*, pp.143-210.

MACLEOD, N., Benfield, M. and Culverhouse, P., 2010. Time to automate identification. *Nature*, *467*(7312), pp.154-155.

MAHONEY, P., Schmidt, C.W., Deter, C., Remy, A., Slavin, P., Johns, S.E., Miszkiewicz, J.J. and Nystrom, P., 2016. Deciduous enamel 3D microwear texture analysis as an indicator of childhood diet in medieval Canterbury, England. *Journal of Archaeological Science*, *66*(12), p.8e136.

MANCHESTER, W., 1992. A World Lit Only B51 Fire: The Medieval Mind and the Renaissance, Portrait of an Age.

MANDER, G.P. and Tildesley, N.W., 1960. *A History of Wolverhampton*.

MARESH, M.M., 1955. Linear growth of long bones of extremities from infancy through adolescence: continuing studies. *AMA American journal of diseases of children*, *89*(6), pp.725-742.

MARTINEZ-ABADIAS, N., Mitteroecker, P., Parsons, T.E., Esparza, M., Sjøvold, T., Rolian, C., Richtsmeier, J.T. and Hallgrímsson, B., 2012. The developmental basis of quantitative craniofacial variation in humans and mice. *Evolutionary biology*, *39*(4), pp.554-567.

MASSLER, M., Schour, I. and Poncher, H.G., 1941. Developmental pattern of the child as reflected in the calcification pattern of the teeth. *American Journal of Diseases of Children*, *62*(1), pp.33-67.

MAYS, S.A., 1985. The relationship between Harris line formation and bone growth and development. *Journal of archaeological science*, *12*(3), pp.207-220.

MAYS, S., 1993. Infanticide in Roman Britain. *Antiquity*, *67*(257), pp.883-888.

MAYS, S., 1995. The relationship between Harris lines and other aspects of skeletal development in adults and juveniles. *Journal of Archaeological Science*, *22*(4), pp.511-520.

MAYS, S.A., 1999. 12 Linear and appositional long bone growth in earlier human populations. *Human growth in the past: Studies from bones and teeth*, *25*, p.290.

MAYS, S., 2003. The rise and fall of rickets in England. *The environmental archaeology of industry. Oxford: Oxbow.* pp.144-153.

MAYS, S. 2007. The human remains, pp. 77-192, 337-97 in Mays, S., Heighway, C. and Harding, C., *Wharram: A study of settlemtn on the Yorkshire Wolds, XI: The Churchyard* (York University Archaeological Publications 13). York University Department of Archaeology.

MAYS, S., 2013. A discussion of some recent methodological developments in the osteoarchaeology of childhood. *Childhood in the Past*, *6*(1), pp.4-21.

MAYS, S.A., Richards, M.P. and Fuller, B.T., 2002. Bone stable isotope evidence for infant feeding in Mediaeval England. *Antiquity*, *76*(293), pp.654-656.

MAYS, S., Brickley, M. and Ives, R., 2006. Skeletal manifestations of rickets in infants and young children in a historic population from England. *American Journal of Physical Anthropology*, *129*(3), pp.362-374.

MAYS, S., Harding, C., Heighway, C., Barclay, C., Marlow-Mann, E. and Heritage, E., 2007. *The Churchyard*. York University Department of Archaeology.

MAYS, S., Brickley, M. and Ives, R., 2008. Growth in an English population from the Industrial Revolution. *American journal of physical anthropology*, *136*(1), pp.85-92.

MAYS, S., Ives, R. and Brickley, M., 2009b. The effects of socioeconomic status on endochondral and appositional bone growth, and acquisition of cortical bone in children from 19th century Birmingham, England. *American journal of physical anthropology*, *140*(3), pp.410-416.

MCCAMMON, R.W., 1970. Human growth and development. *Human growth and development.*

MCGRATH, J.W. 1992. Behavioral change and the evolution of human host-pathogen systems. MASCA: Research Papers in Science and Archaeology 9,13-22.

MCNULTY, K.P. and Vinyard, C.J., 2015. Morphometry, geometry, function, and the future. *The Anatomical Record*, *298*(1), pp.328-333.

MENSFORTH, R.P., Lovejoy, C.O., Lallo, J.W. and Armelagos, G.J., 1978. Part two: The role of constitutional factors, diet, and infectious disease in the etiology of porotic hyperostosis and periosteal reactions in prehistoric infants and children. *Medical Anthropology*, *2*(1), pp.1-59.

MERCHANT, V.L. and Ubelaker, D.H., 1977. Skeletal growth of the protohistoric Arikara. *American Journal of Physical Anthropology*, *46*(1), pp.61-72.

METCALFE, N.B. and Monaghan, P., 2001. Compensation for a bad start: grow now, pay later?. *Trends in ecology & evolution*, *16*(5), pp.254-260.

MITTEROECKER, P., 2013, January. How to measure phenotypic variation in human development and evolution? *American Journal of Physical Anthropology* (Vol. 150, pp. 200-200).

MITTEROECKER, P. and Gunz, P., 2009. Advances in geometric morphometrics. *Evolutionary Biology*, *36*(2), pp.235-247.

MITTEROECKER, P. and Bookstein, F., 2011. Linear discrimination, ordination, and the visualization of selection gradients in modern morphometrics. *Evolutionary Biology*, *38*(1), pp.100-114.

MITTEROECKER, P., Gunz, P., Bernhard, M., Schaefer, K. and Bookstein, F.L., 2004. Comparison of cranial ontogenetic trajectories among great apes and humans. *Journal of Human Evolution*, *46*(6), pp.679-698.

MITTEROECKER, P., Gunz, P. and Bookstein, F.L. 2005.Heterochrony and geometric morphometrics: a comparison of cranial growth in Pan paniscus versus Pan troglodytes. *Evolution & development*, *7*(3), 244-258.

MOLLESON, T. and Cox, M., 1993. The Spitalfields Project: The Anthropology The Middling Sort.

MOLLESON, T., Cruse, K. and Mays, S., 1998. Some sexually dimorphic features of the human juvenile skull and their value in sex determination in immature skeletal remains. *Journal of Archaeological Science*, *25*(8), pp.719-728.

MORANT, G.M., 1939. The use of statistical methods in the investigation of problems of classification in anthropology: Part I. The general nature of the material and the form of intraracial distributions of metrical characters. *Biometrika*, *31*(1/2), pp.72-98.

MORIMOTO, N., De León, M.S.P., Nishimura, T. and Zollikofer, C.P., 2011. Femoral morphology and femoropelvic musculoskeletal anatomy of humans and great apes: a comparative virtopsy study. *The Anatomical Record*, *294*(9), pp.1433-1445.

MORO, M., Van der Meulen, M.C.H., Kiratli, B.J., Marcus, R., Bachrach, L.K. and Carter, D.R. 1996. Body mass is the primary determinant of midfemoral bone acquisition during adolescent growth. *Bone*, *19*(5), pp.519-526.

MUNOZ-MUNOZ F., Quinto-Sánchez, M. and González-José, R., 2016. Photogrammetry: a useful tool for three-dimensional morphometric analysis of small mammals. *Journal of Zoological Systematics and Evolutionary Research*.

NEUBAUER, S., Gunz, P. and Hublin, J.J., 2009. The pattern of endocranial ontogenetic shape changes in humans. *Journal of anatomy*, *215*(3), pp.240-255.

NITSCH, E.K., Humphrey, L.T. and Hedges, R.E., 2011. Using stable isotope analysis to examine the effect of economic change on breastfeeding practices in Spitalfields, London, UK. *American journal of physical anthropology*, *146*(4), pp.619-628.

O'HIGGINS, P. 2000. The study of morphological variation in the hominid fossil record: biology, landmarks and geometry. *The Journal of Anatomy*, *197*(1), pp.103-120.

O'HIGGINS, P. and Jones, N., 1998. Facial growth in Cercocebus torquatus: an application of three-dimensional geometric morphometric techniques to the study of morphological variation. *Journal of Anatomy*, *193*(2), 251-272.

O'HIGGINS, P., Chadfield, P. and Jones, N., 2001. Facial growth and the ontogeny of morphological variation within and between the primates Cebus apella and Cercocebus torquatus. *Journal of Zoology*, *254*(3), pp.337-357.

O'HIGGINS, P. and Collard, M., 2002. Sexual dimorphism and facial growth in papionin monkeys. *Journal of Zoology*, *257*(2), pp.255-272.

ORME, CDL, Freckleton RP, Thomas G, Petzoldt T, Fritz SA, Isaac N, Pearse W. 2011. CAPER: comparative analysis of phylogenetics and evolution in R. R package version 3.1–104.

ORTNER, D.J. and Mays, S., 1998. Dry-bone manifestations of rickets in infancy and early childhood. *International Journal of Osteoarchaeology*, *8*(1), pp.45-55.

ORTNER, D.J., Kimmerle, E.H. and Diez, M., 1999. Probable evidence of scurvy in subadults from archeological sites in Peru. *American Journal of Physical Anthropology*, *108*(3), pp.321-331.

ORTNER, D.J., Butler, W., Cafarella, J. and Milligan, L., 2001. Evidence of probable scurvy in subadults from archeological sites in North America. *American Journal of Physical Anthropology*, *114*(4), pp.343-351.

OTTAWAY, P. 1992. *Archaeology in British Towns: From the Emperor Claudius to the Black Death*, London: Routledge

OWSLEY, D.W. and Jantz, R.L., 1983. Formation of the permanent dentition in Arikara Indians: timing differences that affect dental age assessments. *American Journal of Physical Anthropology*, *61*(4), pp.467-471.

OXNARD, C., 1973. Form and pattern in human evolution: some mathematical, physical, and engineering approaches. University of Chicago Press.

OXNARD, C.E., 2000. Morphometrics of the primate skeleton and the functional and developmental underpinnings of species diversity. In *Linnean Society Symposium Series* (Vol. 20, pp. 235-264).

PARR, W.C.H., Soligo, C., Smaers, J., Chatterjee, H.J., Ruto, A., Cornish, L. and Wroe, S., 2014. Three-dimensional shape variation of talar surface morphology in hominoid primates. *Journal of anatomy*, *225*(1), pp.42-59.

PAUWELS, F. 1980. *Biomechanics of the locomotor aparatus*. Berlin: Springer-Verlag.

PAVLIDIS, G., Koutsoudis, A., Arnaoutoglou, F., Tsioukas, V. and Chamzas, C. 2007. Methods for 3D digitization of cultural heritage. *Journal of cultural heritage*, *8*(1), pp.93-98.

PEARSON, Karl. 1895. Note on Regression and Inheritance in the Case of Two Parents. *Proceedings of the Royal Society*, 58: 272–272.

PEARSON, K., 1901. Mathematical contributions to the theory of evolution. VII. On the correlation of characters not quantitatively measurable. *Philosophical Transactions of the Royal Society of London. Series A, Containing Papers of a Mathematical or Physical Character*, *195*, pp.1-405.

PEARSON, K.L., 1997. Nutrition and the early-medieval diet. *Speculum*, *72*(1), pp.1-32.

PEARSON, O.M. and Lieberman, D.E., 2004. The aging of Wolff's "law": ontogeny and responses to mechanical loading in cortical bone. *American journal of physical anthropology*, *125*(S39), pp.63-99.

PENIN, X., Berge, C. and Baylac, M., 2002. Ontogenetic study of the skull in modern humans and the common chimpanzees: neotenic hypothesis reconsidered with a tridimensional Procrustes analysis. *American Journal of Physical Anthropology*, *118*(1), pp.50-62.

PEREZ, S.I., Bernal, V. and Gonzalez, P.N., 2006. Differences between sliding semi-landmark methods in geometric morphometrics, with an application to human craniofacial and dental variation. *Journal of anatomy*, *208*(6), pp.769-784.

PHYSIOPEDIA. Gait Cycle http://www.physio-pedia.com/Gait_Cycle (accessed 23 September 2017)

PINHASI, R., Teschler-Nicola, M., Knaus, A. and Shaw, P., 2005. Cross-population analysis of the growth of long bones and the os coxae of three early medieval Austrian populations. *American Journal of Human Biology*, *17*(4), pp.470-488.

POLLY, P.D., 2008. Adaptive zones and the pinniped ankle: a three-dimensional quantitative analysis of carnivoran tarsal evolution. In *Mammalian evolutionary morphology* (pp. 167-196). Springer Netherlands.

POLLY, P.D. and MacLeod, N. 2008. Locomotion in fossil Carnivora: an application of eigensurface analysis for morphometric comparison of 3D surfaces. *Palaeontologia Electronica*, *11*(2), pp.10-13.

POLLY, P.D., Dundas, R., Lawing, A.M. 2011. Standing up to climate change: community locomotor ecomorphology and paleoenvironment in the Plio-Pleistoene. In *Journal of vertebrate Paleontology* (Vol. 31, pp. 175-175). 60 Revere dr, STE 500, Northbrook, IL 60062 USA: Soc Vertebrate Paleontology.

POWERS, R. 1980. A tool for coping with juvenile human bones from archaeological excavations. In: *Skeletal Remains from the Cemetery of St Nicholas Shambles, City of London* (edited by W.J. White). London: London and Middlesex Archaeological Trust: 74-78.

PRIVAT, KL, O'Connell TC, Richards MP. 2002. Stable isotope analysis of human and faunal remains from the Anglo-Saxon cemetery at Berinsfield, Oxfordshire: dietary and social implications. *J Archaeol Sci* **29**:779–790.

PUENTE, J., 2013. Distances and algorithms to compare sets of shapes for automated biological morphometrics.

PUJOL, A., Rissech, C., Ventura, J., Badosa, J. and Turbón, D. 2014. Ontogeny of the female femur: geometric morphometric analysis applied on current living individuals of a Spanish population. *Journal of anatomy*, *225*(3), pp.346-357.

RANDO, OJ. 2012. Daddy issues: paternal effects on phenotype. Cell 151:702–708.

RAUCH, F., Neu, C., Manz, F. and Schoenau, E. 2001. The development of metaphyseal cortex—implications for distal radius fractures during growth. *Journal of Bone and Mineral Research*, *16*(8), pp.1547-1555.

R Coding Team. 2012. R: a language and environment for statistical computing. R Foundation for Statistical Computing. Vienna, Austria.

REDFERN, R.C., Millard, A.R. and Hamlin, C., 2012. A regional investigation of subadult dietary patterns and health in late Iron Age and Roman Dorset, England. *Journal of Archaeological Science*, *39*(5), pp.1249-1259.

REGA, E., 1997. Age, gender and biological reality in the Early Bronze Age cemetery at Mokrin. *Invisible people and processes: Writing gender and childhood into European Archaeology*, pp.229-47.

REITSEMA, L.J. and Vercellotti, G., 2012. Stable isotope evidence for sex-and status-based variations in diet and life history at medieval Trino Vercellese, Italy. *American journal of physical anthropology*, *148*(4), pp.589-600.

REYMENT, R.A., 1991. Multidimensional paleobiology. Pergamon Press, New York

RIBOT, I. and Roberts, C., 1996. A study of non-specific stress indicators and skeletal growth in two mediaeval subadult populations. *Journal of Archaeological Science*, *23*(1), pp.67-79.

RICE, S.H., 1997. The analysis of ontogenetic trajectories: when a change in size or shape is not heterochrony. *Proceedings of the National Academy of Sciences*, *94*(3), pp.907-912.

RICHARDS, M.P., Mays, S. and Fuller, B.T., 2002. Stable carbon and nitrogen isotope values of bone and teeth reflect weaning age at the Medieval Wharram Percy site, Yorkshire, UK. *American Journal of Physical Anthropology*, *119*(3), pp.205-210.

RICHMOND, B. G. and Jungers, W. L. 2008. *Orrorin tugenensis* femoral morphology and the evolution of hominin bipedalism. *Science*, *319*, 1662–1665

ROBERTS, D.F., 1995. The pervasiveness of plasticity. *Human variability and plasticity*, pp.1-17.

ROBERTS, DF. 2012. The pervasiveness of plasticity. In: Mascie-Taylor CGN, Bogin B, editors. Human variability and plasticity. Cambridge: Cambridge University Press. p 1–17.

ROBERTS, C. and Manchester, K., 1995. The Archaeology of Disease 2nd edition Sutton Publishing: Gloucester.

ROBERTS, JS, Hall BK, Olson WM. 2001. Bridging the gap between developmental systems theory and evolutionary developmental biology. BioEssays 23:954–962.

ROBERTS, C.A. and Cox, M., 2003. *Health and disease in Britain: from prehistory to the present day*. Sutton publishing.

ROBERTS, B.W., Caspi, A. and Moffitt, T.E., 2001. The kids are alright: growth and stability in personality development from adolescence to adulthood. *Journal of personality and social psychology*, *81*(4), p.670.

ROHLF, F.J., 1986. Relationships among eigenshape analysis, Fourier analysis, and analysis of coordinates. *Mathematical Geology*, *18*(8), pp.845-854.

ROHLF, F.J., 1998. On applications of geometric morphometrics to studies of ontogeny and phylogeny. *Systematic Biology*, *47*(1), pp.147-158.

ROHLF, F.J., 1990. Morphometrics. *Annual Review of ecology and Systematics*, *21*(1), pp.299-316.

ROHLF, F.J., 1999. Shape statistics: Procrustes superimpositions and tangent spaces. *Journal of Classification*, *16*(2), pp.197-223.

ROHLF, F.J., 2000. On the use of shape spaces to compare morphometric methods. *Hystrix, the Italian Journal of Mammalogy*, *11*(1).

ROHLF, F.J. and Marcus, L.F., 1993. A revolution morphometrics. *Trends in Ecology & Evolution*, *8*(4), pp.129-132.

ROSAS, A. and Bastir, M., 2002. Thin-plate spline analysis of allometry and sexual dimorphism in the human craniofacial complex. *American Journal of Physical Anthropology*, *117*(3), pp.236-245.

ROZZI, F.V.R., Gonzalez-Jose, R. and Pucciarelli, H.M., 2005. Cranial growth in normal and low-protein-fed Saimiri. An environmental heterochrony. *Journal of human evolution*, *49*(4), pp.515-535.

RUFF, C., 1987. Sexual dimorphism in human lower limb bone structure: relationship to subsistence strategy and sexual division of labor. *Journal of Human Evolution*, *16*(5), pp.391-416.

RUFF, C.B., 1999. Skeletal structure and behavioral patterns of prehistoric Great Basin populations. Prehistoric lifeways in the Great Basin wetlands: bioarchaeological reconstruction and interpretation. Salt Lake City: University of Utah Press. p, pp.290-320.

RUFF, C.B., 2000. Body size, body shape, and long bone strength in modern humans. *Journal of Human Evolution*, *38*(2), pp.269-290.

RUFF, C., 2003. Growth in bone strength, body size, and muscle size in a juvenile longitudinal sample. *Bone*, *33*(3), pp.317-329.

RUFF, C., 2007. Body size prediction from juvenile skeletal remains. *American Journal of Physical Anthropology*, *133*(1), pp.698-716.

RUFF, C., 2009. Relative limb strength and locomotion in Homo habilis. *American Journal of Physical Anthropology*, *138*(1), pp.90-100.

RUFF, C.B. and Hayes, W.C., 1984. Bone-mineral content in the lower limb. Relationship to cross-sectional geometry. *J Bone Joint Surg Am*, *66*(7), pp.1024-1031.

RUFF, CB, Walker A, Trinkaus E. 1994. Postcranial robusticity in *Homo*, III: ontogeny. *Am J Phys Anthropol* **93**: 35–54.

RUFF, C.B., Scott, W.W. and Liu, A.Y.C., 1991. Articular and diaphyseal remodeling of the proximal femur with changes in body mass in adults. *American Journal of Physical Anthropology*, *86*(3), pp.397-413.

RUFF, C.B., Walker, A. and Trinkaus, E., 1994. Postcranial robusticity in Homo. III: ontogeny. *American Journal of Physical Anthropology*, *93*(1), pp.35-54.

RUFF, C., Holt, B. and Trinkaus, E., 2006. Who's afraid of the big bad Wolff?:"Wolff's law" and bone functional adaptation. *American journal of physical anthropology*, *129*(4), pp.484-498.

RUFF, C.B., Garofalo, E. and Holmes, M.A., 2013. Interpreting skeletal growth in the past from a functional and physiological perspective. *American journal of physical anthropology*, *150*(1), pp.29-37.

RUFF, C.B. and Larsen, C.S., 2014. Long bone structural analyses and the reconstruction of past mobility: a historical review. In *Reconstructing Mobility* (pp. 13-29). Springer US.

RYAN, T.M. and Krovitz, G.E., 2006. Trabecular bone ontogeny in the human proximal femur. *Journal of human evolution*, *51*(6), pp.591-602.

SAARINEN, U.M., 1978. Need for iron supplementation in infants on prolonged breast feeding. *The Journal of pediatrics*, *93*(2), pp.177-180.

SAUNDERS, S.R., 1992. Subadult skeletons and growth related studies. *Skeletal biology of past peoples: research methods*, pp.1-20.

SAUNDERS, S.R. and Hoppa, R.D., 1993. Growth deficit in survivors and Non-survivors: biological mortality bias in subadult skeletal samples. *American journal of physical anthropology*, *36*(S17), pp.127-151.

SAUNDERS, S., Hoppa, R. and Southern, R., 1993. Diaphyseal growth in a nineteenth century skeletal sample of subadults from St Thomas' Church, Belleville, Ontario. *International Journal of Osteoarchaeology*, *3*(4), pp.265-281.

SCHAFER, K., Mitteroecker, P., Gunz, P., Bernhard, M. and Bookstein, F.L., 2004. Craniofacial sexual dimorphism patterns and allometry among extant hominids. *Annals of Anatomy-Anatomischer Anzeiger*, *186*(5-6), pp.471-478.

SCHELL, L.M., 1995. Human biological adaptability with special emphasis on plasticity: history, development and problems for future research. *Human variability and plasticity. Cambridge: Cambridge University Press.* pp.213-237.

SCHEUER, B., 2000. SCHEUER (L.), Black (S.)–Development juvenile osteology.

SCHOENAU, E. 1997. The development of the skeletal system in children and the influence of muscular strength. *Hormone Research in Paediatrics*, *49*(1), pp.27-31.

SCHOENAU, E., Neu, C.M., Mokov, E., Wassmer, G. and Manz, F. 2000. Influence of puberty on muscle area and cortical bone area of the forearm in boys and girls. *The Journal of Clinical Endocrinology & Metabolism*, *85*(3), pp.1095-1098.

SCHOFIELD, J. and Vince, A., 1994. Medieval Towns.

SCHOUR, I. and Massler, M., 1941. *The development of the human dentition*. publisher not identified.

SCHUG, G.R. and Goldman, H.M., 2014. Birth is but our death begun: a bioarchaeological assessment of skeletal emaciation in immature human skeletons in the context of environmental, social, and subsistence transition. *American journal of physical anthropology*, *155*(2), pp.243-259.

SCHURR, M.R., 1997. Stable nitrogen isotopes as evidence for the age of weaning at the Angel site: a comparison of isotopic and demographic measures of weaning age. *Journal of Archaeological Science*, *24*(10), pp.919-927.

SCHURR, M.R., 1998. Using stable nitrogen-isotopes to study weaning behavior in past populations. *World Archaeology*, *30*(2), pp.327-342.

SCHUTKOWSKI, H., 1993. Sex determination of infant and juvenile skeletons: I. Morphognostic features. *American Journal of Physical Anthropology*, *90*(2), pp.199-205.

SCOTT, A.B. and Hoppa, R.D., 2015. A re-evaluation of the impact of radiographic orientation on the identification and interpretation of Harris lines. *American journal of physical anthropology*, *156*(1), pp.141-147.

SELDEN, J., Perttula, T. and O'Brien, M. 2014. Advances in documentation, digital curation, virtual exhibition, and a test of 3D geometric morphometrics: a case study of the Vanderpool vessels from the ancestral Caddo territory. *Advances in Archaeological Practice*, *2*(2), pp.64-79.

SERRAT, M.A., Reno, P.L., McCollum, M.A., Meindl, R.S. and Lovejoy, C.O., 2007. Variation in mammalian proximal femoral development: comparative analysis of two distinct ossification patterns. *Journal of anatomy*, *210*(3), pp.249-258.

SHAPIRO, Harry L. 1939 *Migration and Environment*. London : Oxford University Press.

SHAW, C. 2009. The influence of habitual athletic activity on diaphyseal morphology in modern humans, and its impact on interpretations of hominin activity patterns. Doctoral thesis. University of Cambridge.

SHEFELBINE, S.J., Tardieu, C. and Carter, D.R. 2002. Development of the femoral bicondylar angle in hominid bipedalism. *Bone*, *30*(5), 765-770.

SHEA, B.T. 1983. Allometry and heterochrony in the African Apes. *American Journal of Physical Anthropology., 62. pp. 275-289*

SHROUT, P.E., Fleiss, J.L. 1979. Intraclass correlations: Uses in assessing rater reliability. Psychological Bulletin 86:420-428.

SLICE, D.E., 2005. Modern morphometrics. In *Modern morphometrics in physical anthropology* (pp. 1-45). Springer US.

SLICE, D.E. 2007. Geometric morphometrics. *Annu. Rev. Anthropol.*, *36*, 261-281.

SMALL, C.G., 1996. *The statistical theory of shape*. Springer Science & Business Media.

SMITH, B.H., 1991. Standards of human tooth formation and dental age assessment. *Advances in dental anthropology. New York: Wiley-Liss. p*, *25*.

SOFAER, DEREVENSKI, J, 1994. Where are the children? Accessing children in the past. *Archaeological review from Cambridge*, *13*(2), pp.7-20.

SOFAER, J., 2000. Material culture shock. Confronting expectations in the material culture of children.

SOFAER, J.R., 2006. *The body as material culture: a theoretical osteoarchaeology* (Vol. 4). Cambridge

SOMNER, W., 1703. The Antiquities of Canterbury. EP Publishing Limited

SOMNER, W. and Battely, N., 1977. *The Antiquities of Canterbury*. EP Pub..University Press.

SOROKIN, P. and Zimmerman, C.C., 1970. Rural and Urban Worlds. *Urban Man and Society: A Reader in Urban Sociology. New York: Alfred A Knopf*.

SPARKS, R., 1988. To Treat or Not to Treat Bioethics and the Handicapped Newborn.

SPARKS, M., 2001. The Refitting of the Quire of Canterbury Cathedral 1660–1716: Pictorial and Documentary Evidence. *Journal of the British Archaeological Association*, *154*(1), pp.170-190.

SPARKS, C.S. and Jantz, R.L., 2002. A reassessment of human cranial plasticity: Boas revisited. *Proceedings of the National Academy of Sciences*, *99*(23), pp.14636-14639.

STARK, S. 2013. Sexual Dimorpism of the Foramen Magnum: A Statistical and Morphological Approach. M.A. Thesis, University of Southampton.

STINSON, S., 2012. Growth variation: biological and cultural factors. *Human Biology: An Evolutionary and Biocultural Perspective, Second Edition*, pp.587-635.

STOCK, J.T., 2002. A test of two methods of radiographically deriving long bone cross-sectional properties compared to direct sectioning of the diaphysis. *International Journal of Osteoarchaeology*, *12*(5), pp.335-342.

STOCK, J.T., 2006. Hunter-gatherer postcranial robusticity relative to patterns of mobility, climatic adaptation, and selection for tissue economy. *American Journal of Physical Anthropology*, *131*(2), pp.194-204.

STOCK, J. T. 2012. Human evolution after the origin of our species: Bridging the gap between palaeoanthropology and bioarchaeology. In *Proceedings of the 12th Annual Conference of the British Association for Biological Anthropology and Osteoarchaeology (BABAO),* P. Mitchell and J. Buckberry, eds. Oxford: Archaeopress, 3–15.

STOCK, J. and Pfeiffer, S., 2001. Linking structural variability in long bone diaphyses to habitual behaviors: foragers from the southern African Later Stone Age and the Andaman Islands. *American Journal of Physical Anthropology*, *115*(4), pp.337-348.

STOCK, J.T. and Pfeiffer, S.K., 2004. Long bone robusticity and subsistence behaviour among Later Stone Age foragers of the forest and fynbos biomes of South Africa. *Journal of Archaeological Science*, *31*(7), pp.999-1013.

STOODLEY, N., 2000. From the cradle to the grave: age organization and the early Anglo-Saxon burial rite. *World Archaeology*, *31*(3), pp.456-472.

STOREY, R., 1992. Preindustrial urban lifestyle and health. *Health and lifestyle change*, pp.33-42.

STRAND Viðarsdóttir, U., O'Higgins, P. and Stringer, C., 2002. A geometric morphometric study of regional differences in the ontogeny of the modern human facial skeleton†. *Journal of Anatomy*, *201*(3), pp.211-229.

STRAND Viðarsdóttir, U., and Cobb, S. 2004. Inter-and intra-specific variation in the ontogeny of the hominoid facial skeleton: testing assumptions of ontogenetic variability. *Annals of Anatomy-Anatomischer Anzeiger*, *186*(5), pp.423-428.

STUART-MACADAM, P., 1985. Porotic hyperostosis: representative of a childhood condition. *American Journal of Physical Anthropology*, *66*(4), pp.391-398.

STUART-MACADAM, P., 1992. Porotic hyperostosis: a new perspective. *American Journal of Physical Anthropology*, *87*(1), pp.39-47.

SUMNER, D.R. and Andriacchi, T.P., 1996. Adaptation to differential loading: comparison of growth-related changes in cross-sectional properties of the human femur and humerus. *Bone*, *19*(2), pp.121-126.

SUNDICK, R.I., 1978. Human skeletal growth and age determination. *Homo Gottingen*, *29*(4), pp.228-249.

SWARDSTEDT, T., 1966. Odontological aspects of a Medieval population in the province of Jämtland, mid-Sweden. University of Lund.

TANNAHILL, R., 1973. Food in history.

TANNER, J.M., 1978. *Education and physical Growth: Implications of the study of children's Growth for educational theory and practice*. International Universities PressInc.

TANNER, J.M., 1981. *A history of the study of human growth*. Cambridge University Press.

TANNER, J.M., 1994. Growth from birth to two: a critical review. *Acta Med Auxol*, *26*, pp.1-51.

TANNER, J.B., Zelditch, M.L., Lundrigan, B.L. and Holekamp, K.E., 2010. Ontogenetic change in skull morphology and mechanical advantage in the spotted hyena (Crocuta crocuta). *Journal of Morphology*, *271*(3), pp.353-365.

TARDIEU, C. and Damsin, J.P. 1997. Evolution of the angle of obliquity of the femoral diaphysis during growth—correlations. *Surgical and Radiologic Anatomy*, *19*(2), 91-97.

TAYLOR, M.E., Tanner, K.E., Freeman, M.A.R. and Yettram, A.L., 1996. Stress and strain distribution within the intact femur: compression or bending?. *Medical engineering & physics*, *18*(2), pp.122-131.

TEMPLE, D.H., 2008. What can variation in stature reveal about environmental differences between prehistoric Jomon foragers? Understanding the impact of systemic stress on developmental stability. *American Journal of Human Biology*, *20*(4), pp.431-439.

TEMPLE, D.H. and Goodman, A.H., 2014. Bioarcheology has a “health” problem: Conceptualizing “stress” and “health” in bioarcheological research. *American journal of physical anthropology*, *155*(2), pp.186-191.

TEMPLE, D.H., Bazaliiskii, V.I., Goriunova, O.I. and Weber, A.W., 2014. Skeletal growth in early and late Neolithic foragers from the Cis-Baikal region of Eastern Siberia. *American journal of physical anthropology*, *153*(3), pp.377-386.

TERHUNE, C.E. 2013. How effective are geometric morphometric techniques for assessing functional shape variation? An example from the great ape temporomandibular joint. *The Anatomical Record*, *296*(8), 1264-1282.

THAYER, ZM, Kuzawa CW. 2011. Biological memories of past environments. Epigenetic pathways to health disparities. Epigenetics 6:798–803.

THOMPSON, D. A. W. 1915. Morphology and mathematics. *Transactions of the Royal Society of Edinburgh, 50*, 857–895.

THOMPSON, D.A.W. 1917. On Growth and Form. Cambridge University Press, Cambridge.

THOMPSON, B. 1984. Infant Mortality in Nineteenth-Century Bradford. In R Woods and J Woodward (eds.): Urban Disease andMortality in Nineteenth Century England. London: Batsford, pp. 120-147.

TOOGOOD, P.A, Skalak, A., and Cooperman, D.R. 2009. Proximal femoral anatomy in the normal human population. *Clinical orthopaedics and related research, 467* (4), 876.

TRINKAUS, E., 1993. Femoral neck-shaft angles of the Qafzeh-Skhul early modern humans, and activity levels among immature Near Eastern Middle Paleolithic hominids. *Journal of Human Evolution*, *25*(5), pp.393-416.

TRINKAUS, E., Churchill, S.E., Ruff, C.B. and Vandermeersch, B., 1999. Long bone shaft robusticity and body proportions of the Saint-Césaire 1 Châtelperronian Neanderthal. *Journal of archaeological science*, *26*(7), pp.753-773.

TURNER, B.L., Edwards, J.L., Quinn, E.A., Kingston, J.D. and Van Gerven, D.P., 2007. Age-related variation in isotopic indicators of diet at medieval Kulubnarti, Sudanese Nubia. *International Journal of Osteoarchaeology*, *17*(1), pp.1-25.

TURNER, B.L. and Armelagos, G.J., 2012. Diet, residential origin, and pathology at Machu Picchu, Peru. *American journal of physical anthropology*, *149*(1), pp.71-83.

UBELAKER, D.H. 1989. The estimation of age at death from immature human bone. *Age markers in the human skeleton*, pp.55-70.

VAN DER MEULE, M.C., Beaupre, G.S. and Carter, D.R. 1993. Mechanobiologic influences in long bone cross-sectional growth. *Bone*, *14*(4), pp.635-642.

VAN DER VLIET, V. 1974. Growing up in traditional society. In: Hammond-Tooke WD, editor. *The Bantu speaking peoples of Southern Africa, 2nd edition*. London: Routledge and Kegan Paul. p 211–245.

VAN GERVEN, D.P., Hummert, J.R. and Burr, D.B., 1985. Cortical bone maintenance and geometry of the tibia in prehistoric children from Nubia's Batn el Hajar. *American journal of physical anthropology*, *66*(3), pp.275-280.

VLAK, D., Roksandic, M. and Schillaci, M.A., 2008. Greater sciatic notch as a sex indicator in juveniles. *American Journal of Physical Anthropology*, *137*(3), pp.309-315.

WADDINGTON, CH. 1942. The epigenotype. Endeavor 1: 18-20 (Reprinted in the International Journal of Epidemiology 2012; 41:10-13).

WALDRON, T. 1994. “The human remains”. In; Evison, V. (ed.) *An Anglo-Saxon Cemetery at Great Chesterford, Essex.* York: Council for British Archaeology Research Report 91. 52-66.

WALL, C.E., 1991. Evidence of weaning stress and catch-up growth in the long bones of a Central California Amerindian sample. *Annals of human biology*, *18*(1), pp.9-22.

WALLACE, I.J., Tommasini, S.M., Judex, S., Garland, T. and Demes, B., 2012. Genetic variations and physical activity as determinants of limb bone morphology: an experimental approach using a mouse model. *American journal of physical anthropology*, *148*(1), pp.24-35.

WATERS-RIST, A.L. and Katzenberg, M.A., 2010. The effect of growth on stable nitrogen isotope ratios in subadult bone collagen. *International Journal of Osteoarchaeology*, *20*(2), pp.172-191.

WATTS, R., 2013. Childhood development and adult longevity in an archaeological population from Barton-upon-Humber, Lincolnshire, England. *International Journal of Paleopathology*, *3*(2), pp.95-104.

WEBER, G.W. and Bookstein, F.L. 2011. Virtual anthropology: a guide to a new interdisciplinary field. Springer.

WEBER, G.W., Bookstein, F.L. and Strait, D.S. 2011. Virtual anthropology meets biomechanics. *Journal of biomechanics*, *44*(8), pp.1429-1432.

WEEDON, M.N., Lango, H., Lindgren, C.M., Wallace, C., Evans, D.M., Mangino, M., Freathy, R.M., Perry, J.R., Stevens, S., Hall, A.S., et al. 2008. Genome-wide association analysis identifies 20 loci that influence adult height. *Nature Genetics* 40(5): 575-83.

WELLS, J,C.K. and Stock, J.T. 2007. The biology of the colonizing ape. *Yearbook of Physical Anthropology* 50:191-222.

WELLS, J.C.K. and Stock, J.T. 2011. Re-examining heritability: genetics, life history and plasticity. *Trends in Endrocrinology and Metabolism* 22(10): 421-428.

WESCOTT, D.J., 2006. Ontogeny of femur subtrochanteric shape in Native Americans and American Blacks and Whites. *Journal of forensic sciences*, *51*(6), pp.1240-1245.

WESCOTT, D. and Jantz, R., 2005. Assessing craniofacial secular change in American blacks and whites using geometric morphometry. *Modern morphometrics in physical anthropology*, pp.231-245.

WILEY, A.S. and Pike, I.L., 1998. An alternative method for assessing early mortality in contemporary populations. *American journal of physical anthropology*, *107*(3), pp.315-330.

WILEY, D.F., Amenta, N., Alcantara, D.A., Ghosh, D., Kil, Y.J., Delson, E., Harcourt-Smith, W., Rohlf, F.J., St John, K. and Hamann, B., 2005, October. Evolutionary morphing. In *Visualization, 2005. VIS 05. IEEE* (pp. 431-438). IEEE.

WILLIAMS, N. and Galley, C., 1995. Urban-rural differentials in infant mortality in Victorian England. *Population studies*, *49*(3), pp.401-420.

WILSON L.A., MacLeod, N. and Humphrey, L.T. 2008. Morphometric criteria for sexing juvenile human skeletons using the ilium. *Journal of Forensic Sciences*, *53*(2), pp.269-278.

WILSON, L.A., Cardoso, H.F. and Humphrey, L.T. 2011. On the reliability of a geometric morphometric approach to sex determination: A blind test of six criteria of the juvenile ilium. *Forensic science international*, *206*(1), pp.35-42.

WILSON, L.A.B., and Humphrey, L.T. 2017. Voyaging into the third dimension: A perspective on virtual methods and their application to studies of juvenile sex estimation and the ontogeny of sexual dimorphism. *Forensic Science International, 278,* 32-46.

WOOD, J.W., Milner, G.R., Harpending, H.C., Weiss, K.M., Cohen, M.N., Eisenberg, L.E., Hutchinson, D.L., Jankauskas, R., Cesnys, G., Katzenberg, M.A. and Lukacs, J.R., 1992. The osteological paradox: problems of inferring prehistoric health from skeletal samples [and comments and reply]. *Current anthropology*, *33*(4), pp.343-370.

WORTHMAN, C.M. and Kuzara, J., 2005. Life history and the early origins of health differentials. *American Journal of Human Biology*, *17*(1), pp.95-112.

YANG, J., Benyamin, B., McEvoy, B.P., Gordon, S., Henders, A.K., Nyholt, D.R Nyholt, D.R., Madden, P.A., Heath, A.C., Martin, N.G., Montgomery, G.W., Goddard, M.E., and Visscher, P.M. 2010. Common SNPs explain a large proportion of the heritability for human height. *Nature Genetics* 42(7): 565-569.

YOUNG, N.M., Wagner, G.P. and Hallgrímsson, B., 2010. Development and the evolvability of human limbs. *Proceedings of the National Academy of Sciences*, *107*(8), pp.3400-3405.

ZELDITCH, M.L., Sheets, H.D. and Fink, W.L., 2003. The ontogenetic dynamics of shape disparity. *Paleobiology*, *29*(1), pp.139-156.

ZELDITCH, M.L., Lundrigan, B.L. and Garland, T., 2004. Developmental regulation of skull morphology. I. Ontogenetic dynamics of variance. *Evolution & development*, *6*(3), pp.194-206.

ZELDITCH, M.L., Swiderski, D.L. and Sheets, H.D. 2012. *Geometric morphometrics for biologists: a primer*. Academic Press.

ZOLLIKOFER, C.P.E. and Ponce De León, M.S., 2004. Kinematics of cranial ontogeny: heterotopy, heterochrony, and geometric morphometric analysis of growth models. *Journal of Experimental Zoology Part B: Molecular and Developmental Evolution*, *302*(3), pp.322-340.